DESIGN AND MODELLING OF NOVEL ABSORPTION REFRIGERATION CYCLES

by

Stephen David White

Thesis submitted for the degree of

Doctor of Philosophy

The University of Adelaide

(Department of Chemical Engineering)

(February 1993)

CONTENTS

SUMMARY

Increased concern over the continued availability of oil and gas, combined with environmental concern over the large scale combustion of fossil fuels, has led to renewed interest in absorption refrigeration. However, the low thermal efficiency and high capital cost of absorption refrigeration provide major obstacles to the widespread application of this technology.

In this study, a number of novel absorption cycle heatpumps were investigated in an effort to increase the thermodynamic performance of the conventional cycle. These novel cycles employ a liquid - liquid separation step to separate the volatile working fluid from the rich absorbent stream returning from the absorber. By eliminating the distillation column and condenser from the conventional cycle, it was hoped that generator losses and cycle capital costs could be reduced.

A number of candidate working fluid pairs were examined for application in the novel cycles. Of these pairs, the diethylmethylamine - water, dimethylethylamine - water and trimethylamine - water pairs were selected for further investigation in refrigeration applications. The cyclohexane - aniline pair were selected for further investigation in heat transformer cycles.

To supplement existing data, experimental liquid - liquid and vapour - liquid phase equilibrium data was generated for the dimethylethylamine - water and trimethylamine - water mixtures. This data was correlated by a five parameter NRTL model. The resulting thermodynamic models were used to simulate the performance of the novel absorption cycle heat pumps on the PROCESS™ chemical plant simulation software package.

Simulations of the novel refrigeration cycle showed that refrigeration could only be obtained over a limited range of temperatures. Cycle performance fell dramatically with decreasing evaporator temperature.

In view of the poor performance of this cycle, a number of "hybrid" cycles were synthesized. These cycles combined both the liquid phase separation step and a distillation step for recovering refrigerant. The additional distillation step was employed to increase the purity of either the absorbent or refrigerant phase exiting the liquid phase separation drum.

Of the "hybrid" cycles investigated, optimum performance was obtained from the cycle with refrigerant phase rectification. However, the thermodynamic performance of this cycle did not compare favourably with that obtained from the conventional cycle employing the same working fluid pair.

Similar results were obtained from the novel heat transformer cycles. Indeed, the boiling point elevation which could be achieved between the evaporator and the absorber was even more constrained in these cycles by the insensitivity of the cyclohexane - aniline mixture vapour pressure at high cyclohexane concentrations.

While the results of these simulations were not encouraging, the potential for recycling liquid blowdown from the evaporator, to provide reflux to the distillation column, was highlighted. This modification can be employed to eliminate the use of fresh refrigerant, from the condenser, as reflux in a conventional aqua-ammonia absorption refrigeration cycle. Such a cycle has not been reported to date. The potential of this modified aqua - ammonia absorption refrigeration cycle was investigated.

Simulations of the modified cycle, using the equation of state proposed by Ziegler and Trepp, predicted an increase in thermodynamic performance of approximately five percent with a nett reduction in the total heat transfer area required. Pilot scale demonstration of this cycle is recommended.

DECLARATION

This thesis contains no material which has been accepted for the award of any other degree or diploma in any university or other tertiary institution and, to the best of my knowledge and belief, contains no material previously published or written by another person, except where due reference has been made in the text.

I give consent to this copy of my thesis, when deposited in the University Library, being available for photocopying and loan.

Signed Date 18/2/93

ACKNOWLEDGEMENTS

I would like to thank to all those who have helped make the last three years such an enjoyable and rewarding experience.

In particular, I would like to thank Dr. Brian. O'Neill for supporting my novel research ideas and for his wide-ranging advice over the last three years. I am particularly indebted to him for his assistance in the preparation of this thesis. I would also like to thank Mr. Chris Colby and Mr. Mark Collis for the frequent use of their Macs.

I would like to express my gratitude to the South Australian Energy Research Advisory Committee, the National Energy Research and Development Council and the Australian Research Council for their financial support.

I would like to thank my family, for their love and encouragement through out my studies. I particularly acknowledge the support of my wife, Debra, as she managed the children and the new house over this period. Thanks also to Mum, Dad and the Peacock family for the working bees and the child minding.

Chapter 1
INTRODUCTION

Absorption refrigeration has been used extensively since the development of the first continuously operating ammonia/ water machines in the middle of the nineteenth century by Ferdinand P.E. Carre. While the early popularity of these machines was curbed by the development of vapour compression machines, absorption refrigeration remains of interest when suitable quality waste heat is available at low cost. In such applications, absorption refrigeration machines provide low cost cooling without consuming valuable high grade energy.

Potential problems affecting the continued availability of cheap supplies of oil and gas, combined with environmental concern over the large scale combustion of fossil fuels, has led to renewed interest in absorption refrigeration. With reduced primary fuel consumption and reduced emissions of green-house gases, the importance of absorption refrigeration is sure to increase.

However, the range of applications suitable for absorption refrigeration will continue to be limited by the economics of absorption refrigeration compared with that of vapour compression refrigeration machines. In particular, the low thermal efficiency and increased cost of absorption refrigeration have been identified as major obstacles to the future development and application of absorption refrigeration.

A number of previous attempts to improve the performance of the conventional absorption refrigeration cycle have concentrated on the search for new working fluids. These have met with limited success.

Numerous papers have also been published discussing improved methods for internal heat recovery in the cycle. Unfortunately, the increased heat exchange surface area required in these cycles often outweighs the economic advantage of the improved performance. Perhaps the most promising improvement over the conventional absorption refrigeration cycle, is the application of two stage absorption refrigeration cycles in the chemical process industries.

In this study, a new approach is taken with the development and analysis of a novel absorption refrigeration cycle. The novel absorption refrigeration cycle utilises the partial miscibility of some binary mixtures, at elevated temperatures, to separate the refrigerant from the absorbent in the liquid phase. This modification eliminates the distillation column in the conventional cycle.

The desirable characteristics of absorbent - refrigerant pairs in this cycle is described. Based on these characteristics, a number of absorbent - refrigerant pairs with potential for application in the novel refrigeration cycle are identified.

Experimental phase equilibrium data is generated to supplement existing literature data for these absorbent - refrigerant pairs. Thermodynamic models are generated to correlate this data in a form suitable for application in the PROCESS™ chemical plant simulation software package

The thermodynamic performance of the novel absorption refrigeration cycle is then simulated on PROCESS and the potential of the cycle is discussed. Variations of the basic novel absorption refrigeration cycle are developed and comparisons are made with the conventional absorption refrigeration cycle.

A modification to the conventional absorption refrigeration cycle, resulting from the novel cycle analysis, is also analysed. Comparitive costings of the modified absorption refrigeration cycle are employed to assess the commercial potential of this modified cycle.

Chapter 2
LITERATURE REVIEW

In this chapter, a brief history of the development of the absorption refrigeration cycle is given. Working fluids for the conventional absorption refrigeration cycle are discussed and a number of recent improvements which have been made to the conventional cycle are described. The concept of utilising alternative separation techniques in place of the conventional distillation column regenerator is introduced and a number of such novel cycles are discussed.

2.1 History

The first commercial absorption heat pumps were manufactured in the middle of the nineteenth century. Early machines using sulphuric acid and water were replaced by the continuously operating ammonia / water machines of Ferdinand Carre. These machines were very reliable and were fabricated in great numbers in France, England and Germany. However, by the end of the nineteenth century, absorption machines had largely been displaced by the vapour compression machines of C. V. Linde (Stephan, 1983).

High fuel prices during the 1920's and 30's led to a resurgence in the popularity of absorption machines. Research undertaken during this period led to a large body of literature and significant advances in the design of absorption machines. In particular, E. Altenkirch (1954) carried out fundamental investigations on reversible heat production and absorption refrigeration. He provided numerous suggestions for useful process cycles, including multistage cycles and variations to the internal heat exchange network. G. Maiuri (1939) devised a number important construction improvements including the wetted wall absorber .

Since this time, significant improvements in the efficiency of electrical power generation have resulted in the declining importance of the absorption cycle heat pump. Today, the absorption cycle heat pump is employed in only a limited number of applications where waste heat is available. Economies of scale particularly favour applications in the process industries. In these applications, low cost cooling can be provided without consuming valuable high grade energy.

2.2 Working Fluids

Ammonia - water and lithium bromide - water mixtures are the most widely used working fluids in absorption cycle heat pumps. Both offer high thermodynamic performance and low capital cost. However these mixtures have some disadvantages:

The ammonia/ water cycle is limited by the stability of ammonia at temperatures above 200°C and the high vapour pressure of ammonia at ambient temperatures. This generally makes ammonia/ water mixtures unsuitable for application in the more efficient two stage cycles. Ammonia is also toxic.

The evaporator temperature in the lithium bromide/ water cycle must exceed 0°C to prevent ice formation. Crystallisation of lithium bromide in the generator also limits the allowable concentration of the absorbent and may cause plugging.

These limitations have led to extensive research in the hope of discovering better refrigerant/ absorbent pairs (Zellhoefer, 1937, Iedema, 1982, Ando and Takeshita, 1984). Desirable characteristics for working fluids in an absorption refrigeration cycle have been identified by a number of workers (Buffington, 1949, Macriss, 1976 and Manscori and Patil, 1979). These characteristics include:

(i) The working fluids should exhibit appropriate vapour pressure - temperature characteristics. The high - side pressure is determined by the bubble point pressure of the refrigerant at temperatures just above ambient. Excessive pressures will increase plant construction costs. The low-side pressure is determined by the required evaporator temperature and the purity of the working fluids exiting the distillation column. Cycles operating under vacuum must be hermetically sealed to prevent air leakage and subsequent reduction in absorber efficiency.

(ii) The difference between the normal boiling point of the absorbent and the refrigerant should be large. The difference between the boiling points of the refrigerant and the absorbent generally gives an indication of the maximum boiling point elevation which can be achieved and hence the minimum evaporator temperature. A large boiling point difference also infers a high relative volatility and, consequently, easy separation in the generator.

(iii) The latent heat of the selected refrigerant should be high to minimise the circulation rate of refrigerant and reduce capital costs.

(iv) The selected working fluids should be non corrosive and non toxic.

(v) The working fluids should have good stability to ensure long 'charge life' and minimise the effect of decomposition products on performance and safety.

(vi) The working fluids should not form a solid phase. This eliminates the potential for crystallisation and subsequent plugging.

(vii) The working fluids should exhibit good transport properties, condusive to effective mass and heat transfer and good fluid flow.

The "affinity" of the absorbent - refrigerant pair was also thought to be important. Strong affinity, manifested as a large negative deviation from Raoults Law, reduces absorbent circulation rate with consequent reductions in associated sensible heat losses. However, Jacob et al. (1969) showed that high refrigerant concentrations at the absorber outlet may lead to overall reductions in thermodynamic performance.

Some recent studies of new absorbent/ refrigerant pairs have investigated the potential of various fluorocarbon/ organic solvent pairs for application in residential air conditioning (Ando and Takeshita, 1984, Uemura and Hasaba, 1968 and Kriebel and Loffler, 1965). However, selection of suitable organic solvents with good thermal stability and high refrigerant solubility has proved a difficult task.

A number of recent studies have also investigated the potential of various electrolyte solutions as working fluids in the absorption cycle heat pumps (Grover et. al., 1989, Morrissey and O'Donnell, 1986 and Iedema, 1982). Some improvements have been made to the thermodynamic performance of absorption cycle heat pumps with these mixtures. However, the potential for crystallisation and subsequent plugging remains.

Unfortunately, the search for improved working fluids has met with limited success. It appears that further investigation of new working pairs is unlikely to provide significant potential for further improvements in cycle thermodynamic efficiency or cost. O'Neill and Roach (1990) confirmed this observation by demonstrating that the selection of absorbent/ refrigerant pair does not significantly alter the maximum theoretical performance achievable in an absorption refrigeration cycle employing an ideal distillation column generator.

2.3 Modified Absorption Heat Pump Cycles

The concept of an ideal second law absorption refrigeration cycle, consisting of a Carnot heat pump driven by a Carnot engine, is useful for comparing the performance of the real cycle. Dalichaouch (1990) calculated second law efficiencies for an aqueous lithium bromide absorption refrigeration cycle. He demonstrated that, over a wide range of conditions, the performance of this cycle was less than 30% of the performance predicted by the ideal second law cycle. Clearly, there is significant potential for improvement in cycle performance. Modification of the conventional absorption cycle appears to hold the greatest potential for realising improved performance, as the search for alternative working fluids has met with limited success.

An investigation into the losses encountered in conventional absorption refrigeration cycles provides a starting point in the search for new cycles. Recent papers by Briggs (1971) and Karakas et. al. (1990) have detailed an exergy balance on the conventional absorption refrigeration cycle. The exergy losses calculated by Briggs (1971) are summarised in table 2.1. These studies demonstrate that the majority of losses occur in the absorber and the generator.

COMPONENT	LOST WORK (% OF WORK INPUT TO CYCLE)
Generator	39.0
Liquid heat exchanger	2.5
Weak liquid capillary	0.4
Absorber	33.1
Condenser	6.1
Precooler	0.7
Refrigerant Capillary	1.0
Evaporator	7.2
Net Refrigeration	10.0

TABLE 2.1: BREAKDOWN OF LOSSES IN A CONVENTIONAL ABSORPTION REFRIGERATION CYCLE

Based on these findings, modifications of the conventional absorption cycle with improved heat recovery in the absorber and generator would be expected to exhibit superior performance. Alternatively, improved performance could be achieved by creating a new type of absorption cycle, where the conventional distillation column is replaced by an alternative separation process capable of operating closer to the thermodynamic ideal.

2.3.1 Variations to the Conventional Absorption Cycle Heat Pump

A number of ideas have been proposed for improving the efficiency of the conventional absorption cycle heat pump illustrated in figure 2.1. These ideas could be broadly grouped into three areas; cycles for evaporator blowdown minimisation, cycles for heat recovery from the absorber and multistage cycles. The desirability of these options is largely dependent on the quality, cost and availability of the hot and cold utilities. The following discussion of these modifications particularly relates to ammonia/ water absorption refrigeration cycles.

(i) Cycles for evaporator blowdown minimisation

One of the most significant advances in this area was the recognition of the benefits of careful rectification in the distillation column to prevent accumulation of absorbent in the evaporator. One such improvement to the rectification section of the column employs two condensers in series (Bogart, 1981). In this cycle (figure 2.2), the first partial condenser (dephlegamator) provides the reflux to the distillation column and the second total condenser provides fresh refrigerant to the evaporator. This allows any "carry-over" of absorbent from the distillation column to be returned to the distillation column and prevents build up of absorbent in the evaporator.

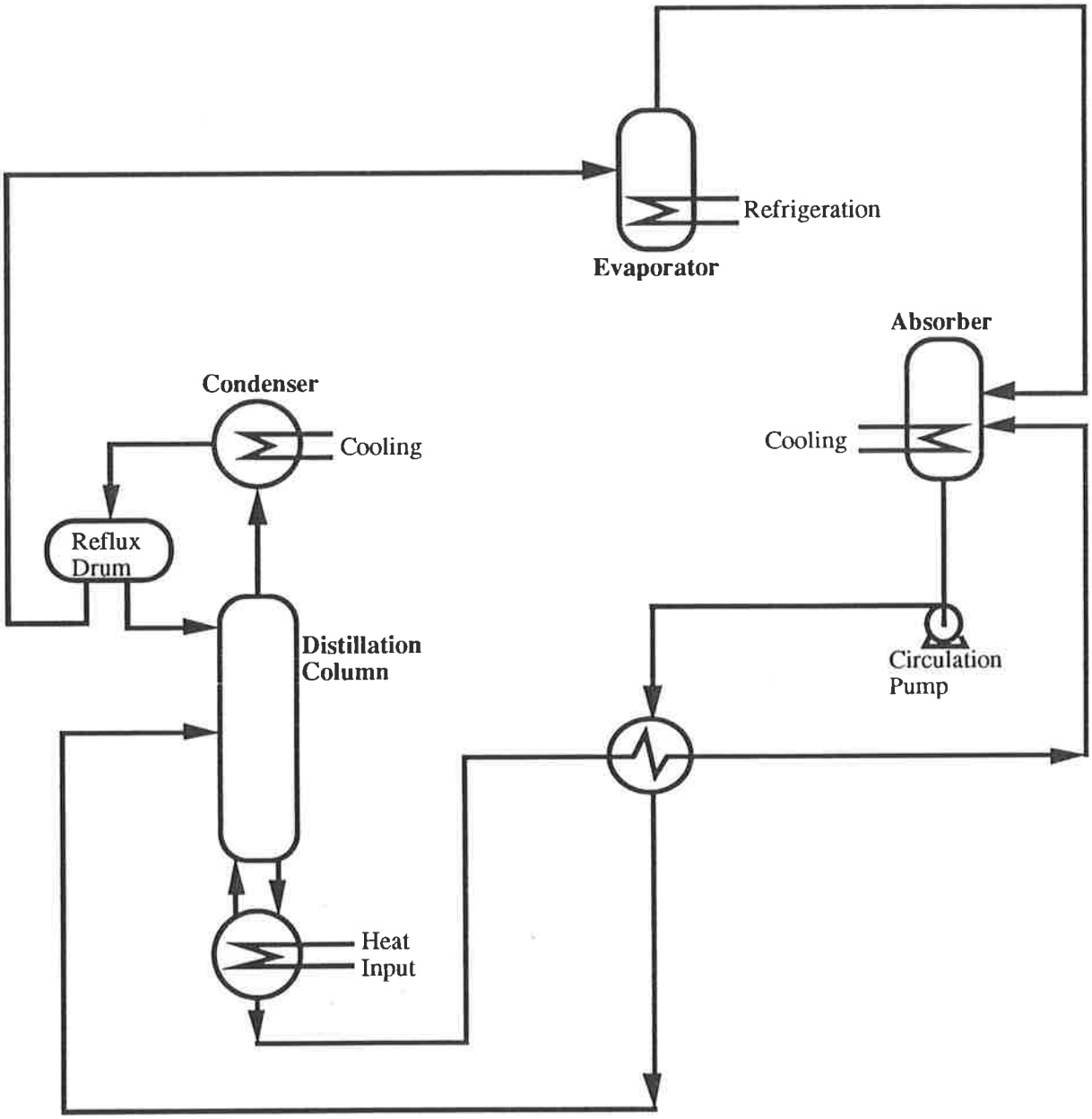

FIGURE 2.1: FLOW SCHEMATIC OF A CONVENTIONAL ABSORPTION REFRIGERATION CYCLE

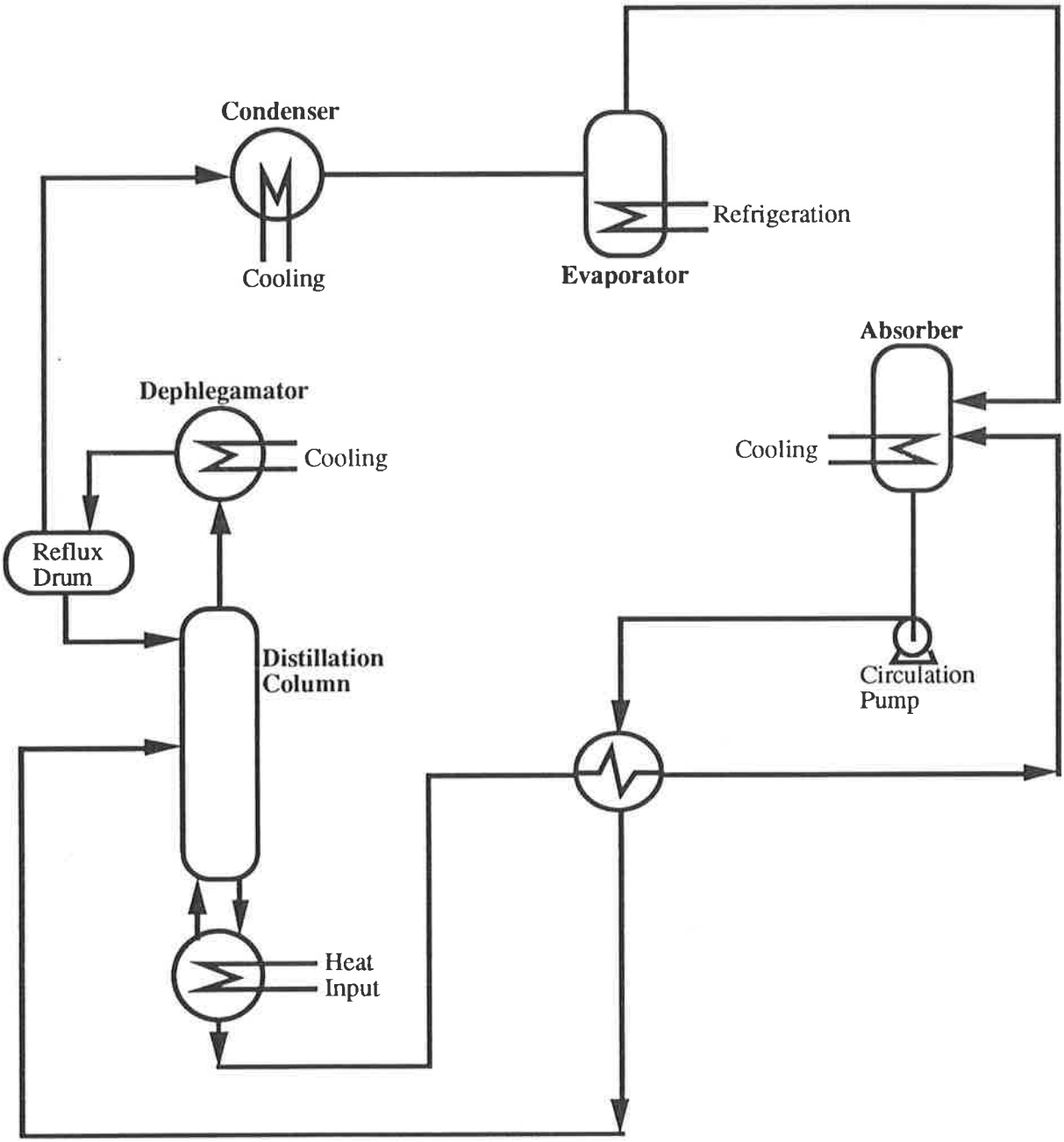

FIGURE 2.2: FLOW SCHEMATIC OF A CONVENTIONAL ABSORPTION REFRIGERATION CYCLE WITH A TWO STAGE CONDENSER

Another improvement to the rectification section of the column involves splitting the returning strong aqua stream prior to the solution heat exchanger (Blass, 1974). This cycle is illustrated in figure 2.3. One fraction of the strong aqua is heated in the solution heat exchanger and fed to the distillation column. The other fraction is added directly to the rectification section of the distillation column. This technique increases the amount of heat that can be recovered from the weak aqua stream with a consequent reduction in the required duty in the generator. The cold feed stream also induces additional reflux in the distillation column as its temperature is raised, by direct contact heat transfer, to the operating temperature of the column. This additional reflux is achieved without the use of expensive heat transfer equipment.

(ii) Cycles for heat recovery from the absorber

A number of options have been presented for recovering the heat released in the absorber (Auh, 1977, Kandlikar, 1982 and Kumar and Kaushik, 1991). The heat of absorption is generally employed to preheat the returning strong aqua. Alternatively, the strong aqua stream exiting the pump can be split, so that one fraction of the stream is used to precool the weak absorbent and the other fraction used to recover heat from the absorber (Bogart, 1981).

(iii) Multi-stage Cycles

Trepp (1983) presented a summary of the fundamental performance limitations of two stage cycles. In these cycles, an intermediate pressure level is introduced so that heat added in the first, high pressure / temperature stage can provide heat to a second, low pressure / temperature stage. This can substantially increase the thermodynamic performance of the cycle. However, successful operation of these machines requires a high temperature heat source. This is a significant limitation because absorption heat pumps are not usually selected in applications where relatively high grade heat sources are available.

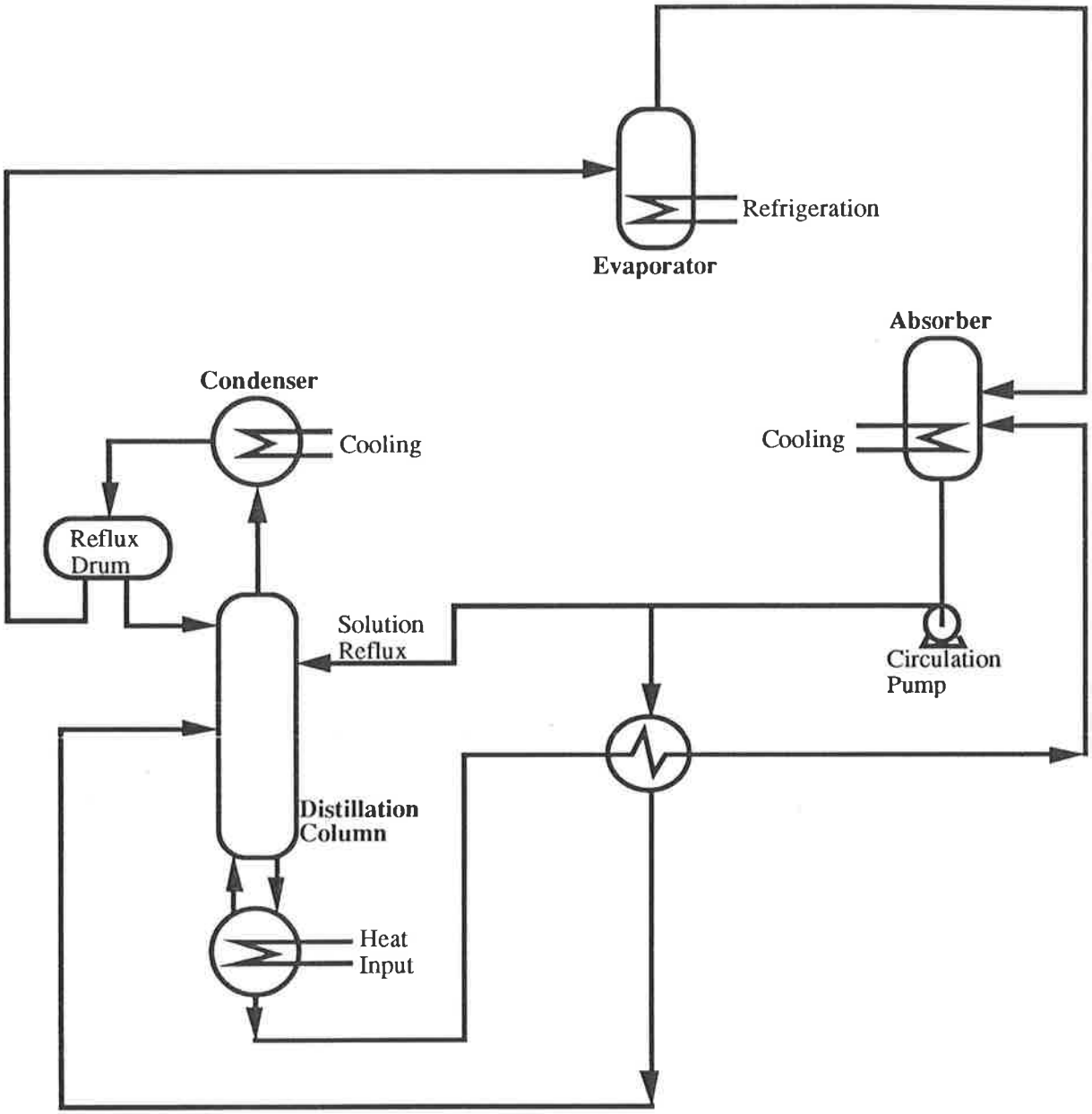

FIGURE 2.3: FLOW SCHEMATIC OF A CONVENTIONAL ABSORPTION REFRIGERATION CYCLE WITH SOLUTION REFLUX

One of the more favourable two stage cycles discussed by Trepp (1983), employs the concept of resorption. The cycle is illustrated in figure 2.4. It employs two evaporators in series operating at different pressures. The first evaporator receives the pure liquid refrigerant from the condenser, allowing it to operate at relatively high pressures. The refrigerant vapour leaving the evaporator is passed to the resorber where it is absorbed into the liquid stream exiting the second evaporator. The resulting two component mixture is then passed to the second evaporator, operating at low pressure, where the refrigerant is evaporated from solution. While pure refrigerant in the first evaporator will boil at constant temperature, a counter current heat exchanger can be used to obtain refrigeration over a range of temperatures in the second evaporator.

Analysis of the benefits of these cycle improvements must reflect a variety of economic criteria in addition to thermodynamic performance. The low value generally placed on the waste heat supplied to the generator may preclude the selection of improved heat recovery networks, with increased capital cost, in most industrial applications. Unfortunately, modern literature abounds with COP comparisons but rarely quotes capital costs or investment comparisons between absorption units and vapour compression units. Holldorf (1979) claimed that the sum of the heat exchange surface areas in an absorption refrigeration cycle provides a measure of investment expenditure. Cockshott (1976) provided a detailed comparison of investment and operating costs between an ammonia/ water absorption refrigeration cycle and a conventional propane vapour compression cycle. The analysis was based on an application in a natural gas liquids processing plant.

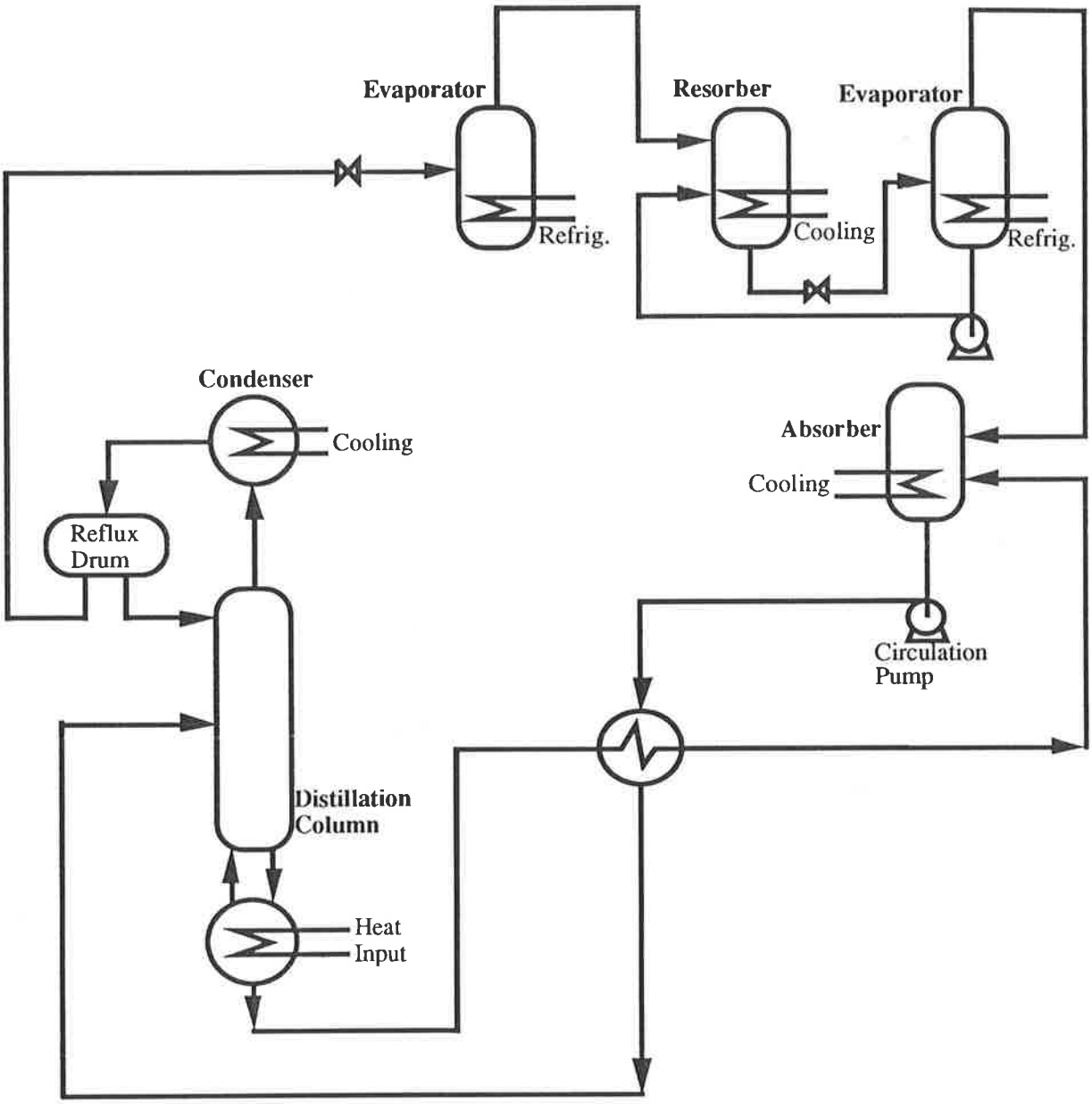

FIGURE 2.4: FLOW SCHEMATIC OF A TWO STAGE ABSORPTION REFRIGERATION CYCLE WITH RESORPTION

2.4 Alternative Separation Techniques for Absorption Heat Pump Generators

References in the literature to the application of alternative separation technologies in absorption refrigeration are sparse. Consequently, the development of such novel cycles is a potentially fruitful area for further investigation.

A number of separation techniques could be selected. The principal criterion is that low grade energy (preferably waste heat) provide the bulk of the required work to the separation device. Some of the separation techniques which could be employed include absorption/ desorption on solids, fractional crystallization, liquid extraction and pervaporation.

Absorption/ desorption on solids has been examined in some detail because of the potential for intermittently operating absorption machines. Altenkirch (1954) and Backstrom (1953) proposed a number of of liquid - solid mixtures for these machines. Examples include calcium chloride/ water, zinc-sulphate/ ammonia and silica gel/ water mixtures. Machines of this type were manufactured by the Humboldt Company in Cologne and Siemens - Schukert Company in Berlin.

Open cycle absorption refrigeration has received considerable attention in recent years because of its potential in solar driven air conditioning applications (Kaushik and Kaudinya, 1989, Lenz et. al., 1986). In this cycle, lithium chloride and water are employed as working fluids. In contrast to a conventional generator, water is removed from solution by (i) reducing the partial pressure of water in the vapour phase with the addition of air as a diluent, and (ii) heating the lithium chloride solution in a solar panel. Water is evaporated into the air stream passing over the solution before it is rejected to the atmosphere. The evaporated water is replaced by fresh make-up water.

While the regeneration step in these cycles is significantly different to the conventional generator, vaporisation of the refrigerant is still required to achieve separation. Consequently, the heat load on these cycles must be high.

In 1958, the Battelle Memorial Institute submitted a report to the American Gas Association regarding the application of solution systems, exhibiting lower critical solution temperature behaviour, in absorption refrigeration. The report recognized that the behaviour of these mixtures could provide the means to separate a refrigerant from an absorbent. However, the report does not describe an operating system which could be employed for this purpose.

Mehta (1981) patented an absorption refrigeration cycle utilising the partial miscibility of these binary mixtures, at elevated temperatures, to separate the refrigerant from the absorbent. By eliminating the steps of vaporization and condensation of the refrigerant, the cycle could potentially realise savings in energy and capital cost. However, the simplified cycle analysis presented in the patent is insufficient to to assess the potential of this cycle and the cycle has not been developed further in the literature.

The cycle described by Mehta (1981) was chosen for further examination with the intention of demonstrating that vaporisation of the refrigerant is not required for recovery of refrigerant in an absorption refrigeration cycle.

2.5 Prediction of the Thermodynamics of Absorption Cycle Working Fluids

Successful simulation of the various absorption refrigeration cycles requires a thermodynamic model capable of accurate prediction of phase equilibria for the selected working fluid mixtures. In a conventional absorption refrigeration cycle, the thermodynamic model is employed to predict vapour - liquid equilibria only. However, the thermodynamic model for the novel absorption refrigeration cycle must be capable of accurate prediction of both vapour - liquid and liquid - liquid phase equilibria. Information on the pure component thermodynamic properties is also required.

A number of thermodynamic models are available for predicting phase equilibria. These models can be classified into four groups; equations of state, liquid activity coefficient models, electrolytic models and group contribution models.

(i) Equation of state models

Equations of state are often used for mixtures of non-polar comopounds. Generalised equation of state models, based on the pure component critical properties, provide a complete thermodynamic description of the system including phase equilibria, enthalpies and entropies. Examples include the Peng Robinson and Swoave Redlich Kwong equations of state. Unfortunately, a number of additional parameters are required to predict the excess properties for mixtures of polar compounds and model formulation becomes a curve fitting exercise. In this study, the 46 parameter equation of state of Ziegler and Trepp (1984) was used for the prediction of the thermodynamic properties for mixtures of ammonia and water.

(ii) Group contribution models

Group contribution models have been used with some success for the prediction of pure component thermodynamic properties. However, these models are generally unsuitable for the prediction of two component phase equilibria of polar compounds. Reid, Prausnitz and Poling (1987) provide recommendations on the applications of these models. In this study, pure component thermodynamic properties have been calculated for a number of low molecular weight tertiary amines using these methods.

(iii) Liquid activity coefficient models

Liquid activity coefficient models are particularly suitable for the prediction of phase equilibria for polar mixtures at low pressure. Gmehling et. al. (1977) provide values for the adjustable parameters of five different liquid activity coefficient models for an extensive range of binary mixtures. Examination of these listings suggests that the non -random two linear (NRTL) model proposed by Renon and Prausnitz (1968) generally provides the most accurate fit to experimental data. Unfortunately, conventional activity coefficient models are only valid for isothermal data. This limits the capability of these models to predict heats of mixing because the Gibbs Free Energy Function can not be differentiated with respect to temperature. To overcome this difficulty, additional parameters can be employed in the NRTL model (Asselineau and Renon, 1970). In this model, the energies of interaction (g_{ij}–g_{jj}) are linear functions of temperature. This enables a single model to predict phase equilibria and heats of mixing over a range of temperatures.

Chapter 3
EXPERIMENTAL METHOD

Additional phase equilibrium data was required to supplement existing data for two low molecular weight tertiary amine/ water mixtures. In this chapter, the experimental apparatus and experimental technique for determining the required liquid - liquid and vapour - liquid equilibrium data is described.

A suitable refrigerant/ absorbent pair for the novel absorption refrigeration cycle must exhibit "lower critical solution temperature behaviour" when mixed. Relatively few mixtures exhibit such behaviour. The bulk of these mixtures are composed of amines with either water or ethanol. In these systems, miscibility at low temperatures is a consequence of hydrogen bonding between the amine group and the polar solvent. At higher temperatures the hydrogen bonds breakdown, reducing the affinity between the amine and the solvent.

Such unusual thermodynamic behaviour has been studied by Copp (1955) who presented liquid - liquid equilibrium data for diethylmethylamine - water mixtures. Davison et. al.(1960,1966) also presented liquid - liquid equilibrium data for a variety of aliphatic tertiary and secondary amine - water mixtures. However, liquid - phase separation has not been reported for the lower molecular weight tertiary amines, namely, dimethylethylamine and trimethylamine in mixture with water.

Chun et. al. (1971) and Copp (1955) presented extensive tabulations of vapour - liquid equilibrium data for mixtures of diethylmethylamine and water. However, vapour - liquid equilibrium data was not available for dimethylethylamine - water mixtures and the solubility data presented by Felsing and Phillips (1936), for trimethylamine in water, was limited to very low amine concentrations (< 4 mol %).

Of these mixtures, the dimethylethylamine - water and trimethylamine - water pairs were thought to posess the greatest potential in the novel absorption refrigeration cycle. However, additional experimental data was required to provide sufficient information to accurately predict the thermodynamic properties of these mixtures.

To supplement the experimental data reported in the literature, experimental vapour - liquid and liquid - liquid equilibrium data was generated for the dimethylethylamine - water and trimethylamine - water mixtures. In this chapter, the experimental apparatus used to generate this data is described in detail and the operation of these experiments is discussed.

3.1 Liquid-Liquid Equilibrium Experiments.

Two methods of determining the liquid phase coexistance curve are widely used in the literature. For binary mixtures, liquid - liquid equilibrium data can be obtained by heating a mixture of known concentration inside a sealed glass ampoule and recording the temperature at which phase separation first occurs.

Liquid phase equilibrium data can also be obtained by sampling from each phase of a two phase mixture. This method is particularly suitable for determining equilibrium tie - lines in multicomponent mixtures.

Both of these experiments were used for determining the liquid phase co-existance curves for dimethylethylamine - water and trimethylamine - 3% salt solution mixtures. The former method was used for obtaining equilibrium compositions when the recorded temperature was close to the lower critical solution temperature. In this region, good temperature control is required because the equilibrium composition is sensitive to temperature.

The direct phase sampling method was employed at temperatures significantly higher than the lower critical solution temperature where the equilibrium temperature is very sensitive to composition.

3.1.1 Equilibrium Determination Inside Sealed Glass Ampoules

Pyrex tubes, constricted near their open end, were charged with various concentration mixtures of water and tertiary amine. The concentration measurement procedure is discussed in section 3.3. The filled ampoules were then frozen in liquid nitrogen, evacuated and sealed. Sealed ampoules were placed in a well stirred water bath and heated until phase separation occured.

The water bath consisted of a glass beaker filled with litium bromide solution. Lithium bromide solution was used in the bath to enable bath temperatures of up to 150°C. A Eurotherm P818 temperature controller (with an ISA type K thermocouple and internal cold junction compensation) supplied power to a 150W cartridge heater inserted in the bath. Stirring was provided by a rotating impeller to eliminate thermal gradients in the bath. This arrangement, illustrated in figure 3.1, allowed the temperature to be controlled to within 0.2K of the setpoint. A 4 wire, 3mm O.D., sheathed platinum resistance probe, connected to a Leeds and Northrop 8078 precision temperature bridge, was used in preference to the controller thermocouple as the standard for determining bath temperature.

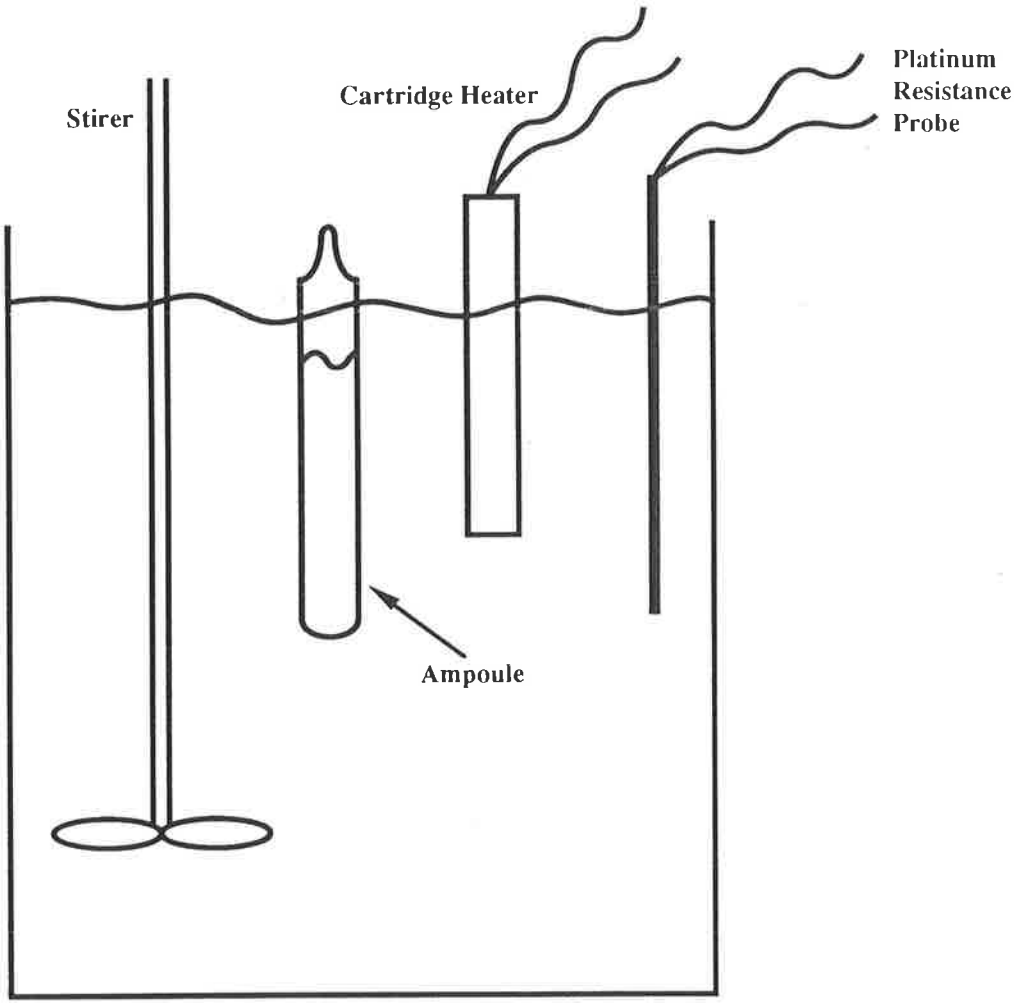

FIGURE 3.1: WATER BATH SCHEMATIC DIAGRAM

The bath was carefully heated until phase separation was observed in the ampoule. The temperature was then held constant at various temperatures above and below the equilibrium temperature, gradually converging on the equilibrium temperature. Each temperature was held for more than 30 minutes to ensure thermal equilibrium had been achieved. However, some hysteresis was observed in values obtained for the equilibrium temperature when comparing values obtained by increasing the temperature (approaching from the region of total miscibility) with values obtained by decreasing the temperature (approaching from the region of phase immiscibility). The accuracy of equilibrium temperature determinations was better than ±0.5K.

At the temperatures encountered in these experiments, the pressure inside the ampoules exceeded atmospheric pressure. However, it was not possible to measure pressure inside the sealed ampoules. This is unfortunate, as the high pressures expected inside the ampoule constitute the major source of systematic experimental error. The error between the measured composition and the liquid phase composition present in the ampoule at elevated temperature, results from evaporation of the more volatile amine into the vapour phase. The actual amine composition was estimated to be between 1.5% and 5.0% less than the measured value for mixtures of dimethylethylamine and water. The actual amine composition for trimethylamine - water mixtures, was estimated to be between 6% and 11% less than the measured value.

In some initial experiments with dimethylethylamine - water mixtures, ampoules were not evacuated prior to sealing. In these experiments, the cloud point temperature appeared to decrease with time and a yellow colour change was observed. The influence of this phenomena on the measured phase separation temperatures was quite dramatic at high amine concentrations. Fourier transform NMR spectra were obtained from samples of the discoloured mixture to identify and quantify the source of discolouration. A typical spectra is presented in figure 3.2. The discolouration appears as a consequence of amine decomposition with approximately two percent decomposition measured in one sample. Clearly, industrial applications employing these amines as solvents would be severly constrained by the poor stability of the amine.

Unfortunately, this technique was plagued by ampoule failures when testing mixtures of trimethylamine and salt solution at high temperature and consequently high pressure. This led to the eventual abandonment of further testing at concentrations above 26.5 mol% trimethylamine.

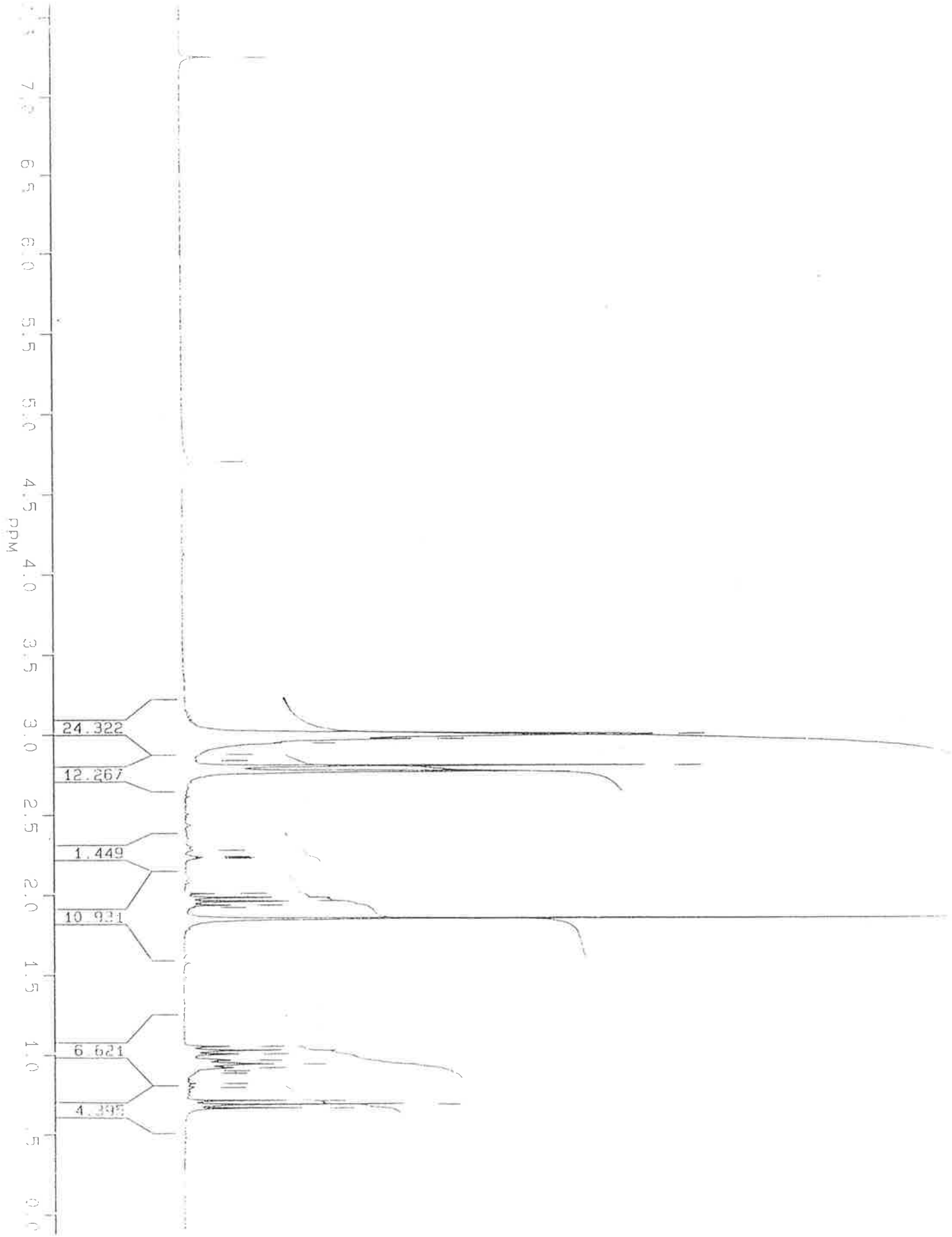

FIGURE 3.2: FOURIER TRANSFORM NMR SPECTRA OF DISCOLOURED AMINE - WATER MIXTURE

3.1.2 Equilibrium Determination By Direct Sampling of Phases

An obvious method for determining the boundaries of the liquid phase equilibrium curve is to establish the two liquid phases in a sealed container and measure the composition of samples taken from each phase. Despite the appeal of such a technique, some practical difficulties are encountered with volatile amine - water mixtures. High pressures are encountered at the temperatures required for phase separation, making it difficult to prevent flashing as the sample is taken.

To overcome these difficulties, an equilibrium cell was constructed from a 10mm O.D. stainless steel tube with a central isolation valve. The equilibrium cell is illustrated in figure 3.3. The cell was charged with the amine - water mixture and heated. After phase separation had been established, the top and bottom halves of the tube were isolated prior to cooling and subsequent composition analysis.

FIGURE 3.3: LIQUID PHASE EQUILIBRIUM CELL WITH ISOLATION VALVE

The concentration of the charge mixture was chosen to ensure that a two phase mixture would form upon heating. By selecting a concentration above or below the lower critical solution concentration, the liquid predominantly forms either the amine rich phase or an aqueous phase inside the tube.

The tube was then suspended in the constant temperature water bath (ref section 3.1.1) and heated to the desired temperature. After 30 minutes equilibration time, the top and bottom half of the tube was isolated to create one sample of liquid corresponding to either the amine phase or aqueous phase (depending on the concentration of the feed). This sample was cooled to prevent flashing of the volatile amine and the composition measured. The other sample of liquid was discarded as it contained both liquid phases.

3.2 Vapour - Liquid Equilibrium Experiments.

Experimental devices for obtaining vapour - liquid equilibrium data are well documented for binary mixtures. These experiments can be classified into two groups; circulating stills and static devices.

Circulating stills consist of a boiling chamber, condenser and condensate receiver. The boiling chamber is charged with a binary mixture and the apparatus evacuated. The mixture is then heated until boiling occurs. The resulting vapour is condensed and returned to the boiling chamber. After a suitable time, the temperature and pressure in the boiling chamber is measured. Liquid samples are also taken from the boiling chamber and condensate receiver to determine the composition of the liquid and vapour phases. Circulating stills eliminate the problem of dissolved gases in the charge mixture and also provide vapour phase compositions which can be used to test for thermodynamic consistency.

Static equilibrium devices consist of a vessel connected to a mercury manometer. The vessel is charged with a degassed binary liquid mixture and the entire apparatus is immersed in a constant temperature bath. The vapour pressure of the mixture is measured at various temperatures. The composition of the liquid phase is then measured and the composition of the vapour phase is calculated from the liquid phase composition, temperature and pressure. These devices are simpler to operate than the circulating stills and data can be accumulated more rapidly.

The experimental data in this study was required for an initial screening of potential refrigerant/ absorbent pairs. Therefore, high precision data was not considered of major importance. In this study, the static equilibrium experiment was chosen for its ease of construction and operation, although some error was evident as a result of inadequate degassing. The final experiment resembled that described by Davison et. al. (1967).

The apparatus constructed for these experiments consisted of a stainless steel vessel connected to an 850mm mercury manometer. 9.5mm O.D. stainless steel tubing was used to connect the vessel to the manometer and the vacuum source. The apparatus is illustrated in figure 3.4.

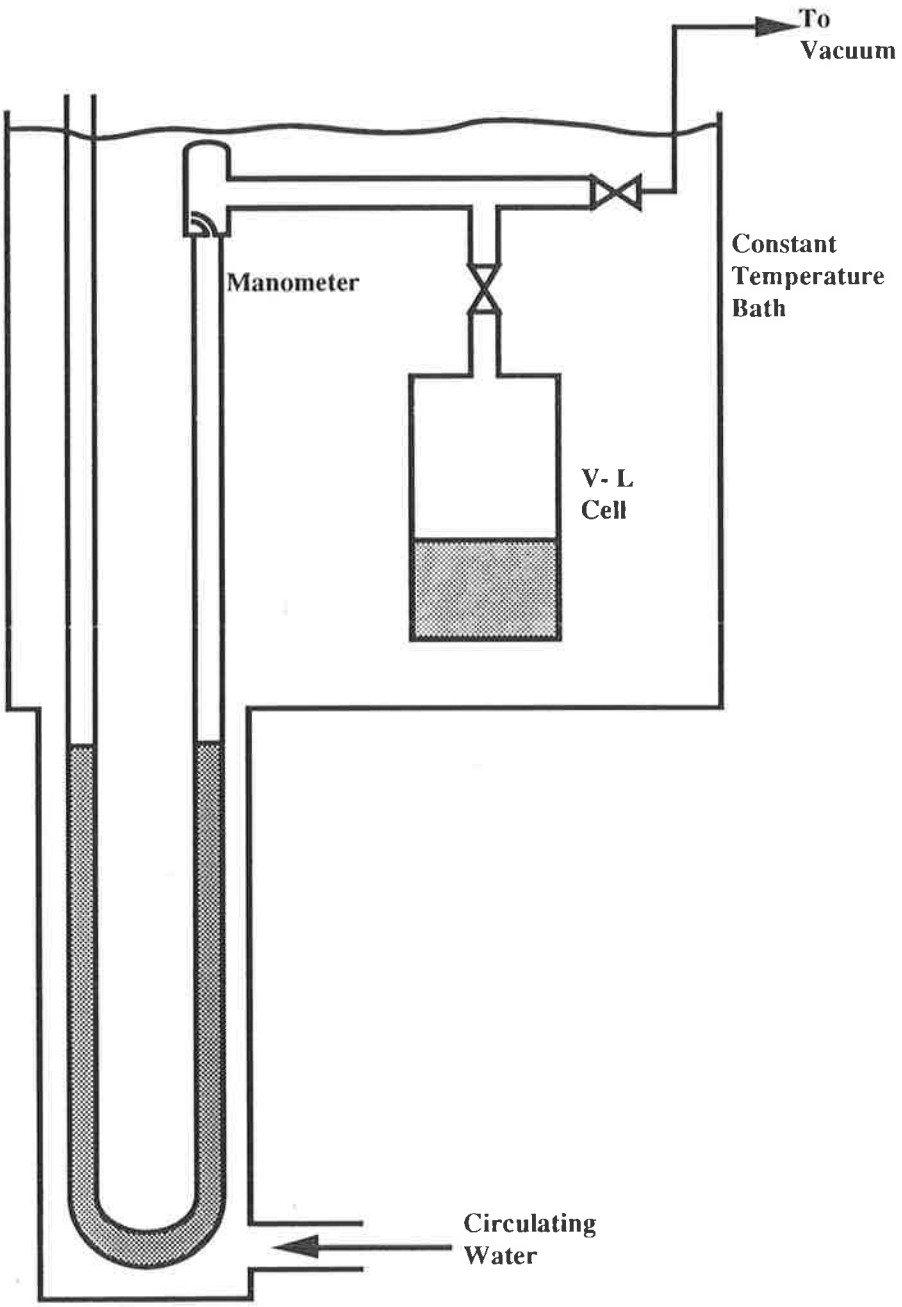

FIGURE 3.4: STATIC VAPOUR PRESSURE APPARATUS

The principal difference between this apparatus and that of Davison et. al. (1967) was the length of the mercury manometer. By increasing the length of the manometer, vapour pressures of up to two atmospheres absolute could be obtained with the opposite leg of the manometer open to the atmosphere. Atmospheric pressure was measured by an aneroid barometer with bimetallic strip temperature compensation (Ota Keiki Seisakusho Co. Ltd.), accurate to ±0.1mmHg. This contrasts with the apparatus of Davison, where a second fluid was employed to exert a known balancing vapour pressure on the opposite leg of the manometer.

Degassing of the teriary amine - water charge mixture was achieved by refluxing at atmospheric pressure for 10 minutes to remove any dissolved gases. The mixture was then frozen in liquid nitrogen and the evolved gases were evacuated from the cell. The degassed liquid, contained in the vessel, was connected to the evacuated manometer and the entire apparatus immersed in a well stirred water bath.

A bath heater/ refrigerator (Neslab RTE - 110) was employed to control water bath temperature to within ±0.2K. The charge was assumed to be in equilibrium when no further change in vapour pressure was observed (approx 2h.). A 4 wire, 3mm O.D., sheathed platinum resistance detector, connected to a Leeds and Northrop 8078 portable precision temperature bridge, was used to measure water bath temperature.

Vapour pressure readings were determined from the mercury manometer using a cathetometer accurate to better than ±0.1mm. These values were adjusted for ambient pressure and bath temperature.

Liquid from the equilibrium cell was sampled and its composition determined by the method discussed in section 3.3. Some change in the liquid phase composition could be expected over the course of a run due to changes in temperature and vapour pressure. The magnitude of this composition change would depend on the volume of the vapour space. Composition measurements were not corrected for changing temperature in the equilibrium cell as the volume of the vapour space changes with charge volume and measured vapour pressure. The error between the measured amine composition and the actual amine composition at equilibrium conditions, was estimated to be less than 3% for the bulk of the equilibrium data obtained in this study. However, the error in the composition determination is significantly greater at the lowest amine compositions (< 2 mol%).

Tests with mixtures of ammonia and water indicate that inadequate outgassing elevated the experimentally determined vapour pressure by up to 1 kPa. This constitutes the major source of error, especially at low amine concentrations.

3.3 Amine Concentration Determination

In all experiments, amine concentrations were determined by titration. The sample was added to a measured excess of standard hydrochloric acid (1.0 N). The excess acid was then titrated with standard caustic soda (0.1 N). The end point was detected with methyl red indicator. Titrations were repeated until agreement was within ±2% of the established value. When preparing mixtures to be sealed in ampoules, it was necessary to provide agitation with a magnetic stirrer pellet to ensure consistent concentration measurements.

Chapter 4
EXPERIMENTAL RESULTS

In this chapter, results are presented for vapour - liquid and liquid - liquid equilibrium experiments conducted on dimethylethylamine - water and trimethylamine - water mixtures. The significance of these results are discussed. The experimental data is fitted to a five parameter NRTL thermodynamic model for the prediction of mixture phase equilibria. Heat of mixing data is also generated, for these mixtures, by differentiation of the temperature dependent Gibbs Free Energy function.

Successful simulation of the various absorption refrigeration cycles requires a thermodynamic model capable of accurate prediction of phase equilibria for mixtures of the selected working fluids. In a conventional absorption refrigeration cycle, the thermodynamic model is employed to predict vapour - liquid equilibria only. However, the thermodynamic model for the novel absorption refrigeration cycle should also be capable of accurate prediction of both vapour - liquid and liquid - liquid phase equilibria.

The thermodynamic model is generally obtained by fitting adjustable parameters to experimental phase equilibrium data. Ideally, the experimental data should cover the entire range of temperatures encountered in the refrigeration cycle. In many instances, the necessary data can be found in the literature. However, phase equilibrium data for most of the mixtures with potential for application in the novel absorption refrigeration cycle is scarce or non-existent.

Binary mixtures of dimethylethylamine and trimethylamine with water were selected as candidate working fluids with good potential in the novel absorption refrigeration cycle. However, additional experimental data was required to provide sufficient information to accurately predict the thermodynamics of these mixtures.

In this chapter, results are presented for vapour - liquid and liquid - liquid equilibrium experiments conducted on dimethylethylamine - water and trimethylamine - water mixtures. Thermodynamic models which fit the experimental data are also presented.

4.1 Liquid-Liquid Equilibrium Experiments.

The liquid - liquid equilibrium phase diagram for mixtures of dimethylethylamine and water is summarised in figure 4.1. This figure is based on equilibrium data presented in Appendix A. The shape of the equilibrium curve is typical of other aliphatic amine - water mixtures, exhibiting lower critical solution temperature behaviour. Of particular interest is the high temperature (approximately 372K) at which phase separation commences and the high concentrations of both water in the amine phase and amine in the aqueous phase.

Phase separation was not observed for mixtures of trimethylamine and water at temperatures below 433K. This represents the limit of the available equipment. However, phase separation was induced by the addition of salt to mixtures of trimethylamine and water. This is not surprising as Davison et. al. (1966) and Ting et. al. (1992) have also reported reductions in the lower critical solution temperature for aliphatic amine - water mixtures with the addition of salt.

The liquid - liquid equilibrium phase diagram for mixtures of trimethylamine and 3% sodium chloride solution is presented in figure 4.2. It is important to note that, for any given temperature, the amine phase composition and aqueous phase composition read from figure 4.2 will not give the composition of two phases in equilibrium with each other. Each point on the coexistence curve is determined separately with a fixed salt to water ratio. However, if a stream containing trimethylamine, water and salt was separated into two liquid phases, the ratio of salt to water would be different in each phase. Clearly, the addition of an extra component creates an extra degree of freedom and a two dimensional equilibrium curve can only be obtained by adding a suitable constraint (e.g. fixing the ratio of salt to water).

It is evident from figure 4.2 that phase separation begins at even higher temperatures for mixtures of trimethylamine in 3% salt solution. Significant scatter in the experimental data is indicative of the sensitivity of phase separation behaviour to small variations in the salt concentration and to the presence of amine oxidation products (ref Section 3.1.1)

Errors between the measured salt concentration and that experienced in the ampoule at phase separation conditions result from evaporation inside the ampoule upon heating, and flashing during ampoule preparation.

Examination of the experimental data for other tertiary amine - water mixtures (Davison et. al., 1960), highlights a trend toward increasing lower critical solution temperature and reduced phase purity as the molecular weight of the tertiary amine decreases. The experimental data presented for mixtures of dimethylethylamine and trimethylamine in water follows this trend.

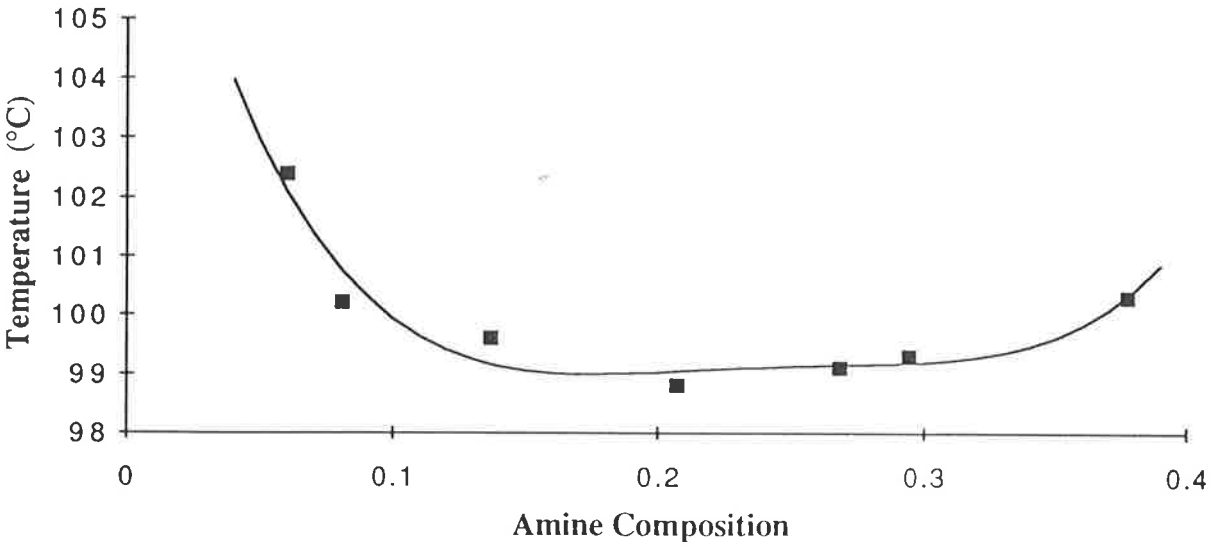

FIGURE 4.1: LIQUID - LIQUID EQUILIBRIUM DIAGRAM
FOR DIMETHYLETHYLAMINE - WATER MIXTURES

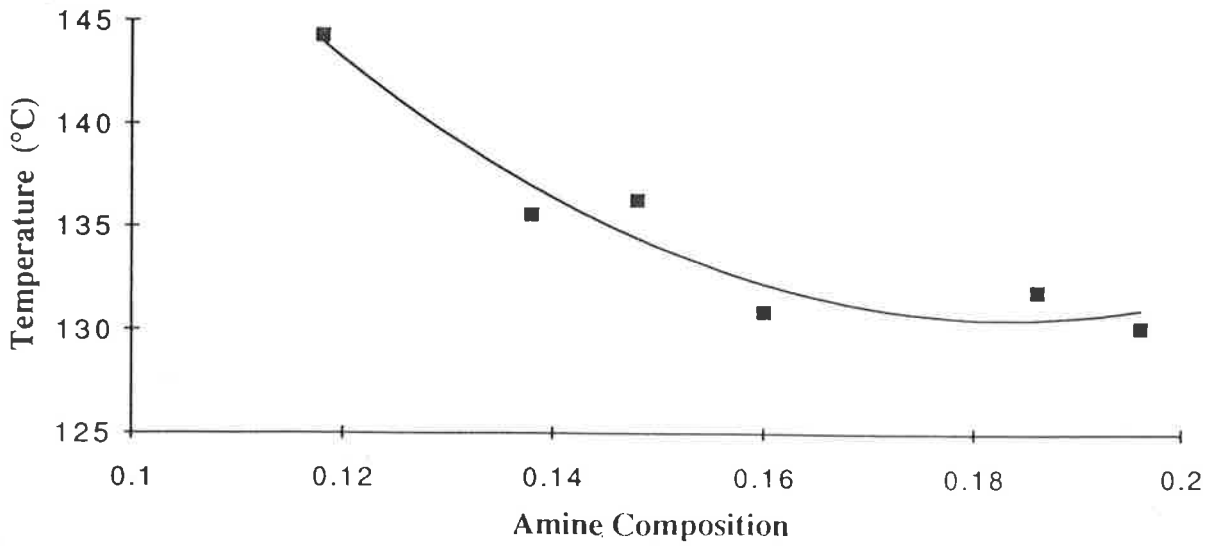

FIGURE 4.2: LIQUID - LIQUID EQUILIBRIUM DIAGRAM
FOR TRIMETHYLAMINE - 3% NaCl SOLUTION MIXTURES

4.1.1 Correlation of Liquid - Liquid Equilibrium Data.

For a consistent thermodynamic description of these mixtures, the liquid - liquid equilibrium correlation must also correlate the vapour - liquid equilibrium data. If a separate correlation is required to predict vapour - liquid equilibria, a discontinuity will appear in the thermodynamic description of the system.

Unfortunately, attempts to obtain a single model capable of accurate vapour - liquid and lquid - liquid equilibrium prediction were unsuccessful. A more detailed thermodynamic model would be required to simulate the complex temperature dependence of the liquid phase co-existence curve.

Consequently, a more black box approach was used in simulations of the novel absorption cycle heat pumps.

4.2 Vapour - Liquid Equilibrium Experiments.

The vapour pressure of dimethylethylamine - water mixtures was determined over the full range of concentrations, at temperatures of 283.1 K, 292.6 K, 302.3 K, 312.0 K and 321.7 K. The experimental data is presented in Appendix A.

The vapour pressure of trimethylamine - water mixtures was determined over the full range of concentrations for temperatures of 283.8 K and 293.0 K. At higher temperatures, the vapour pressure of some mixtures exceeded the range of the manometer. This restricted the concentration range which could be examined at 297.5 K, 302.7 K, 312.4 K and 322.0 K. The experimental vapour pressure data is summarized in Appendix A.

4.2.1 Correlation of Vapour Pressure Data.

At low pressures, the vapour phase composition can be calculated from the experimental data by equating vapour and liquid phase fugacities for each component. Under these conditions, the fugacity coefficients nearly cancel each other and the Poynting corrections are close to unity. This leads to the simplified expressions in equations 4.1 and 4.2.

$$y_{H_2O} P_{meas} = \gamma_{H_2O} x_{H_2O} P_{vap,H_2O} \quad .....(4.1)$$

$$y_{Amine} P_{meas} = \gamma_{Amine} x_{Amine} P_{vap,Amine} \quad .....(4.2)$$

Solution of these equations requires expressions for the liquid phase activity coefficients (γ_i) and the pure component vapour pressures ($P_{vap,i}$). Ideally the model should also be capable of predicting the heats of mixing and hence the composition dependence of stream enthalpy.

The vapour pressure of trimethylamine can be calculated using the Antoine equation presented in equation 4.3 (Lange, 1961). As no data exists for the vapour pressure of dimethylethylamine, the static vapour - liquid equilibrium apparatus was used to experimentally determine the vapour pressure of pure dimethylethylamine over a range of temperatures. The observed vapour pressure data (presented in Appendix A) was correlated by equation 4.4 with an accuracy of ±2.6mmHg.

$$\log_{10}(P_{vap,\ trimethylamine}) = 6.81628 - \frac{937.49}{T\ (K) - 37.79} \qquad .....(4.3)$$

$$\log_{10}(P_{vap,\ dimethylethylamine}) = 7.06702 - \frac{1171.74}{T\ (K) - 29.71} \qquad .....(4.4)$$

Activity coefficient prediction is complicated by the complex dependence on both temperature and composition. The majority of prediction models are only valid for isothermal data so that heats of mixing can not be calculated by differentiation of the Gibbs Free Energy Function. To overcome this difficulty, the five parameter NRTL (Renon & Prausnitz, 1968) model given in equation 4.5, was used for the prediction of activity coefficients. In this model the energies of interaction (g_{ij}–g_{jj}) are temperature dependent and one model can be used to predict phase separation over a range of temperatures.

$$\ln(\gamma_1) = x_2^2\left[\tau_{21}\left(\frac{G_{21}}{x_1+x_2G_{21}}\right)^2 + \frac{\tau_{12}G_{12}}{(x_2+x_1G_{12})^2}\right] \qquad ..... (4.5a)$$

$$\ln(\gamma_2) = x_1^2\left[\tau_{12}\left(\frac{G_{12}}{x_2+x_1G_{12}}\right)^2 + \frac{\tau_{21}G_{21}}{(x_1+x_2G_{21})^2}\right] \qquad ..... (4.5b)$$

where $G_{12} = \exp(-\alpha\tau_{12})$ ..... (4.5c)

$G_{21} = \exp(-\alpha\tau_{21})$ ..... (4.5d)

$\tau_{12} = \frac{g_{12} - g_{22}}{RT}$ ..... (4.5e)

$$\tau_{21} = \frac{g_{21} - g_{11}}{RT} \qquad \text{..... (4.5f)}$$

$$g_{12} - g_{22} = a_1 + b_1 T \qquad \text{..... (4.5g)}$$

$$g_{21} - g_{11} = a_2 + b_2 T \qquad \text{..... (4.5h)}$$

The adjustable parameters a_1, a_2, b_1, b_2 and α were obtained by minimising the error function given in equation 4.6. The minimisation was solved, numerically, using a two stage Powell's algorithm. For given values of b_1 and b_2, the error function was minimised by manipulation of a_1, a_2 and α. New values for b_1 and b_2 were chosen, and optimum values for a_1, a_2 and α recalculated. The process continued until no further reduction in the error could be achieved. This two stage approach was chosen for its robustness. Attempts to minimise the error function with a single stage Powell algorithm yielded varying results depending on the initial values chosen for a_1, a_2, b_1, b_2 and α. The computer code for determining the adjustable parameters is presented in Appendix B.

$$\text{Error} = \sum \left(\frac{P_{meas} - \gamma_{H_2O}\, x_{H_2O}\, P_{vap.H_2O} - \gamma_{Amine}\, x_{Amine}\, P_{vap.Amine}}{P_{meas}} \right)^2 \qquad \text{.....(4.6)}$$

Values for the five adjustable parameters are presented in table 4.1 for mixtures of dimethylethylamine and trimethylamine in water. Using these parameters, the experimental vapour pressures could be predicted with an average accuracy of ±4.9% and ±5.9% for dimethylethylamine - water and trimethylamine - water mixtures respectively. Adjustable parameters were also obtained for diethylmethylamine/ water and cyclohexane/ aniline mixtures by fitting the 5 parameter NRTL model to literature experimental data. Values for these parameters are also presented in table 1.

	a_1	a_2	b_1	b_2	α
Cyclohexane - aniline	1123.6	2453.8	0.833	–4.821	0.4108
Diethylmethylamine - water	–3485.8	–2584.1	13.05	11.20	0.5021
Dimethylethylamine - water	4620.0	–2413.5	–12.42	9.90	0.6146
Trimethylamine - water	3842.4	–4599.5	–9.88	16.58	0.6107

TABLE 4.1: LEAST SQUARES FITTED NRTL PARAMETERS FOR TERTIARY AMINE - WATER VAPOUR - LIQUID PHASE EQUILIBRIUM PREDICTION

Figures 4.3, 4.4 and 4.5 present comparisons between the calculated and experimental vapour pressures of dimethylethylamine - water mixtures at 283.1K, 302.3K and 321.7K respectively. The calculated dew point curves are also illustrated in these figures.

Examination of these figures suggests the presence of an azeotrope at a concentration of approximately 98% dimethylethylamine. There is insufficient experimental evidence to confirm or deny this observation. The bubble point curve also appears to flaten out at 321.7K and a composition of around 14% dimethylethylamine. This trend is consistent with the formation of two liquid phases in this concentration range at higher temperatures.

Figures 4.6 and 4.7 present comparisons between the calculated and experimental vapour pressures of trimethylamine - water mixtures at 283.8K, 302.7K respectively. The calculated dew point curves are also illustrated in these figures. The thermodynamic model is most accurate at low amine concentrations due to the limited vapour pressure data available at concentrations above 65 mol%.

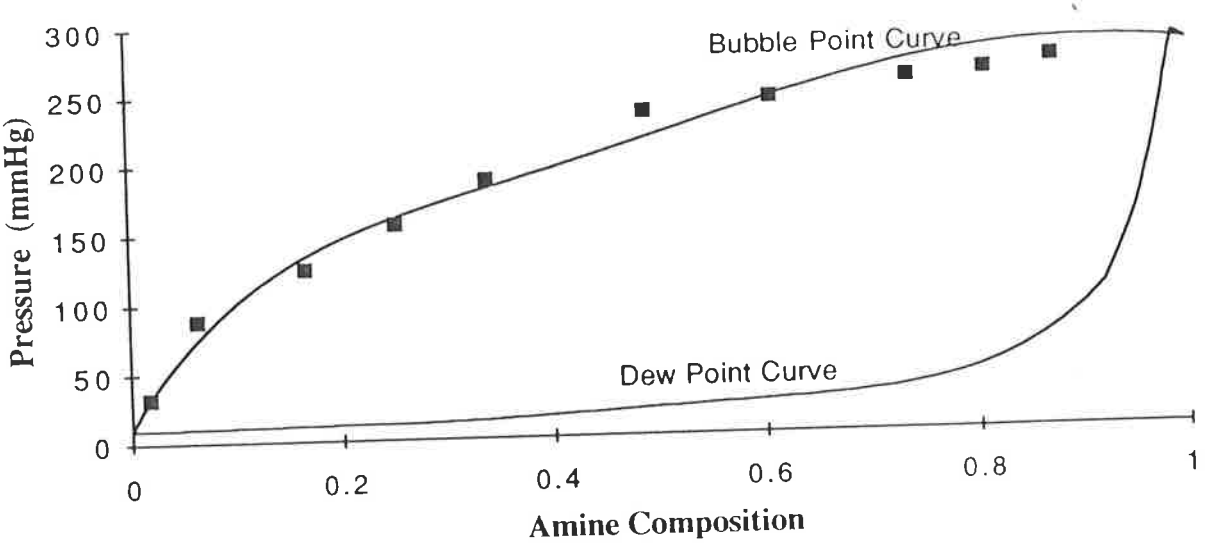

FIGURE 4.3: VAPOUR - LIQUID PHASE ENVELOPE FOR DIMETHYLETHYLAMINE - WATER MIXTURES AT 283.1K

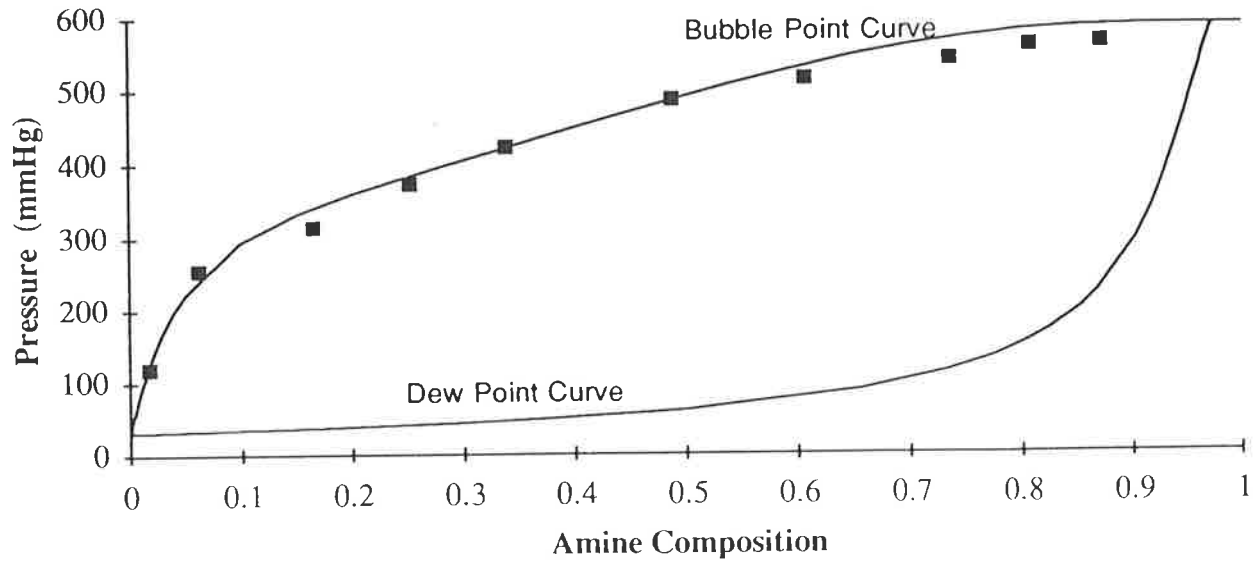

FIGURE 4.4: VAPOUR - LIQUID PHASE ENVELOPE FOR DIMETHYLETHYLAMINE - WATER MIXTURES AT 302.3K

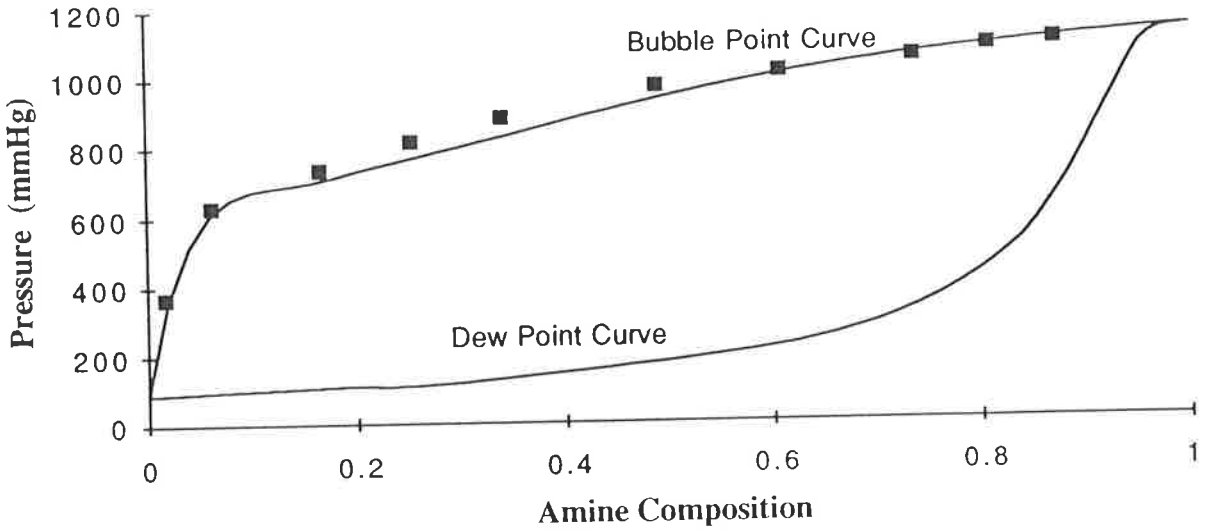

FIGURE 4.5: VAPOUR - LIQUID PHASE ENVELOPE FOR DIMETHYLETHYLAMINE - WATER MIXTURES AT 321.7K

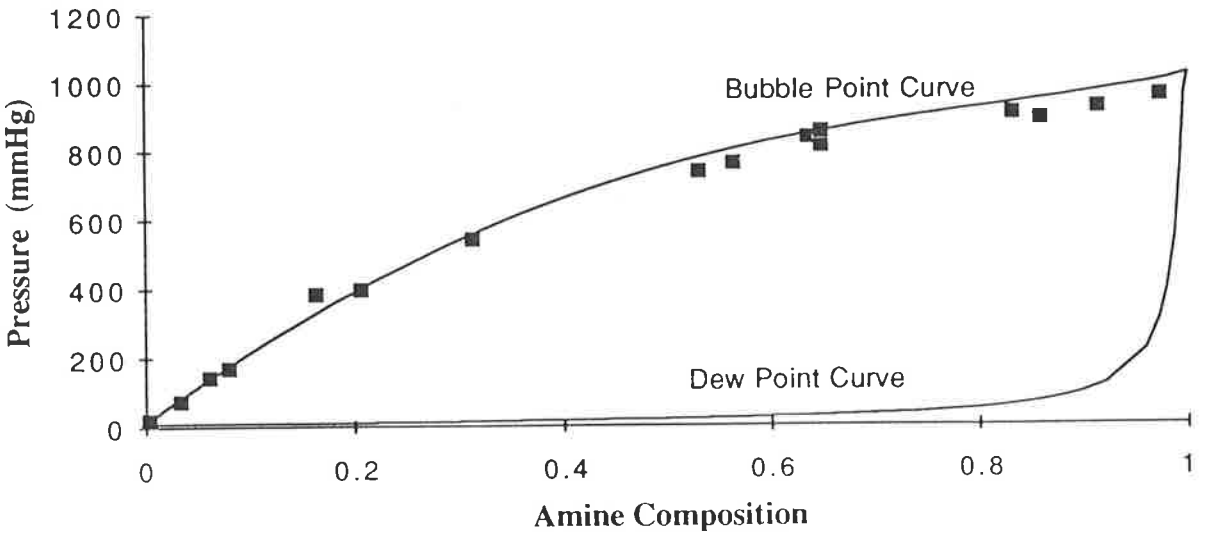

FIGURE 4.6: VAPOUR - LIQUID PHASE ENVELOPE FOR TRIMETHYLYAMINE - WATER MIXTURES AT 283.8K

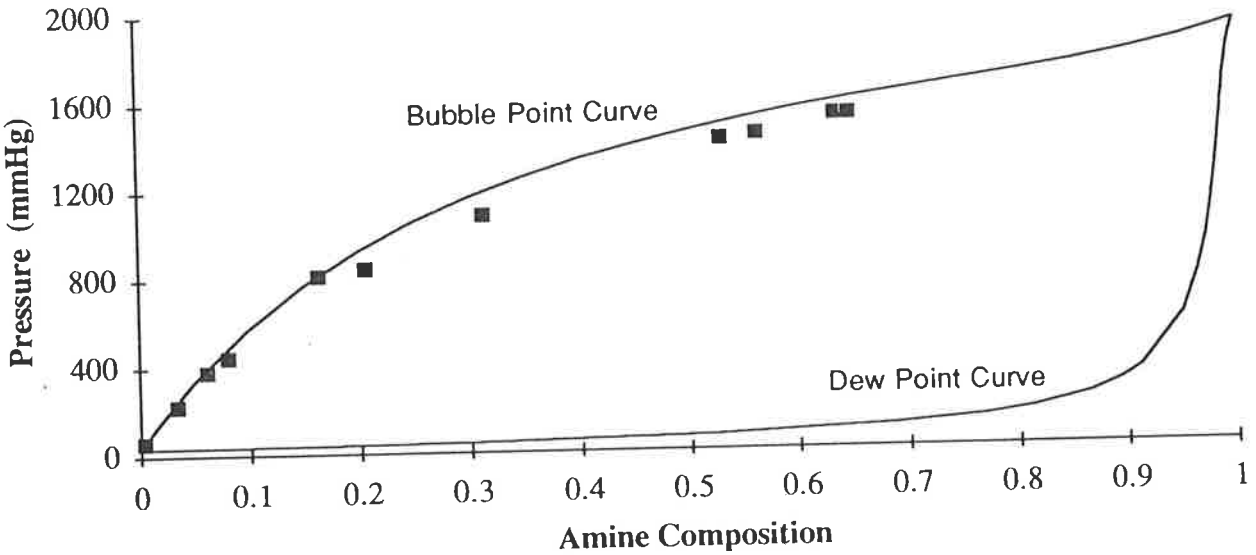

FIGURE 4.7: VAPOUR - LIQUID PHASE ENVELOPE FOR TRIMETHYLYAMINE - WATER MIXTURES AT 302.7K

4.3 Calculation of Heats of Mixing.

As experimental heat of mixing data is not available for these mixtures, the heat of mixing was calculated by differentiating the excess Gibbs Free Energy function (equation 4.7). The 5 parameter NRTL model Gibbs Free Energy function is obtained by manipulation of equations 4.5a and 4.5b to give equation 4.8.

$$H_e = -RT^2 \frac{d\left(\frac{G_e}{RT}\right)}{dT} \qquad .....(4.7)$$

$$\frac{G_e}{RT} = x_1 x_2 \left[\frac{\tau_{21} G_{21}}{x_1 + x_2 G_{21}} + \frac{\tau_{12} G_{12}}{x_2 + x_1 G_{12}} \right] \qquad ..... (4.8)$$

where τ_{21}, τ_{21}, G_{21} and G_{21} are defined by equations 4.5c to 4.5h

This approach should provide reasonably accurate heat of mixing predictions over the temperature range of the available experimental data (Skjold-Jorgensen et. al., 1980). However, extrapolation into the region of liquid phase separation is not possible because the Gibbs Free Energy function of equation 4.8 does not predict the true minimum energy in this region.

graph gives °C

Calculated heat of mixing data, at 283 K, 303 K and 323 K, are plotted in figures 4.8 and 4.9 for mixtures of dimethylethylamine and trimethylamine in water respectively. It is interesting to note that the calculated heats of mixing appear to be quite sensitive to temperature. There is no available experimental data to verify this result. However, these calculations should be reasonably accurate over this temperature range because the temperature dependence of the Gibbs Free Energy Function has been fitted to the experimental phase equilibrium data.

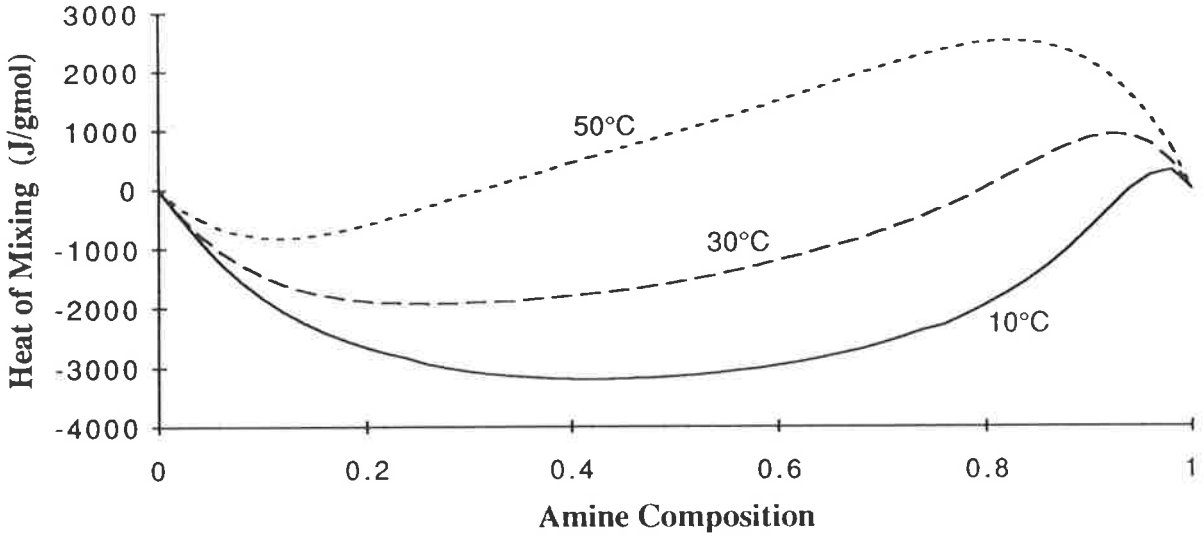

FIGURE 4.8: CALCULATED HEATS OF MIXING FOR DIMETHYLETHYLAMINE - WATER MIXTURES

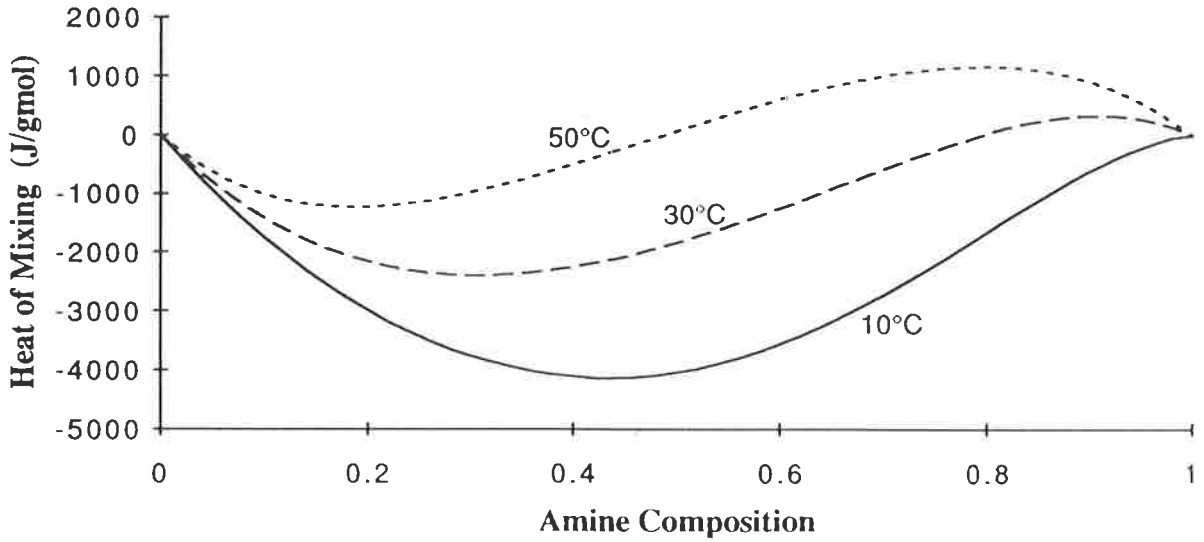

FIGURE 4.9: CALCULATED HEATS OF MIXING FOR TRIMETHYLAMINE - WATER MIXTURES

4.4 Calculation of Other Thermodynamic Parameters.

The bulk of the necessary pure component physical properties of diethylmethylamine and dimethylethylamine have not been measured. Hence, established group contribution estimation techniques were employed to calculate these properties. The techniques used follow the recommendations of Reid, Prausnitz and Poling (1987) and are summarised in table 4.2. For a wide variety of compounds, the typical error between predicted and actual values using these methods is less than 2%. Data for other compounds was available in the PROCESS™ library.

PROPERTY	ESTIMAT'N TECHNIQUE	UNITS	FORMULAE DEVELOPED FOR DIMETHYLETHYLAMINE	FORMULAE DEVELOPED FOR DIETHYLMETHYLAMINE
Ideal gas heat capacity	Joback (1984)	$Jmol^{-1}K^{-1}$	$23.23 - 1.144\times10^{-2}\,T + 2.54\times10^{-4}\,T^2 - 1.021\times10^{-7}\,T^3 + 1.85\times10^{-11}\,T^4$	$16.45 - 1.23\times10^{-2}\,T + 3.01\times10^{-4}\,T^2 - 1.203\times10^{-7}\,T^3 + 2.143\times10^{-11}\,T^4$
Liquid heat capacity	Chueh - Swanson (1973)	$Jmol^{-1}K^{-1}$	171.8	202.2
Heat of vaporisation	Riedel (1954)	$kJ\ kg^{-1}$	$317.6\left(\frac{511 - T}{511 - 309}\right)^{0.38}$	$336.2\left(\frac{508 - T}{508 - 339}\right)^{0.38}$

TABLE 4.2: THERMODYNAMIC PROPERTY ESTIMATION TECHNIQUES EMPLOYED IN THE ANALYSIS OF THE NOVEL ABSORPTION REFRIGERATION CYCLE

Chapter 5
THE NOVEL ABSORPTION REFRIGERATION CYCLE

In this chapter, a novel absorption refrigeration cycle is proposed. A computer model of the cycle is developed, based on the thermodynamic model described in chapter 4, and the results of cycle performance simulations are presented. Based on these results, the potential of the cycle is discussed.

A large body of literature, addressing various aspects of absorption cycle heat pumps has developed since the pioneering work of Carre and Altenkirch (Stephan, 1983). A large fraction of this research effort has focussed on the discovery of new refrigerant/ absorbent pairs. However, the only working pairs to have found widespread commercial application are the ammonia/ water and water/ lithium bromide pairs.

More desireable working fluid pairs may exist with improved properties such as toxicity, transport properties or corrosivity. However, further investigation of new working pairs does not appear to provide significant potential for further improvements in cycle thermodynamic efficiency. O'Neill & Roach (1990) confirmed this observation by demonstrating that the selection of an absorbent/ refrigerant pair does not significantly alter the maximum theoretical performance achievable in an absorption refrigeration cycle employing an ideal distillation column generator.

Consequently, further examination and synthesis of alternative absorption refrigeration cycles appears to offer the greatest potential for improving the performance and cost of absorption cycle heat pumps. An investigation into the losses encountered in conventional absorption refrigeration cycles provides an ideal starting point in the search for new cycles.

Recent papers by Briggs (1971) and Karakas et. al. (1990) have detailed an exergy balance on the conventional absorption refrigeration cycle. These studies demonstrate that the majority of losses are confined to the absorber and the generator. Dalichaouch (1990) calculated second law efficiencies for an aqueous lithium bromide absorption refrigeration cycle. He showed that, over a wide range of conditions, the performance of this cycle was less than thirty percent of the performance predicted by the ideal second law.

Clearly, there is significant room for improvement in cycle performance. Two avenues exist for improving the design of absorption refrigeration cycles . Firstly, improvements could be achieved through modification of the conventional absorption cycle. Alternatively, performance could be improved by creating a new type of absorption cycle. One example of the latter approach replaces the conventional distillation column with a new separation process capable of operating closer to the thermodynamic ideal.

References to the application of alternative separation techniques in absorption refrigeration are sparse, suggesting that this is a potentially fruitful area for further investigation. With this in mind, a novel absorption refigeration cycle was devised. The cycle was selected for further investigation in this study.

The novel cycle, first proposed by Mehta (1981), employs a liquid - liquid separation step to separate the absorbent from the refrigerant. The cycle has attracted scant attention in the literature and analysis of the cycle appears to be restricted to the original patent. The cycle was chosen for further examination with the intention of demonstrating the feasibility of eliminating the distillation column generator in an absorption cycle heat pump.

The novel absorption cycle heat pump was simulated on a computer using the PROCESS™ chemical plant simulation software package. Results of the computer simulations are presented, and the potential of the cycle is discussed.

5.1 Refrigeration Cycle Description

Mehta (1981) describes a refrigeration cycle utilising the partial miscibility of some binary mixtures, at elevated temperatures, to separate the refrigerant from the absorbent in an absorption refrigeration cycle.

The cycle is illustrated in the flow schematic presented in figure 5.1. The physical significance of each stream in the cycle is illustrated in the phase diagrams presented in figure 5.2. Refrigerant vapour from the evaporator is dissolved in lean absorbent at low pressure. The rich absorbent is pumped to high pressure and heated until the refrigerant becomes immiscible in the absorbent. The refrigerant and absorbent are then separated in a settling drum. Recovered refrigerant from the settling drum is cooled and passed to the evaporator. The lean absorbent is returned to the absorber. The novelty of this cycle lies in the method for separation of the refrigerant from the absorbent. This is carried out in the liquid phase.

There are significant differences between the cycle illustrated in figure 5.1 and the original cycle proposed by Mehta (1981). These differences are listed below;

(i) The liquid blowdown (containing the bulk of the less volatile component) is continuously removed from the evaporator, pumped to high pressure and returned to the settling drum. In contrast, the evaporator blowdown was passed to the absorber in the cycle proposed by Mehta. Analysis shows that this modification provides a significant improvement in thermodynamic efficiency. Unfortunately, the liquid - phase separation is imperfect. Hence, the absorbent stream retains a fraction of the more volatile component and some of the less volatile component remains in the refrigerant. Consequently, the evaporator blowdown stream is large. By returning the evaporator blowdown directly to the generator, the load on the absorber is reduced and thermodynamic performance is increased.

(ii) A heat exchange network for recovering heat from the hot refrigerant and absorbent streams is defined. These heat exchangers preheat the feed to the settling drum.

The principal differences between the novel absorption refrigeration cycle and the conventional absorption refrigeration cycle (illustrated in figure 2.1) are as follows:

(i) The liquid - liquid separation drum replaces the distillation column in the conventional cycle.
(ii) Liquid blowdown from the evaporator is recycled to the separation drum generator.
(iii) The novel absorption refrigeration cycle does not require a condenser

Preliminary examination of the cycle highlights the potential for reductions in capital cost, over the conventional cycle, through the elimination of the condenser. There is also potential for increasing thermodynamic performance as heat is not required to vaporise the refrigerant. Ideally, the bulk of the heat required to raise the temperature of the rich absorbent and the evaporator blowdown can be recovered by cooling the fresh absorbent and fresh refrigerant.

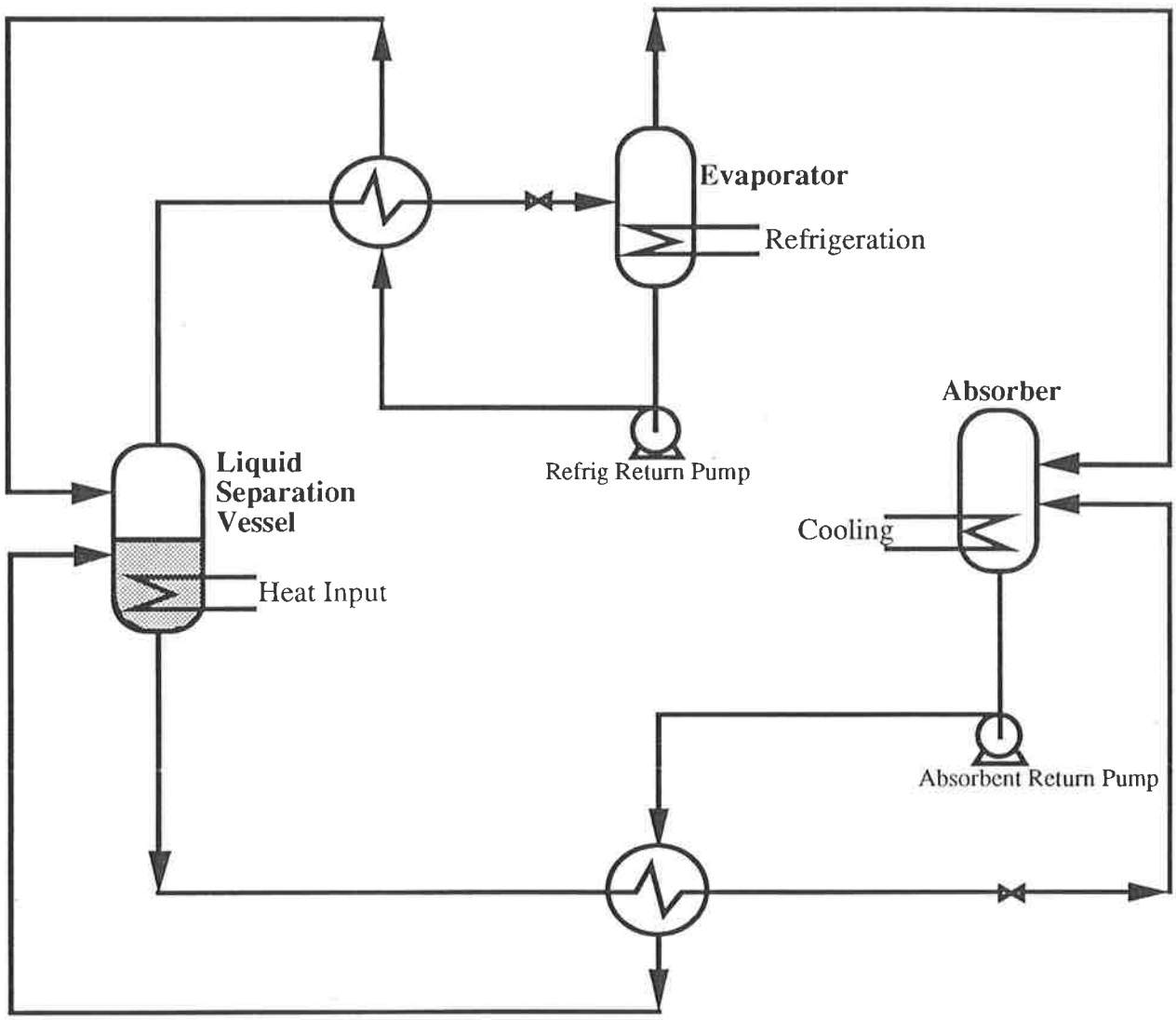

FIGURE 5.1: FLOW SCHEMATIC OF THE NOVEL ABSORPTION REFRIGERATION CYCLE

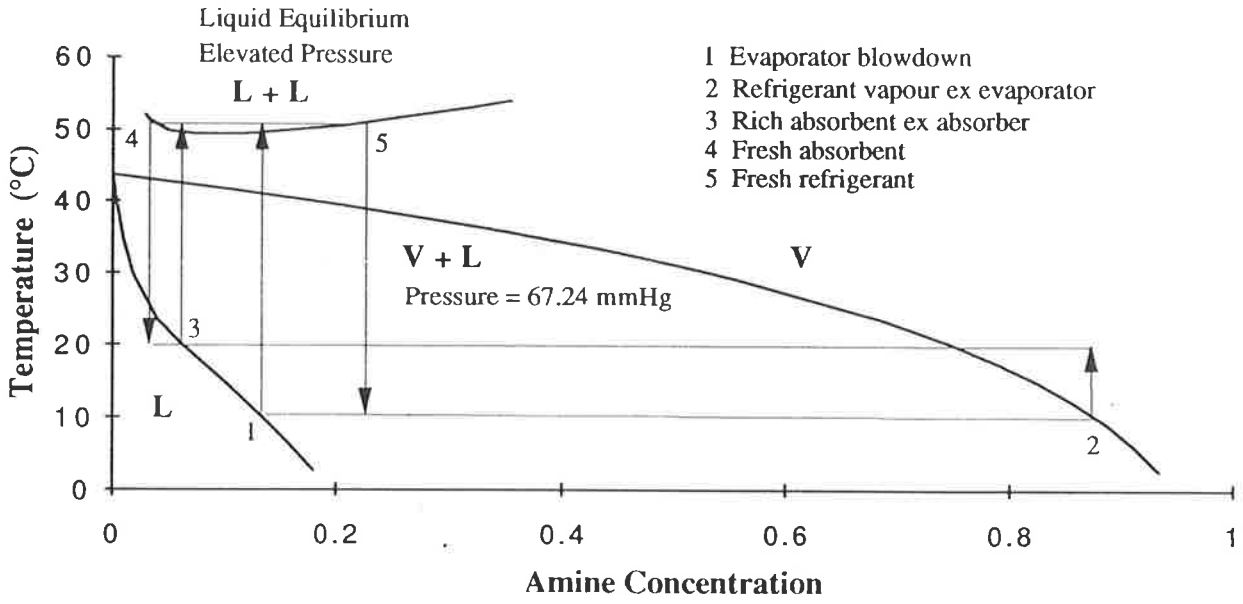

FIGURE 5.2: PHASE DIAGRAM OF WORKING FLUID MIXTURES WITH NOVEL ABSORPTION REFRIGERATION CYCLE PROCESS CONDITIONS SUPERIMPOSED

5.2 Selection of Working Fluids for the Novel Cycle

A suitable refrigerant/ absorbent pair for this cycle must exhibit "lower critical solution temperature behaviour" when mixed. The selected pair should also possess properties which are desirable in conventional absorption refrigeration working fluids. These properties are discussed in chapter 2.

Relatively few mixtures exhibit lower critical solution temperature behaviour. The bulk of such mixtures are composed of amines with either water or ethanol. In these systems, miscibility at low temperatures is a consequence of hydrogen bonding between the amine group and the polar solvent. At higher temperatures the hydrogen bonds breakdown, reducing the affinity between the amine and the solvent.

Figure 5.3 summarizes the liquid-liquid equilibrium co-existence curves for mixtures of dimethylethylamine, diethylmethylamine and triethylamine with water. It demonstrates that the lower boiling point amines have a higher "lower critical solution temperature" and reduced purity in the equilibrium phases. Examination of other amine - water phase diagrams (Davison et. al., 1960) indicate that such behaviour is typical of amine - water mixtures.

Consequently, if a low boiling point amine is used as a refrigerant in this cycle (with water as the absorbent), the thermodynamic performance of the cycle will be lowered by imperfect separation in the settling drum. Subsequent distillation of these phases may be required to improve performance.

Conversely, if a high boiling point amine is selected in the cycle as the absorbent (with water as the refrigerant), then the refrigerant and absorbent will be immiscible at all reasonable refrigeration temperatures. For this reason, it would not be practical to design the cycle under these conditions.

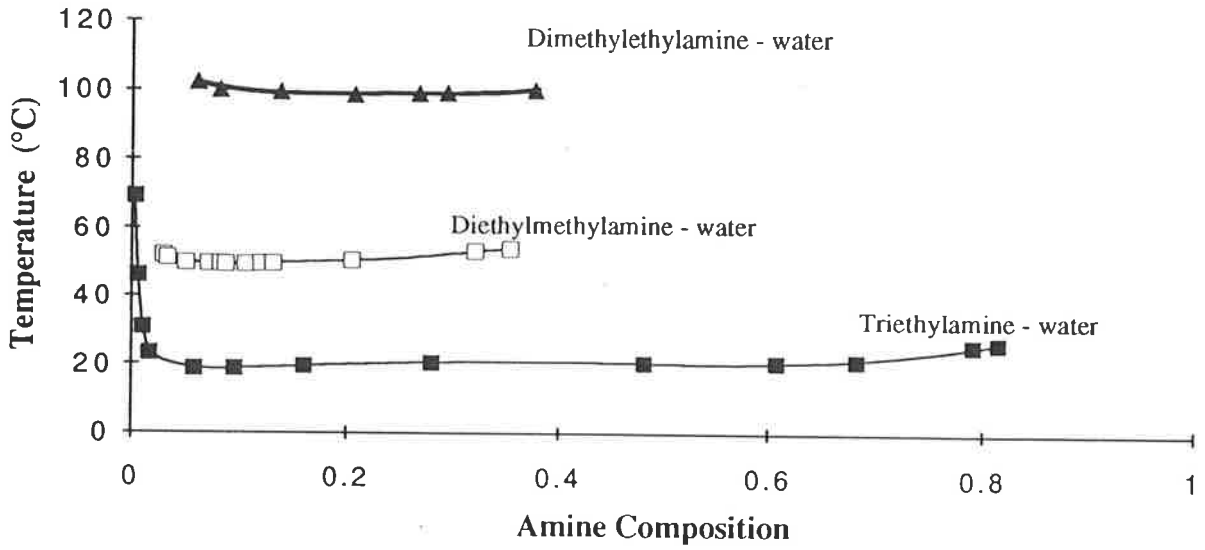

FIGURE 5.3: LIQUID - LIQUID PHASE EQUILIBRIA FOR VARIOUS TERTIARY AMINE/ WATER MIXTURES

5.3 Computer Simulation of the Novel Cycle

Computer models were constructed for the novel absorption cycle heat pumps to determine the process conditions through out the cycle and the cycle thermodynamic performance. The results of these simulations provide evidence of the feasibility of the proposed cycle.

5.3.1 Thermodynamics

Detailed thermodynamic models for the prediction of phase equilibria and state properties such as enthalpy and entropy are required to obtain accurate simulation results. Equilibrium predictions and excess properties were calculated using a five parameter NRTL model (Asselineau and Renon, 1970) fitted to the experimental data. Pure component heat capacities and latent heats were calculated using established group contribution methods (Chueh and Swanson, 1973, Joback, 1984 and Riedel, 1954). The five parameter NRTL model and the appropriate group contribution methods are described in more detail in chapter 4.

In subsequent computer simulations of the novel absorption cycle heat pumps, the thermodynamic models were extrapolated to temperatures above the range of the experimentally determined data. Unfortunately, higher temperature experimental data could not be obtained because of the limited measurement range of the mercury manometer.

Attempts to obtain a single model capable of accurate vapour - liquid and lquid - liquid equilibrium prediction were unsuccessful. In computer simulations of cycle performance, either a second thermodynamic model or a black box component splitter was used to simulate the liquid - liquid separation step. Both techniques imply a discontinuity in the thermodynamics of the cycle.

5.3.2 The PROCESS™ Simulation Package

The PROCESS™ chemical plant simulation software package was used in all computer simulations of the absorption cycle heat pumps. This package is used extensively in the design and operation of commercial hydrocarbon processing and petrochemical plants. It can solve complex material and energy balances and, with an appropriate thermodynamic model, it can predict phase equilibria. This makes the program particularly useful for the design of complex physical separation processes which include recycle streams and distillation columns. PROCESS assumes perfect mixing in all phase separation calculations.

Sample PROCESS input and output files, used in simulations of the novel absorption cycles, are presented in Appendix D. The solution procedure employed by the PROCESS simulation program in these cases is also presented.

Unless otherwise specified in the input file, PROCESS calculates new values for the process conditions of the recycle stream by direct substitution. It is interesting to note that the results obtained from these simulations were often sensitive to the allowable error (tolerance) between the old and new recycle stream temperature. Care was taken to ensure that the specified tolerances were sufficiently tight to prevent this from significantly influencing the results.

5.3.3 Simulation Constraints

There are a number of variables which influence the cost and performance of absorption cycle heat pumps. The performance of an ideal, reversible absorption cycle is defined solely by the temperatures at which heat is added and rejected from the cycle. However, the performance of any real cycle is also dependent on a number of variables specific to the cycle. These variables are discussed below. From this list, a consistent set of design constraints was selected to enable comparison of the various cycles.

(i) Generator, condenser and absorber temperatures.

These temperatures are largely set by the temperatures of the available heat source and heat sink. However, some allowance must also be made for a reasonable temperature difference between the fluid on the utility side and the fluid on the heat pump side of each heat exchanger. When simulating the performance of the novel absorption refrigeration cycles, the generator and absorber temperatures were fixed with the assumption that the hot and cold utilities were available at appropriate temperatures. This was required because the boiling point elevation between the evaporator and the absorber was not sufficient to achieve realistic absorber temperatures.

(ii) Evaporator temperature.

While other parameters are generally set within a reasonably narrow band for all absorption refrigeration applications, the evaporator temperature can vary dramatically depending on the required refrigeration task. For this reason, the influence of evaporator temperature on the objective parameter was investigated in some detail.

(iii) Approach temperature in the heat recovery heat exchangers.

Reducing the approach temperature in the heat recovery heat exchangers increases cycle COP but also increases capital costs. In conventional cycles, one would expect approach temperatures of around 10 to 20 K. However, significantly lower approach temperatures were required for the novel absorption cycles because of the low boiling point elevation achievable with the selected mixtures. An approach temperature of 2 K was selected for the basic novel absorption heat pump cycles and 5 K for the novel cycles with distillation.

(iv) Rich absorbent quality.

Rich absorbent exiting the absorber must be a liquid to ensure that it can be pumped up to the pressure of the generator. However, sub-cooling of the rich absorbent results in an undesirable increase in absorbent circulation rate. The lean absorbent flowrate was set to ensure that liquid at its bubble point exits the absorber in all simulations. This would be difficult to achieve in practice but sets an upper limit on cycle performance.

(iv) Evaporator blowdown.

The fraction of fresh refrigerant boiled in the evaporator has a dramatic influence on the performance of the novel absorption cycle heat pumps. If the fraction of refrigerant boiled in the evaporator is increased, the evaporator (and hence absorber) pressure goes down and the flowrate of required absorbent increases. This is balanced to some extent by the increase in refrigeration achieved. An optimum exists for a given absorber temperature, evaporator temperature and working fluid purity.

An example of this is presented in figure 5.4 for the basic novel absorption refrigeration cycle with methyldiethylamine and water as the working fluids. For a 10°C evaporator temperature and 20°C absorber temperature, the optimum COP was obtained when around 70% of the incoming refrigerant was returned to the generator.

While the influence of evaporator blowdown is more dramatic for the novel absorption cycles, an optimum blowdown rate also exists for the conventional cycle. The evaporator blowdown was optimised to achieve the maximum coefficient of performance in simulations of each absorption refrigeration cycle investigated.

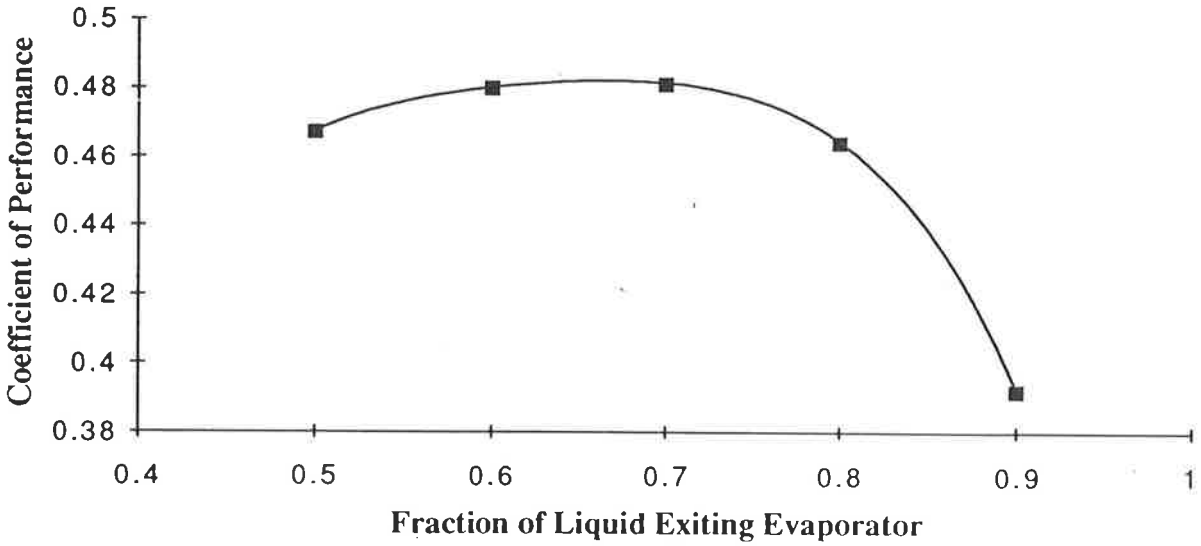

FIGURE 5.4: OPTIMUM BLOWDOWN EXAMPLE FOR THE NOVEL ABSORPTION REFRIGERATION CYCLE

5.4 Novel Absorption Refrigeration Cycle Simulation Results

The performance of the novel absorption refrigeration cycle was investigated using the general constraints detailed above. Initial simulations employed diethylmethylamine and water as working fluids in the cycle. This provided an ideal starting point as experimental phase equilibrium data was available in the literature and comparisons could be made with the analysis presented by Mehta (1981).

A generator temperature of 80°C was used for all simulations with diethylmethylamine and water. At this temperature the slope of the co-existence curve is very steep and only small improvements in phase purity are possible.

A process flow diagram of the novel absorption refrigeration cycle, with the evaporator temperature and absorber temperature fixed at 10°C and 20°C respectively, is presented in Figure 5.5. The diagram includes details of the process conditions for each stream in the cycle. Examination of the stream data highlights the following points.

(i) The refrigerant exiting the generator is not very pure in the more volatile amine. This necessitates a large recycle stream for the spent refrigerant exiting the evaporator.

(ii) The evaporator must operate under vacuum to achieve even modest refrigerant temperatures in the evaporator.

(iii) The ratio of absorbent to refrigerant flowrates is very high compared to conventional cycles, despite the small temperature difference between the evaporator and the absorber. Poor cycle performance would be expected as a consequence of the high absorbent circulation rate.

Figure 5.6 illustrates the effect of evaporator temperature on the optimum coefficient of performance with the absorber temperature fixed at 20°C. Thermodynamic performance is reduced as the evaporator temperature is decreased and the cycle ceases operation at evaporator temperatures below about 2°C.

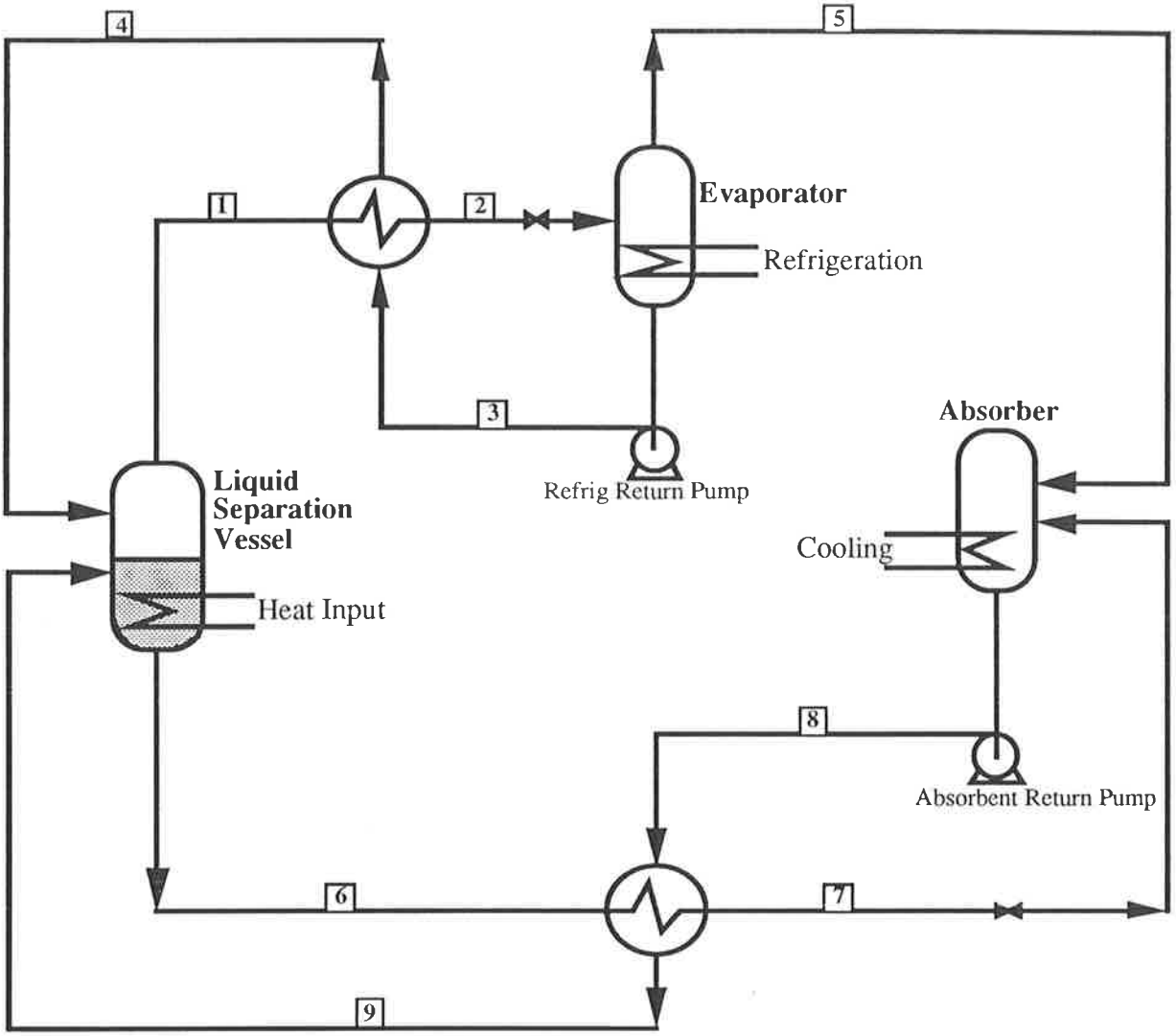

Generator Duty = 1.28MW Evaporator Duty = 0.62MW Absorber Duty = 1.92MW
Absorbent Heat Recovery Duty = 7.72MW Refrigerant Heat Recovery Duty = 1.04MW
Absorbent Return Pump = 0.02MW Refrigerant Return Pump = 0.002MW

STREAM NO	1	2	3	4	5	6	7	8	9
Flowrate (kmol h^{-1})	326	326	215	215	111	6014	6014	6125	6125
Composition (mole%)	65.0	65.0	52.8	52.8	88.7	1.1	1.1	2.7	2.7
Temperature (°C)	80.0	32.3	10.1	78.0	10.0	80.0	22.1	20.1	71.9
Pressure (kPa)	333	333	333	333	8.96	333	333	333	333
Liquid Fraction	1.0	1.0	1.0	1.0	0.0	1.0	1.0	1.0	1.0

FIGURE 5.5: PROCESS FLOW DIAGRAM OF THE NOVEL ABSORPTION REFRIGERATION CYCLE

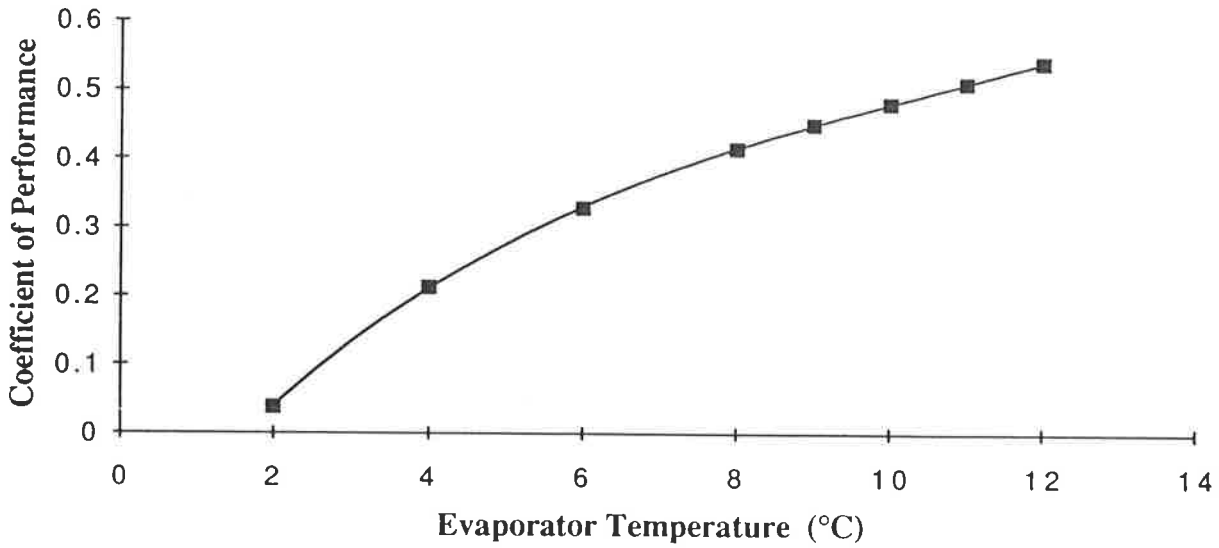

FIGURE 5.6: THE INFLUENCE OF EVAPORATOR TEMPERATURE ON THE PERFORMANCE OF THE NOVEL ABSORPTION REFRIGERATION CYCLE (DIETHYLMETHYLAMINE AND WATER WORKING FLUIDS)

This behaviour can be explained by inspection of the phase diagram presented in figure 5.2. As the evaporator temperature decreases, the evaporator (and hence absorber) pressure decreases. The absorbent circulation rate must then be increased to lower the concentration of amine in the rich absorbent, and maintain the desired temperature in the absorber. Increased losses and reduced performance result from the increased circulation rate.

Further reduction in the rich absorbent amine concentration is not possible when the equilibrium composition exiting the absorber equals that of the lean absorbent entering the absorber. The minimum possible evaporator temperature is achieved under these conditions.

In another set of simulations with the diethylmethylamine - water pair, the coefficient of performance of the cycle was determined over a range of absorber temperatures with the evaporator temperature fixed at 10°C. The coefficient of performance decreased with increasing absorber temperature (figure 5.7).

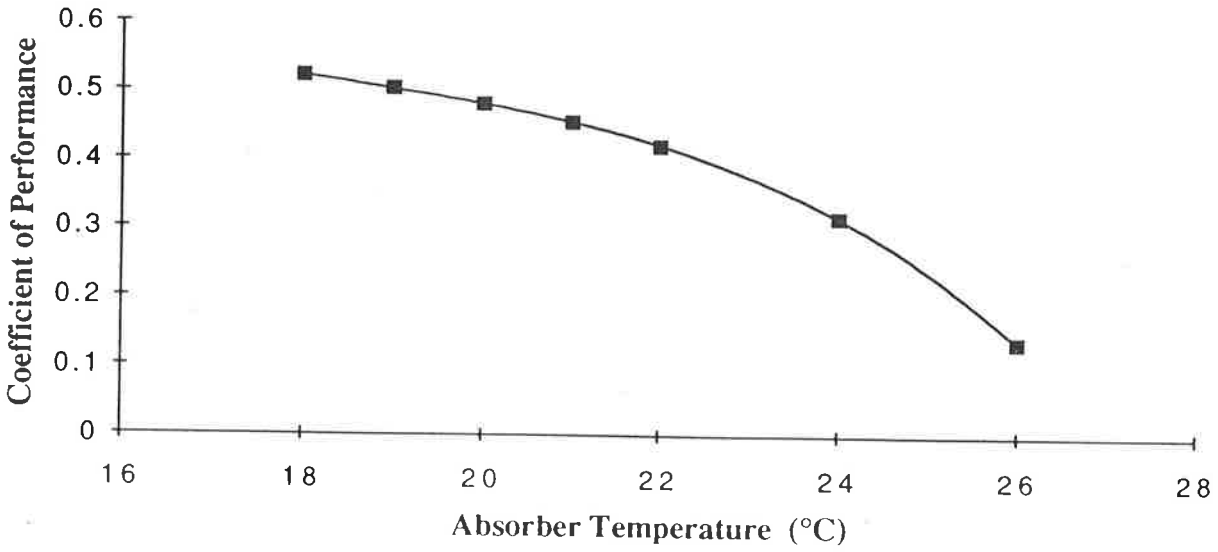

FIGURE 5.7: THE INFLUENCE OF ABSORBER TEMPERATURE ON THE PERFORMANCE OF THE NOVEL ABSORPTION REFRIGERATION CYCLE (DIETHYLMETHYLAMINE AND WATER WORKING FLUIDS)

The boiling point elevation achieved in the novel absorption refrigeration cycle with diethylmethylamine and water is clearly inadequate for practical refrigeration. New working fluids were sought in an attempt to improve the performance of the cycle and raise the allowable absorber temperature. Working fluids with increased normal boiling point difference were particularly sought after with the expectation that increased boiling point elevations could be achieved between the evaporator and the absorber.

Dimethylethylamine - water and trimethylamine - water mixtures were selected as candidate working fluids with potential in the novel cycle. While dimethylethylamine and trimethylamine have low boiling points, liquid phase immiscibility had not previously been observed for these mixtures. The necessary experimental data was gathered to allow simulation of the novel absorption cycle with dimethylethylamine - water mixtures. The experimental difficulties of obtaining high pressure vapour - liquid equilibrium data for a three component mixture dictated that a more limited experimental investigation and cycle analysis be conducted with mixtures of trimethylamine, water and salt. This analysis is described in chapter 6.

A fixed generator temperature of 100°C was used in simulations of the novel absorption refrigeration cycle with dimethylethylamine and water. Figure 5.8 illustrates the influence of evaporator temperature on performance for this cycle. The boiling point elevation achieved was very similar to that obtained in the diethylmethylamine - water cycle. However, the coefficient of performance was considerably lower. This reduction in performance is attributed to the high specific heat of the refrigerant, caused by water (absorbent) contamination. Synthesis of an improved heat recovery design could reduce the apparent difference in cycle performance when using alternative working fluids.

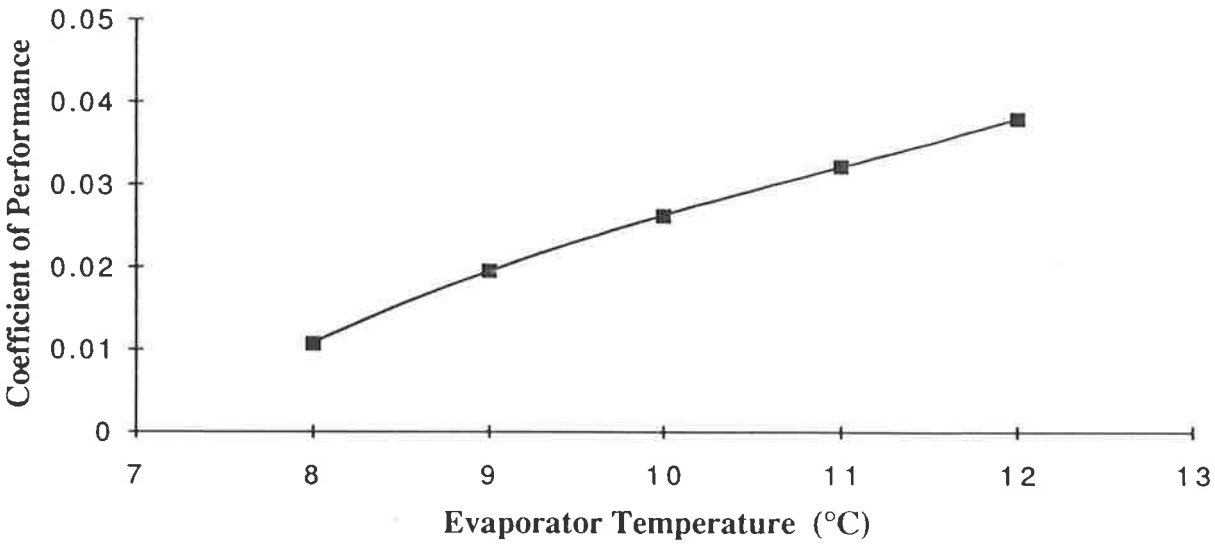

FIGURE 5.8: THE INFLUENCE OF EVAPORATOR TEMPERATURE ON THE PERFORMANCE OF THE NOVEL ABSORPTION REFRIGERATION CYCLE (DIMETHYLETHYLAMINE AND WATER WORKING FLUIDS)

5.5 Discussion

It is clear from these simulations, that the novel absorption refrigeration cycle is inferior to the conventional cycle. Cycle operation is only possible over a limited range of temperatures, and the coefficient of performance is poor compared with conventional absorption refrigeration units using ammonia and water as the refrigerant/ absorbent pair.

However, these calculations are significant as a tool to verify the feasibility of the proposed cycle. If the cycle is feasible, then vaporisation of the refrigerant is not a requirement for refrigerant recovery and other candidate unit operations should be investigated in more detail.

5.5.1 Thermodynamic Analysis

To confirm the results of these simulations and explain why the cycle is a valid method for obtaining refrigeration, we must investigate the phase behaviour of these mixtures in more detail.

A typical lower critical solution temperature phase equilibrium curve is presented in Figure 5.9. Superimposed upon the liquid phase co-existence curve are two constant pressure bubble point curves. At low pressures, the bubble point temperature increases as the concentration of the more volatile component is increased. At higher pressures the bubble point curve intersects the region of liquid phase immiscibility. Over this concentration range, the bubble point temperature remains constant. Either side of the immiscible region, the bubble point temperature increases as the concentration of the more volatile component is increased.

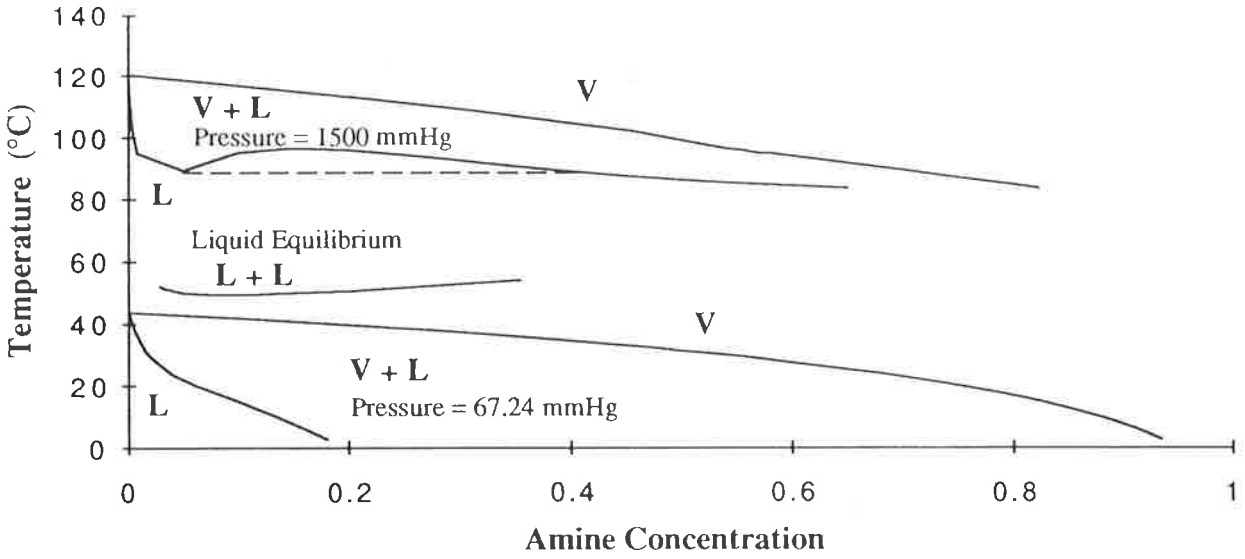

FIGURE 5.9: PHASE EQUILIBRIUM DIAGRAMS FOR TYPICAL MIXTURES EXHIBITING LOWER CRITICAL SOLUTION TEMPERATURE BEHAVIOUR

The behaviour of the bubble point curves, described above, can be deduced by inspection of equation 5.1 (Bett et. al., 1975).

$$\left[\frac{dT}{dx_2}\right]_P = \frac{-T\, g_{2x}\, \Delta x_2}{y_1\, \Delta h_1 + y_2\, \Delta h_2} \qquad \text{.....(5.1)}$$

where Δx_2 is $(y_2 - x_2)$, Δh_i is the difference between the partial enthalpies of component i in the vapour and liquid phases $(h_i^g - h_i^l)$, g_{2x} is the second derivative of the partial Gibbs Free Energy function at constant pressure and temperature, and $(dT / dx_2)_p$ is the derivative along the saturation curve.

The second derivative of the partial Gibbs Free Energy function, and hence the derivative of the bubble point temperature, are zero at the lower critical solution temperature. Elsewhere the second derivative of the partial Gibbs Free Energy function must be positive to ensure phase stability (equation 5.2).

$$\text{i.e.} \qquad \left[\frac{\partial^2 g}{\partial x^2}\right]_P > 0 \qquad \text{.....(5.2)}$$

The tertiary amine - water mixtures, employed in simulations of the novel absorption refrigeration cycle, do not exhibit azeotropic behaviour near the immiscible region. This can be deduced from the calculated vapour phase compositions which are rich in the more volatile amine. Given these constraints, Δx_2 must be negative and $(dT / dx_2)_P$ must be positive in the region below the liquid - liquid phase equilibrium curve.

Now, if we take a mixture in the immiscible region where $(dT / dx_2)_P$ is zero, it will separate into two liquid phases of equal boiling point. If we drop the pressure of the two streams to a region of total miscibility (where $(dT / dx_2)_P$ is positive) then a difference must occur between the boiling points of the two streams. This difference in boiling points can be used to create the the necessary boiling point elevation between the evaporator and the absorber, and confirms the feasibility of the proposed novel absorption refrigeration cycle.

5.5.2 Comparison with Literature Results

The novel refrigeration cycle has attracted little attention in the literature. The limited analysis of cycle performance by Mehta (1981), in the original patent, appears to be the sole reference for comparison of the results obtained in this study.

Differences between the assumptions used in the performance calculations presented by Mehta (1981) and those employed in this study are given below.

(i) Assumed stream compositions

The compositions of the refrigerant and absorbent steams, employed by Mehta, were 88.0wt% and 3.0wt% amine respectively. In this study, the assumed compositions of the refrigerant and absorbent streams were 90wt% and 5.1wt% respectively. These values were obtained from experimental data presented in graphical form by Hood and Davison (1960).

(ii) Evaporator blowdown return

In this study, performance was improved by recycling the evaporator blowdown directly to the generator. This is explained in more detail in section 5.1.

(iii) Heat recovery heat exchanger network

Performance calculations presented by Mehta assume a 4 K difference between the temperature of the streams entering and exiting the liquid phase separator. A 4 K temperature difference between the lean absorbent entering the absorber and the rich absorbent exiting the absorber was also assumed. The heat exchanger network used to achieve this level of heat recovery was not described. In this study, a realistic heat exchanger network was employed.

For an absorber temperature of 29°C and evaporator temperature of 10°C Mehta obtained a COP of 0.84. This performance is significantly better than that obtained in this study, even though a superior cycle was employed.

The difference in performance can be traced to the ideal heat exchanger network employed in the analysis presented by Mehta. The exergy analysis presented in section 5.5.3 demonstrates that the majority of losses in this cycle occur in the heat recovery exchangers. For this reason, improving the heat exchange network would be expected to make significant improvements to the performance of the cycle. Alternatively, the cycle could be improved by blending a portion of the rich absorbent with the returning evaporator blowdown to better match the required cooling duties in the two heat recovery exchangers. Even so, a constant thermal driving force across these heat exchangers is unlikely to be achieved because of the large changes occuring in the stream partial excess enthalpies at constant composition.

5.5.3 Exergy Analysis

In an attempt to identify the reasons for the poor performance of this cycle, an exergy analysis was conducted on the novel cycle. For ease of calculation, the total exergy loss from each unit in the cycle was calculated using the simplified equations proposed by Linhoff & Carpenter (1981). The accuracy of the available data did not warrant more detailed availability calculations. The calculated exergy losses (summarized in table 5.1) are based on a refrigeration duty of 478kW and consumption of LP steam at 100°C.

UNIT	EXERGY LOSS (kW)	PERCENTAGE OF TOTAL (%)
Generator	35.3	19.1
Absorbent heat recovery	61.9	33.4
Refrigerant heat recovery	28.1	15.2
Absorber	50.7	27.4
Valve	3.3	1.8
Evaporator	6.0	3.2

TABLE 5.1: SOURCE OF EXERGY LOSSES IN THE NOVEL CYCLE

The percentage of losses occurring in the generator of the novel cycle is considerably lower than that reported by Briggs (1971) for conventional absorption cycle generators (approximately 39.0%). Clearly, the new design was successful in reducing relative losses in the generator, but the increased circulation rate of absorbent and refrigerant required in this design resulted in large losses in the two heat - recovery heat exchangers.

These results suggest that it may be possible to increase the performance of the novel cycle by employing a distillation step to improve refrigerant or absorbent purity. This would effectively reduce losses in the heat exchangers but additional losses would be incurred in the distillation column. The potential of these cycles is discussed further in chapter 6.

Chapter 6.
VARIATIONS OF THE NOVEL ABSORPTION REFRIGERATION CYCLE

In this chapter, a number of variations of the basic novel absorption refrigeration cycle are proposed. These cycles include an additional distillation step to improve refrigerant and/ or absorbent purity. Results of computer simulations are presented and the potential of these cycles is discussed. The potential of trimethylamine - 3% aqueous salt solution is also analysed.

In chapter 5, inferior thermodynamic performance was obtained in simulations of the basic novel absorption refrigeration cycle employing the available absorbent/ refrigerant pairs. Unfortunately, there are very few alternative absorbent/ refrigerant pairs, exhibiting suitable phase behaviour, which can be considered to overcome the limitations of this cycle.

However, further improvements in cycle performance could be obtained by modifying the basic cycle. A number of variations to the basic cycle can be devised by including additional distillation steps in the cycle. These modifications improve the purity of the absorbent and/ or refrigerant with a consequent reduction in the absorbent circulation rate. Unfortunately, the addition of the distillation step also adds complexity to the basic novel absorption refrigeration cycle. A general discussion of these modifications is presented in this chapter together with the results of computer simulations of each cycle's thermodynamic performance.

In chapter 5, discussion of the basic novel absorption refrigeration cycle, with trimethylamine and water, was deferred because of the difficulty in conducting a full analysis with the limited available experimental data. A simplified analysis of the application of these mixtures in the novel absorption refrigeration cycles is presented in this chapter.

6.1 Description of Novel Absorption Refrigeration Cycles Which Include An Additional Distillation Step

A number of cycles which include an additional distillation step can be devised. The primary goal of the additional distillation step is to increase the purity of the absorbent and/ or the refrigerant streams so that increased boiling point elevations can be achieved between the evaporator and the absorber. Increasing absorbent purity also reduces absorbent circulation rates, with a consequent improvement in cycle performance.

If the boiling point elevation between the absorber and the evaporator is increased beyond that obtained in the basic novel absorption refrigeration cycle, the concentration of amine in either the evaporator blowdown or the rich absorbent stream will be outside the concentration range of the immiscible region. Consequently, it will not be possible to purify this stream in the liquid phase separation drum. Purification would, instead, be achieved by feeding the stream directly to the distillation column. Cycles can be devised which employ the liquid phase separation step for partially purifying either the evaporator blowdown or the rich absorbent.

Low molecular weight tertiary amine - water mixtures can separate into two liquid phases at elevated temperatures. However, the aqueous phase generally contains a significant quantity of amine and the amine phase contains large quantities of water. The poor separation obtained in this liquid separation step makes additional distillation steps particularly attractive when utilising these mixtures as working fluids. One or both of the streams exiting the liquid phase separation drum can be distilled.

6.1.1 Absorbent Phase Distillation

Figure 6.1 illustrates a cycle which combines distillation and liquid phase separation steps to recover refrigerant from the rich absorbent stream returning from the absorber. The rich absorbent first enters the liquid phase separation drum where a portion of the refrigerant is recovered. The partially regenerated absorbent is then passed to the top tray of the distillation column and a more pure absorbent is removed from the bottom of the column. The column overheads are combined with the refrigerant rich phase exiting the liquid phase separation drum to produce the fresh refrigerant feed to the evaporator. In this cycle, the evaporator blowdown is passed to the absorber in a similar manner to the conventional absorption refrigeration cycle.

Unfortunately, for all known working fluid pairs, the fresh refrigerant entering the evaporator contains a significant quantity of the absorbent. Consequently, the flowrate of the evaporator blowdown is high and the absorbent flowrate must be increased to prevent evaporation of the evaporator blowdown in the absorber.

Losses, resulting from the high absorbent circulation rates, can be reduced by returning the evaporator blowdown to the regeneration section of the cycle. However, the available feed locations for the returning evaporator blowdown are unattractive.

The liquid phase separation drum is not an ideal feed location because the concentration of amine in the evaporator blowdown is too high for effective liquid phase separation.

A better cycle is illustrated in figure 6.2. In this cycle, the evaporator blowdown is used as reflux to the distillation column. The partially regenerated absorbent is fed into the column below the top tray. The resulting rectification section of the column produces a significantly higher purity refrigerant. Simulation results for this cycle are presented in section 6.3.1.

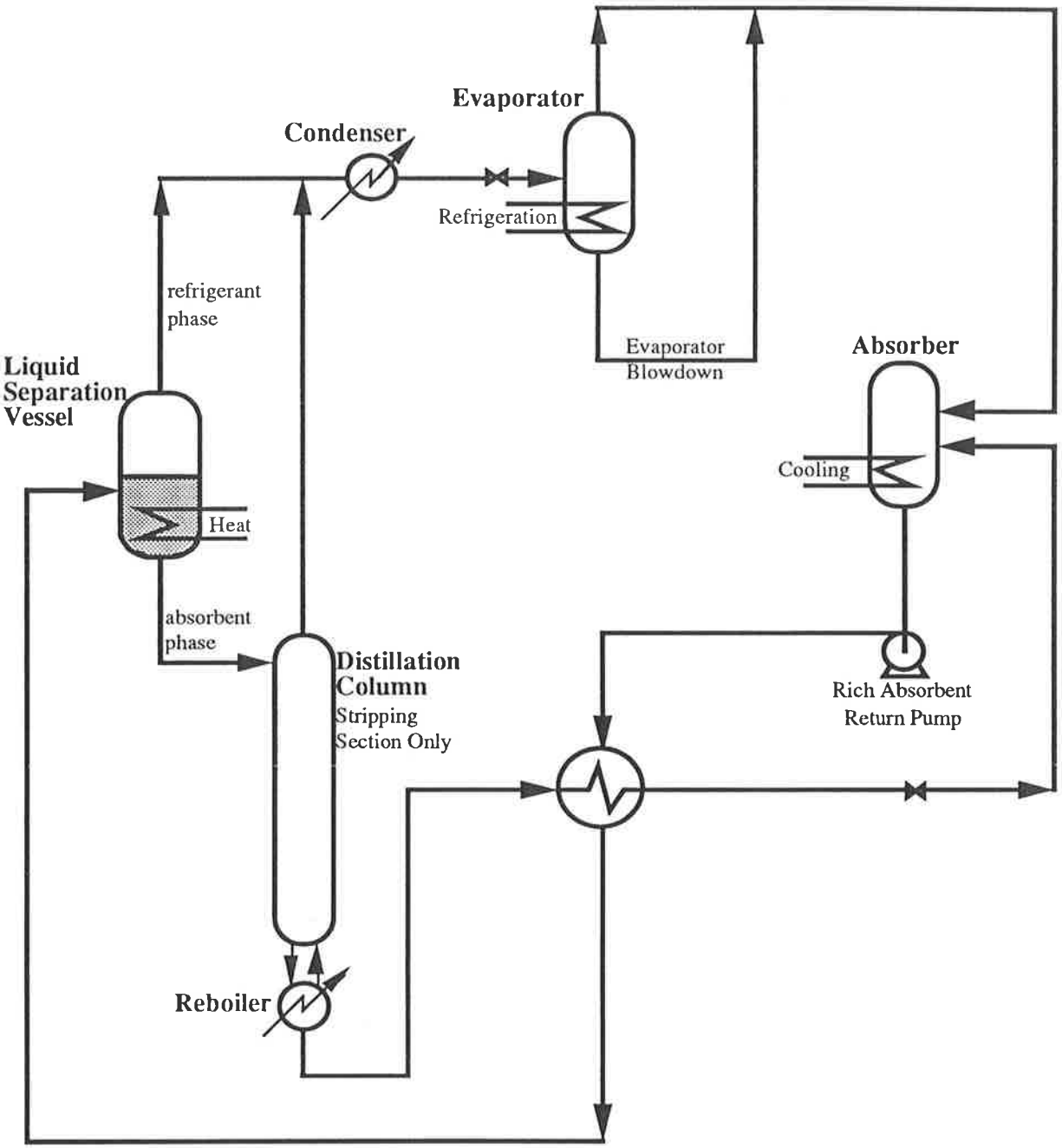

FIGURE 6.1: FLOW SCHEMATIC OF A NOVEL ABSORPTION REFRIGERATION CYCLE WITH ABSORBENT PHASE DISTILLATION AND EVAPORATOR BLOWDOWN TO THE ABSORBER

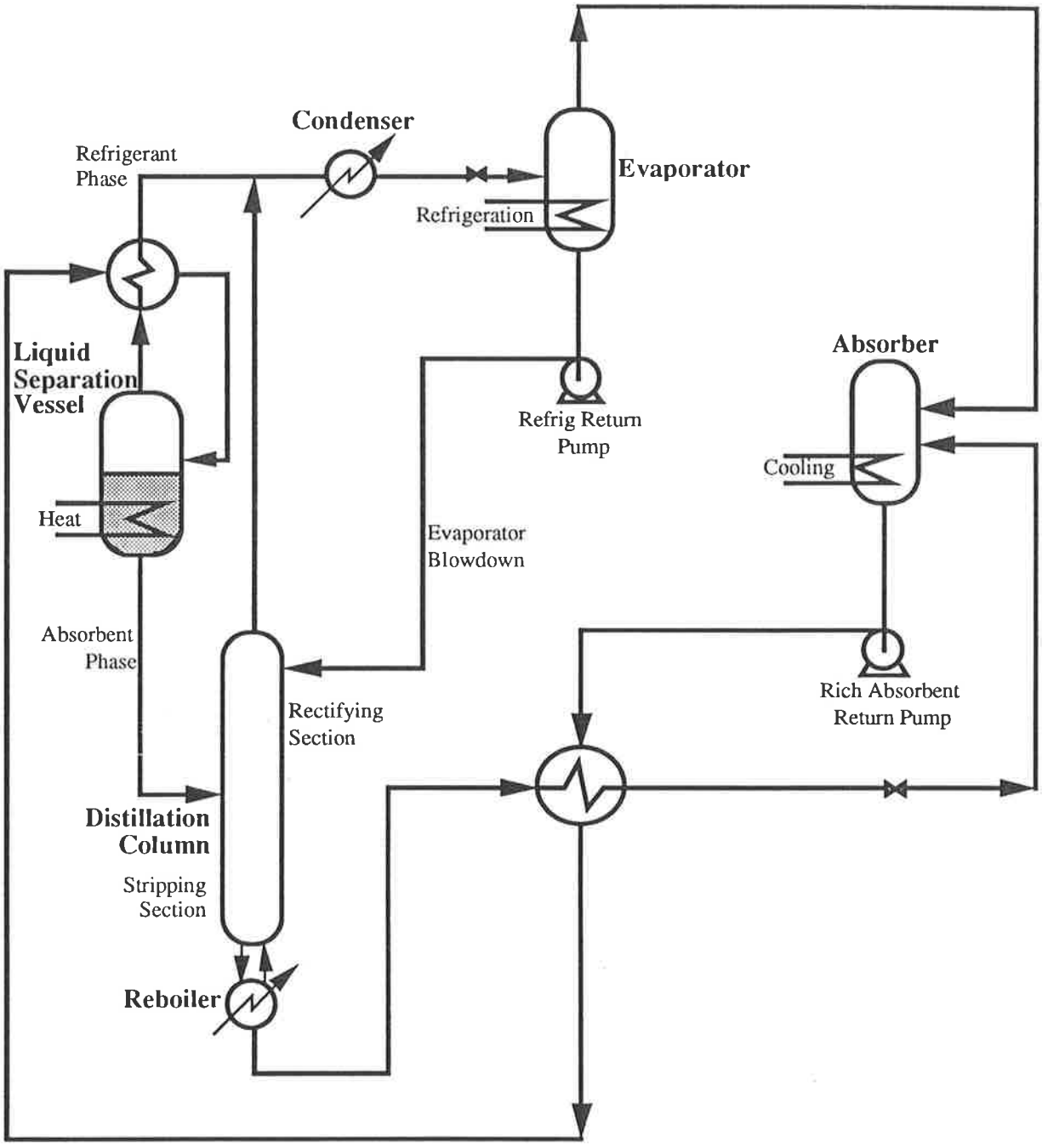

FIGURE 6.2: FLOW SCHEMATIC OF A NOVEL ABSORPTION REFRIGERATION CYCLE WITH ABSORBENT PHASE DISTILLATION AND EVAPORATOR BLOWDOWN RETURNED TO THE DISTILLATION COLUMN.

The low concentration of refrigerant in the refrigerant rich phase exiting the separation drum compared with that exiting the distillation column suggests the possibility of feeding both streams from the separation drum onto separate trays in the column. However, the optimum feed location for the two streams would be identical because of the small difference in the boiling point of the two streams. Clearly, this creates a cycle identical to that of the conventional cycle.

6.1.2 Refrigerant Phase Rectification

Figure 6.3 illustrates an alternative cycle in which the refrigerant rich phase exiting the liquid separation drum is distilled to increase the purity of the refrigerant. First, the rich absorbent enters the liquid phase separation drum where the refrigerant is separated from the absorbent. The refrigerant rich stream is then passed to a distillation column containing both rectification and stripping sections. Pure refrigerant is removed from the top of the column and lean absorbent, removed from the bottom of the column, is combined with the absorbent stream exiting the liquid separation drum.

Unfortunately, all fresh refrigerant produced in this cycle is obtained by vapourisation in a distillation column. This partially defeats the purpose of the original cycle which eliminates the necessity for a phase change in the regeneration step. However, the advantage of this cycle lies in the small fraction of the refrigerant rich absorbent stream which must be processed in the distillation column. Simulation results for this cycle are presented in section 6.3.2

As the refrigerant can be distilled to achieve high purity, the evaporator blowdown stream will be small. This allows the blowdown to be passed to the absorber without excessive penalty. However, one would still expect superior performance if the evaporator blowdown were returned to the distillation column as reflux. Analysis of the benefits of returning the evaporator blowdown as reflux to the distillation column in a conventional cycle will be discussed in detail in Chapter 8.

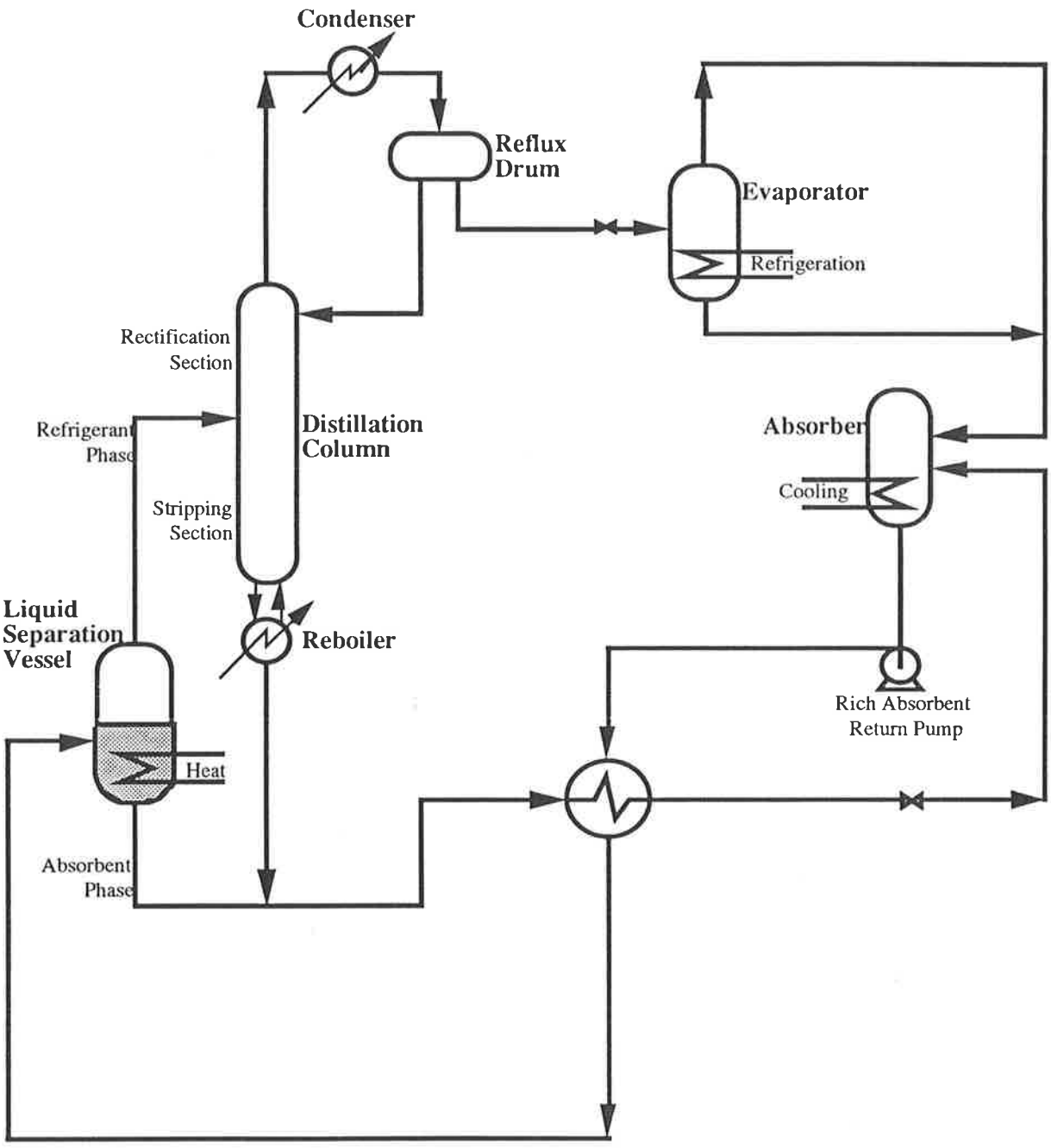

FIGURE 6.3: FLOW SCHEMATIC OF A NOVEL ABSORPTION REFRIGERATION CYCLE WITH REFRIGERANT PHASE RECTIFICATION

6.1.3 Liquid Phase Refrigerant Recovery from the Evaporator Blowdown

Figure 6.4 illustrates an alternative novel absorption refrigeration cycle in which refrigerant in the evaporator blowdown is partially recovered in a liquid phase separation drum. The blowdown stream exiting the evaporator is heated in a heat recovery exchanger. It is then passed to the liquid phase separation drum where additional heat is supplied and phase separation occurs. The refrigerant rich phase is combined with the fresh refrigerant and returned to the evaporator. The absorbent rich phase exiting the liquid separation drum is passed to the absorber.

In this cycle, the composition of the liquid blowdown from the evaporator is such that liquid phase separation will occur upon heating. However, to achieve significant boiling point elevation between the evaporator and the absorber, the refrigerant concentration in the rich absorbent must be below that required for liquid phase separation. Consequently, separation of refrigerant from the rich absorbent is achieved in a single distillation column containing both rectifying and stripping sections.

The attraction of this cycle lies in the ability of the cycle to obtain useful refrigeration from a greater fraction of the fresh refrigerant from the distillation column. Unfortunately, the cycle requires a reasonably elaborate heat recovery network. Simulation results for this cycle are presented in section 6.3.3

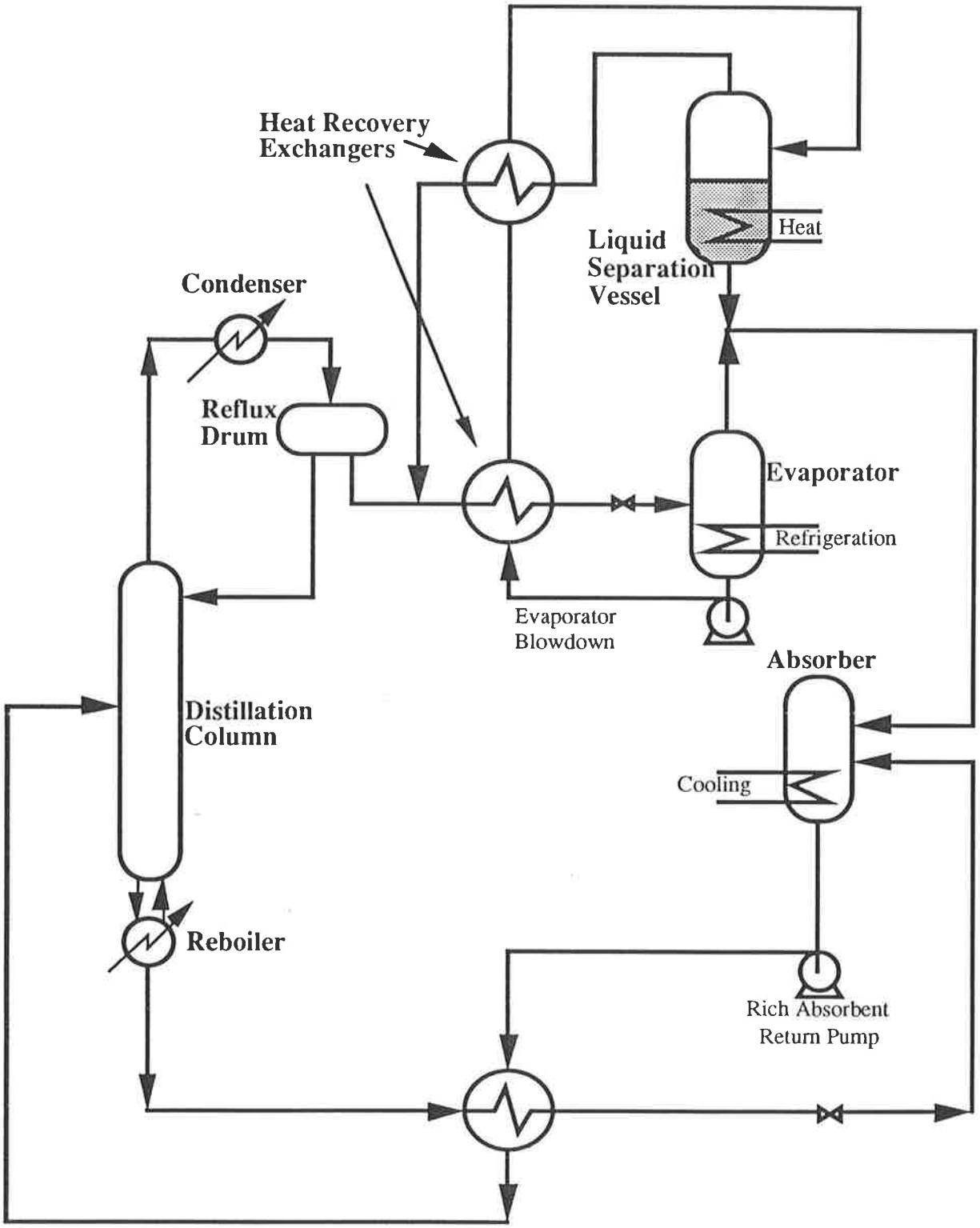

FIGURE 6.4: FLOW SCHEMATIC OF A NOVEL ABSORPTION REFRIGERATION CYCLE WITH LIQUID PHASE EVAPORATOR BLOWDOWN REFRIGERANT RECOVERY

6.2 Computer Simulation of Cycles Including Distillation

The PROCESS^{TM} chemical plant simulation package was used to model the performance of each cycle variation. The main differences between the solution procedure employed for these cycles and that employed for the basic novel absorption refrigeration cycle, discussed in chapter 5, result from the inclusion of the distillation column. This, combined with the more complex heat exchange network, considerably increased the amount of computer time required for each simulation.

The distillation column was solved, rigorously, using mass and energy balances on each tray in the column. Six ideal tray columns were employed in all simulations, giving near maximum performance. Increasing the number of ideal trays did not improve performance significantly as the temperature difference between the trays, at the feed tray, was less than 1.5 K.

The dimethylethylamine - water working fluid pair was the only pair to be used in these simulations. The small difference between the boiling point of diethylmethylamine and water made this pair unsuitable for application in cycles which include distillation. The available experimental data was insufficient for such a detailed analysis to be completed with trimethylamine/ water/ salt working fluid mixtures.

In all simulations, liquid phase separation was achieved at 102°C. Inspection of the liquid phase coexistence curve indicates that increasing the temperature in the liquid phase separation drum further would have minimal impact on the purity of the two phases.

The performance of the novel absorption refrigeration cycles including distillation were compared with the performance of the conventional absorption refrigeration cycle. To remove ambiguity in this comparison, the dimethylethylamine - water working fluid pair was also employed in the conventional cycle, and a 5 K approach temperature was assumed in all heat recovery heat exchangers. Other, more general, considerations on the simulation procedure and simulation constraints are discussed in chapter 5.

6.3 Simulation Results and Discussion

6.3.1 Cycle With Absorbent Phase Distillation

A process flow diagram of the novel absorption refrigeration cycle with absorbent phase distillation and evaporator blowdown return is presented in figure 6.5. In this example, the evaporator and the absorber temperatures were fixed at 15°C and 30°C respectively. The optimum reboiler temperature was calculated to be 81°C.

The equivalent conventional cycle, employing the same working fluids, is presented in figure 6.6. Comparison of the process conditions in the two cycles highlights the following points:

(i) The purity of the refrigerant in the novel cycle is dramatically improved by the inclusion of the distillation step. However, refrigerant purity is still well below that obtained in the conventional cycle with the same working fluids.

(ii) The purity of the refrigerant in the conventional cycle employing dimethylethylamine and water as working fluids, is significantly lower than that obtained with commercial working fluids. Higher purity refrigerant is difficult to achieve because of the azeotrope which is predicted to form at a concentration of approximately 98 mol% dimethylethylamine.

(iii) The amine (refrigerant) phase exiting the liquid separation drum makes minimal contribution to the overall refrigeration duty. This is because the stream contributes a significant portion (approximately 30%) of the total absorbent carried over in the refrigerant. The high amine concentration in the evaporator blowdown also ensures that the bulk of the amine phase exiting the liquid separation drum ends up as blowdown from the evaporator, without achieving useful refrigeration.

(iv) High absorbent circulation rates, relative to the refrigerant flowrate, contribute to the poor performance of the cycle.

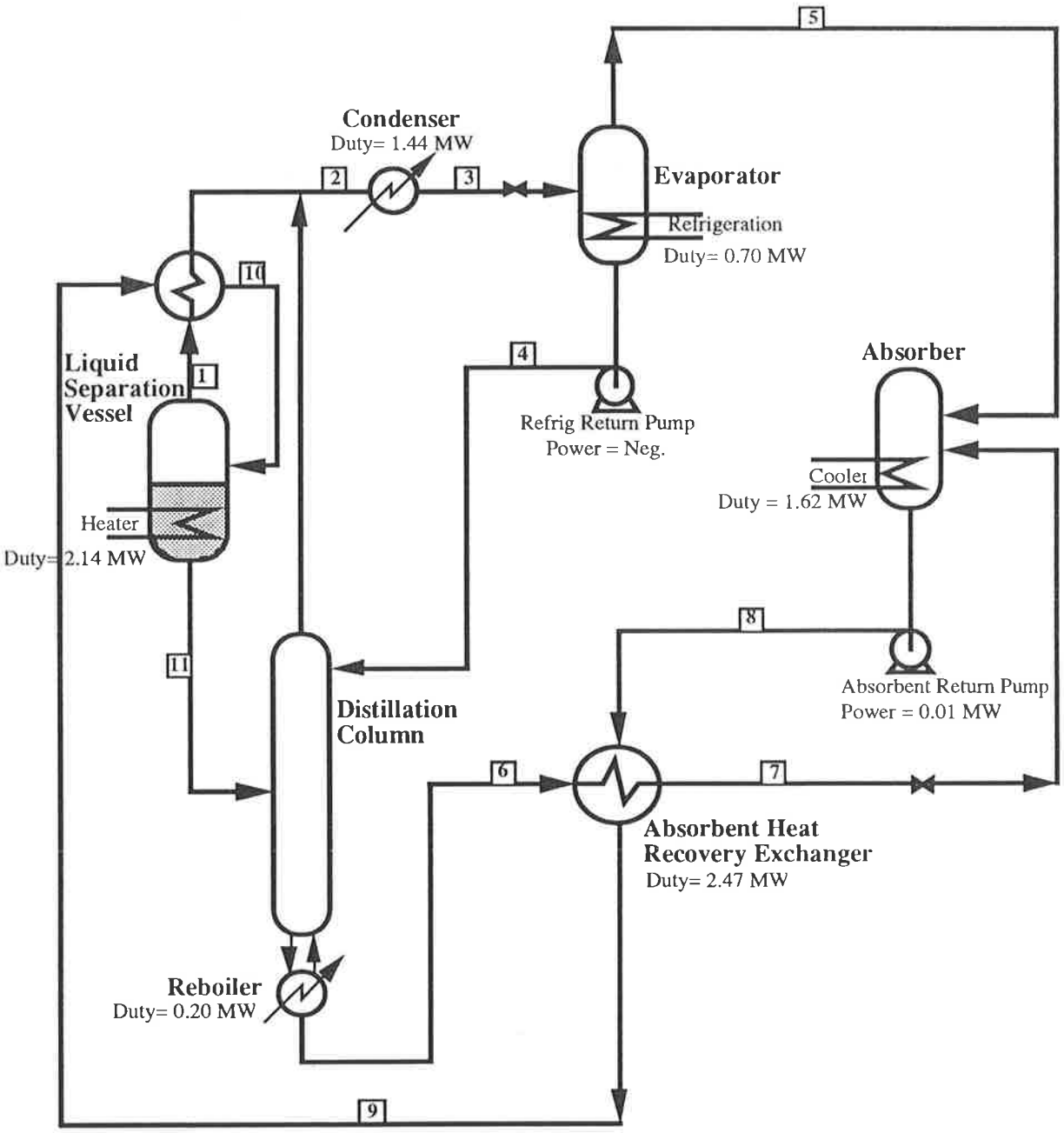

STREAM NO	1	2	3	4	5	6	7	8	9	10	11
Flowrate (kmol h^{-1})	19	181	181	57	124	2537	2537	2661	2661	2661	2642
Composition (mol%)	37.0	77.0	77.0	36.3	95.7	0.81	0.81	5.2	5.2	5.2	5.0
Temperature (°C)	102.0	65.2	30.0	15.0	15.0	80.9	35.2	30.0	68.1	68.5	102.0
Pressure (kPa)	466.5	146.6	146.6	466.5	31.6	146.6	146.6	466.5	466.5	466.5	466.5
Liquid Fraction	1.0	1.0	1.0	1.0	0.0	1.0	1.0	1.0	1.0	1.0	1.0

FIGURE 6.5: PROCESS FLOW DIAGRAM OF THE NOVEL ABSORPTION REFRIGERATION CYCLE WITH ABSORBENT PHASE DISTILLATION AND EVAPORATOR BLOWDOWN RETURN

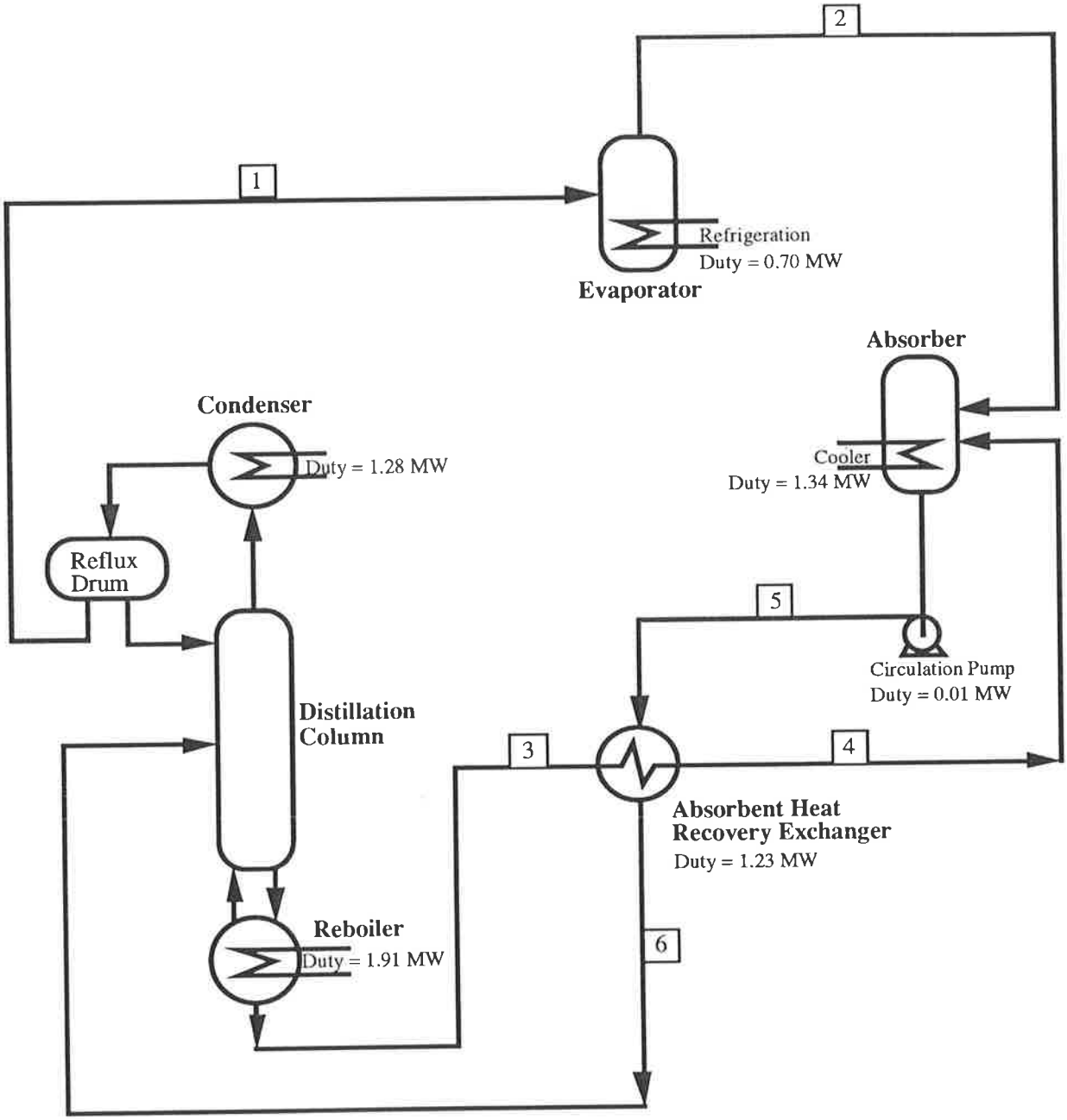

STREAM NO	1	2	3	4	5	6
Flowrate (kmol h^{-1})	127	127	1350	1350	1477	1477
Composition (mol %)	95.1	95.1	1.1	1.1	9.2	9.2
Temperature (°C)	30.0	15.0	77.7	35.2	30.2	59.7
Pressure (kPa)	146.6	39.6	146.6	146.6	146.6	146.6
Liquid Fraction	1.0	0.056	1.0	1.0	1.0	1.0

FIGURE 6.6: PROCESS FLOW DIAGRAM OF THE CONVENTIONAL ABSORPTION REFRIGERATION CYCLE WITH DIMETHYLETHYLAMINE AND WATER

Figure 6.7 illustrates the effect of evaporator temperature on the optimum coefficient of performance of the novel absorption refrigeration cycle with rich absorbent distillation and evaporator blowdown return. The influence of evaporator temperature on the conventional absorption refrigeration cycle is also illustrated in figure 6.7. The absorber temperature was fixed at 30°C in both cycles.

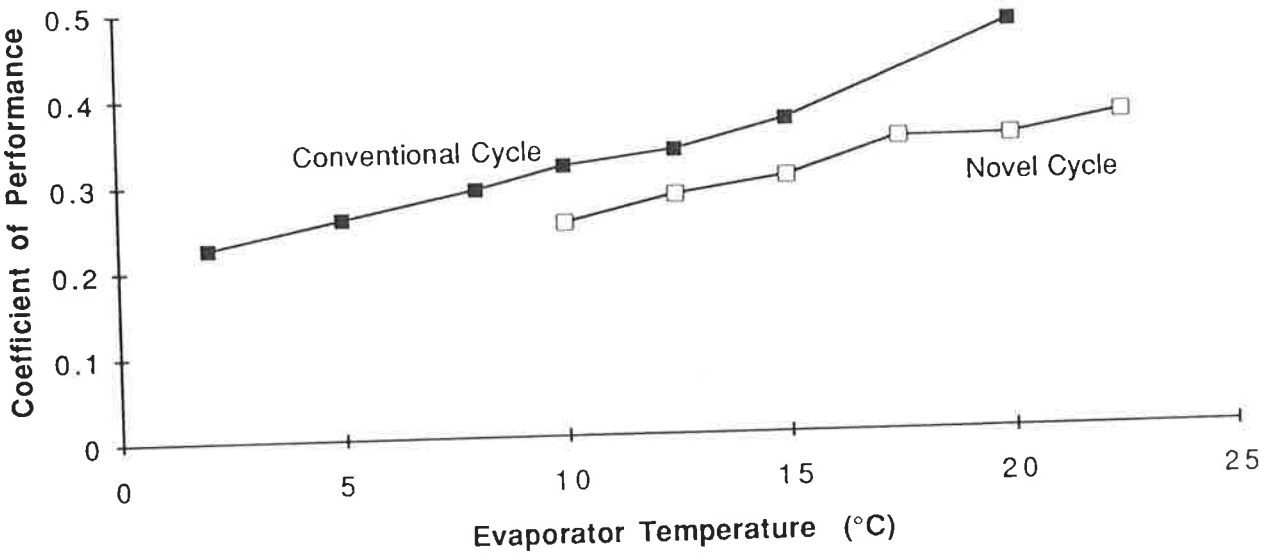

FIGURE 6.7: COMPARISON OF THE PERFORMANCE OF THE NOVEL CYCLE WITH ABSORBENT DISTILLATION AND THE CONVENTIONAL CYCLE

As expected, the performance of the novel cycle with absorbent distillation decreases as the evaporator temperature is reduced. As the evaporator temperature is decreased, the absorbent circulation rate must be increased to maintain an acceptable absorber temperature. Consequently, the performance of the cycle decreases.

Figure 6.7 also shows that the performance of the conventional cycle is superior to that of the novel cycle with absorbent distillation. The reduced performance of the novel cycle can be explained by the low purity of the refrigerant from the liquid separation drum. Consequently, a significant fraction of the available refrigeration duty is required to cool the large evaporator blowdown stream to the evaporator temperature.

6.3.2 Cycle With Refrigerant Phase Rectification

A process flow diagram of the novel absorption refrigeration cycle with refrigerant phase rectification is presented in figure 6.8. In this example, the evaporator and the absorber were fixed at 15°C and 30°C respectively. The optimum reboiler temperature was 110°C.

Comparison with the conventional cycle, illustrated in figure 6.6, highlights the following points:

(i) The composition of the lean absorbent is considerably higher than that obtained in simulations of the conventional cycle. This effectively limits the minimum evaporator temperature which can be achieved. In order to lower the composition of the lean absorbent, the fraction of absorbent sourced from the distillation column bottom product must be increased. However, this can only be achieved by increasing the composition of the rich absorbent exiting the absorber. Consequently, the desired increase in boiling point elevation is diminished.

(ii) The generator temperature is significantly higher than the generator temperature in the conventional cycle. In the novel cycle with refrigerant phase rectification, the flowrate of absorbent exiting the bottom of the distillation column is limited by the separation achieved in the liquid phase separation drum. Consequently, a high generator temperature is required to minimise the concentration of the combined lean absorbent stream.

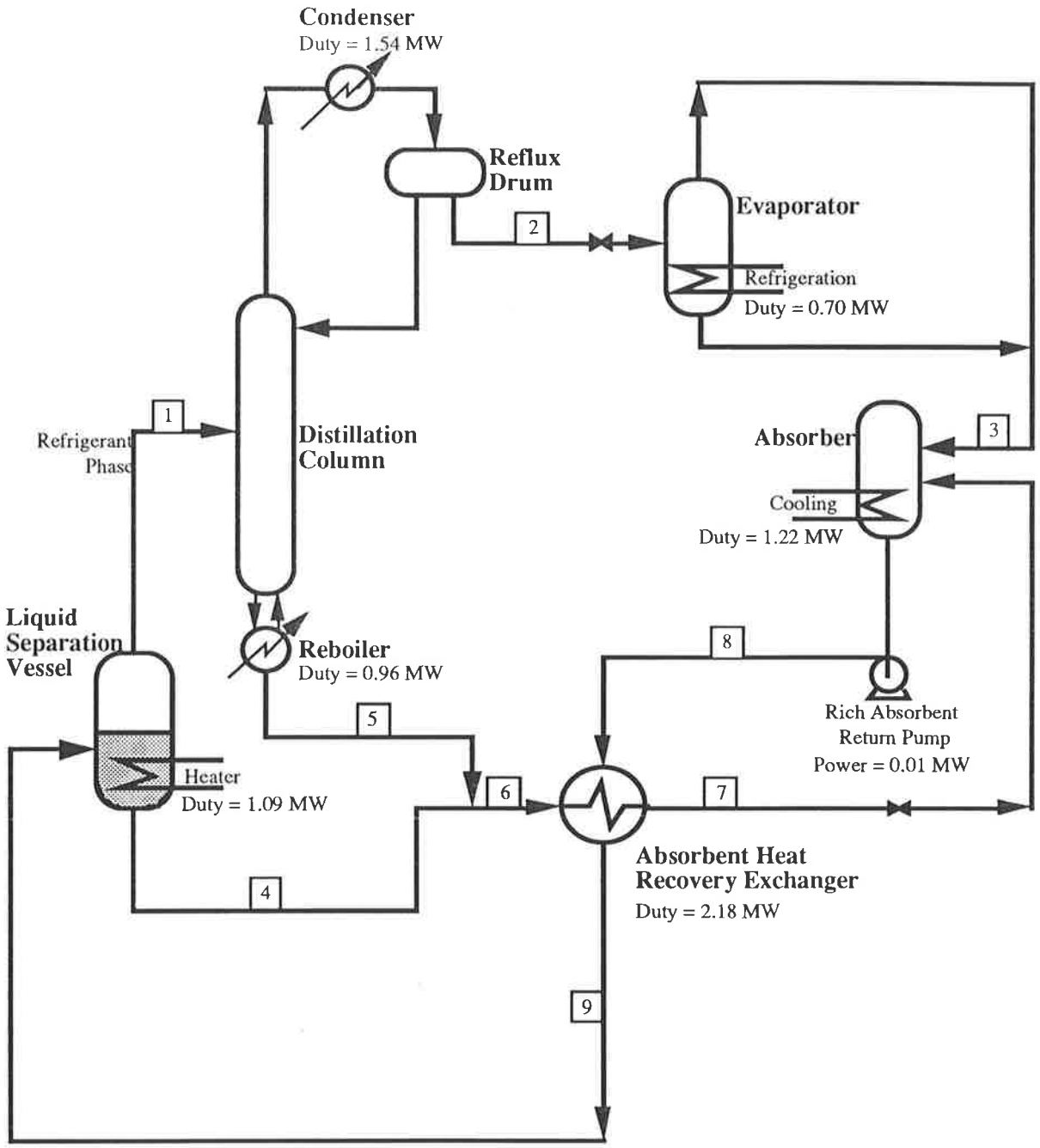

STREAM NO	1	2	3	4	5	6	7	8	9
Flowrate (kmol h^{-1})	333	128	128	1152	205	1357	1357	1485	1485
Composition (mol %)	37.0	96.4	96.4	5.0	0.0	4.2	4.2	12.2	12.2
Temperature (°C)	102.0	30.0	15.0	102.0	110.0	101.3	35.2	30.2	78.5
Pressure (kPa)	466.5	146.6	43.3	146.6	146.6	466.5	466.5	466.5	466.5
Liquid Fraction	1.0	1.0	0.056	1.0	1.0	0.992	1.0	1.0	1.0

FIGURE 6.8: PROCESS FLOW DIAGRAM OF THE NOVEL ABSORPTION REFRIGERATION CYCLE WITH REFRIGERANT PHASE RECTIFICATION

(iii) Higher purity refrigerant is employed in the novel cycle with refrigerant phase rectification compared with that used in the conventional cycle. This is required to offset the deleterious effect of the high lean absorbent concentration.

Figure 6.9 illustrates the influence of evaporator temperature on the optimum coefficient of performance of the novel absorption refrigeration cycle with refrigerant phase rectification. The performance of the conventional cycle is also illustrated in figure 6.9 to enable comparison. The absorber temperature was fixed at 30°C in both cycles.

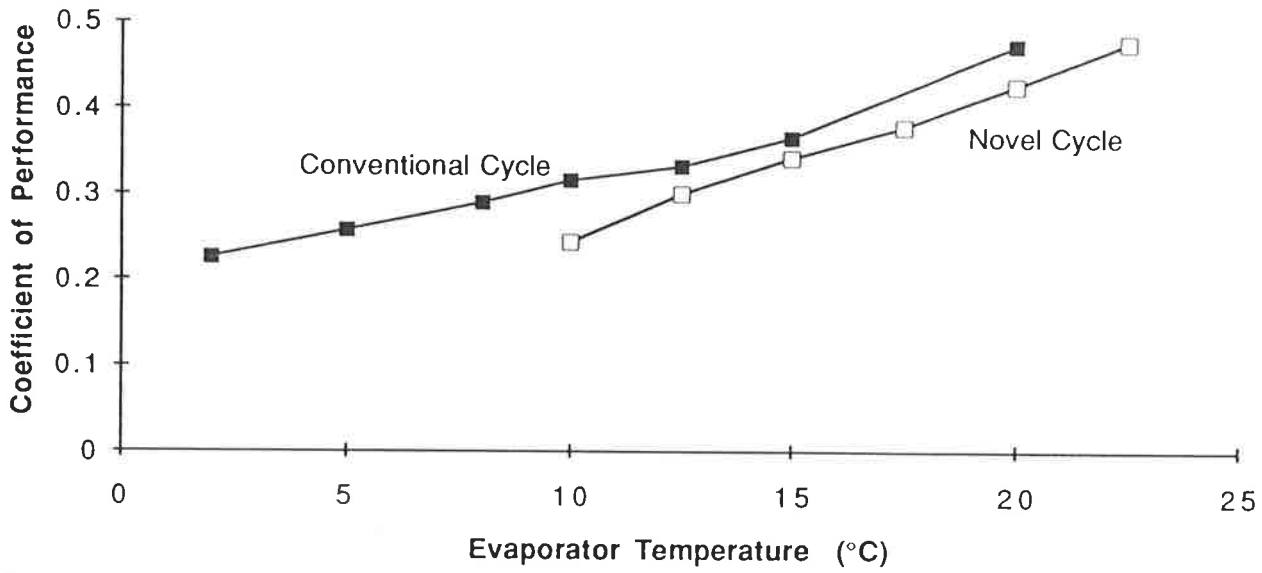

FIGURE 6.9: PERFORMANCE COMPARISON BETWEEN THE NOVEL CYCLE WITH REFRIGERANT PHASE RECTIFICATION AND THE CONVENTIONAL CYCLE

As expected, the performance of the novel cycle with refrigerant phase rectification decreases as the evaporator temperature is reduced. This is because the absorbent circulation rate must be increased to maintain the desired absorber temperature as the evaporator temperature is decreased.

While the performance of the novel cycle with refrigerant rectification is superior to that of the novel cycle with absorbent distillation (see section 6.3.1), figure 6.9 shows that the best performance is still obtained from the conventional cycle.

The reduced performance of the novel cycle with refrigerant rectification can be explained by the inherent high concentration of refrigerant in the lean absorbent. Consequently, the absorbent circulation rate or the refrigerant purity must be increased. Losses also result from the mixing of the absorbent streams exiting the liquid separation drum and the distillation column.

6.3.3 Cycle With Refrigerant Recovery from the Evaporator Blowdown

A process flow diagram of the novel absorption refrigeration cycle with refrigerant phase rectification is presented in figure 6.10. In this example, the temperatures of the evaporator and the absorber were fixed at 15°C and 30°C respectively. The optimum reboiler temperature was 80.5°C. Examination of the stream data presented in figure 6.10 highlights the following points.

(i) The combination of high purity fresh refrigerant from the distillation column and low purity evaporator blowdown (necessary for subsequent liquid phase separation) ensures that the flowrate of the evaporator blowdown stream is very small. Consequently, the amount of extra refrigerant recovered using this flowsheet is minimal.

(ii) The evaporator pressure is less than that obtained in the conventional cycle because of the low purity of the evaporator blowdown. Consequently, the absorber pressure is low and the required absorbent circulation rate must be high. This leads to poor performance.

The coefficient of performance of the cycle in this example was 0.27, considerably worse than that obtained from the other cycles. In view of the poor performance, further investigations of this cycle were abandoned.

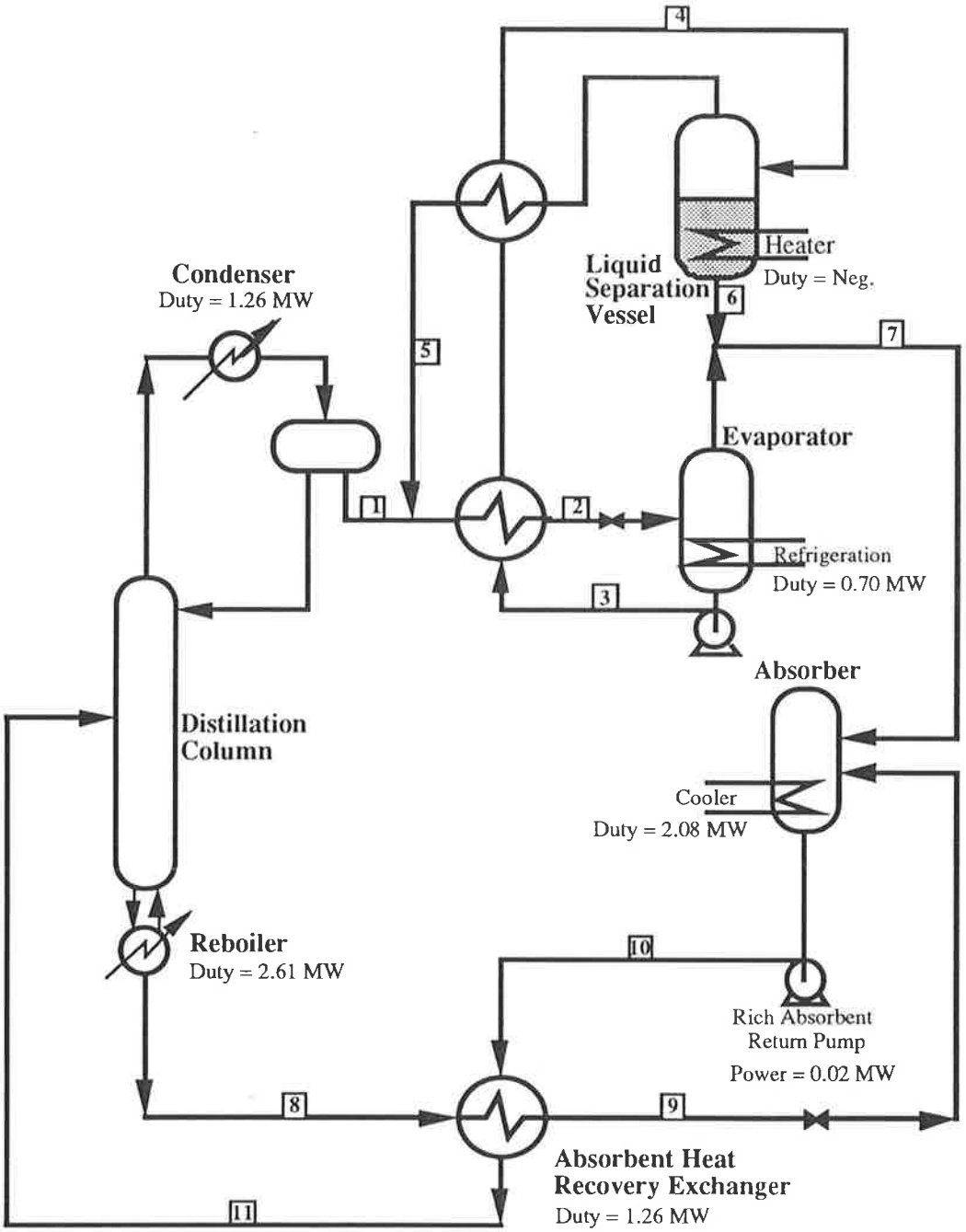

STREAM NO	1	2	3	4	5	6	7	8	9	10	11
Flowrate (kmol h^{-1})	140	141	1.09	1.09	0.61	0.48	140	4548	4548	4688	4688
Composition (mol %)	94.1	93.8	23.0	23.0	37.0	5.0	94.1	0.83	0.83	3.6	3.6
Temperature (°C)	48.0	47.6	15.2	78.3	47.8	102	15.1	80.5	35.2	30.2	70.7
Pressure (kPa)	146.6	146.6	466.5	466.5	466.5	466.5	26.3	146.6	146.6	146.6	146.6
Liquid Fraction	1.0	1.0	1.0	1.0	1.0	1.0	0.003	1.0	1.0	1.0	1.0

FIGURE 6.10: PROCESS FLOW DIAGRAM OF THE NOVEL ABSORPTION REFRIGERATION CYCLE WITH REFRIGERANT RECOVERY FROM THE EVAPORATOR BLOWDOWN

6.4 Simplified Analysis of Cycles With Trimethylamine and Water

In chapter five, low molecular weight, tertiary amines were selected as candidate refrigerants in the novel absorption refrigeration cycle, with water as the absorbent. In particular, diethylmethylamine and dimethylethylamine were employed as refrigerants in simulations of the basic novel absorption refrigeration cycle.

With the introduction of a distillation step to the novel cycle in this chapter, diethylmethylamine was discarded as a refrigerant because of its high boiling point. In contrast, the difference between the boiling point of dimethylethylamine and water was sufficient to enable the hybrid novel absorption refrigeration cycles to be modelled and compared with the conventional cycle. However, the performance of the conventional cycle employing dimethylethylamine and water as the working fluid pair was considerably worse than the performance expected with conventional refrigerant/ absorbent pairs. Clearly, alternative refrigerant/ absorbent pairs with a greater difference in normal boiling point are required.

Unfortunately, there are very few alternative mixtures known to exhibit the required thermodynamic behaviour for application in the novel cycles. Trimethylamine and water were identified as one alternative refrigerant/ absorbent pair. While the boiling point of trimethylamine is the lowest of all the tertiary amines (approximately 2°C), experiments showed that liquid phase separation in trimethylamine - water mixtures could not be achieved unless salt was added.

Unfortunately, these factors add significant complexity to the formulation of a suitable thermodynamic prediction model for detailed analysis of the novel absorption refrigeration cycles discussed above. In particular, experimental limitations prevented the aquisition of sufficient experimental data, at high temperatures, for the prediction of phase equilibria in the distillation column. The addition of the third component also necessitates a more sophisticated thermodynamic model such as that proposed by Tan and Ti (1989)

A more simplified analysis of the potential of trimethylamine - water mixtures as candidate pairs for application in absorption refrigeration cycles was devised. This analysis procedure was employed to assess the merit of pursuing an extended experimental program. If the results of this analysis were favourable, the commercial potential of this working fluid pair would be considered sufficient to justify reconstruction of the experimental apparatus to obtain the required experimental data for a more complete analysis.

6.4.1 Description of the Simplified Absorption Refrigeration Cycle Analysis.

The simplified analysis compares the ratio of lean absorbent flowrate to refrigerant flowrate in absorption refrigeration cycles which employ trimethylamine/ water and ammonia/ water as the refrigerant/ absorbent pair. A high value for this ratio results in increased losses in the heat recovery exchanger and the distillation column with concomitant poor cycle performance.

Assumptions made on the lean absorbent composition, refrigerant composition and evaporator blowdown fraction are employed to eliminate the necessity for simulating the generator. Calculations are based on an evaporator temperature of 4°C and an absorber exit temperature of 35°C. The flow sheet employed to simulate the absorbent/ refrigerant flow ratio is illustrated in figure 6.11. The thermodynamic model used for predicting the phase equilibria of mixtures of trimethylamine and water is described in chapter 4.

Figure 6.12 illustrates the influence of lean absorbent composition on the ratio of absorbent to refrigerant flowrate for the two refrigerants trimethylamine and ammonia. Figure 6.12 shows that the absorbent to refrigerant flow ratio for the absorption of trimethylamine into solution with water is an order of magnitude greater than that obtained with ammonia and water. Clearly, the trimethylamine/ water working fluid pair will not challange the performance of the conventional aqua - ammonia absorption refrigeration cycle.

The addition of salt to mixtures of trimethylamine and water is required to obtain liquid phase separation in the novel absorption refrigeration cycles. However, the addition of salt reduces the affinity between trimethylamine and water. For this reason, the addition of salt would further increase the absorbent to refrigerant flow ratio.

On the basis of these findings it was decided not to pursue detailed phase equilibrium experiments on mixtures of trimethylamine, water and salt.

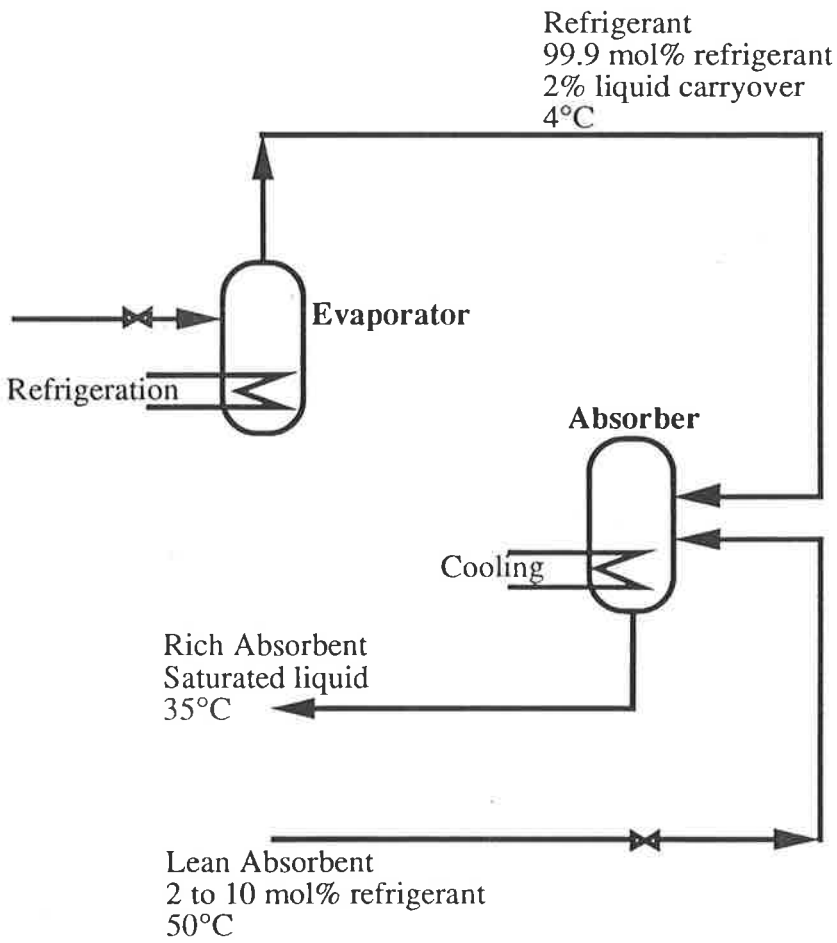

FIGURE 6.11: FLOW SCHEMATIC FOR DETERMINING THE ABSORBENT REFRIGERANT FLOW RATIO

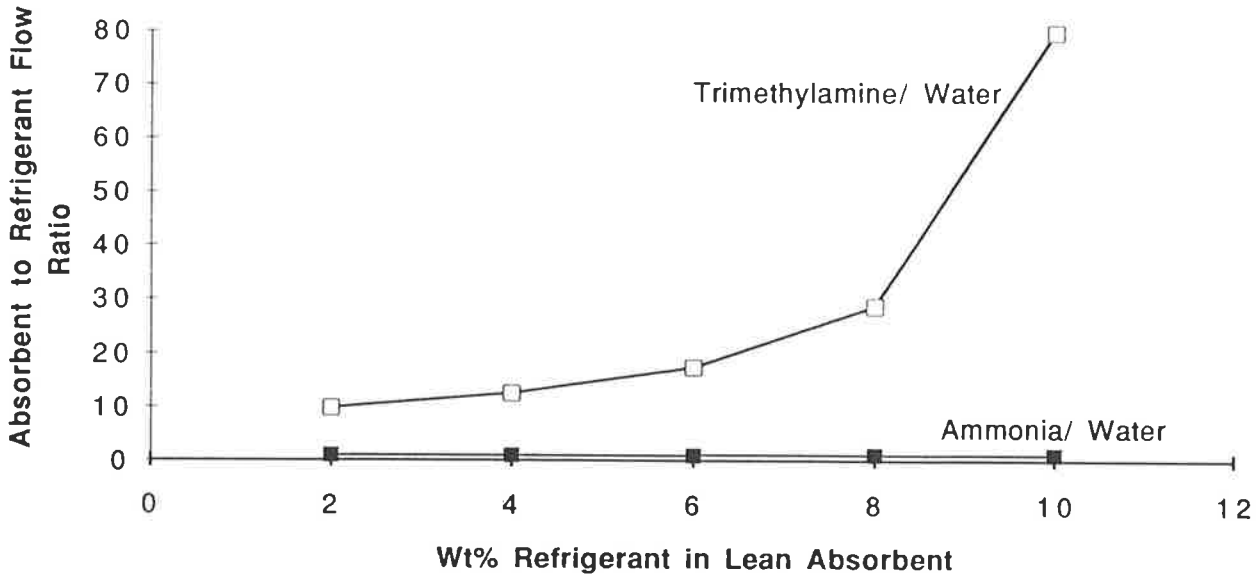

FIGURE 6.12: THE INFLUENCE OF ABSORBENT COMPOSITION ON ABSORBENT REFRIGERANT FLOW RATIO

6.5 Conclusions

In this chapter a number of "hybrid" absorption refrigeration cycles were investigated which include both a liquid phase separation step and a distillation step to separate refrigerant from the rich absorbent returning from the absorber. The thermodynamic performance of these cycles was modelled with the PROCESS™ chemical plant simulation package using dimethylethylamine and water as the working fluid pair.

In one of these cycles, the absorbent phase exiting the liquid separation drum was passed to a distillation column, where the bulk of the remaining refrigerant was stripped from the absorbent. Optimum performance was obtained from this cycle when the liquid blowdown from the evaporator was employed as reflux to the distillation column. Despite this improvement, the low purity of the fresh refrigerant entering the evaporator resulted in reduced performance compared with that obtained from the conventional absorption refrigeration cycle employing the same absorbent/ refrigerant working fluid pair.

The "hybrid" cycle with the best thermodynamic performance employed a distillation step to recover absorbent from the refrigerant rich phase exiting the liquid phase separation drum. Unfortunately, the purity of the lean absorbent, in this cycle, is limited by the composition and flowrate of the absorbent phase exiting the bottom of the liquid separation drum. Consequently, the boiling point elevation between the evaporator and the absorber is significantly reduced compared with the conventional absorption refrigeration cycle.

A cycle can also be devised where refrigerant is recovered from the liquid blowdown exiting the evaporator in a liquid phase separation step. However, the high purity of the refrigerant, obtained from the conventional distillation column, severely limits the amount of refrigerant which can be recovered. The thermodynamic performance of this cycle was significantly worse than that obtained from the other cycles investigated.

The absorbent to refrigerant flow ratio, required in an absorption refrigeration cycle employing the trimethylamine - water working fluid pair, was calculated over a range of lean absorbent concentrations. The results of these calculations were compared with the results of similar calculations with the conventional ammonia - water working fluid pair. This comparison was used to demonstrate that the thermodynamic performance of absorption refrigeration cycles employing trimethylamine and water would be insufficient to justify commercial application of this absorbent/ refrigerant pair.

It is apparent from these results, that the application of a liquid phase separation step in an absorption refrigeration cycle is unlikely to find commercial application in any form.

Chapter 7.
THE NOVEL ABSORPTION CYCLE HEAT-PUMP

In this chapter, a type II absorption cycle heat-pump is proposed. This cycle employs working fluid pairs which exhibit "upper critical solution temperature behaviour" to effect the separation of volatile working fluid from the absorbent in a low temperature generator. A number of variations to this cycle which include a distillation step are also proposed. Simulations of the performance of each cycle are presented and the potential of these cycles is discussed.

In chapters 5 and 6, mixtures exhibiting lower critical solution temperature behaviour were employed as working fluids in a series of novel absorption refrigeration cycles. Unfortunately, low coefficients of performance were predicted in simulations of these cycle with the working fluid pairs known to exhibit the required thermodynamic behaviour. In view of the limited number of mixtures which exhibit lower critical solution temperature behaviour, it is unlikely that a more suitable alternative working fluid pair will be found.

In contrast, numerous binary mixtures exhibit upper critical solution temperature behaviour. While such mixtures are unsuitable for the refrigeration cycles described in chapters 5 and 6, they could find application in a heat pump cycle where volatile working fluid recovery occurs at low temperature.

Figure 7.1 illustrates the direction of energy flow in the two possible types of absorption cycle heat pump. In this figure, the horizontal lines represent the temperature levels of the available heat sources/ sinks, and the arrows represent the direction of the energy flow. Arrows pointing into the line represent heat input to the cycle and arrows pointing out from the line represent heat rejection. The type I cycle utilizes high - grade energy to raise the temperature of a low - grade heat source. The useful heat from this process is rejected at an intermediate temperature. The type II cycle employs heat at an intermediate temperature and rejects heat at both low and high temperatures.

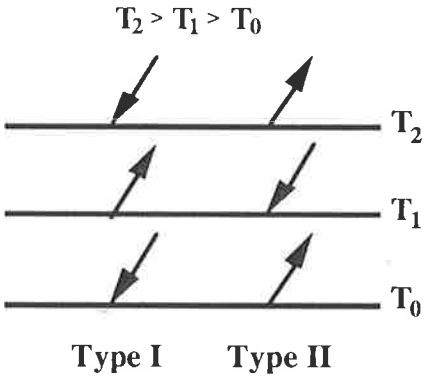

FIGURE 7.1: DIRECTION OF ENERGY FLOW FOR THE TWO FEASIBLE HEAT PUMP TYPES

In this chapter, a type II heat pump is described which employs mixtures exhibiting upper critical solution temperature behaviour as working fluids. The partial miscibility of these mixtures at low temperature is utilized to separate the volatile working fluid from the rich absorbent.

To demonstrate the feasibility of the proposed novel absorption cycle heat pump, cyclohexane and aniline were chosen as candidate working fluids for computer simulation of the novel heat pump. This pair was selected because of the large difference in boiling point between the two compounds and the large composition range over which liquid phase separation occurs.

The thermodynamic performance of a number of cycle variations which include an additional distillation step are also investigated. The performance of these cycles is compared and their potential is discussed.

7.1 Description of the Novel Absorption Cycle Heat Pumps

7.1.1 Basic Novel Type II Heat Pump

The novel type II heat pump cycle is illustrated in figure 7.2. In this cycle, the volatile working fluid is partially boiled in an evaporator using low grade heat. The resulting vapour then dissolves in a high boiling point absorption fluid with the heat of solution released at elevated temperature. The rich absorbent is subsequently cooled until the volatile working fluid becomes immiscible in the absorbent. The resulting two liquid phases are separated in a settling drum, with the recovered volatile working fluid returned to the evaporator and the absorbent phase passed to the absorber.

As the liquid phase separation is imperfect, the absorbent stream contains a fraction of the more volatile component and a fraction of the less volatile absorbent remains in the working fluid. Liquid is removed from the evaporator and returned to the settling drum to prevent build up of the less volatile component in the evaporator. Heat exchangers are employed to preheat the absorbent and working fluid, and to simultaneously precool the settling - drum feeds.

Figure 7.3 details a flow schematic of a conventional type II absorption cycle heat pump for comparison. In contrast to the conventional cycle, the novel cycle includes a liquid - liquid separation drum in place of the conventional distillation column and blowdown from the evaporator is recycled to the generator.

In an attempt to improve the thermodynamic performance of the novel heat pump, a number of hybrid cycles including a distillation step were synthesized. The principal reason for the additional distillation step is to increase the purity of the working fluids, thus reducing the circulation rates of the working fluids and increasing performance.

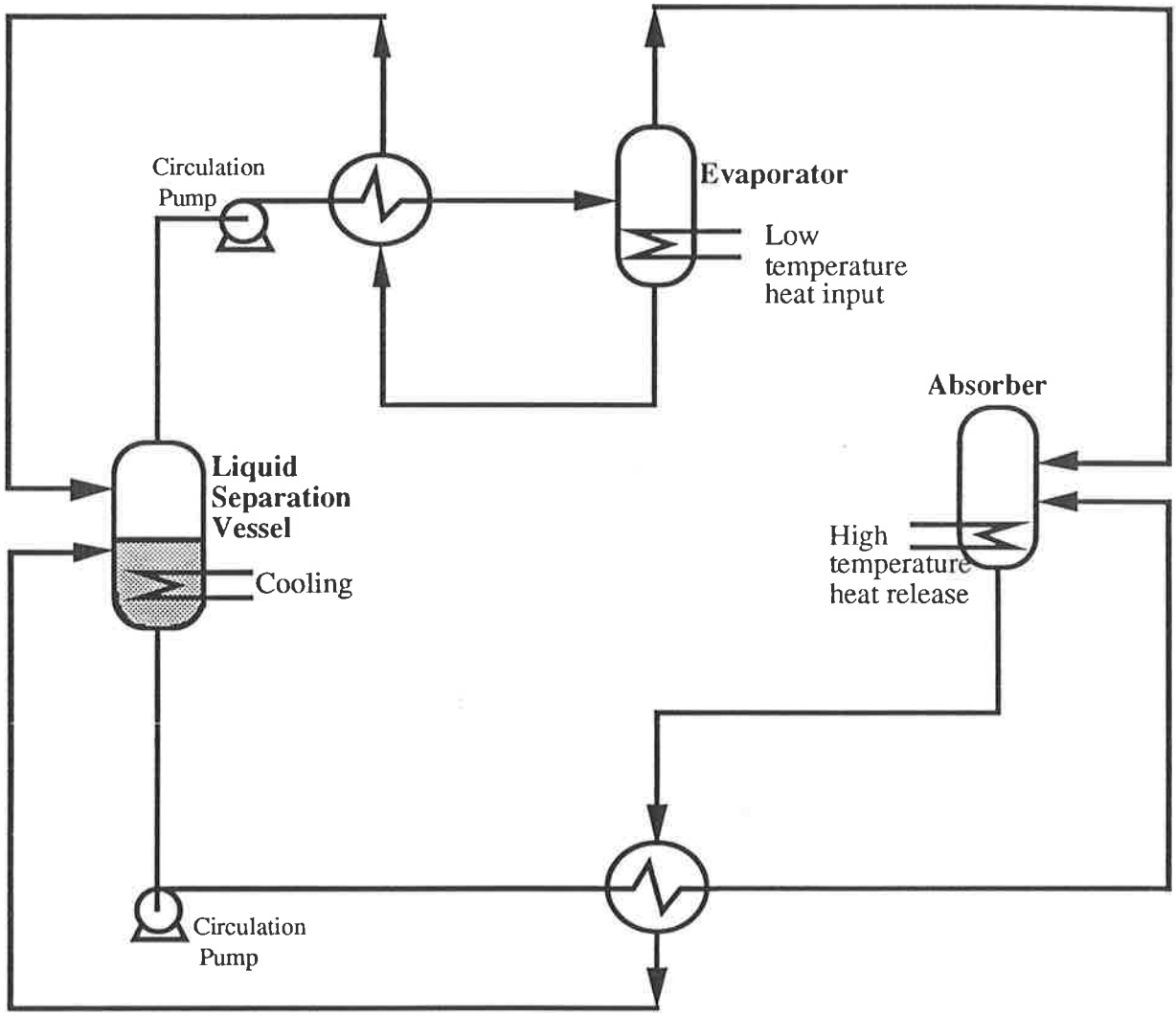

FIGURE 7.2: FLOW SCHEMATIC OF THE NOVEL TYPE II ABSORPTION CYCLE HEAT PUMP

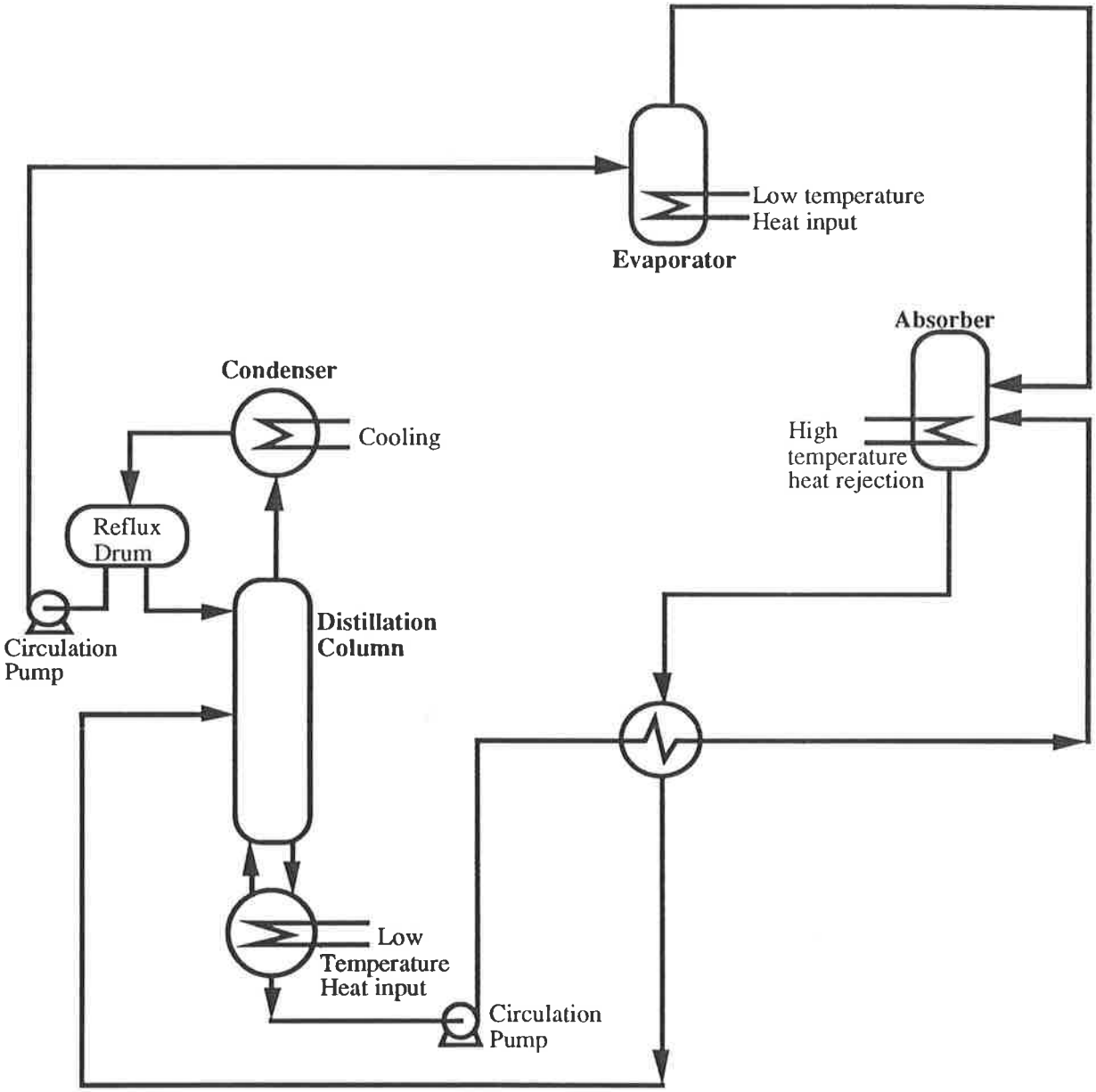

FIGURE 7.3: FLOW SCHEMATIC OF THE CONVENTIONAL TYPE II ABSORPTION CYCLE HEAT PUMP

7.1.2 Novel Type II Heat Pump With Absorbent Phase Distillation

The novel absorption cycle heat pump with absorbent phase distillation is illustrated in figure 7.4. In this cycle, volatile working fluid present in the absorbent phase exiting the liquid separation drum, is stripped in the distillation column. The overheads from the distillation column are condensed and combined with the volatile working fluid phase exiting the liquid separation drum. The resulting stream is pumped to elevated pressure and passed to the evaporator. Blowdown from the evaporator is used as reflux to the distillation column. This cycle is a corollary of the refrigeration cycle illustrated in figure 6.2.

7.1.3 Novel Type II Heat Pump With Volatile Phase Rectification

Figure 7.5 illustrates an alternative heat pump cycle in which the volatile working fluid phase exiting the liquid separation drum is distilled to recover lean absorbent. The rich absorbent first enters the liquid phase separation drum where the volatile working fluid is removed from the absorbent. The volatile working fluid stream is then passed to a distillation column containing both rectification and stripping sections. A pure stream of volatile working fluid is recovered from the top of the column and lean absorbent is removed from the bottom of the column. The lean absorbent from the bottom of the distillation column is then combined with the absorbent stream exiting the liquid separation drum and passed to the absorber. This cycle is a corollary of the refrigeration cycle presented in figure 6.3.

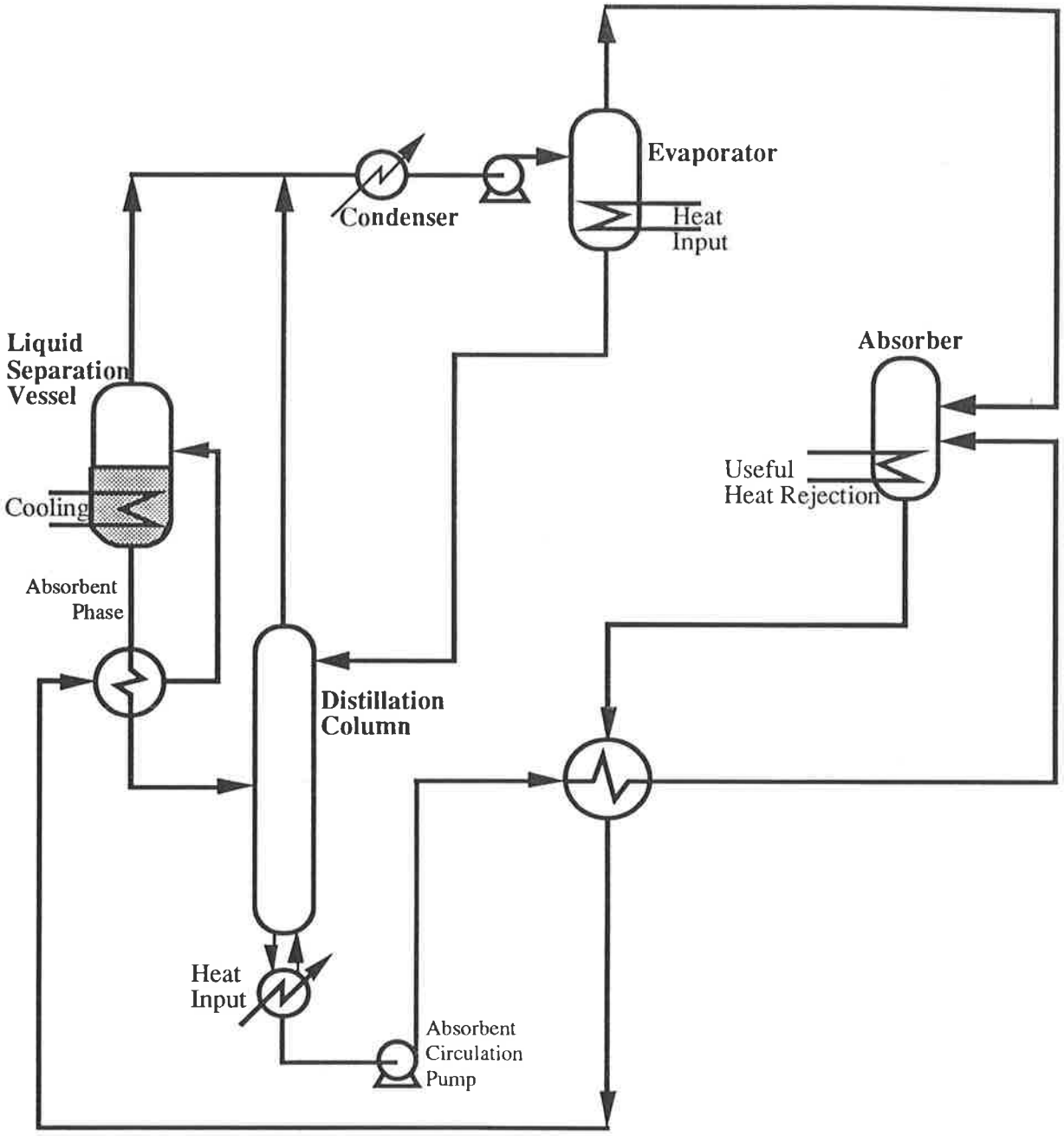

FIGURE 7.4: FLOW SCHEMATIC OF THE NOVEL TYPE II ABSORPTION CYCLE HEAT PUMP WITH ABSORBENT PHASE DISTILLATION

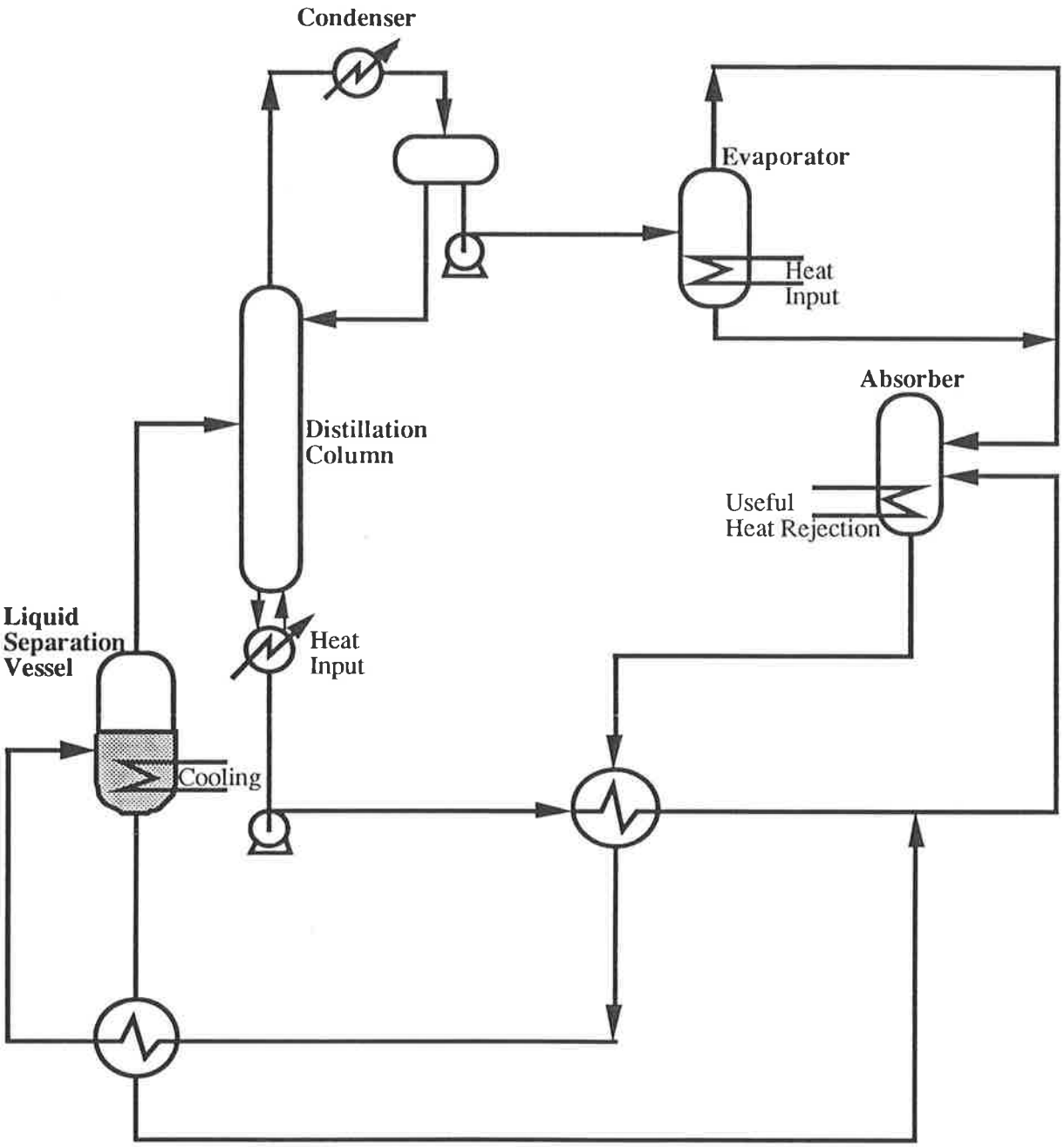

FIGURE 7.5: FLOW SCHEMATIC OF THE NOVEL TYPE II ABSORPTION CYCLE HEAT PUMP WITH VOLATILE WORKING FLUID RECTIFICATION

7.1.4 Novel Type II Heat Pump With Volatile Working Fluid Recovery From the Evaporator Blowdown

Figure 7.6 illustrates an alternative novel absorption cycle heat pump in which volatile working fluid in the evaporator blowdown is partially recovered in a liquid phase separation step. The blowdown stream exiting the evaporator is cooled by heat exchange with the fresh volatile working fluid stream. It is then passed to the liquid phase separation drum where it is cooled until phase separation occurs. The volatile working fluid phase is returned to the evaporator and the absorbent rich phase exiting the liquid separation drum is passed to the absorber. This cycle is a corollary of the refrigeration cycle illustrated in figure 6.4.

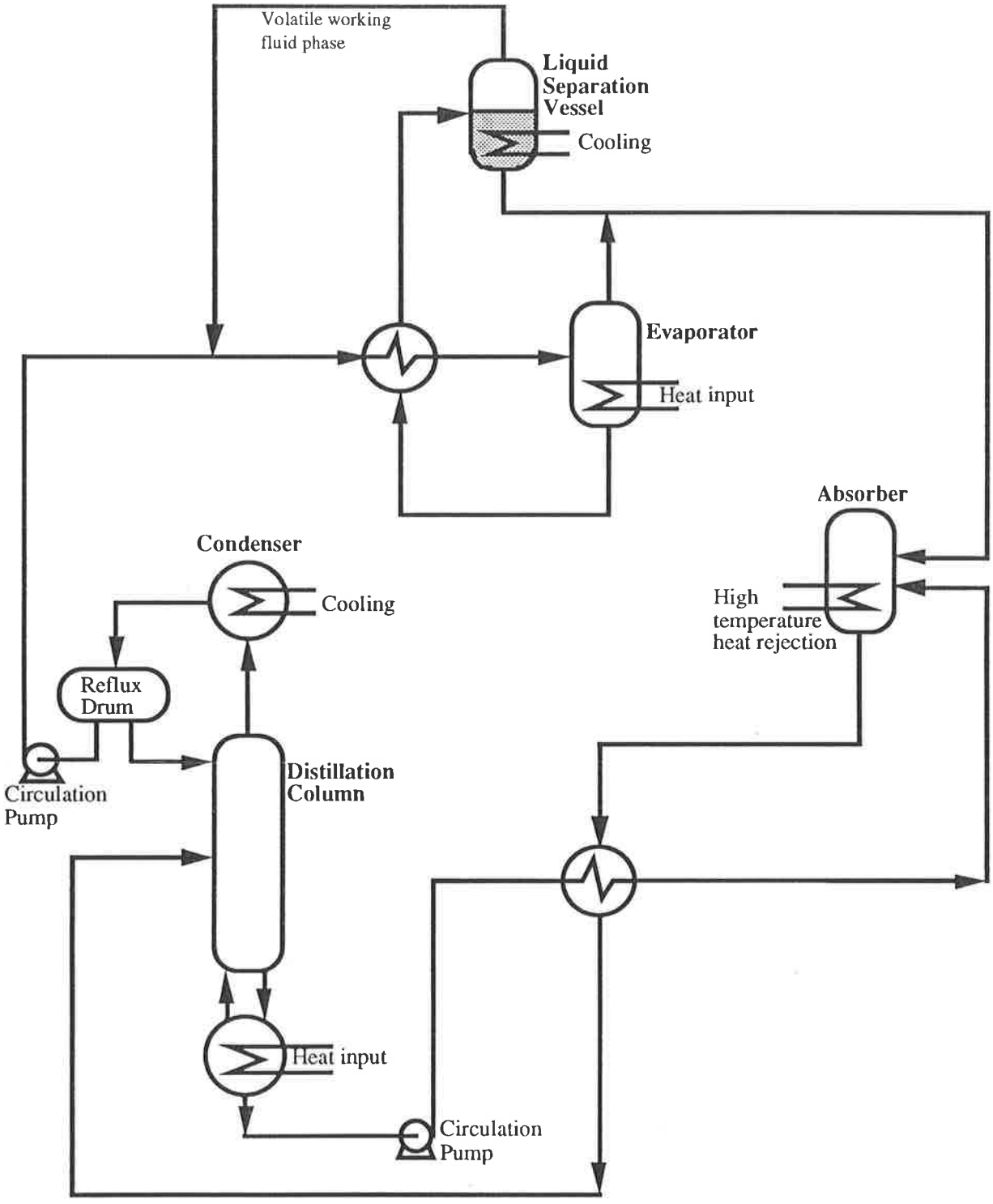

FIGURE 7.6: FLOW SCHEMATIC OF THE NOVEL TYPE II ABSORPTION CYCLE HEAT PUMP WITH VOLATILE WORKING FLUID RECOVERY FROM THE EVAPORATOR BLOWDOWN

7.2 Selection of Working Fluids

Working fluids suitable for application in this cycle must exhibit upper critical solution temperature behaviour upon mixing. As well, the selected pair should possess properties which are desirable in conventional absorption cycle heat pumps. Properties of particular importance include thermal stability and low corrosivity. A large difference between the boiling point of the volatile working fluid and the absorbent is also desirable to ensure sufficient boiling point rise in the absorber.

To demonstrate the feasibility of the proposed novel absorption cycle heat pump, cyclohexane and aniline were chosen as candidate working fluids for computer simulation of the novel heat pump and its variants. This pair was selected because of the large difference in boiling point between the two compounds and the large composition range over which liquid phase separation occurs.

Conveniently, a large body of experimental data is available for the development of an accurate thermodynamic model for mixtures of cyclo-hexane and aniline (Abello et. al., 1968, Hosseini and Schneider, 1963, Korteum and Freier, 1954, Roeck and Sieg, 1955, Buchner and Kleyn, 1924, and Hunter.and Brown, 1947). The five - parameter NRTL model described in chapter 4 was used to predict the phase behaviour of these mixtures. By comparison of model predictions and experimental data, the thermodynamic model was shown to predict mixture vapour pressure with an average accuracy of ±1.8%.

7.3 Computer Simulation of the Novel Heat Pump Cycles

The performance of each of the proposed heatpump cycles was simulated with the PROCESS^{TM} chemical plant simulation package. An approach temperature of 2 K was assumed for the two heat recovery heat exchangers in the basic cycle. Larger approach temperatures were not used for this cycle because of the low boiling point elevation achieved between the evaporator and the absorber. The approach temperature was increased to 5 K for simulations of the heat pump cycles which included the additional distillation step. In all simulations, the temperature in the liquid phase separation drum was fixed at 25°C.

To obtain optimum performance from each cycle, the absorbent flowrate was adjusted to ensure that rich absorbent exiting the absorber remains a saturated liquid. In addition, the fraction of working fluid boiled in the evaporator was optimised. This procedure is described in more detail in section 5.3.3.

Heat pumps are generally employed to raise the temperature of an available low grade heat source. Waste heat from low pressure steam, at a temperature slightly in excess of 100°C, is one common source of low grade heat. For this reason, the evaporator temperature was fixed at 100°C and the influence of absorber exit temperature on cycle performance was investigated.

The performance of the novel absorption cycle heat pumps was then compared with the performance of the conventional absorption cycle heat pump employing cyclohexane and aniline as working fluids.

The simulation procedure and simulation constraints parallel the detailed discussion presented in chapters 5 and 6.

7.4 Simulation Results

7.4.1 Basic Novel absorption Cycle Heatpump

Simulations were conducted on the basic novel absorption cycle heat pump over a range of absorber temperatures and with the evaporator temperature fixed at 100°C. A process flow schematic of this cycle is presented in figure 7.8 with the absorber temperature fixed at 106°C. Examination of the stream data, presented in the flowsheet, highlights the following points:

(i) The boiling point elevation achieved between the evaporator and the absorber is very small despite the large concentration difference between the absorbent and the volatile working fluid. At the low temperatures experienced in the liquid phase separation drum, the boiling point of the absorbent and the volatile working fluid must be identical if liquid phase separation is to occur. However, the small difference between the boiling point of these streams, at the elevated temperatures experienced in the evaporator and the absorber, highlights the relative insensitivity of the shape of the cyclohexane - aniline phase envelope to increasing temperature.

(ii) In order to increase the boiling point elevation between the evaporator and the absorber a large fraction of the volatile working fluid must be recycled to the liquid phase separation drum.

Figure 7.7 illustrates the influence of absorber temperature on the optimum coefficient of performance for the basic novel absorption cycle heat pump. Performance falls dramatically as the absorber temperature is increased until the cycle ceases operation with an absorber temperature in excess of 108°C.

The reduction in performance with increasing absorber temperature can be attributed to the increased circulation rate of absorbent required to dissolve the volatile working fluid. The maximum absorber exit temperature corresponds to the saturation temperature of the lean absorbent. At this temperature, the lean absorbent cannot absorb any vapour from the evaporator.

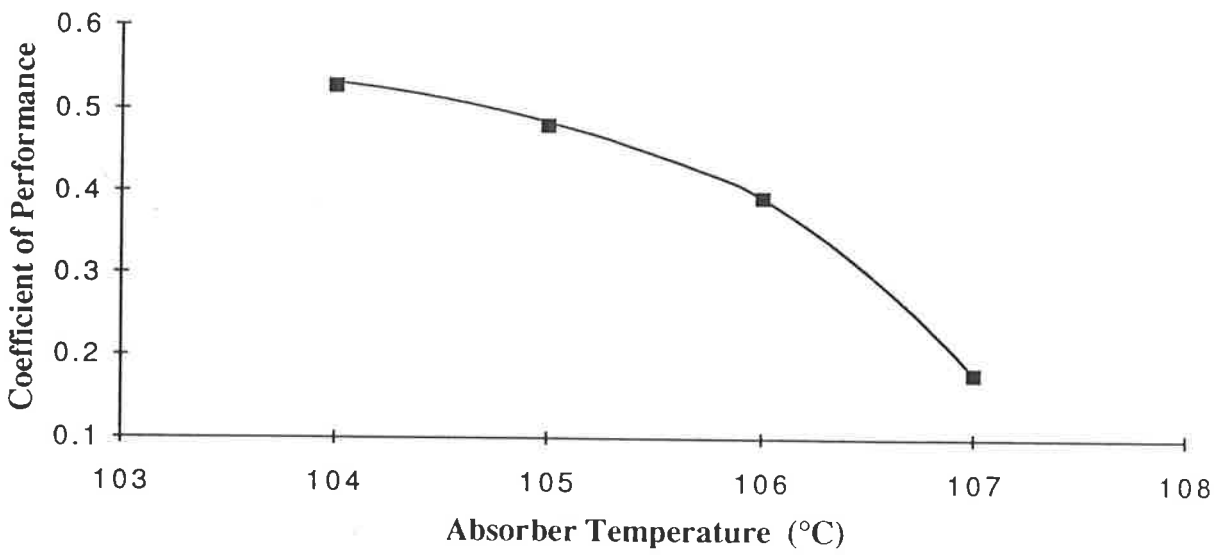

FIGURE 7.7: THE INFLUENCE OF ABSORBER EXIT TEMPERATURE ON THE PERFORMANCE OF THE NOVEL ABSORPTION CYCLE HEAT PUMP

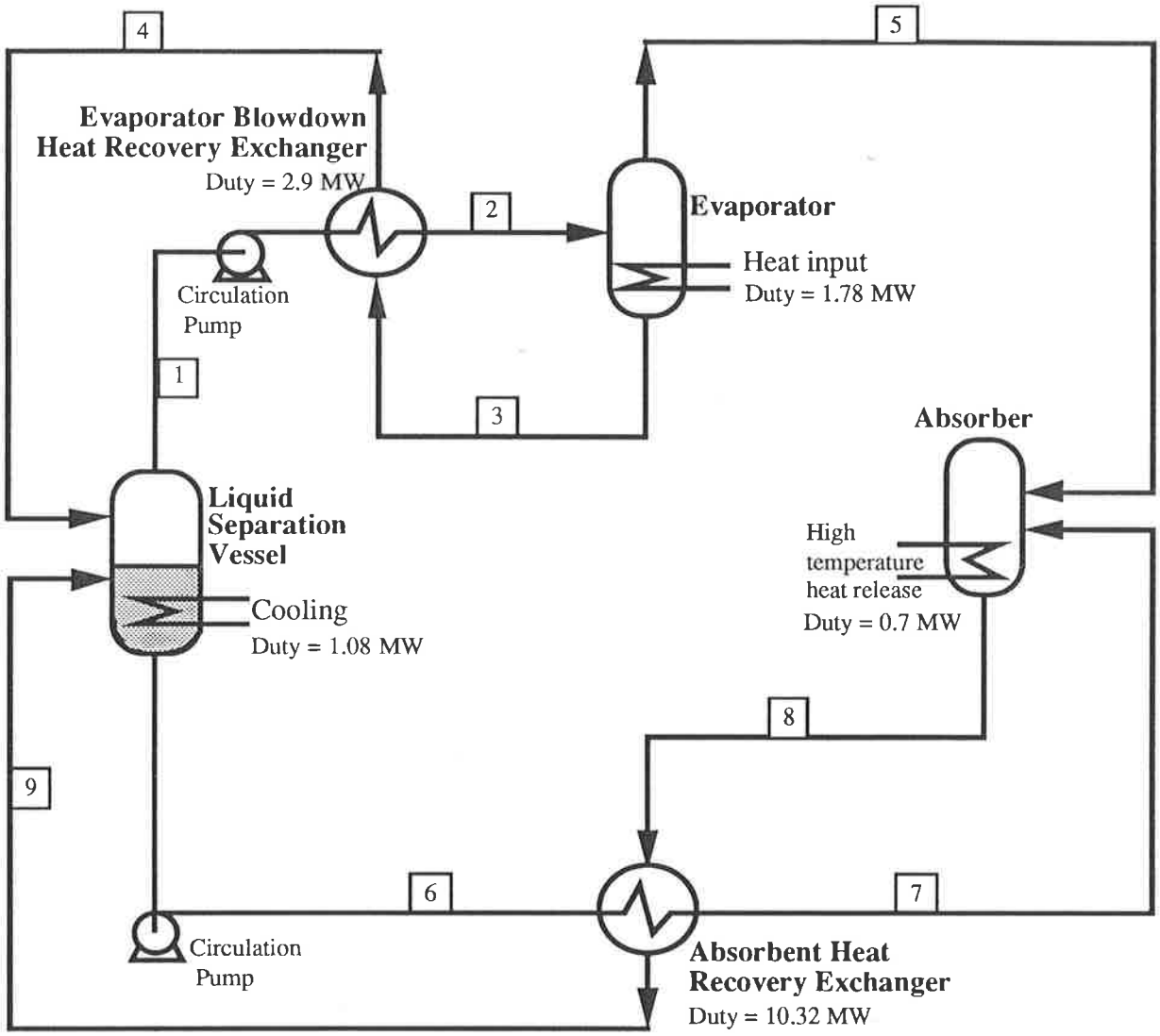

STREAM NO	1	2	3	4	5	6	7	8	9
Flowrate (kmol h^{-1})	988	988	840	840	148	2881	2881	3030	3030
Composition (mol %)	87.0	87.0	85.1	85.1	97.5	27.0	27.0	30.5	30.5
Temperature (°C)	25.0	88.2	100.0	27.0	100.0	25.0	104.0	106	32.6
Pressure (kPa)	164.7	164.7	164.7	164.7	164.7	164.7	164.7	164.7	164.7
Liquid Fraction	1.0	1.0	1.0	1.0	0.0	1.0	1.0	1.0	1.0

FIGURE 7.8: PROCESS FLOW DIAGRAM OF THE NOVEL ABSORPTION CYCLE HEAT PUMP

7.4.2 The Novel Type II Heat Pump With Absorbent Phase Distillation and the Novel Type II Heat Pump With Volatile Phase Rectification

Despite the addition of the distillation step in these cycles, the temperature range over which the heat pump can operate is severely constrained when cyclohexane and aniline are employed as working fluids. This is best illustrated by the phase diagram presented in figure 7.9. The bubble point curve presented in this figure was calculated at a constant pressure of 167.5 kPa. Assuming the evaporator temperature is 100°C, this pressure is approximately equal to the pressure expected in the evaporator and absorber of these novel heat pump cycles.

In these two cycles, the rich absorbent exiting the absorber is separated into two phases in the liquid separation drum. Consequently, the concentration of cyclohexane in the rich absorbent stream must be between 27 mol% and 87 mol%. Thus, from figure 7.9, we can deduce that the boiling point elevation between the evaporator and the absorber is limited to approximately 8.5 degrees C for these working fluids. This is significantly less than the boiling point elevation which can be achieved in the conventional cycle (see section 7.4.3). For this reason, no further simulations were conducted to determine the performance of these cycles.

From figure 7.9, we can also see that the boiling point in the evaporator is quite insensitive to the composition of the evaporator liquid blowdown. Consequently, the evaporator pressure can not be varied significantly without influencing the evaporator temperature.

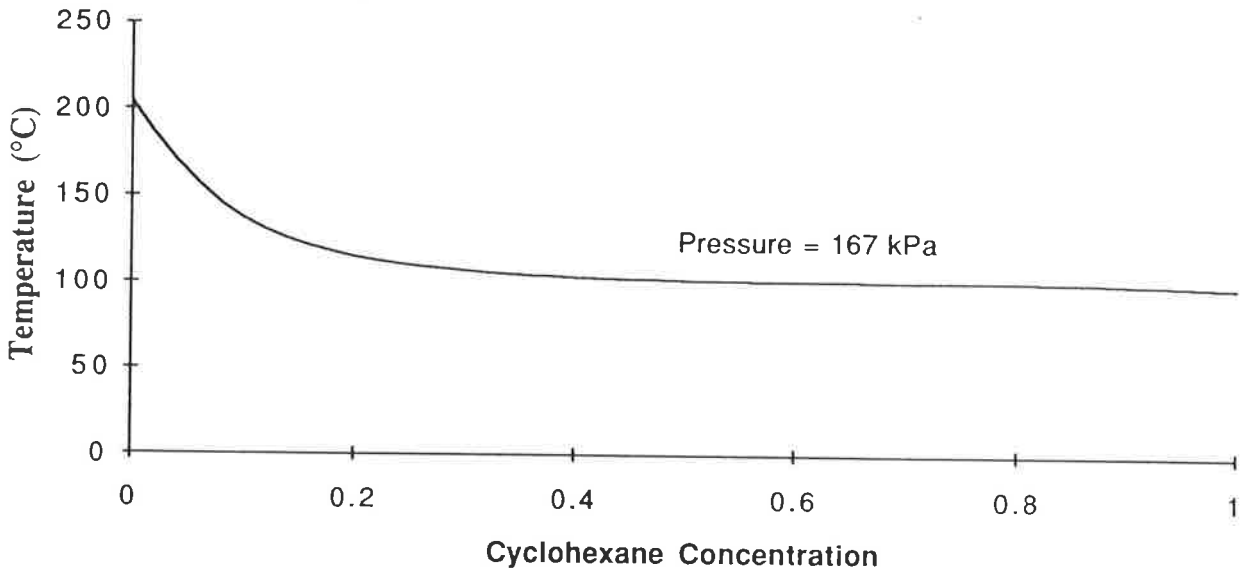

FIGURE 7.9: CALCULATED BUBBLE POINT CURVE FOR MIXTURES OF CYCLOHEXANE AND ANILINE AT 167.5 KPA

7.4.3 The Novel Type II Heat Pump With Volatile Working Fluid Recovery From the Evaporator Blowdown

Simulations were conducted on the novel cycle with volatile working fluid recovery from the evaporator blowdown over a range of absorber temperatures and with the evaporator temperature fixed at 100°C. A process flow diagram of this cycle is presented in figure 7.10 with the absorber temperature fixed at 120°C. A process flow diagram of the conventional type II absorption cycle heat pump under the same conditions is also provided in figure 7.11 for comparison. Examination of stream data, presented in these flowsheets, highlights the following points:

(i) The evaporator pressure in the novel cycle is significantly lower than that obtained in the conventional heat pump. This low evaporator pressure is required to achieve an appropriate concentration of cyclohexane in the evaporator blowdown to enable subsequent purification in the liquid phase separation drum.

(ii) In the novel cycle, the distillation column overhead stream contains a lower concentration of the more volatile component. At the higher distillation column overhead concentrations, the optimum liquid blowdown concentration is too rich in cyclohexane to achieve liquid phase separation. At the lower concentrations, however, the benefit of the liquid phase separation step is increased because a larger fraction of the evaporator blowdown must be recycled.

(iii) The concentration of the rich absorbent returning to the distillation column is higher in the conventional distillation column. This results from the increased pressure in the evaporator (and hence absorber) as previously discussed. The high concentration of the rich absorbent enables reduced absorbent circulation rates and improved performance in the conventional cycle.

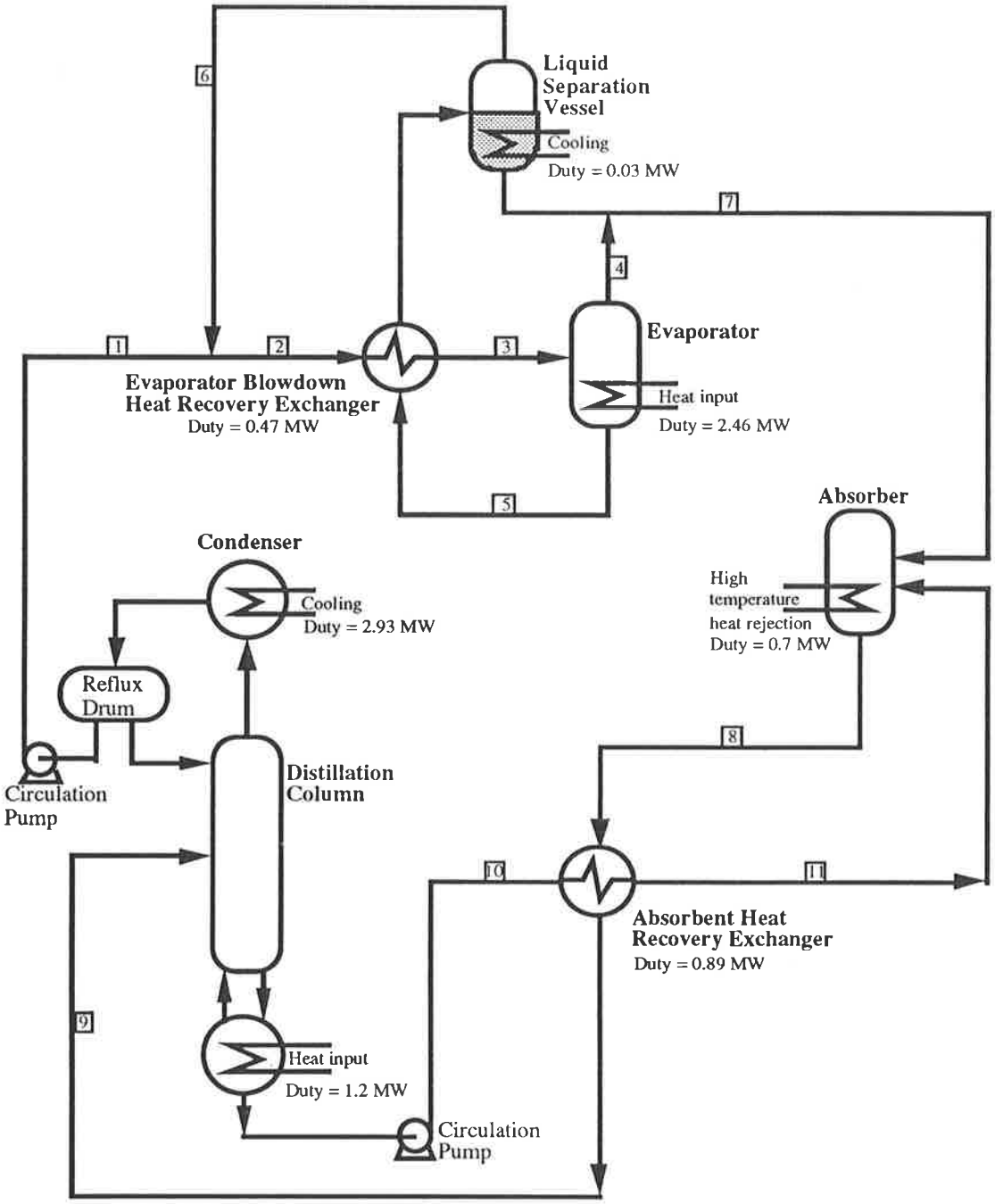

STREAM NO	1	2	3	4	5	6	7	8	9	10	11
Flowrate (kmol h^{-1})	215	350	350	210	140	136	215	1324	1324	1109	1109
Composition (mol %)	96.0	92.5	92.5	97.5	85.0	87.0	96.0	16.1	16.1	0.7	0.7
Temperature (°C)	25.2	25.0	54.7	100.0	100.0	25.0	100.8	120.0	107.8	100.0	115.0
Pressure (kPa)	173.3	164.7	164.7	164.7	164.7	164.7	164.7	164.7	164.7	173.3	173.3
Liquid Fraction	1.0	1.0	1.0	0.0	1.0	1.0	0.037	1.0	1.0	1.0	1.0

FIGURE 7.10: PROCESS FLOW DIAGRAM OF THE NOVEL ABSORPTION CYCLE HEAT PUMP WITH VOLATILE WORKING FLUID RECOVERY FROM THE EVAPORATOR BLOWDOWN

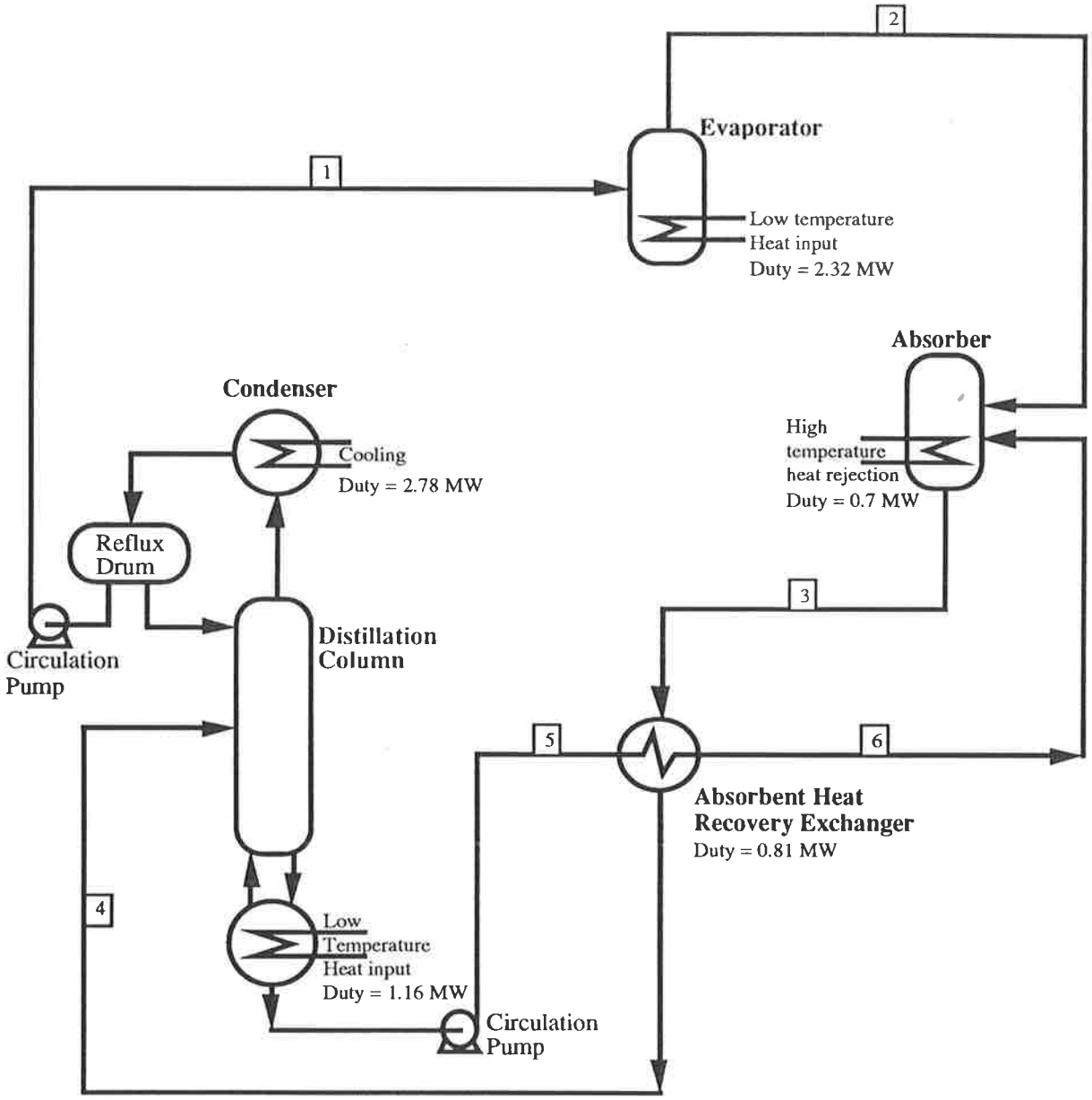

STREAM NO	1	2	3	4	5	6
Flowrate (kmol h^{-1})	202	202	1203	1203	1001	1001
Composition (mol %)	98.6	98.6	17.1	17.1	0.7	0.7
Temperature (°C)	25.2	100.0	120.0	107.9	100.0	115.0
Pressure (kPa)	173.3	170.5	170.5	170.5	173.3	173.3
Liquid Fraction	1.0	0.001	1.0	1.0	1.0	1.0

FIGURE 7.11: FLOW DIAGRAM OF THE CONVENTIONAL ABSORPTION CYCLE HEAT PUMP

Figure 7.12 illustrates the influence of absorber temperature on the optimum coefficient of performance for the novel absorption cycle heat pump with volatile working fluid recovery from the evaporator blowdown. Performance curves are provided for three distillation column pressures of 95 mm Hg, 95.5 mm Hg and 96.5 mm Hg. As the condenser exit temperature was fixed at 25°C in all simulations, these distillation column pressures correspond to overhead cyclohexane compositions of 96.02%, 97.01% and 98.39% respectively. The evaporator and distillation column reboiler temperatures were fixed at 100°C in all simulations.

When the distillation column pressure was set to 96.5mmHg, the optimum liquid blowdown from the evaporator was too rich in cyclohexane to achieve any liquid - phase separation. Hence, the results given at this pressure are essentially those for a conventional absorption cycle heat pump employing cyclohexane and aniline as the working fluids.

From figure 7.12, it is evident that cycle performance decreases with increasing absorber temperature. However, the temperature elevation achieved in the absorber of this cycle is considerably greater than that achieved in the basic novel absorption cycle heat pump and cycle performance is less sensitive to the absorber temperature.

Despite the liquid - phase working fluid recovery step, increasing overhead volatile composition yields improved performance. Indeed, cycle performance continues to increase when the liquid - phase separation step becomes redundant at higher column pressure. This can be attributed to the increased absorber pressure obtained with the higher overhead volatile compositions.

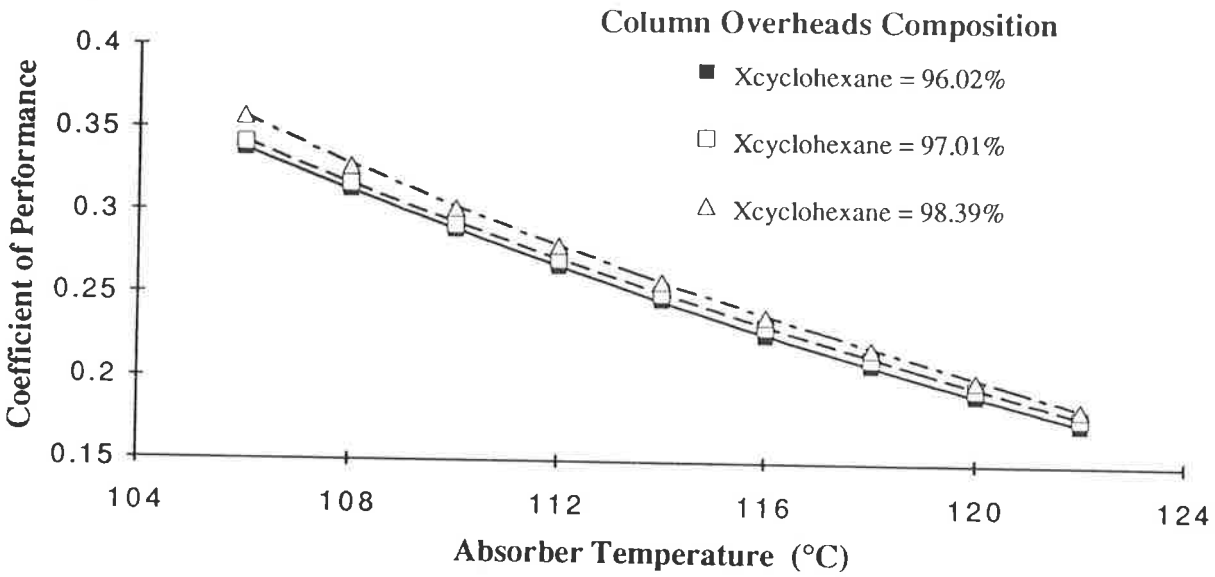

FIGURE 7.12: THE INFLUENCE OF ABSORBER TEMPERATURE ON THE PERFORMANCE OF THE NOVEL ABSORPTION CYCLE HEAT PUMP WITH VOLATILE WORKING FLUID RECOVERY FROM THE EVAPORATOR BLOWDOWN

7.5 Conclusions

In this chapter, a novel type II absorption cycle heat pump, which employs a liquid phase separation step to recover the volatile working fluid from the absorbent, was investigated. Variants of this cycle, which include an additional distillation step, were also analysed. The thermodynamic performance of these cycles was modelled with the PROCESS™ chemical plant simulation package using cyclohexane and aniline as the working fluid pair.

Results of simulations on the basic novel type II absorption cycle heat pump demonstrated that only a small increase in temperature between the evaporator and the absorber could be achieved with the selected working fluid pair. This was attributed to the relative insensitivity of the shape of the cyclohexane - aniline phase envelope to increasing temperature.

With the addition of a distillation step, the purity of either the volatile working fluid or the lean absorbent can be increased. In two such cycles, the rich absorbent exiting the absorber is cooled and passed to the liquid phase separation drum. Either the volatile working fluid phase or the absorbent phase exiting this drum can then be distilled to improve stream purity. Unfortunately, only small improvements were made to the boiling point elevation between the evaporator and the absorber, in these cycles. Further increases in the boiling point elevation could only be achieved by decreasing the concentration of cyclohexane in the rich absorbent stream. However, this would make phase separation in the liquid phase separation drum impossible.

The most effective of the novel heat pump cycles, employed the liquid phase separation step to recover refrigerant from the liquid blowdown exiting the evaporator. Primary separation of volatile working fluid from the rich absorbent was achieved in the distillation column. In this cycle, the purity of the volatile working fluid entering the evaporator must be low to obtain significant volatile working fluid recovery in the liquid phase separation drum. This results in low thermodynamic performance when compared with the conventional type II absorption cycle heat pump employing the same working fluid pair.

Chapter 8.
EVAPORATOR BLOWDOWN RECYCLE IN A CONVENTIONAL AQUA AMMONIA ABSORPTION REFRIGERATION CYCLE

In previous chapters, recycling of the evaporator liquid blowdown to the generator was introduced as a means for reducing performance losses which result from poor refrigerant purity. In this chapter, the principle of returning liquid blowdown from the evaporator to the generator is applied to the conventional aqua - ammonia absorption refrigeration cycle. In this application, the returning liquid can be used as reflux to the distillation column, thus eliminating the necessity for fresh refrigerant reflux. The performance and cost of the cycle with evaporator blowdown return is compared with that of the conventional cycle. The commercial potential of the new cycle is discussed.

In chapters 5 and 6, a series of novel absorption cycle refrigerators were devised which include evaporator blowdown recycle to the generator. The application of evaporator blowdown recycle was found to be particularly attractive in these cycles because of the poor purity of the refrigerant. The recycle effectively reduces the load on the absorber and increases thermodynamic performance.

In conventional absorption refrigeration cycles employing a volatile absorbent, (e.g. organic solvent or water) some fraction of absorbent is carried over into the refrigerant. The absorbent is concentrated in the liquid phase in the evaporator, thus limiting the quantity of refrigerant which can be evaporated. This problem can be reduced by improved rectification in the distillation column. However, the increased duty in the generator which is required to improve product purity may negate any benefit from the reduction in required liquid blowdown. For the aqueous-ammonia system, a refrigerant purity of approximately 99.9% ammonia appears to be close to the optimum (Bogart, 1981).

A number of alternative cycles have been suggested for reducing the quantity of liquid blowdown from the evaporator. One cycle employs a partial condenser (dephlegmator) to produce reflux to the distillation column. Any absorbent "carry-over" in the vapour overheads is preferentially condensed in the partial condenser. The resulting higher purity vapour is then passed to the total condenser to form fresh liquid refrigerant feed to the evaporator. This cycle is illustrated in figure 2.2.

Another cycle employs the principle of resorption. By recirculating liquid from the evaporator, the concentration of the liquid phase in the evaporator can be controlled so that the equilibrium vapour phase composition is equal to that of the fresh refrigerant. In theory, one hundred percent of the fresh refrigerant can be vaporised in this cycle and improved performance is obtained.

Cycles have been devised which employ a pump to enable the evaporator blowdown to be added downstream of the rich absorbent return pump (Bogart, 1981). However, the concept of replacing fresh refrigerant reflux to the distillation column with the returning liquid evaporator blowdown stream does not appear to have been proposed in the literature. This is surprising as the presence of absorbent contamination in the refrigerant stream is evidence of the potential for this approach. In contrast to the other cycles discussed in the previous paragraphs, this cycle does not minimise the fraction of fresh refrigerant appearing as liquid blowdown from the evaporator. Instead, the size of the liquid blowdown stream is controlled to ensure sufficient reflux to the distillation column.

Application of this concept to the conventional aqua - ammonia absorption refrigeration cycle appears to be attractive and worthy of further investigation. For this reason, the performance and cost of the aqua - ammonia absorption refrigeration cycle with evaporator blowdown reflux, was investigated in detail. In this chapter, the results of this investigation are presented. Simulation results are compared with the conventional aqua - ammonia absorption refrigeration cycle and the potential of the modified cycle is discussed.

8.1 Cycle Description

In the conventional absorption refrigeration cycle (figure 2.1), high purity refrigerant from the distillation column is condensed and collected in a reflux drum. A portion of this refrigerant is returned to the column as reflux and the rest is passed to the evaporator to provide useful refrigeration. Any absorbent contamination in the refrigerant is removed from the evaporator as a liquid by entrainment or blowdown.

Spent refrigerant vapour from the evaporator is dissolved/condensed in the absorption fluid and the resulting refrigerant rich absorbent is pumped to high pressure where the refrigerant is recovered from the absorbent by distillation.

If limited waste heat is available or if the heat supplied is valuable, fuel can be conserved by precooling the liquid refrigerant with spent refrigerant vapour from the evaporator (figure 8.1).

The modified cycle eliminates the use of refrigerant exiting the condenser as reflux to the distillation column. However, rectification is still achieved in the distillation column by returning liquid blowdown from the evaporator to the top of the column (figure 8.2). If required, precooling of the refrigerant can be achieved by heat exchange with the evaporator blowdown (figure 8.3) and by heat exchange with spent refrigerant vapour exiting the evaporator (figure 8.4).

In conventional designs, the liquid phase in the evaporator contains the bulk of any absorbent which was carried over from the distillation column. The presence of the absorbent reduces the fraction of the fresh refrigerant which can be boiled in the evaporator, with consequent reduction in performance. In the case of the aqua - ammonia cycle, the resulting liquid removed from the evaporator contains large quantities of ammonia refrigerant (approx 90%) which can not provide useful refrigeration. If the evaporator blowdown is passed to the absorber, additional absorbent is required to dissolve the additional refrigerant.

Useful refrigeration is also lost in conventional designs by using fresh refrigerant as reflux to the distillation column. In the modified cycle, the entire refrigerant stream is passed to the evaporator so that the maximum amount of refrigeration can be obtained per unit of column vapour overheads. In this way, only spent refrigerant is used as reflux to the distillation column. The combination of condenser and evaporator in the modified cycle could be viewed as a partial condenser for the distillation column.

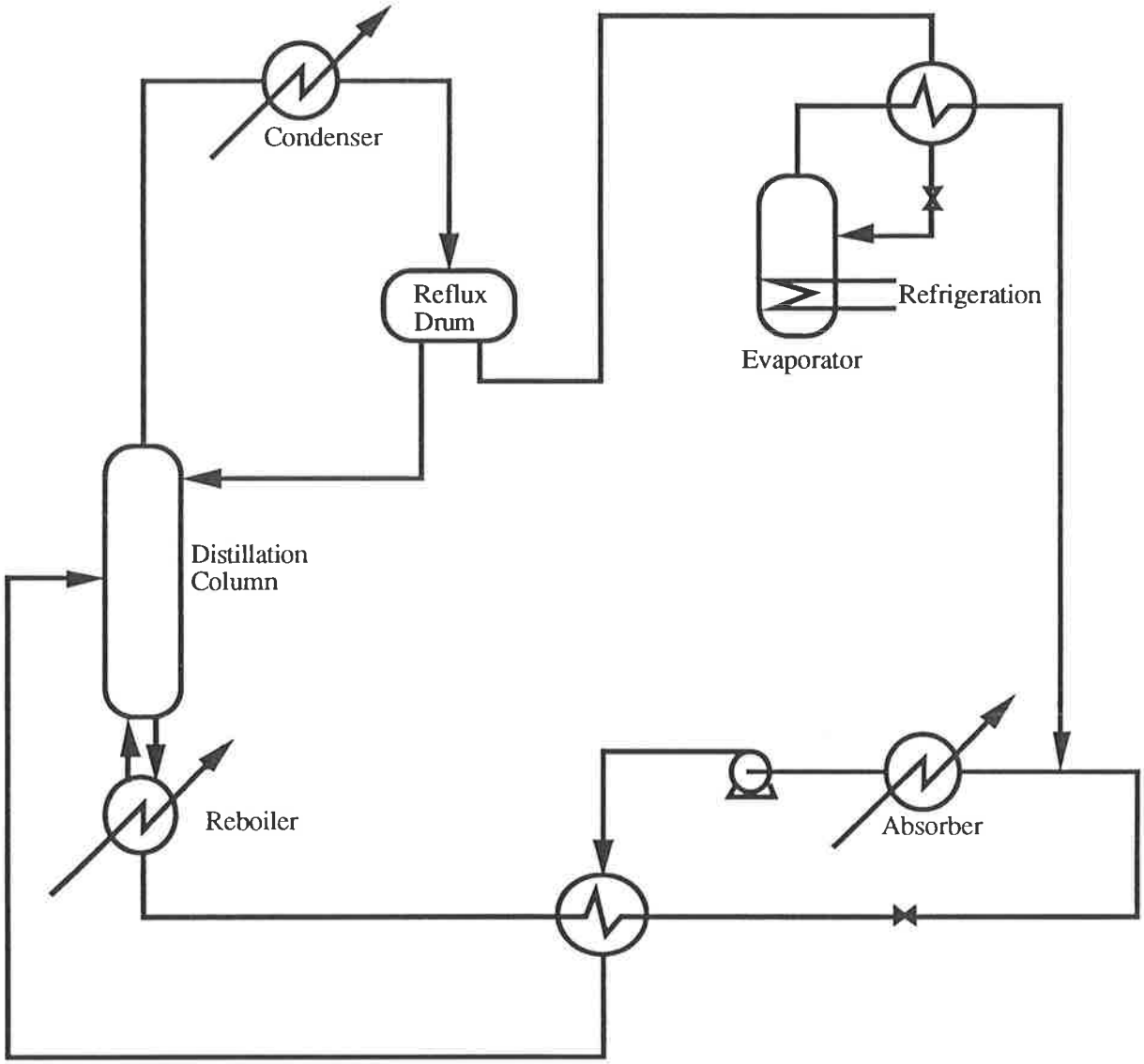

FIGURE 8.1: CONVENTIONAL ABSORPTION REFRIGERATION CYCLE WITH REFRIGERANT PRECOOLING

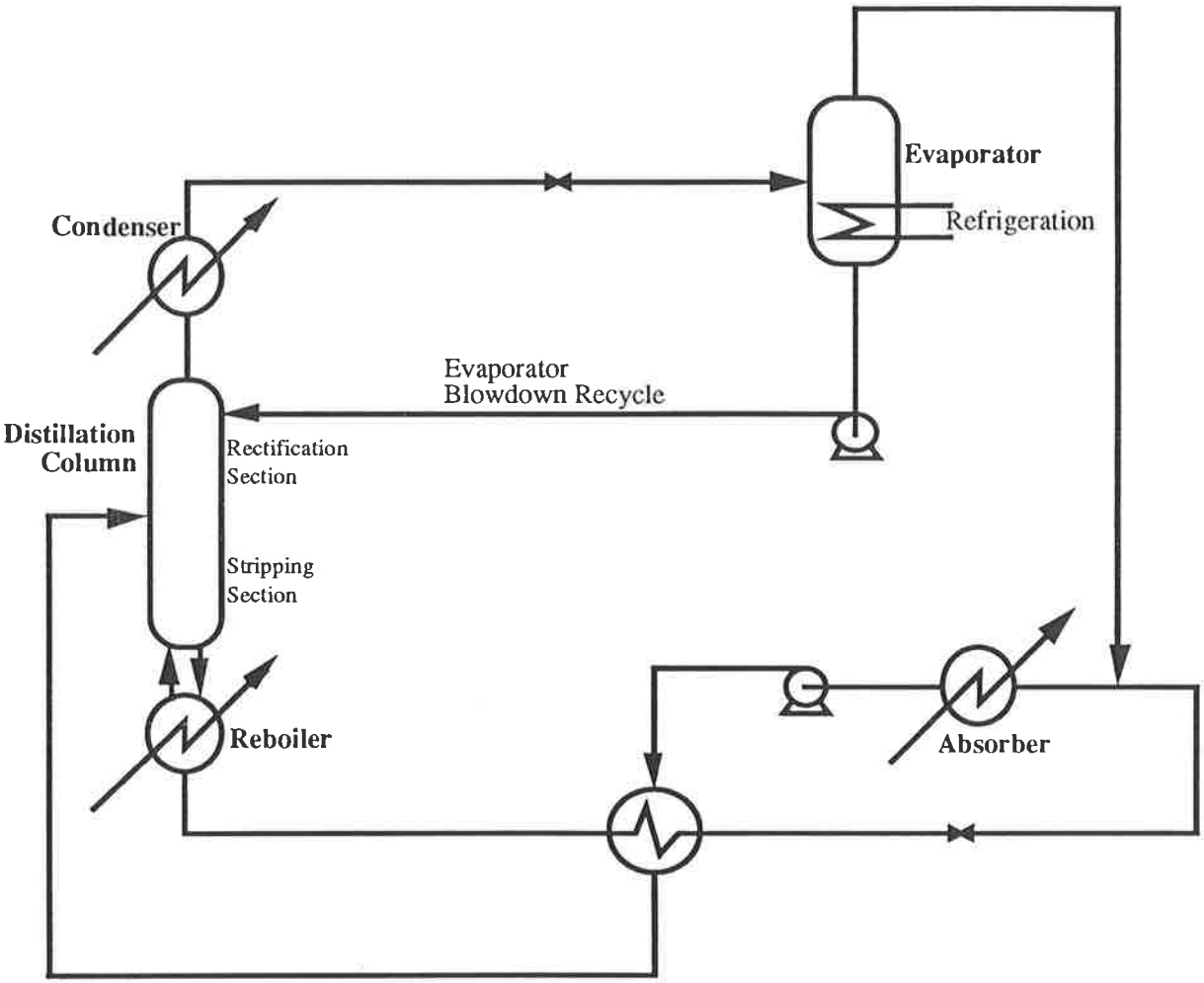

FIGURE 8.2: ABSORPTION REFRIGERATION CYCLE WITH EVAPORATOR BLOWDOWN RETURN

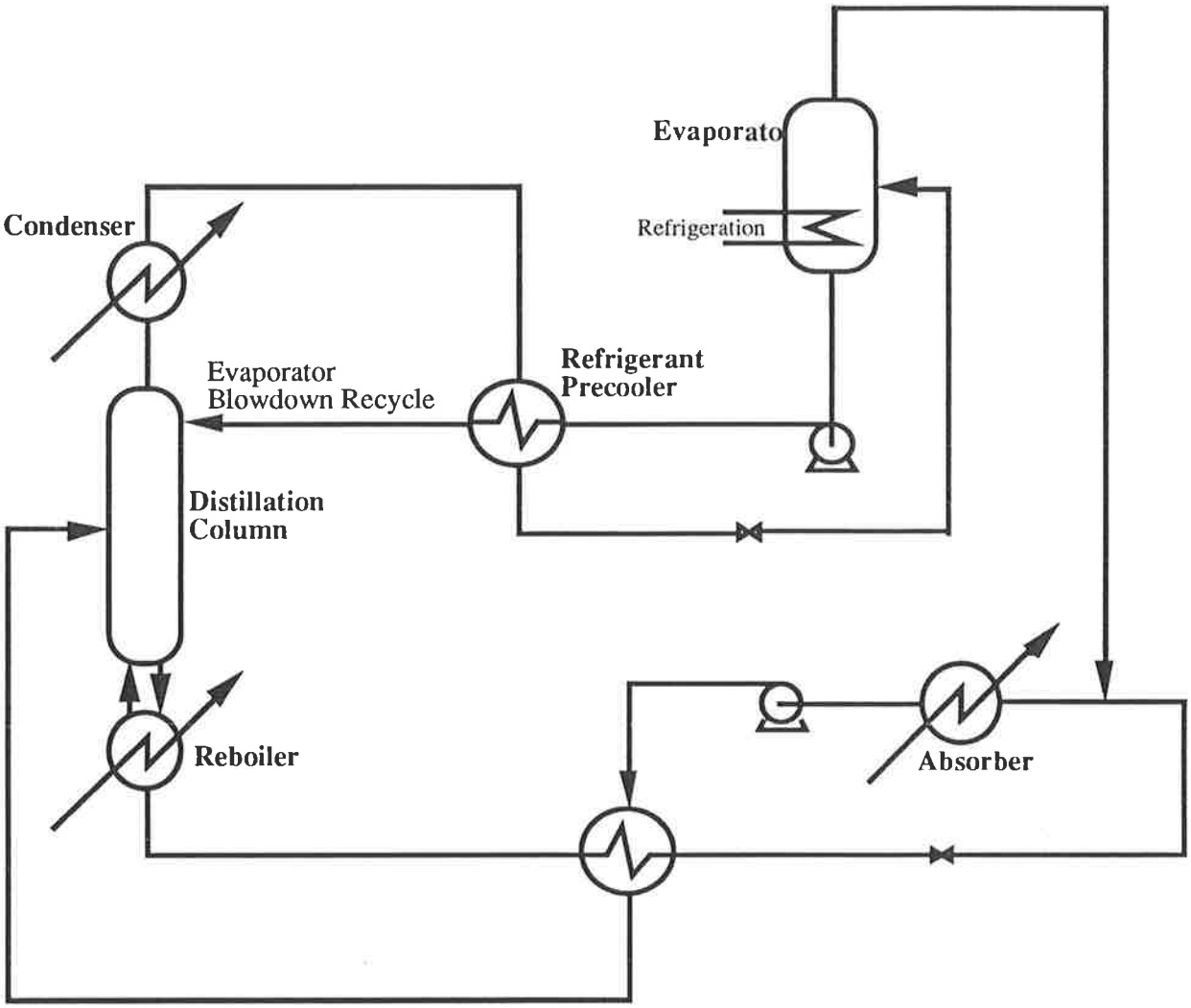

FIGURE 8.3: ABSORPTION REFRIGERATION CYCLE WITH EVAPORATOR BLOWDOWN RETURN AND PARTIAL REFRIGERANT PRECOOLING

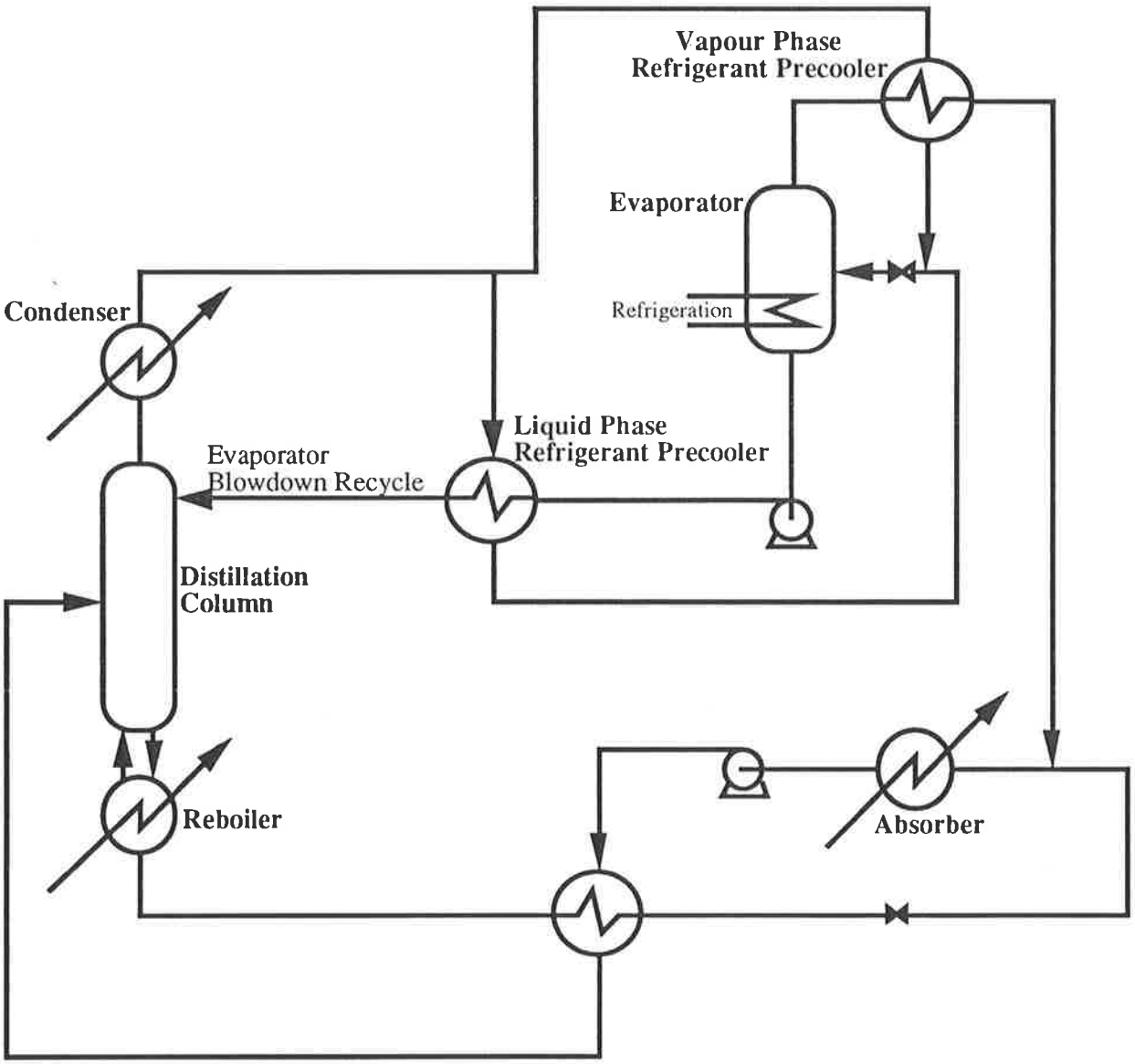

FIGURE 8.4: ABSORPTION REFRIGERATION CYCLE WITH EVAPORATOR BLOWDOWN RETURN AND FULL REFRIGERANT PRECOOLING

8.2 Computer Simulation of the Modified Cycle

Process simulations were conducted to assess the impact of recycling the evaporator blowdown on the performance and cost of the aqua-ammonia absorption refrigeration cycle. These simulations were conducted on the PROCESS^{TM} computer simulation package using the equation of state proposed by Ziegler and Trepp (1984) for predicting the thermodynamic properties of ammonia - water mixtures.

Clearly, there are a number of cycles which could have been chosen for comparison with the modified cycles illustrated in figures 8.2 to 8.4. The conventional cycle (figure 2.1) and the conventional cycle with refrigerant precooling (figure 8.1) were chosen for comparison. With the exception of the proposed modification, these cycles are identical to the modified cycle.

To ensure accurate comparison, all simulations were based on an absorber exit temperature of 44°C and a condenser temperature of 44°C. The generator temperature and the approach temperature in each of the heat recovery heat exchangers were varied to ensure that optimal performance was achieved. For the two conventional cycles, the evaporator liquid blowdown rate was also optimised.

In most simulations, the cycle was optimised by minimising the cost of the required heat exchangers at a fixed refrigeration duty of 0.69MW. This objective was chosen to reflect a scenario where cycle performance is of secondary importance, applicable when the cycle is fired by waste heat of low value. The use of total heat exchanger cost was chosen in place of the overall refrigerator cost to reduce calculation complexity. Experience has shown that this criteria can be used for comparitive estimation of total investment expenditure (Holldorf, 1979).

The heat exchanger cost equation employed in this study (Linhoff and Ahmad, 1990) is presented as equation 8.1. Additional assumptions used in the cost analysis are summarised in table 8.1.

$$\text{Cost} = \$10{,}000 + 350 \text{ area } (m^2) \qquad .....(8.1)$$

Overall Heat Transfer Coefficient (Refrigerant Vapour Heating)	50 W $m^{-2}K^{-1}$
Overall Heat Transfer Coefficient (Other Exchangers)	1000 W $m^{-2}K^{-1}$
Available Steam Temperature	170 °C
Refrig. Vapour Superheater Pressure Drop	12 kPa
Distillation Column Theoretical Plates	5

TABLE 8.1: ASSUMPTIONS IN THE CYCLE COST ANALYSIS.

Further discussion on the simulation procedure and simulation constraints is detailed in chapter 5.

The validity of the conventional aqua-ammonia absorption refrigeration cycle PROCESS model was tested by comparing the value of a number of key parameters calculated by the model with those obtained by other authors. The results of this comparison are presented in table 8.2. Values obtained from the PROCESS model appear to compare well other designs from the literature.

SOURCE	T_{EVAP}	X_{BOT}	ABSORBENT / REFRIGERANT RATIO	REFLUX RATIO	NOTES
Ludwig (1965)	−15°C	25.8 wt%	7.41	0.5-1.0	No account of blowdown
Bogart (1981)	5.6°C	29.4 wt%	1.97	0.11	Maximised heat recovery
Bogart (1981)	−29°C	17.4 wt%	6.05	0.15	Low temp. heat source
Bogart (1981)	16°C & 1.7°C	30.0 wt%	1.77	0.10	Dual evaporator
Bogart (1981)	−20°C	25.0 wt%	6.50	0.41	High value heat source
Bogart (1981)	−3.9°C	20.0 wt%	3.04	0.15-0.36	High temp. heat source
White	−10°C	18.7 wt%	3.68	0.32	This work (fig 8.5)

TABLE 8.2: COMPARISON OF THE CONVENTIONAL AMMONIA WATER ABSORPTION REFRIGERATION CYCLE MODEL WITH OTHER LITERATURE DESIGNS

8.3 Case Study of the Modified Cycle

Ammonia water absorption refrigeration has been successfully employed in ammonia manufacturing plants. In one application 12.6 MW (3580 tons) of refrigeration was required at −10°C (Holldorf, 1979). As a case study for comparison of the new technology, conventional and modified absorption refrigeration cycles were designed for this application. Design assumptions were similar to those discussed in section 8.2 except that the distillation column was increased to 7 theoretical stages and the cost objective function was altered to account for operating costs. Operating cost were calculated from the required cooling water valued at US$0.05 / tonne ($0.19 / 1000 gallon).

Process flow diagrams, including a complete listing of stream conditions, are presented in figures 8.5 and 8.6 for the optimised conventional and modified cycles with partial refrigerant precooling. Technical comparison of the two cycles highlight the following points:

(i) The required absorbent flowrate is lowered in the modified cycle. This results from the increased evaporator (and hence absorber) pressure.

(ii) The apparent reflux ratio is marginally reduced in the modified cycle. However, the actual reflux in the column is higher for the modified design as the returning reflux is sub-cooled. The increased actual reflux rate results from the lower ammonia composition in the modified cycle reflux stream.

(iii) The reflux return pump duty has a negligible effect on the COP in both designs.

(iv) Evaporator blowdown accounts for 23.9% and 5.2% of the evaporator feed in the modified and conventional designs respectively. The increased evaporator blowdown flowrate is required to maintain the optimum reflux flow-rate to the distillation column.

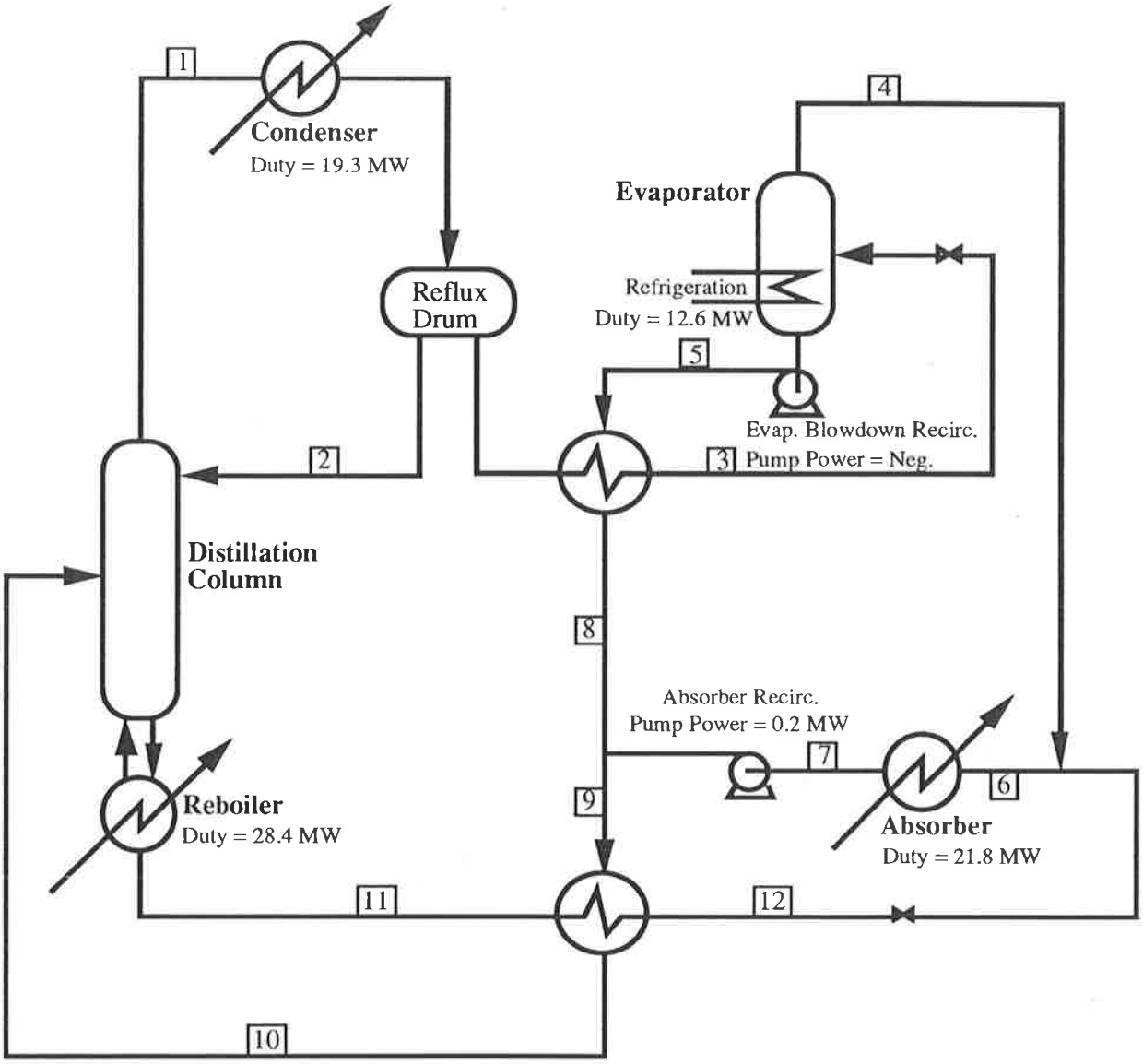

STREAM NO	1	2	3	4	5	6	7	8	9	10	11	12
Flow (kmol h^{-1})	3552	853	2699	2559	140	12032	12032	140	12172	12172	9474	9474
Conc. (mol %)	99.7	99.7	99.7	100.0	94.3	36.72	36.72	94.3	37.38	37.38	19.6	19.6
Temperature (°C)	63.6	44.0	41.6	-10.0	-9.4	67.4	44.0	40.0	45.1	113.9	152.6	59.5
Pressure (atm)	17.1	17.1	17.1	2.712	17.1	2.712	2.592	17.1	17.1	17.1	17.1	17.1
Heat Flow (MW)	?	0.84	2.51	15.17	-0.06	19.22	-2.61	0.10	-2.33	17.02	23.4	4.06
Liquid Fraction	0.0	1.0	1.0	0.0	1.0	0.831	1.0	1.0	1.0	1.0	1.0	1.0

FIGURE 8.5: CONVENTIONAL CYCLE WITH PARTIAL REFRIGERANT PRECOOLING

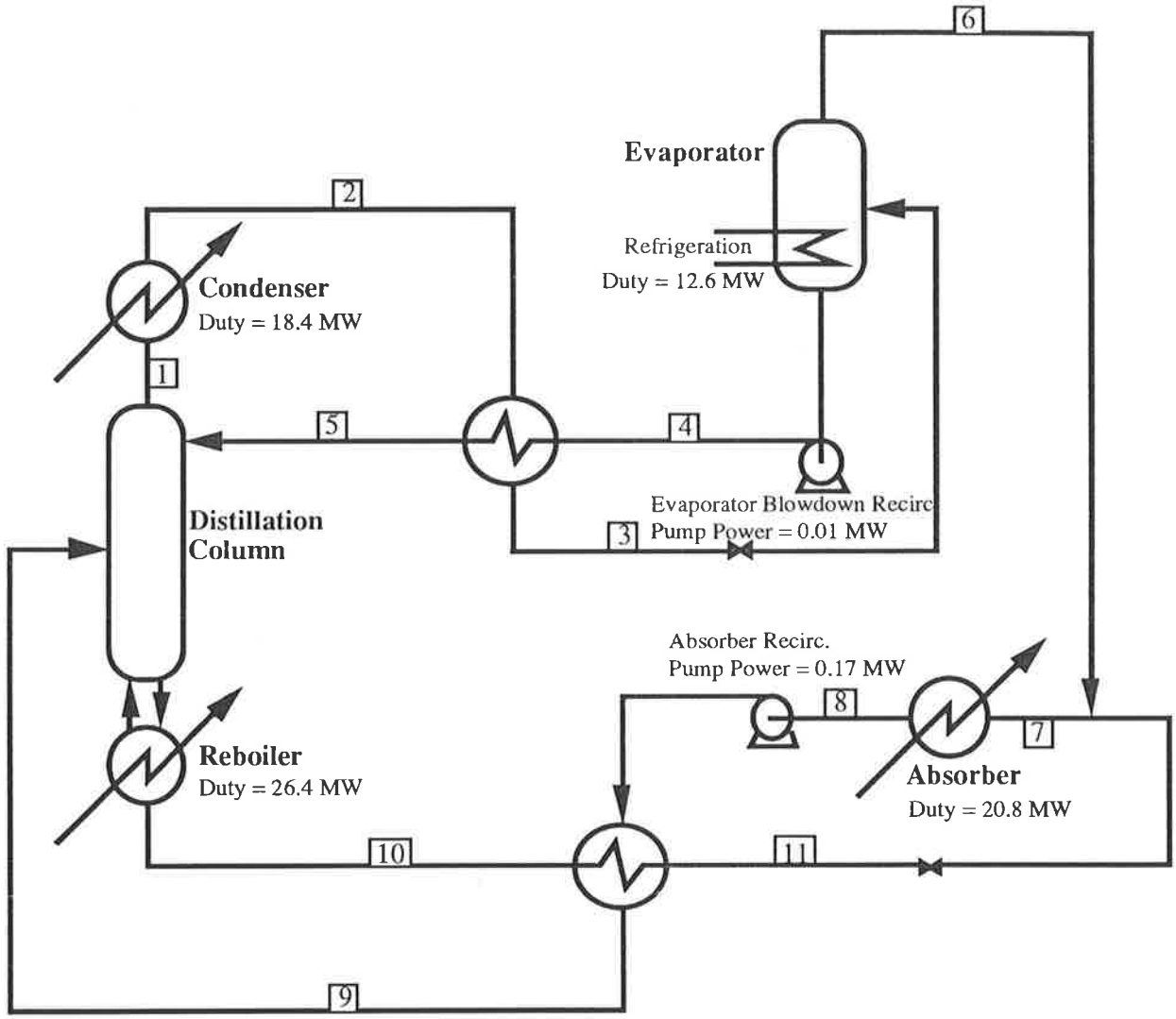

STREAM NO	1	2	3	4	5	6	7	8	9	10	11
Flowrate (kmol h^{-1})	3378	3378	3378	807	807	2570	11611	11611	11611	9041	9041
Concentration (mol %)	99.70	99.70	99.70	98.78	98.78	100.0	37.45	37.45	37.45	19.67	19.67
Temperature (°C)	63.5	44.0	32.3	-9.4	41.7	-10	67.0	44.0	114.6	152.5	54.9
Pressure (atm)	17.05	17.05	17.05	17.1	17.1	2.831	2.831	2.711	17.1	17.05	17.05
Heat Flow (MW)	21.70	3.34	2.41	-0.20	0.73	15.22	18.20	-2.58	16.93	22.31	2.98
Liquid Fraction	0.0	1.0	1.0	0.0	1.0	0.0	0.831	1.0	1.0	1.0	1.0

FIGURE 8.6: MODIFIED CYCLE WITH PARTIAL REFRIGERANT PRECOOLING

An investment summary for the conventional aqua-ammonia absorption refrigeration cycle with partial refrigerant heat recovery is presented in table 8.3. This cycle was the most attractive of the conventional cycles, making it ideal for economic comparison with the modified cycle.

Table 8.3 includes capital and operating costs for the refrigeration unit. The capital cost of the refrigeration unit was obtained by factoring the cost of each item of process equipment. A factor of 5.7 was used to reflect the cost of plant installed at a "green-field" site (Peters and Timmerhaus, 1990). Process equipment costs were obtained from graphs presented by Peters and Timmerhaus (1990).

Refrigeration Duty (MW)	12.6
Capital Investment ($US 1990)	7,110,000
COP	0.4443
Cooling Water Cost ($/yr)	1,106,000

TABLE 8.3: CONVENTIONAL ABSORPTION REFRIGERATION CYCLE INVESTMENT SUMMARY

A comparative investment summary for the modified cycle is presented in table 8.4. In this table, the additional capital expense incurred in two examples of the modified cycle is compared with the savings obtained in operating costs. The two modified cycles examined are the modified cycle with partial refrigerant precooling (figure 8.3) and the modified cycle with full refrigerant precooling (figure 8.4)

Savings in heat exchanger capital cost are offset by the additional expense of the positive displacement evaporator blowdown return pumps. A small (<1%) increase in capital cost results. Heat exchanger surface area is greater in the modified cycle with full refrigerant heat recovery. Consequently, capital cost is increased and operating costs are reduced. The investment returns presented in table 8.4 show that the additional cost of both modified cycles is easily justified on the cooling water savings alone. The modified cycle would be even more attractive if value was placed on the waste heat consumed in the reboiler.

	Modified Cycle With Partial Precooling	Modified Cycle With Full Precooling
Refrigeration Duty (MW)	12.6	12.6
COP	0.4759	0.4782
Capital Cost Increase ($US 1990)	$22,500	$45,400
Cooling Water Savings ($/yr)	$50,800	$54,200
Return On Investment	226%	119%
Pay Back Time (yrs)	0.44	0.84
Incremental NPV* ($ 1990)	$147,800	$136,300

* 15 % discount rate over 5 years

TABLE 8.4: MODIFIED ABSORPTION CYCLE INVESTMENT SUMMARY

8.4 Results of the Modified Cycle Computer Simulations

For each of the five aqua-ammonia absorption refrigeration cycles (figures 2.1 and 8.1 to 8.4), the minimum total cost of the required heat exchangers was determined over a range of evaporator temperatures between 4°C and −12°C. These results are plotted in figure 8.7. The corresponding coefficients of performance obtained in these simulations are presented in figure 8.8 as a function of evaporator temperature.

The capital cost of the heat exchangers in the modified cycle without refrigerant heat recovery was approximately 2.7% less than that of the equivalent conventional cycle. Also, the performance of the modified cycle was approximately 5% greater than the performance of the conventional cycle.

The total capital cost of the heat exchangers in the modified cycle with partial refrigerant pre-cooling was higher than that in the modified cycle without refrigerant pre-cooling due to the increased number of heat exchange units. However, the heat exchange surface area was reduced in this design. In larger refrigeration units, where the fixed charge on each heat exchanger is small compared to the variable charge for increasing heat exchange surface area, the modified cycle with partial refrigerant precooling may be less expensive than the cycle without refrigerant heat recovery.

For the given cost objective function, the cycles with full refrigerant precooling were less attractive due to poor heat transfer and increased pressure drop in the refrigerant vapour superheater.

Within the expected error of these simulations, the coefficients of performance (COP's) obtained for each of the three cycles with refrigerant pre-cooling were identical. The similarity between the two modified cycles with refrigerant pre-cooling can be explained by the size of the refrigerant vapour superheater. When optimised, this heat exchanger becomes very small. Hence, the modified cycle with full precooling is essentially the same as the cycle with partial precooling. The similarity with the conventional cycle with full precooling appears to be fortuitous.

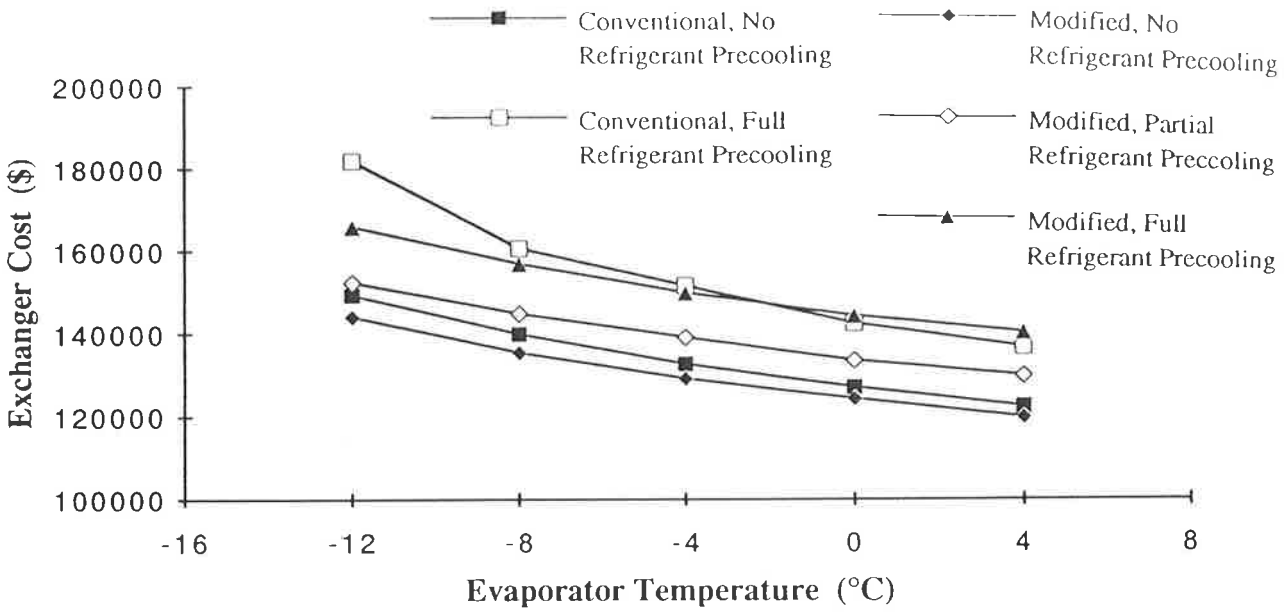

FIGURE 8.7: COMPARISON OF CONVENTIONAL AND MODIFIED CYCLE HEAT EXCHANGER COSTS

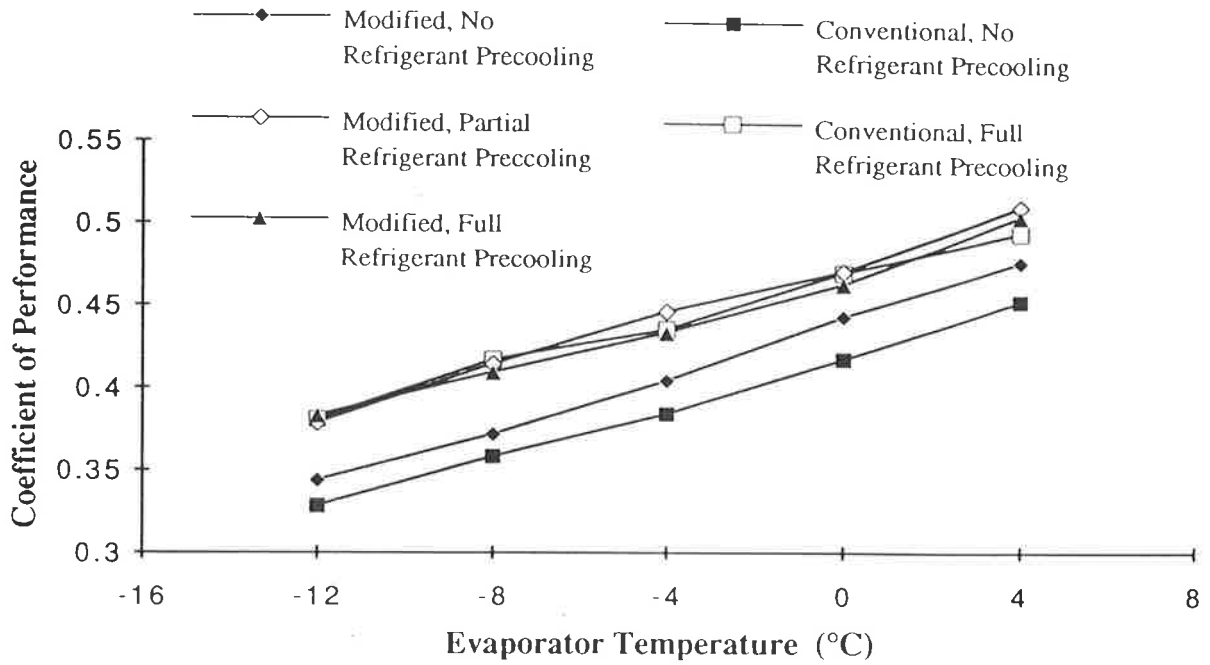

FIGURE 8.8: COMPARISON OF CONVENTIONAL AND MODIFIED CYCLE THERMODYNAMIC PERFORMANCE

On average, the coefficient of performance of the cycles with refrigerant precooling were a further 8.3% greater than the coefficients of performance obtained for the modified cycle without refrigerant precooling.

To investigate the effect of constraints placed on the available heat source, the simulations were repeated with the generator temperature held constant at 120°C. Under these conditions, the influence of evaporator temperature on the minimum heat exchanger cost is presented in figure 8.9.

The capital cost of the required heat exchangers in the modified cycle was less than that required for the equivalent conventional cycle. Indeed, as the evaporator temperature approached the lower feasible operating limit, the difference between the cost and performance of the two cycles increased. At an evaporator temperature of −12°C the cost of the heat exchangers for the modified cycle was 17% below that of the equivalent conventional cycle.

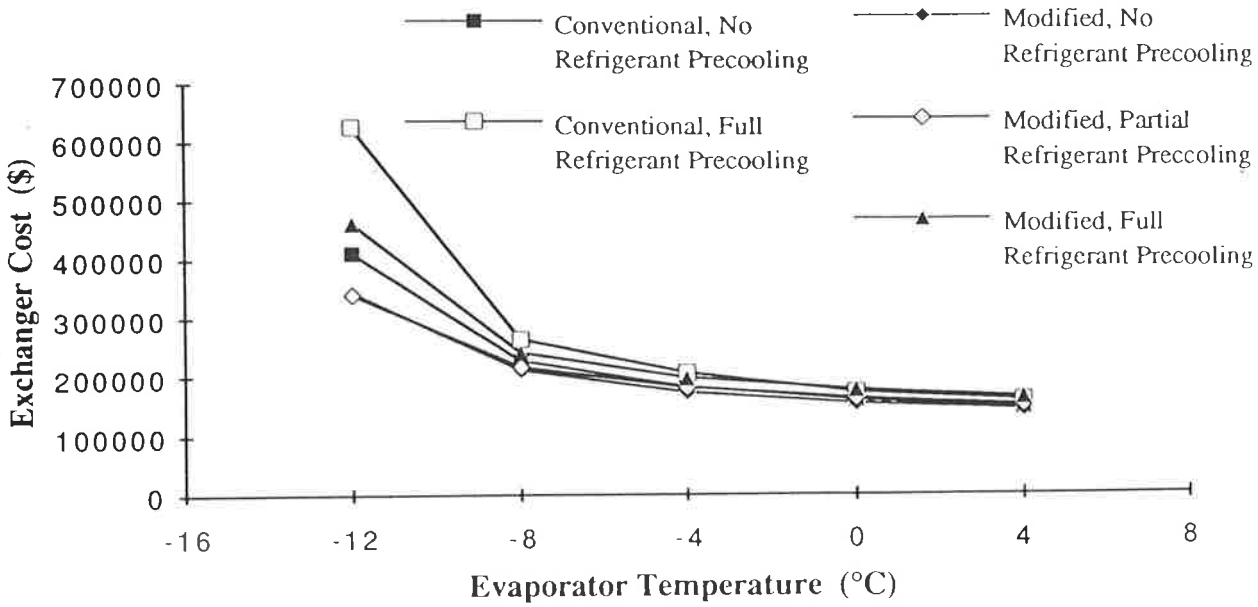

FIGURE 8.9: COMPARISON OF CONVENTIONAL AND MODIFIED CYCLE HEAT EXCHANGER COSTS WITH GENERATOR TEMPERATURE FIXED AT 120°C

The condenser / evaporator combination in the modified cycle may be viewed as a partial condenser for the distillation column. If this were the case, the improvement in performance obtained from the modified cycle could reflect the influence of placing an extra stage in the distillation column only.

To investigate this hypothesis, a number of simulations of the modified and conventional cycles were conducted to investigate the influence of increasing the number of theoretical stages in the distillation column on cost and thermodynamic performance. The results of these simulations are presented in Figure 8.10. The curves presented in figure 8.10 are not smooth because the feed location must be an integral number of plates from the top of the column.

In all cases, the capital cost of the heat exchangers in the modified cycle was lower than that obtained from the conventional cycle. Clearly, figure 8.10 demonstrates that the improvement in performance obtained from the modified cycle cannot be represented solely by the addition of an extra theoretical plate to the distillation column.

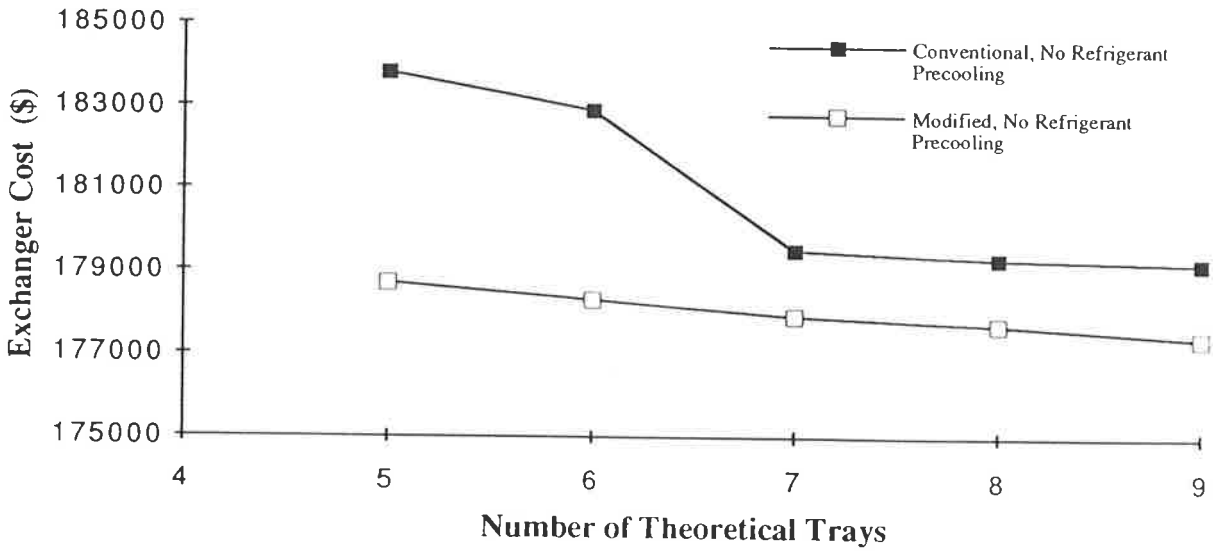

FIGURE 8.10: INFLUENCE OF INCREASING THE NUMBER OF THEORETICAL TRAYS ON CONVENTIONAL AND MODIFIED CYCLE HEAT EXCHANGER CAPITAL COST

The performance of the conventional aqua-ammonia absorption refrigeration cycle is maximised when the refrigerant purity is very high (approx. 99.9wt% NH_3) and drops off as refrigerant purity decreases. Simulations were conducted to investigate the sensitivity of the conventional and modified cycles, without refrigerant pre-cooling, to changing refrigerant purity. In these simulations, refrigerant purity was varied by changing the column pressure at a constant condenser temperature. The results of these simulations are illustrated in figure 8.11.

Figgure 8.11 shows that high purity ammonia refrigerant is required for optimum performance of the modified aqua-ammonia absorption refrigeration cycle. However, the decrease in performance due to increasing water contamination is not as dramatic as that seen in the conventional cycle. This results in a more robust cycle which is more resilient to column foaming or entrainment.

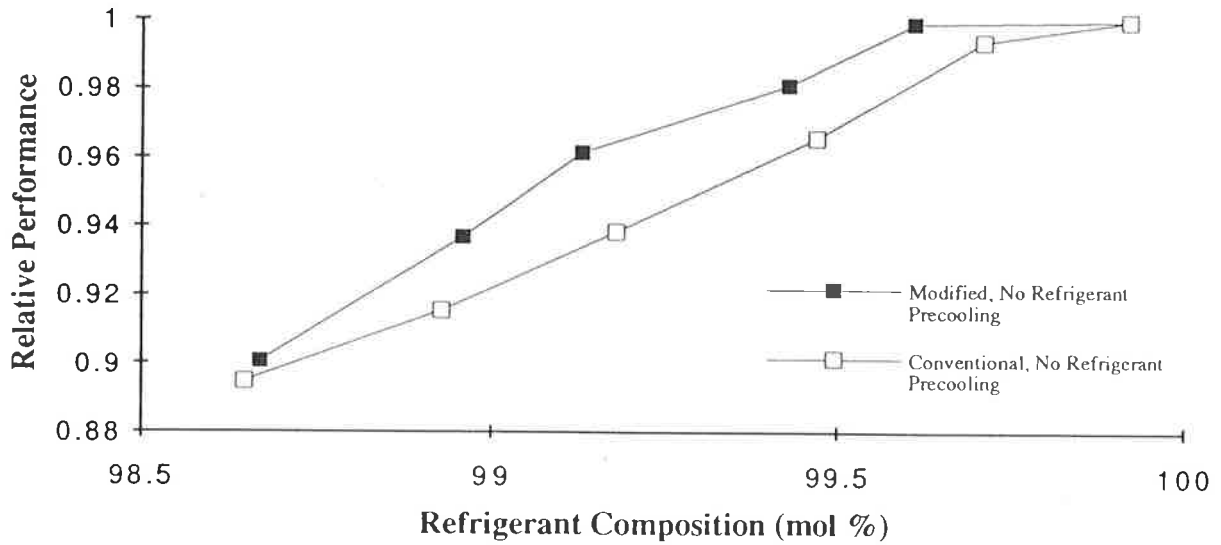

FIGURE 8.11: INFLUENCE OF REFRIGERANT COMPOSITION ON CONVENTIONAL AND MODIFIED CYCLE PERFORMANCE.

8.5 Discussion

On inspection, the proposed absorption refrigeration cycle with evaporator blowdown recycle is very similar to the conventional cycle. However, significant improvements to cycle performance are obtained with negligible increase in capital cost. The following discussion details the reasons for the improved performance obtained from the modified cycle.

8.5.1 Absorbent Flowrate

The reduced circulation rate of absorbent required in the modified cycle is the principal reason for improved performance compared with the conventional cycle.

In order to maintain optimum reflux to the distillation column, a much larger fraction of refrigerant entering the evaporator is returned to the distillation column. Consequently, the composition of the liquid blowdown from the evaporator is richer in refrigerant and, for a given evaporator temperature, the resulting evaporator pressure must be higher. This, in turn, leads to increased pressure in the absorber so that less absorbent is required to dissolve the refrigerant vapour exiting the evaporator.

In conventional designs, the evaporator blowdown is considerably richer in ammonia than the strong absorbent exiting the absorber. (This fact can be deduced by comparing the compositions of saturated liquid mixtures at the temperature of the evaporator and of the absorber). Consequently, additional absorbent is required to dissolve the liquid blowdown stream. By eliminating the practice of "dumping" liquid from the evaporator to the absorber, further reductions in absorbent flowrate can be achieved.

The reduction in required absorbent circulation rate in the modified cycle leads to reduced losses in the heat recovery exchanger and reduced sensible heating losses in the distillation column.

8.5.2 Exergy Losses

Major sources of losses in absorption refrigeration machines result from the following;

(i) The mixing of streams with different composition.

(ii) Flashing of refrigerant across the expansion valve.

(iii) Indirect heat transfer with finite thermal driving force.

In particular, losses occur in the conventional absorber due to mixing of the evaporator blowdown (approx 94 mol% ammonia) with absorption fluid (approx 36.7 mol% ammonia after refrigerant vapour has been absorbed). In the modified cycle, the evaporator blowdown is fed to the top of the distillation column where the concentration of ammonia in the fluid is similar to that of the evaporator blowdown liquid. Consequently, mixing losses are reduced.

Further reductions in cycle losses result from the lower flowrate of absorbent in the modified cycle. This leads to reduced losses in the heat recovery heat exchangers, distillation column and absorber.

An exergy analysis was conducted on both the conventional and modified cycles to further determine the source of the reduced losses observed in the modified absorption refrigeration cycle. The analysis was based on stream availabilities calculated by the PROCESS simulation package using the equation of state proposed by Ziegler and Trepp (1984). The results of this analysis are presented in table 8.5 for a 0.76MW refrigerator. Availability losses calculated by Briggs (1971) are also presented in table 8.5 for comparison.

Availability losses calculated in this study compare reasonably well with those presented by Briggs, with the exception of the absorber and the heat recovery exchanger. In this study, there is a nett gain of work in the absorber. This is due to the 15°C reference temperature employed in this study and the use of cooling water entering at 27°C as the heat sink. Briggs assumed that heat was rejected from the absorber to the heat sink at the reference temperature. Small losses obtained by Briggs in the heat recovery exchanger reflect the close approach temperature (1.1 K) assumed. In this study, the optimal approach temperature was calculated to be 8.8 K.

	Conventional Cycle (Briggs, 1971)	Conventional Cycle	Modified Cycle with Partial Pre-cooling
Evaporator	36.8 kW	53.3 kW	48.4 kW
Refrigerant pre-cooler	3.7	–	3.9
Absorber recirc. pump	5.8	4.2	4.5
Refrigerant recirc. pump	–	0.05	0.37
Absorber	169.0	−55.9	−60.6
Evap Blowdown Absorption	–	2.0	–
Heat recovery exchanger	12.6	62.6	60.7
Distillation column	230.8	319.8	312.7

TABLE 8.5: COMPARISON OF CYCLE EXERGY LOSSES

Detailed examination of this table does not highlight any dramatic savings of work. The reduction in losses obtained in the modified cycle evaporator are primarily due to the refrigerant precooler. Small reductions in losses associated with the heat recovery exchanger and the distillation column, are due to the reduced circulation rate of absorbent as discussed above.

Chapter 9
CONCLUSIONS

Background

Recent papers (Briggs, 1971 and Karakas,1990) have shown that the majority of losses in the conventional absorption refrigeration cycle are confined to the absorber and the generator. Dalichaouch (1990) also showed that, over a wide range of conditions, the performance of the conventional absorption refrigeration cycle is less than thirty percent of the performance predicted by the ideal second law.

Clearly, there is significant room for improvement in cycle performance. Bearing this in mind, investigations were conducted on a novel absorption refrigeration cycle which employs a liquid - liquid separation step to separate the absorbent from the refrigerant. The cycle was chosen for further examination with the intention of demonstrating the feasibility of eliminating the distillation column generator in an absorption cycle heat pump. This could lower capital costs and reduce one of the major sources of exergy losses.

The Thermodynamics of Working Fluid Mixtures

In addition to those characteristics which are desirable for absorbent - refrigerant pairs in the conventional absorption refrigeration cycle, suitable absorbent - refrigerant pairs for the novel cycle must exhibit "lower critical solution temperature behaviour" when mixed. Consequently, a number of low molecular weight tertiary amine - water pairs were selected as suitable candidate pairs for application in the novel absorption refrigeration cycle.

To simulate the performance of the novel cycle, an accurate thermodynamic model was required to predict mixture phase equilibria at all points in the cycle. A five parameter NRTL model was developed for this purpose. For each refrigerant - absorbent pair, the five parameters were obtained by fitting the model to experimental vapour - liquid equilibrium data by least squares regression.

Subsequent simulations of cycle performance employed a "black box" separator for the liquid phase separation step, because no thermodynamic model was found capable of accurately simulating the combined temperature dependent vapour - liquid and liquid - liquid phase equilibria.

Experimental Results

Unfortunately, not all of the required experimental data was available for the selected absorbent - refrigerant pairs. Consequently, experimental vapour - liquid and liquid - liquid equilibrium studies were conducted on dimethylethylamine - water and trimethylamine - water mixtures. Liquid phase immiscibility had not previously been reported for either of these mixtures.

In this study, liquid phase separation was achieved for mixtures of dimethylethylamine and water at temperatures above 99°C and at concentrations between 5 mol% and 37 mol% amine. Liquid phase separation was not observed for mixtures of trimethylamine and water at temperatures up to 160°C. However, with the addition of 3 wt% sodium chloride, liquid phase separation was achieved at temperatures above 130°C. Unfortunately, significant uncertainty is associated with the liquid phase co-existence curve obtained for mixtures of trimethylamine, water and salt. This uncertainty results, primarily, from the high pressure and consequently high evaporation losses inside the sample ampoules at experimental conditions.

Vapour - liquid equilibrium data was obtained in a static equilibrium apparatus for dimethylethylamine - water and trimethylamine - water mixtures between 10°C and 50°C. Vapour pressure data was obtained over the entire concentration range for mixtures of dimethylethylamine and water. Unfortunately, vapour pressure data could only be obtained over a limited concentration range at temperatures above 20°C for mixtures of trimethylamine and water. For high concentrations of trimethylamine, the vapour pressure was too high to be measured on the mercury manometer.

The Novel Absorption Refrigeration Cycle

The basic novel absorption cycle heat pump was simulated on a computer using the PROCESS™ chemical plant simulation software package. Results of these simulations, using diethylmethylamine and water as the refrigerant - absorbent pair, showed that refrigeration could only be obtained over a limited range of temperatures. Performance fell dramatically with decreasing evaporator temperature. The performance of the cycle with dimethylethylamine and water as the working fluid pair was worse because of the higher water (absorbent) content in the refrigerant.

Thermodynamic analysis of the cycle demonstrated that the boiling point elevation between the refrigerant and the absorbent must be zero at the high pressures required in the liquid phase separation drum. Clearly, the rate of change in this boiling point elevation, with decreasing pressure, is insufficient to obtain a reasonable boiling point elevation between the evaporator and the absorber in the novel absorption refrigeration cycle.

Unfortunately, there are very few alternative mixtures which exhibit the required liquid - phase behaviour. For these reasons, the novel absorption refrigeration cycle is unlikely to find commercial application. However, the feasibility of the novel cycle was successfully demonstrated. This result confirms that it is possible to eliminate the necessity for refrigerant vaporisation in the generator and, consequently, it is possible to replace the distillation column with a more thermodynamically efficient unit operation.

The Novel Absorption Refrigeration Cycle With Distillation

The potential of a number of cycles containing both the liquid phase separation step and the distillation step for recovering refrigerant, was also investigated. The performance of these "hybrid" cycles were simulated using PROCESS™ to determine the optimum cycle configuration. Dimethylethylamine and water were used as the working fluids in these simulations because the normal boiling point of dimethylethylamine is significantly lower than that of diethylmethylamine.

One of the cycles developed employed the additional distillation step to further purify the absorbent stream after initial refrigerant recovery was achieved in the liquid phase separation drum. Due to the significant level of absorbent contamination in the refrigerant stream, the concept of returning the evaporator blowdown to the generator (initially applied to the basic novel absorption cycle only) was employed in this cycle. In this case, the evaporator blowdown recycle stream was employed as reflux to the distillation column. This concept was subsequently applied to the conventional aqua - ammonia absorption refrigeration cycle with encouraging results.

Despite this advance, the performance of each of the novel absorption refrigeration cycles including the additional distillation step was worse than the performance of the conventional absorption refrigeration cycle employing the same working fluids. Surprisingly, the novel cycle with the best thermodynamic performance employed the distillation column to rectify the refrigerant phase exiting the liquid phase separation drum. In this cycle, all of the fresh refrigerant must be evaporated and condensed prior to entering the evaporator at low pressure, which defeats the initial purpose of investigating cycles which employ the liquid phase separation step.

Simplified Analysis for Cycles With Trimethylamine and Water

Due to the poor experimental results obtained for mixtures of trimethylamine and water, the potential of the novel absorption refrigeration cycles with trimethylamine as the refrigerant was not examined in detail. Instead, the absorbent flowrate required to completely dissolve refrigerant vapour of assumed concentration, was determined as a ratio of the refrigerant vapour flowrate. By comparison with the conventional ammonia - water working fluid pair, the trimethylamine - water working fluid pair was shown to have no commercial potential in any of these absorption refrigeration cycles.

The Novel Absorption Cycle Heatpump

The previous cycles employed mixtures exhibiting lower critical solution temperature behaviour as working fluids in novel absorption refrigeration cycles. In a further development of this concept, a type II heat pump cycle was proposed and developed. The cycle employs working fluid mixtures exhibiting upper critical solution temperature behaviour. The cycle accepts heat at some intermediate temperature level and rejects a portion of this heat at high temperature.

The performance of this cycle was simulated on the PROCESS™ chemical plant simulation package using cyclohexane and aniline as the working fluids. This working fluid pair was considered ideal as a very large boiling point difference exists between the two compounds and liquid phase separation occurs over a large concentration range at ambient temperature.

Results of these simulations showed that the boiling point elevation which could be achieved between the evaporator and the absorber, with these working fluids, was less than 10 K. Performance was also shown to fall dramatically with increasing absorber temperature. Poor performance was attributed to the high absorbent circulation rate required.

A number of alternative heat pump cycles including the liquid phase separation step and an additional distillation step were also investigated. Unfortunately, the rate of decrease in the bubble point temperature for mixtures of cyclohexane and aniline is very low at cyclohexane concentrations between 30% and 100%. Consequently, the addition of volatile working fluid phase rectification or absorbent phase stripping steps does not significantly increase the boiling point elevation which can be achieved between the evaporator and the absorber.

Increased boiling point elevations were achieved, however, when the liquid phase separation step was applied to the evaporator blowdown stream. Unfortunately, the small size of this stream, the complex heat recovery network required and the low refrigerant purity required to make this cycle feasible resulted in poor thermodynamic performance compared to that obtained in the conventional type II heat pump employing the same working fluid pair.

The Modified Aqua - Ammonia Absorption Refrigeration Cycle

While the feasibility of each of the cycles discussed above was demonstrated, commercial application of these cycles is unlikely due to the low boiling point elevations achieved and the poor cycle thermodynamic performance.

However, these simulations successfully highlighted the potential of recycling the evaporator blowdown in order to supply reflux to the rectification section of the conventional absorption cycle distillation column. This modification to the conventional cycle was simulated on PROCESS™ using the thermodynamic model proposed by Ziegler and Trepp (1984) for predicting the phase behaviour of ammonia - water mixtures.

Over a wide range of conditions, these simulations indicate a reduction in total heat exchange surface area and an increase in thermodynamic performance of approximately five percent (5%) when the modified cycle is compared with the conventional aqua - ammonia absorption refrigeration cycle.

As a much larger fraction of refrigerant entering the evaporator is returned to the distillation column in the modified absorption refrigeration cycle, the composition of the liquid blowdown from the evaporator is richer in refrigerant. Thus, for a given evaporator temperature, the resulting evaporator/ absorber pressure must be higher so that absorbent circulation rates can be reduced. This is the primary reason for the improved performance of the modified cycle.

Recommendations

The results of this study indicate that the conventional absorption cycle heat pump distillation column generator can be replaced by alternative separation techniques. However, the alternative separation technique of liquid phase separation explored in this thesis, did not prove attractive when compared with the conventional cycle. Consequently, further examination of liquid phase separation in an absorption cycle heat pump should be abandoned. Other separation techniques such as fractional crystallisation or membrane filtration are worthy of further investigation.

An interesting modification to the conventional absorption refrigeration cycle, arising from this work, was the application of evaporator blowdown recycle to provide reflux to the rectification section of the conventional distillation column. This modification was shown to provide efficiency improvements with a nett reduction in heat transfer surface area. Consequently, pilot scale demonstration of this cycle is recommended.

Appendix A
EXPERIMENTAL DATA

T °C	P mmHg
5.54	228.88
10.31	282.02
14.92	338.79
14.97	342.59
19.56	409.27
24.51	492.89
26.44	532.39
31.36	632.56
31.90	646.87
34.69	714.29
38.87	825.51
41.51	903.70
44.85	1005.52
48.41	1126.12

TABLE A.1: VAPOUR PRESSURE DATA FOR DIMETHYLETHYLAMINE

T °C	X_{dmea}	P mmHg	T °C	X_{dmea}	P mmHg	T °C	X_{dmea}	P mmHg
10.01	0.0174	32.04	19.53	0.0174	61.85	29.17	0.0174	119.56
	0.0618	87.58		0.0618	150.61		0.0618	254.48
	0.1656	123.74		0.1656	200.63		0.1656	314.76
	0.2533	155.57		0.2533	244.86		0.2533	373.56
	0.3385	186.87		0.3385	283.37		0.3385	423.22
	0.4885	233.3		0.4885	337.65		0.4885	487.48
	0.6077	242.54		0.6077	358.00		0.6077	515.53
	0.7363	255.42		0.7363	374.41		0.7363	541.89
	0.8081	260.22		0.8081	384.50		0.8081	560.00
	0.8719	267.72		0.8719	391.35		0.8719	564.29

T °C	X_{dmea}	P mmHg	T °C	X_{dmea}	P mmHg
38.91	0.0174	219.16	48.59	0.0174	366.38
	0.0618	409.08		0.0618	629.69
	0.1656	490.60		0.1656	735.90
	0.2533	560.93		0.2533	815.21
	0.3385	618.91		0.3385	881.24
	0.4885	699.16		0.4885	972.09
	0.6077	735.28		0.6077	1012.42
	0.7363	742.14		0.7363	1053.86
	0.8081	785.45		0.8081	1083.29
	0.8719	798.04		0.8719	1096.40

TABLE A.2: VAPOUR - LIQUID EQUILIBRIUM DATA FOR DIMETHYLETHYLAMINE - WATER MIXTURES

T °C	X_{tma}	P mmHg	T °C	X_{tma}	P mmHg	T °C	X_{tma}	P mmHg
10.66	0.0034	32.04	19.88	0.0034	34.18	24.43	0.6483	1373.90
	0.0336	75.05		0.0336	133.89		0.8320	1466.60
	0.0614	143.21		0.0614	236.34			
	0.0803	168.50		0.0803	276.08			
	0.1630	382.83		0.1630	562.15			
	0.2062	396.34		0.2062	577.67			
	0.3127	540.49		0.3127	764.71			
	0.5305	736.80		0.5305	1031.33			
	0.5639	761.29		0.5639	1052.13			
	0.6358	837.22		0.6358	1120.92			
	0.6480	810.73		0.6480	1119.45			
	0.6483	855.00		0.6483	1169.88			
	0.8320	907.05		0.8320	1253.4			
	0.8593	890.19		0.8593	1234.13			
	0.9142	923.23		0.9142	1289.56			
	0.9733	956.48		0.9733	1322.61			

T °C	X_{tma}	P mmHg	T °C	X_{tma}	P mmHg	T °C	X_{tma}	P mmHg
29.60	0.0034	60.89	39.28	0.0034	103.62	48.85	0.0034	168.21
	0.0336	224.70		0.0336	342.98		0.0336	489.52
	0.0614	378.96		0.0614	569.37		0.0614	818.25
	0.0803	444.37		0.0803	682.47		0.0803	1013.08
	0.1630	811.92		0.1630	1135.33			
	0.2062	841.21						
	0.3127	1080.63						
	0.5305	1413.61						
	0.5639	1438.17						
	0.6358	1521.91						
	0.6480	1520.94						

TABLE A.3: VAPOUR - LIQUID EQUILIBRIUM DATA FOR TRIMETHYLAMINE - WATER MIXTURES

Amine Composition (mol%)	Temperature (°C)
6.0	102.4
8.1	100.2
13.7	99.6
20.7	98.8
26.8	99.1
29.4	99.3
37.7	100.3

TABLE A.4: LIQUID - LIQUID EQUILIBRIUM DATA FOR DIIMETHYLETHYLAMINE - WATER MIXTURES

Amine Composition (mol%)	Temperature (°C)
11.8	144.3
13.8	135.6
14.8	136.3
16.0	130.9
18.6	131.9
19.6	130.2
23.0	123.6
26.5	120.4

TABLE A.5: LIQUID - LIQUID EQUILIBRIUM DATA FOR TRIMETHYLAMINE - 3% NaCl SOLUTION MIXTURES

Appendix B

NRTL PARAMETER DETERMINATION FROM VAPOUR - LIQUID EQUILIBRIUM DATA

Program Description

A computer program was employed to generate values for the five parameters, required in the NRTL model described in chapter 4, which give the best fit to the experimental data. The program employs the Powell algorithm to minimise the objective function. The objective function was defined as the sum of the squared error between each of the experimental data points and that predicted by the thermodynamic model with the selected five parameters (chapter 4 equation 4.6)

The five adjustable parameters a_1, a_2, b_1, b_2 and α, in the NRTL model, were obtained using a two stage minimisation procedure. This procedure is illustrated in the block diagram presented in figure B.1. For given values of b_1 and b_2, the error function was minimised by manipulation of a_1, a_2 and α. New values for b_1 and b_2 were chosen, and optimum values for a_1, a_2 and α recalculated. The process continued until no further reduction in the error could be achieved. A listing of the fortran computer program is presented below. The subroutines POWELL, LINMIN, MNBRAK, BRENT and F1DIM employed in this procedure, were obtained from Press et. al. (1989) with minor modifications. The reader is refered to this text for further information on these programs.

This two stage approach was chosen for its robustness. Attempts to minimise the error function with a single stage Powell algorithm gave varying results depending on the initial values chosen for a_1, a_2, b_1, b_2 and α.

1. Select initial values for a_1, a_2, b_1, b_2, α and two search vectors.

2. Calculate new a_1, a_2 and α to give the initial minimum error for b_1 and b_2.

3. Search along the first vector to determine the upper and lower bounds (around the minimum) for b_1 and b_2.

4. Using the first vector, shrink the upper and lower bounds for b_1 and b_2.until the minimum error is achieved.

5. Search along the second vector to determine the upper and lower bounds (around the minimum) for b_1 and b_2.

6. Using the second vector, shrink the upper and lower bounds for b_1 and b_2.until the minimum error is achieved.

7. Replace the vector which achieved the largest error reduction with a new vector equal to the change in b_1 and b_2 achieved in the previous two line searches.

8. Repeat procedures 3 to 7 until no further improvement is made to b_1 and b_2.

FIGURE B.1: LOGIC FOR FINDING VALUES FOR THE MODEL PARAMETERS GIVING THE MINIMUM LEAST SQUARE ERROR

Program Listings

program nrtl7

This program runs the outer minimisation loop for determining the best fit values for b1 and b2

```
      dimension xxp(20,20),pp(20)
      common /par/ e,f,g
      data n/2/np/2/ftol/0.001/
      open(unit=4,status='old')
      read(4,11) e                    Reading in initial values for a1,a2,alpha
      read(4,11) f
      read(4,11) g
      close(unit=4)
      do i=1,n          Reading in initial values for b1,b2 and assigning initial search vectors
         read(44,11)pp(i)
         xxp(i,i)=1.0
      end do
11    format(f8.4)
      call powell2(pp,xxp,n,np,ftol,iter,fret)      Calling the powell subroutine to conduct
                                                    the error minimisation search
      do i=1,4
         write(9,20)i,pp(i)
      end do
20    format('a',i2,'=',f10.5)
      end
```

function func2(pp)

This function calculates the error between the experimental data and the correlation for the given correlation parameters.

```
      dimension pp(7)
      common /tem/ a,b
      a=pp(1)
      b=pp(2)
      call nrtl(err)          Calling the subroutine NRTL to determine the optimum values
                              of a1, a2, and α for the selected b1 and b2
      write(6,12)err,a,b
12    format(' error=',f9.3,x,f10.6,x,f10.6)
```

```
    func2=err
    return
    end
```

subroutine nrtl(fret)

This subroutine returns the minimum error between the experimental data and the NRTL equation which can be obtained by manipulating a_1, a_2 and α for given values of b_1 and b_2. This is the inner minimisation loop

```
    dimension xxp(20,20),p(20)
    common /par/ e,f,g
    data n/3/np/3/ftol/0.001/
    p(1)=e
    p(2)=f
    p(3)=g
    call powell(p,xxp,n,np,ftol,iter,fret)      Calling the POWELL subroutine to conduct the
                                                minimisation
    do i=1,n
        write(9,20)i,p(i)
    end do
20  format('a',i2,'=',f12.5)
    return
    end
```

function func(p)

```
    dimension p(7)
    common /tem/ ta1,ta2
    open(unit=14,status='old')
    read(14,1000)nvl                Reading the number of isothermal V-L data sets
1000  format(i2)
    err=0.0
    do i=1,nvl
        read(14,1000)np             Reading the number of data points in the i'th V-L data set
        read(14,82)tvl              Reading the temperature of the i'th V-L data set
        tet=tvl+273.14
```

```
      t12=(p(1)+ta1*tet-2.5E-8*tet**4)/1.98721/(tvl+273.14)  Calculating NRTL parameters
      t21=(p(2)+ta2*tet)/1.98721/(tvl+273.14)
      alpha=p(3)
      g12=exp(-alpha*t12)
      g21=exp(-alpha*t21)
      pvap1=10**(7.55466-1002.711/(tvl+247.885))      Calculating pure component
      pvap2=10**(8.07131-1730.63/(tvl+233.426))       vapour pressures
      do j=1,np
         read(14,83)pres,xl
         vllny1=(1-xl)**2*(t21*(g21/(xl+(1-xl)*g21))**2
     *        +t12*g12/(1-xl+xl*g12)**2)
         y1=exp(vllny1)                  Calculating the component 1 activity coefficients
         yp1=xl*y1*pvap1                 and partial pressures at data point j
         vllny2=xl**2*(t12*(g12/(1-xl+xl*g12))**2
     *        +t21*g21/(xl+(1-xl)*g21)**2)
         y2=exp(vllny2)
         yp2=(1-xl)*y2*pvap2
         err=err+(pres-yp1-yp2)**2/pres**2     calculating the normalised error between
      end do                                   experiment and model
   end do
82 format(f8.4)
83 format(f8.2,f8.5)
   func=err
   close(unit=14)
   return
   end
```

SUBROUTINE POWELL2(pp,xxn,N,NP,FTOL,ITER,FRET)

Minimisation of a function FUNC2 of N variables. (FUNC2 is not an argument, it is a fixed function name) Input consists of an initial starting point PP that is a vector of length N; an initial matrix XXN whose logical dimensions are N by N, physical dimensions NP by NP, and whose columns contain the initial set of directions (usually the N unit vectors); and FTOL, the fractional tolerance in the function value such that failure to decrease by more than this amount on one iteration signals doneness. On output, PP is set to the best point found, XI is the then - current direction set, FRET is the returned function value at PP, and ITER is the number of iterations taken. The routine LINMIN2 is used.

```
      PARAMETER (NMAX=20,ITMAX=200)
      DIMENSION pp(6),xxn(6,6),PT(NMAX),PTT(NMAX),xiT(NMAX)
      FRET=FUNC2(pp)
      DO 11 J=1,N
          PT(J)=pp(J)
11    CONTINUE
      ITER=0
1     ITER=ITER+1
      FP=FRET
      IBIG=0
      DEL=0.
      DO 13 I=1,N
          DO 12 J=1,N
              XIT(J)=xxn(J,I)
12        CONTINUE
          CALL LINMIN2(pp,XIT,N,FRET)
          IF(ABS(FP-FRET).GT.DEL)THEN
              DEL=ABS(FP-FRET)
              IBIG=I
          ENDIF
13    CONTINUE
      IF(2.*ABS(FP-FRET).LE.FTOL*(ABS(FP)+ABS(FRET)))RETURN
      IF(ITER.EQ.ITMAX) PAUSE 'Powell exceeding maximum iterations.'
      DO 14 J=1,N
          PTT(J)=2.*pp(J)-PT(J)
          XIT(J)=pp(J)-PT(J)
          PT(J)=pp(J)
14    CONTINUE
      FPTT=FUNC2(PTT)
      IF(FPTT.GE.FP)GO TO 1
      T=2.*(FP-2.*FRET+FPTT)*(FP-FRET-DEL)**2-DEL*(FP-FPTT)**2
      IF(T.GE.0.)GO TO 1
      CALL LINMIN2(pp,XIT,N,FRET)
      DO 15 J=1,N
          xxn(J,IBIG)=XIT(J)
15    CONTINUE
      GO TO 1
      END
```

SUBROUTINE POWELL(P,xxn,N,NP,FTOL,ITER,FRET)

Minimisation of a function FUNC of N variables. (Func is not an argument, it is a fixed function name) Input consists of an initial starting point P that is a vector of length N; an initial matrix XI whose logical dimensions are N by N, physical dimensions NP by NP, and whose columns contain the initial set of directions (usually the N unit vectors); and FTOL, the fractional tolerance in the function value such that failure to decrease by more than this amount on one iteration signals doneness. On output, P is set to the best point found, XI is the then - current direction set, FRET is the returned function value at P, and ITER is the number of iterations taken. The routine LINMIN is used.

```
      PARAMETER (NMAX=20,ITMAX=200)
      DIMENSION P(6),xxn(6,6),PT(NMAX),PTT(NMAX),xiT(NMAX)
      FRET=FUNC(P)
      xxn(1,1)=1.
      xxn(2,2)=1.
      xxn(3,3)=0.02
      DO 11 J=1,N       Save the initial points
        PT(J)=P(J)
11    CONTINUE
      ITER=0
1     ITER=ITER+1
      FP=FRET
      IBIG=0
      DEL=0.                  Will be the biggest function decrease
      DO 13 I=1,N             In each iteration, loop over all directions in the set.
        DO 12 J=1,N           Copy the direction
          XIT(J)=xxn(J,I)
12      CONTINUE
        CALL LINMIN(P,XIT,N,FRET)          Minimise along it
        IF(ABS(FP-FRET).GT.DEL)THEN        And record it if it is the largest decrease so far
          DEL=ABS(FP-FRET)
          IBIG=I
        ENDIF
13    CONTINUE
      IF(2.*ABS(FP-FRET).LE.FTOL*(ABS(FP)+ABS(FRET)))RETURN  Termination Criterion
      IF(ITER.EQ.ITMAX) PAUSE 'Powell exceeding maximum iterations.'
      DO 14 J=1,N       Construct the extrapolated point and the average direction moved.
```

```
      PTT(J)=2.*P(J)-PT(J)          Save the old starting point
      XIT(J)=P(J)-PT(J)
      PT(J)=P(J)
14  CONTINUE
    FPTT=FUNC(PTT)                  Function value at the extrapolated point
    IF(FPTT.GE.FP)GO TO 1           One reason not to use new direction
    T=2.*(FP-2.*FRET+FPTT)*(FP-FRET-DEL)**2-DEL*(FP-FPTT)**2
    IF(T.GE.0.)GO TO 1              Other reason not to use new direction
    CALL LINMIN(P,XIT,N,FRET)       Move to the minimum of the new direction
    DO 15 J=1,N                     And save the new direction
      xxn(J,IBIG)=XIT(J)
15  CONTINUE
    GO TO 1          Back for another iteration
    END
```

SUBROUTINE LINMIN2(pp,XI,N,FRET)

Given an N dimensional point pp and an N dimensional direction XI, this program moves and resets pp to where the function FUNC(pp) takes on a minimum along the direction XI from pp. The program also replaces XI by the actual vector displacement that pp was moved. The value of FUNC at the returned location P is returned as FRET. These tasks are accomplished by calling the subroutines MNBRAK2 and BRENT2.

```
    PARAMETER (NMAX=50,TOL=3.E-3)
    EXTERNAL F1DIM2
    DIMENSION pp(4),XI(N)
    COMMON /F1COM2/ NCOM,PCOM(NMAX),XICOM(NMAX)
    NCOM=N
    PCOM(J)=pp(J)
    XICOM(J)=XI(J)
11  CONTINUE
    AX=0.
    XX=1.
    BX=2.
    CALL MNBRAK2(AX,XX,BX,FA,FX,FB,F1DIM2)
    FRET=BRENT2(AX,XX,BX,F1DIM2,TOL,XMIN)
    DO 12 J=1,N
```

```
      XI(J)=XMIN*XI(J)
      pp(J)=pp(J)+XI(J)
12  CONTINUE
    RETURN
    END
```

SUBROUTINE LINMIN(P,XI,N,FRET)

Given an N dimensional point P and an N dimensional direction XI, this program moves and resets P to where the function FUNC(P) takes on a minimum along the direction XI from P. The program also replaces XI by the actual vector displacement that P was moved. The value of FUNC at the returned location P is returned as FRET. These tasks are accomplished by calling the subroutines MNBRAK and BRENT.

```
    PARAMETER (NMAX=50,TOL=3.E-3)
    EXTERNAL F1DIM
    DIMENSION P(N),XI(N)
    COMMON /F1COM/ NCOM,PCOM(NMAX),XICOM(NMAX)
    NCOM=N                                    set up common block
    DO 11 J=1,N
      PCOM(J)=P(J)
      XICOM(J)=XI(J)
11  CONTINUE
    AX=0.                                     Initial guess for brackets
    XX=1.
    BX=2.
    CALL MNBRAK(AX,XX,BX,FA,FX,FB,F1DIM)
    FRET=BRENT(AX,XX,BX,F1DIM,TOL,XMIN)
    DO 12 J=1,N                               Constructing the vector results to return
      XI(J)=XMIN*XI(J)
      P(J)=P(J)+XI(J)
12  CONTINUE
    RETURN
    END
```

```
      SUBROUTINE MNBRAK2(AX,BX,CX,FA,FB,FC,FUNC2)
      PARAMETER (GOLD=1.618034, GLIMIT=100., TINY=1.E-20)
      FA=FUNC2(AX)
      FB=FUNC2(BX)
      IF(FB.GT.FA)THEN
        DUM=AX
        AX=BX
        BX=DUM
        DUM=FB
        FB=FA
        FA=DUM
      ENDIF
      CX=BX+GOLD*(BX-AX)
      FC=FUNC2(CX)
1     IF(FB.GE.FC)THEN
        R=(BX-AX)*(FB-FC)
        Q=(BX-CX)*(FB-FA)
        U=BX-((BX-CX)*Q-(BX-AX)*R)/(2.*SIGN(MAX(ABS(Q-R),TINY),Q-R))
        ULIM=BX+GLIMIT*(CX-BX)
        IF((BX-U)*(U-CX).GT.0.)THEN
          FU=FUNC2(U)
          IF(FU.LT.FC)THEN
            AX=BX
            FA=FB
            BX=U
            FB=FU
            GO TO 1
          ELSE IF(FU.GT.FB)THEN
            CX=U
            FC=FU
            GO TO 1
          ENDIF
          U=CX+GOLD*(CX-BX)
          FU=FUNC2(U)
        ELSE IF((CX-U)*(U-ULIM).GT.0.)THEN
          FU=FUNC2(U)
          IF(FU.LT.FC)THEN
```

```
            BX=CX
            CX=U
            U=CX+GOLD*(CX-BX)
            FB=FC
            FC=FU
            FU=FUNC2(U)
        ENDIF
    ELSE IF((U-ULIM)*(ULIM-CX).GE.0.)THEN
        U=ULIM
        FU=FUNC2(U)
    ELSE
        U=CX+GOLD*(CX-BX)
        FU=FUNC2(U)
    ENDIF
    AX=BX
    BX=CX
    CX=U
    FA=FB
    FB=FC
    FC=FU
    GO TO 1
ENDIF
RETURN
END
```

SUBROUTINE MNBRAK(AX,BX,CX,FA,FB,FC,FUNC)

Given a function FUNC, and given distinct initial points AX and BX, this routine searches in the downhill direction (defined by the function as evaluated at the initial points) and returns new points AX, BX and CX which bracket a minimum of the function. Also returned are the function values at the three points FA, FB and FC

```
PARAMETER (GOLD=1.618034, GLIMIT=100., TINY=1.E-20)
FA=FUNC(AX)
FB=FUNC(BX)
IF(FB.GT.FA)THEN              Switch roles of A and B so that we can go downhill
    DUM=AX                      in the direction from A to B
```

```
      AX=BX
      BX=DUM
      DUM=FB
      FB=FA
      FA=DUM
    ENDIF
    CX=BX+GOLD*(BX-AX)              first guess for C
    FC=FUNC(CX)
1   IF(FB.GE.FC)THEN                Keep returning here until we bracket
      R=(BX-AX)*(FB-FC)
      Q=(BX-CX)*(FB-FA)
      U=BX-((BX-CX)*Q-(BX-AX)*R)/(2.*SIGN(MAX(ABS(Q-R),TINY),Q-R))
      ULIM=BX+GLIMIT*(CX-BX)  Compute U by parabolic extrapolation from A, B & C
      IF((BX-U)*(U-CX).GT.0.)THEN   Parabolic U is between B and C
        FU=FUNC(U)
        IF(FU.LT.FC)THEN            Got a minimum between B and C
          AX=BX
          FA=FB
          BX=U
          FB=FU
          GO TO 1
        ELSE IF(FU.GT.FB)THEN               Got a minimum between A and U
          CX=U
          FC=FU
          GO TO 1
        ENDIF
        U=CX+GOLD*(CX-BX)       Parabolic fit was no use. Use default magnification
        FU=FUNC(U)
      ELSE IF((CX-U)*(U-ULIM).GT.0.)THEN        Parabolic fit is between C and its
        FU=FUNC(U)                                allowed limit
        IF(FU.LT.FC)THEN
          BX=CX
          CX=U
          U=CX+GOLD*(CX-BX)
          FB=FC
          FC=FU
```

```
            FU=FUNC(U)
          ENDIF
        ELSE IF((U-ULIM)*(ULIM-CX).GE.0.)THEN     Limit parabolic U to max allowed
          U=ULIM
          FU=FUNC(U)
        ELSE            Reject parabolic U.  Use default magnification
          U=CX+GOLD*(CX-BX)
          FU=FUNC(U)
        ENDIF
        AX=BX
        BX=CX
        CX=U
        FA=FB
        FB=FC
        FC=FU
        GO TO 1
      ENDIF
      RETURN
      END
```

FUNCTION BRENT2(AX,BX,CX,F,TOL,XMIN)

Given a function F, and given a bracketing triplet of abscissas AX, BX, CX (such that BX is between AX and CX, and F(BX) is less than both F(AX) and F(CX)), this routine isolates the minimum to a fractional precision of about TOL using Brent's method. The abscissa of the minimum is returned as XMIN, and the minimum function value is returned as BRENT2, the returned function value.

```
      PARAMETER (ITMAX=100,CGOLD=.3819660,ZEPS=1.0E-10)
      A=MIN(AX,CX)
      B=MAX(AX,CX)
      V=BX
      W=V
      X=V
      E=0.
      FX=F(X)
      FV=FX
```

```
      FW=FX
      mm=1
      m=1
      DO 11 ITER=1,ITMAX
        XM=0.5*(A+B)
        TOL1=TOL*ABS(X)+ZEPS
        TOL2=2.*TOL1
        IF(ABS(X-XM).LE.(TOL2-.5*(B-A))) GOTO 3
        if(m.eq.5) then                    As the program is so slow, the following code is
          write(6,56)                      used to allow the user to make judicious decisions
56        format('are we close enough? yes=2 no=1')    about when to finish minimising
          read(5,57)mm
57        format(i2)
          if(mm.eq.2) goto 3
          m=1
        end if
        m=m+1
        write(6,57)m
        IF(ABS(E).GT.TOL1) THEN
          R=(X-W)*(FX-FV)
          Q=(X-V)*(FX-FW)
          P=(X-V)*Q-(X-W)*R
          Q=2.*(Q-R)
          IF(Q.GT.0.) P=-P
          Q=ABS(Q)
          ETEMP=E
          E=D
          IF(ABS(P).GE.ABS(.5*Q*ETEMP).OR.P.LE.Q*(A-X).OR.
     *       P.GE.Q*(B-X)) GOTO 1
          D=P/Q
          U=X+D
          IF(U-A.LT.TOL2 .OR. B-U.LT.TOL2) D=SIGN(TOL1,XM-X)
          GOTO 2
        ENDIF
1       IF(X.GE.XM) THEN
          E=A-X
```

```
      ELSE
          E=B-X
      ENDIF
      D=CGOLD*E
2     IF(ABS(D).GE.TOL1) THEN
          U=X+D
       ELSE
          U=X+SIGN(TOL1,D)
      ENDIF
      FU=F(U)
      IF(FU.LE.FX) THEN
          IF(U.GE.X) THEN
              A=X
          ELSE
              B=X
          ENDIF
          V=W
          FV=FW
          W=X
          FW=FX
          X=U
          FX=FU
      ELSE
           IF(U.LT.X) THEN
              A=U
          ELSE
              B=U
          ENDIF
          IF(FU.LE.FW .OR. W.EQ.X) THEN
              V=W
              FV=FW
              W=U
              FW=FU
          ELSE IF(FU.LE.FV .OR. V.EQ.X .OR. V.EQ.W) THEN
              V=U
              FV=FU
```

```
        ENDIF
      ENDIF
11  CONTINUE
    write(6,38)
38  format('Brent2 exceed maximum iterations.')
3   XMIN=X
    BRENT2=FX
    RETURN
    END
```

FUNCTION BRENT(AX,BX,CX,F,TOL,XMIN)

Given a function F, and given a bracketing triplet of abscissas AX, BX, CX (such that BX is between AX and CX, and F(BX) is less than both F(AX) and F(CX)), this routine isolates the minimum to a fractional precision of about TOL using Brent's method. The abscissa of the minimum is returned as XMIN, and the minimum function value is returned as BRENT, the returned function value.

```
    PARAMETER (ITMAX=100,CGOLD=.3819660,ZEPS=1.0E-10)
    A=MIN(AX,CX)          A and B must be in ascending order, though the input abscissas
    B=MAX(AX,CX)          need not be
    V=BX
    W=V
    X=V
    E=0.          This will be the distance moved on the step before last
    FX=F(X)
    FV=FX
    FW=FX
    DO 11 ITER=1,ITMAX
      XM=0.5*(A+B)
      TOL1=TOL*ABS(X)+ZEPS
      TOL2=2.*TOL1
      IF(ABS(X-XM).LE.(TOL2-.5*(B-A))) GOTO 3      Test for done here
      IF(ABS(E).GT.TOL1) THEN                  Construct a trial parabolic fit
        R=(X-W)*(FX-FV)
        Q=(X-V)*(FX-FW)
        P=(X-V)*Q-(X-W)*R
```

```
      Q=2.*(Q-R)
      IF(Q.GT.0.) P=-P
      Q=ABS(Q)
      ETEMP=E
      E=D
      IF(ABS(P).GE.ABS(.5*Q*ETEMP).OR.P.LE.Q*(A-X).OR.
     *   P.GE.Q*(B-X)) GOTO 1      The above conditions determine the acceptability
                                   of the parabolic fit.
      D=P/Q                        Take the parabolic step
      U=X+D
      IF(U-A.LT.TOL2 .OR. B-U.LT.TOL2) D=SIGN(TOL1,XM-X)
      GOTO 2
    ENDIF
1   IF(X.GE.XM) THEN               Here we take the golden section step into the larger of
      E=A-X                        the two segments
    ELSE
      E=B-X
    ENDIF
    D=CGOLD*E
2   IF(ABS(D).GE.TOL1) THEN
      U=X+D
    ELSE
      U=X+SIGN(TOL1,D)
    ENDIF
    FU=F(U)                        This is the one function evaluation per iteration
    IF(FU.LE.FX) THEN              And now we have to decide what to do with our function
      IF(U.GE.X) THEN              evaluation.  Housekeeping follows:
        A=X
      ELSE
        B=X
      ENDIF
      V=W
      FV=FW
      W=X
      FW=FX
      X=U
```

```
        FX=FU
      ELSE
      IF(U.LT.X) THEN
        A=U
      ELSE
        B=U
      ENDIF
      IF(FU.LE.FW .OR. W.EQ.X) THEN
        V=W
        FV=FW
        W=U
        FW=FU
      ELSE IF(FU.LE.FV .OR. V.EQ.X .OR. V.EQ.W) THEN
        V=U
        FV=FU
      ENDIF
    ENDIF
11  CONTINUE
    write(6,38)
38  format('Brent exceed maximum iterations.')
3   XMIN=X          Arrive here ready to exit with best values
    BRENT=FX
    RETURN
    END
```

```
    FUNCTION F1DIM2(X)
    PARAMETER (NMAX=50)
    COMMON /F1COM2/ NCOM,PCOM(NMAX),XICOM(NMAX)
    DIMENSION XT(NMAX)
    DO 11 J=1,NCOM
    XT(J)=PCOM(J)+X*XICOM(J)
11  CONTINUE
    F1DIM2=FUNC2(XT)
    RETURN
    END
```

```
      FUNCTION  F1DIM(X)
      PARAMETER (NMAX=50)
      COMMON /F1COM/ NCOM,PCOM(NMAX),XICOM(NMAX)
      DIMENSION XT(NMAX)
      DO 11 J=1,NCOM
      XT(J)=PCOM(J)+X*XICOM(J)
11    CONTINUE
      F1DIM=FUNC(XT)
      RETURN
      END
```

Appendix C

THERMODYNAMIC MODEL FOR THE PREDICTION OF AMMONIA - WATER THERMODYNAMIC PROPERTIES

The equation of state proposed by Ziegler and Trepp (1984) was used for predicting the thermodynamic properties of ammonia - water mixtures. A separate "user supplied" FORTRAN subroutine was written for this purpose, as there is no suitable thermodynamic model for these mixtures built into the PROCESS™ computer simulation package. A listing of these subroutines is presented below. Common variables and subroutine arguments used in these programs are defined in the PROCESS™ User Added Subroutines Manual. The reader is refered to this manual for further information on these definitions and for further information on the structure of the PROCESS™ chemical plant simulation package.

The accuracy of these programs was investigated by comparing phase equilibrium curves generated by PROCESS with equilibrium data presented by Bogart (1981). Figures C.1 and C.2 illustrate the close agreement obtained between the computer model and the data presented by Bogart.

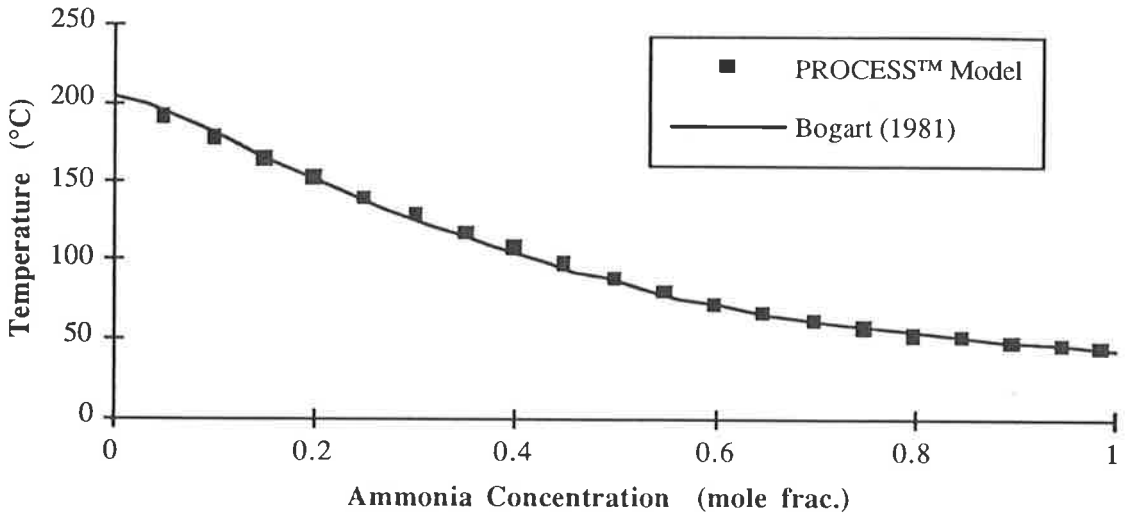

FIGURE C.1: COMPARISON OF COMPUTER GENERATED BUBBLE POINT CURVE AT 1724 KPA AND LITERATURE DATA

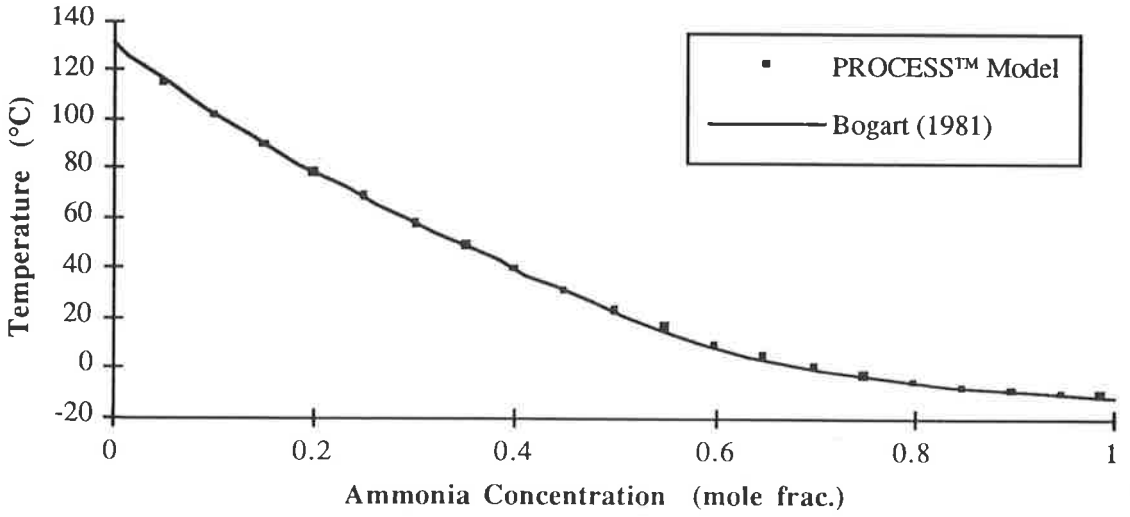

FIGURE C.2: COMPARISON OF COMPUTER GENERATED BUBBLE POINT CURVE AT 276 KPA AND LITERATURE DATA

Program Listings

```
      SUBROUTINE  UKHS2
C ** This subroutine calculates k values for the ammonia water system
C ** based on the equation of state proposed by Ziegler & Trepp
      COMMON /FACTOR/ TCONVT,TFAC,PCONVT,PFAC,TIMFAC,WTFAC,VVFAC,
     *     ARFAC,XLVFAC,SPGFAC,HSFAC,WKFAC,VISFAC,TCFAC,VVFACA,STFAC,
     *     FACA,FACB,EXPFAC,XM3FAC,FTOR,CTOK,XKTOR,ATM,VVTOML,RCONST
      COMMON /UTHERM/IFLAG,NOCX,IFAZE,IWATER,IOUT,TEMPR,TDELTR,
     *     PRESR,XV(50),XL(50),XL2(50),YSAT,XSOL,XKAY(50),DRIV(50),HS1,HS2,
     *     Z1,Z2,JFLAG,IFLG(10)
      DIMENSION STREAM(60),VPS(50)
      IF(IFLAG.NE.-1) GOTO 10
      JFLAG=3
      RETURN
10    IF(IFLG(4).GT.0) GOTO 20
      IFLG(4)=1

C ** Assigning values to the equation of state parameters
      HLORA=4.878573
      HGORA=26.468879
      SLORA=1.644773
      SGORA=8.339026
      TORA=3.2252
      PORA=2.0000
      HLORW=21.821141
      HGORW=60.965058
      SLORW=5.733498
      SGORW=13.45343
      TORW=5.0705
      PORW=3.0000
      A1A=3.971423E-2
      A2A=-1.790557E-5
      A3A=-1.308905E-2
      A4A=3.752836E-3
      B1A=1.634519E1
      B2A=-6.508119
      B3A=1.448937
```

C1A=-1.049377E-2
C2A=-8.288224
C3A=-6.647257E2
C4A=-3.045352E3
D1A=3.673647
D2A=9.989629E-2
D3A=3.617622E-2
A1W=2.748796E-2
A2W=-1.016665E-5
A3W=-4.452025E-3
A4W=8.389246E-4
B1W=1.214557E1
B2W=-1.898065
B3W=2.911966E-1
C1W=2.136131E-2
C2W=-3.169291E1
C3W=-4.634611E4
C4W=0.0
D1W=4.019170
D2W=-5.17555E-2
D3W=1.951939E-2
A1A=3.971423E-2
A2A=-1.790557E-5
A3A=-1.308905E-2
A4A=3.752836E-3
E1=-4.626129E1
E2=2.060225E-2
E3=7.292369
E4=-1.032613E-2
E5=8.074824E1
E6=-8.461214E1
E7=2.452882E1
E8=9.598767E-3
E9=-1.475383
E10=-5.038107E-3
E11=-9.640398E1

```
      E12=1.226973E2
      E13=-7.582637
      E14=6.012445E-4
      E15=5.487018E1
      E16=-7.667596E1

20    IF(IFLAG.EQ.0) RETURN
      IF(IFLAG.EQ.1) GOTO 30
      JFLAG=99
      WRITE(IOUT,60) IFLAG
60    FORMAT(50H0 ** FATAL ERROR -USER THERMO U2 IS KVALUES-IFLAG=,I5)
      RETURN
30    II=0

C ** Converting from program units to SI units
      TDEGK=(TEMPR+TCONVT)*TFAC/XKTOR
      PBAR=(PRESR+PCONVT)*PFAC/14.50
      TR=TDEGK/100
      PR=PBAR/10

C ** Calculating the normalised liquid phase Gibbs Free Energy of Ammonia
40    GLRA=HLORA-TR*SLORA+B1A*TR+B2A/2*TR**2+B3A/3*TR**3-
     *      B1A*TR*LOG(TR)
      GLRA=GLRA-B2A*TR**2-B3A/2*TR**3-B1A*TORA-B2A/2*TORA**2-
     *      B3A/3*TORA**3
      GLRA=GLRA+TR*B1A*LOG(TORA)+B2A*TR*TORA+B3A/2*TR*TORA**2
      GLRA=GLRA+(A1A+A3A*TR+A4A*TR**2)*(PR-PORA)+A2A*(PR**2-PORA**2)/2
C ** Calculating the normalised liquid phase Gibbs Free Energy of Water
      GLRW=HLORW-TR*SLORW+B1W*TR+B2W/2*TR**2+B3W/3*TR**3-
     *      B1W*TR*LOG(TR)
      GLRW=GLRW-B2W*TR**2-B3W/2*TR**3-B1W*TORW-B2W/2*TORW**2-
     *      B3W/3*TORW**3
      GLRW=GLRW+TR*B1W*LOG(TORW)+B2W*TR*TORW+B3W/2*TR*TORW**2
      GLRW=GLRW+(A1W+A3W*TR+A4W*TR**2)*(PR-PORW)+A2W*(PR**2-
     *      PORW**2)/2
```

```
C ** Calculating the normalised vapour phase Gibbs Free Energy of Ammonia
      GGRA=HGORA-TR*SGORA+D1A*TR+D2A/2*TR**2+D3A/3*TR**3-
     *     D1A*TR*LOG(TR)
      GGRA=GGRA-D2A*TR**2-D3A/2*TR**3-D1A*TORA-D2A/2*TORA**2-
     *     D3A/3*TORA**3
      GGRA=GGRA+TR*D1A*LOG(TORA)+D2A*TR*TORA+D3A/2*TR*TORA**2
      GGRA=GGRA+C1A*(PR-PORA)+C2A*(PR/TR**3-4*PORA/TORA**3
     *     +3*PORA*TR/TORA**4)
      GGRA=GGRA+C3A*(PR/TR**11-12*PORA/TORA**11+11*PORA*TR/TORA**12)
      GGRA=GGRA+C4A*(PR**3/TR**11-12*PORA**3/TORA**11+11*PORA**3*TR
     *     /TORA**12)/3+TR*LOG(PR/PORA)
C ** Calculating the normalised vapour phase Gibbs Free Energy of Water
      GGRW=HGORW-TR*SGORW+D1W*TR+D2W/2*TR**2+D3W/3*TR**3-
     *     D1W*TR*LOG(TR)
      GGRW=GGRW-D2W*TR**2-D3W/2*TR**3-D1W*TORW-D2W/2*TORW**2-
     *     D3W/3*TORW**3
      GGRW=GGRW+TR*D1W*LOG(TORW)+D2W*TR*TORW+D3W/2*TR*TORW**2
      GGRW=GGRW+C1W*(PR-PORW)+C2W*(PR/TR**3-4*PORW/TORW**3
     *     +3*PORW*TR/TORW**4)
      GGRW=GGRW+C3W*(PR/TR**11-12*PORW/TORW**11
     *     +11*PORW*TR/TORW**12)
      GGRW=GGRW+C4W*(PR**3/TR**11-12*PORW**3/TORW**11+11*PORW**3*TR
     *     /TORW**12)/3+TR*LOG(PR/PORW)
C ** Calculating the normalised excess Gibbs Free Energy of mixing
      X=XL(1)
      CE1=E1+E2*PR+(E3+E4*PR)*TR+E5/TR+E6/TR**2
      CE2=E7+E8*PR+(E9+E10*PR)*TR+E11/TR+E12/TR**2
      CE3=E13+E14*PR+E15/TR+E16/TR**2
      GE=(CE1+CE2*(2*X-1)+CE3*(2*X-1)**2)*X*(1-X)
      DGEDX=GE/X/(1-X)*(1-2*X)+X*(1-X)*(2*CE2+4*CE3*(2*X-1))

C ** Calculating the vapour phase composition
      ULRW=GLRW+TR*LOG(1-X)+GE-X*DGEDX
      ULRA=GLRA+TR*LOG(X)+GE+(1-X)*DGEDX
      YW=1-EXP((ULRW-GGRW)/TR)
      YA=EXP((ULRA-GGRA)/TR)
```

```
C ** Calculating the equilibrium K values and the temperature derivative
      XK1=YA/XL(1)
      XK2=YW/(1-XL(1))
      IF(TDELTR.EQ.0.) GOTO 77
      IF(II.GT.0) GOTO 50
      II=II+1
      XKAY(1)=XK1
      XKAY(2)=XK2
      TR=(TDEGK+0.01)/100
      GOTO 40
50    DRIV(1)=(XK1-XKAY(1))/0.01
      DRIV(2)=(XK2-XKAY(2))/0.01
77    CONTINUE
      RETURN
      END
```

```
      SUBROUTINE  UKHS3
C **** This subroutine calculates H  values for the ammonia water system
C **** based on the equation of state proposed by Ziegler & Trepp
      COMMON /FACTOR/ TCONVT,TFAC,PCONVT,PFAC,TIMFAC,WTFAC,VVFAC,
     * ARFAC,XLVFAC,SPGFAC,HSFAC,WKFAC,VISFAC,TCFAC,VVFACA,STFAC,CA,
     * FAFACB,EXPFAC,XM3FAC,FTOR,CTOK,XKTOR,ATM,VVTOML,RCONST
      COMMON /UTHERM/IFLAG,NOCX,IFAZE,IWATER,IOUT,TEMPR,TDELTR,
     * PRESR,XV(50),XL(50),XL2(50),YSAT,XSOL,XKAY(50),DRIV(50),HS1,HS2,
     * Z1,Z2,JFLAG,IFLG(10)
      JFLAG=1
      IF(IFLAG.EQ.2) GOTO 10
      WRITE(IOUT,90) IFLAG
90    FORMAT(48H0***ERROR-USER METHOD U3 IS ENTHALPIES - IFLAG=,I5,//)
      JFLAG=99
      RETURN

C ** Assigning values to the equation of state parameters
10    HLORA=4.878573
      HGORA=26.468879
      SLORA=1.644773
      SGORA=8.339026
      TORA=3.2252
      PORA=2.0000
      HLORW=21.821141
      HGORW=60.965058
      SLORW=5.733498
      SGORW=13.45343
      TORW=5.0705
      PORW=3.0000
      A1A=3.971423E-2
      A2A=-1.790557E-5
      A3A=-1.308905E-2
      A4A=3.752836E-3
      B1A=1.634519E1
      B2A=-6.508119
      B3A=1.448937
```

C1A=-1.049377E-2
C2A=-8.288224
C3A=-6.647257E2
C4A=-3.045352E3
D1A=3.673647
D2A=9.989629E-2
D3A=3.617622E-2
A1W=2.748796E-2
A2W=-1.016665E-5
A3W=-4.452025E-3
A4W=8.389246E-4
B1W=1.214557E1
B2W=-1.898065
B3W=2.911966E-1
C1W=2.136131E-2
C2W=-3.169291E1
C3W=-4.634611E4
C4W=0.0
D1W=4.019170
D2W=-5.17555E-2
D3W=1.951939E-2
E1=-4.626129E1
E2=2.060225E-2
E3=7.292369
E4=-1.032613E-2
E5=8.074824E1
E6=-8.461214E1
E7=2.452882E1
E8=9.598767E-3
E9=-1.475383
E10=-5.038107E-3
E11=-9.640398E1
E12=1.226973E2
E13=-7.582637
E14=6.012445E-4
E15=5.487018E1
E16=-7.667596E1

```
C ** Converting to SI units
      TDEGK=(TEMPR+TCONVT)*TFAC/XKTOR
      PBAR=(PRESR+PCONVT)*PFAC/14.50
      TB=100
      II=0
20    TR=TDEGK/100
      PR=PBAR/10
      IF(IFAZE.EQ.1) GOTO 30

C  ** Calculating the liquid phase enthalpy
      X=XL(1)
      CPLRA=B1A*(TR-TORA)+B2A*(TR**2-TORA**2)/2+B3A*(TR**3-TORA**3)/3
      CPLRA=CPLRA/TR**2
      CPLRW=B1W*(TR-TORW)+B2W*(TR**2-TORW**2)/2+B3W*(TR**3-TORW**3)/3
      CPLRW=CPLRW/TR**2
      HLR=(1-X)*(-HLORW/TR**2-CPLRW+(A4W-A1W/TR**2)*(PR-PORW))+X*(
     *     -HLORA/TR**2-CPLRA+(A4A-A1A/TR**2)*(PR-PORA))
      HLR=HLR+(-2*E5/TR**3-3*E6/TR**4-(E1+E2*PR)/TR**2)*X*(1-X)+X*
     *     (1-X)*(2*X-1)*(-(E7+E8*PR)/TR**2-2*E11/TR**3-3*E12/TR**4)
      HLR=HLR+X*(1-X)*(2*X-1)*(-(E13+E14*PR)/TR**2-2*E15/TR**3-3*E16
     *     /TR**4)
      HLR=-HLR*TR**2*TB/TDEGK
      H=HLR
      GOTO 77

C  ** Calculating the vapour phase enthalpy
30    Y=XV(1)
      CPVRA=D1A*(TR-TORA)+D2A*(TR**2-TORA**2)/2+D3A*(TR**3-TORA**3)/3
      CPVRA=CPVRA/TR**2
      CPVRW=D1W*(TR-TORW)+D2W*(TR**2-TORW**2)/2+D3W*(TR**3-TORW**3)/3
      CPVRW=CPVRW/TR**2
      HVR=(1-Y)*(-HGORW/TR**2-CPVRW-C1W/TR**2*(PR-PORW)+C2W*(4*PORW/
     *     TORW**3/TR**2-4*PR/TR**5)+C3W*(12*PORW/TORW**11/TR**2-12*PR/
     *     TR**13)+C4W*(4*PORW**3/TORW**11/TR**2-4*PR**3/TR**13))
      HVR=HVR+Y*(-HGORA/TR**2-CPVRA-C1A/TR**2*(PR-PORA)+C2A*(4*PORA/
     *     TORA**3/TR**2-4*PR/TR**5)+C3A*(12*PORA/TORA**11/TR**2-12*PR/
     *     TR**13)+C4A*(4*PORA**3/TORA**11/TR**2-4*PR**3/TR**13))
```

```
      HVR=-HVR*TR**2*TB/TDEGK
      H=HVR

77    CONTINUE
      II=II+1
      TDEGK=TDEGK+TDELTR
      IF(II.EQ.2) GOTO 40
      HS1=H
C     ** Calculating the enthalpy at a small increment higher temperature
      GOTO 20
40    HS2=H
      RETURN
      END
```

```
      SUBROUTINE  UKHS4
C  ** This subroutine calculates entropy values for the ammonia water system
C  ** based on the equation of state proposed by Ziegler & Trepp
      COMMON /FACTOR/ TCONVT,TFAC,PCONVT,PFAC,TIMFAC,WTFAC,VVFAC,
     *     ARFAC,XLVFAC,SPGFAC,HSFAC,WKFAC,VISFAC,TCFAC,VVFACA,CA,
     *     STFAC,FA,FACB,EXPFAC,XM3FAC,FTOR,CTOK,XKTOR,ATM,
     *     VVTOML,RCONST
      COMMON /UTHERM/IFLAG,NOCX,IFAZE,IWATER,IOUT,TEMPR,TDELTR,
     *     PRESR,XV(50),XL(50),XL2(50),YSAT,XSOL,XKAY(50),DRIV(50),HS1,
     *     HS2,Z1,Z2,JFLAG,IFLG(10)
      JFLAG=1
      IF(IFLAG.EQ.3) GOTO 10
      WRITE(IOUT,99) IFLAG
99    FORMAT(48H0***ERROR-USER METHOD U4 IS ENTROPIES - IFLAG=,I5,//)
      JFLAG=99
      RETURN

C  ** Assigning values to equation of state parameters
10    HLORA=4.878573
      HGORA=26.468879
      SLORA=1.644773
      SGORA=8.339026
      TORA=3.2252
      PORA=2.0000
      HLORW=21.821141
      HGORW=60.965058
      SLORW=5.733498
      SGORW=13.45343
      TORW=5.0705
      PORW=3.0000
      A1A=3.971423E-2
      A2A=-1.790557E-5
      A3A=-1.308905E-2
      A4A=3.752836E-3
      B1A=1.634519E1
      B2A=-6.508119
      B3A=1.448937
```

C1A=-1.049377E-2
C2A=-8.288224
C3A=-6.647257E2
C4A=-3.045352E3
D1A=3.673647
D2A=9.989629E-2
D3A=3.617622E-2
A1W=2.748796E-2
A2W=-1.016665E-5
A3W=-4.452025E-3
A4W=8.389246E-4
B1W=1.214557E1
B2W=-1.898065
B3W=2.911966E-1
C1W=2.136131E-2
C2W=-3.169291E1
C3W=-4.634611E4
C4W=0.0
D1W=4.019170
D2W=-5.17555E-2
D3W=1.951939E-2
E1=-4.626129E1
E2=2.060225E-2
E3=7.292369
E4=-1.032613E-2
E5=8.074824E1
E6=-8.461214E1
E7=2.452882E1
E8=9.598767E-3
E9=-1.475383
E10=-5.038107E-3
E11=-9.640398E1
E12=1.226973E2
E13=-7.582637
E14=6.012445E-4
E15=5.487018E1
E16=-7.667596E1

```
      TDEGK=(TEMPR+TCONVT)*TFAC/XKTOR
      PBAR=(PRESR+PCONVT)*PFAC/14.50
      TB=100
      II=0
20    TR=TDEGK/100
      PR=PBAR/10
      IF(IFAZE.EQ.1) GOTO 30

C ** Calculating the liquid phase entropy
      X=XL(1)
      CPLRA=B1A*LOG(TR/TORA)+B2A*(TR-TORA)+B3A*(TR**2-TORA**2)/2
      CPLRW=B1W*LOG(TR/TORW)+B2W*(TR-TORW)+B3W*(TR**2-TORW**2)/2
      SLR=(1-X)*(-SLORW-CPLRW+(A3W+2*A4W*TR)*(PR-PORW))+X*(-SLORA
     *     -CPLRA+(A3A+2*A4A*TR)*(PR-PORA))
      SLR=SLR+(E3+E4*PR-E5/TR**2-2*E6/TR**3)*X*(1-X)+X*(1-X)*(2*X-1)
     *    *(E9+E10*PR-E11/TR**2-2*E12/TR**3)+X*(1-X)*(2*X-1)**2*
     *    (-E15/TR**2-2*E16/TR**3)
      SLR=-SLR
      H=SLR
      GOTO 77

C ** Calculating the vapour phase entropy
30    Y=XV(1)
      CPVRA=D1A*LOG(TR/TORA)+D2A*(TR-TORA)+D3A*(TR**2-TORA**2)/2
      CPVRW=D1W*LOG(TR/TORW)+D2W*(TR-TORW)+D3W*(TR**2-TORW**2)/2
      SVR=(1-Y)*(-SGORW-CPVRW+LOG(PR/PORW)+C2W*(3*PORW/TORW**4-3*
     *    PR/TR**4)+C3W*(11*PORW/TORW**12-11*PR/TR**12)+C4W*(11*PORW**3
     *    /TORW**12-11*PR**3/TR**12))
      SVR=SVR+Y*(-SGORA-CPVRA+LOG(PR/PORA)+C2A*(3*PORA/TORA**4-3*
     *    PR/TR**4)+C3A*(11*PORA/TORA**12-11*PR/TR**12)+C4A*(11*PORA**3
     *    /TORA**12-11*PR**3/TR**12))
      SVR=-SVR
      H=SVR
```

```
77  CONTINUE
    II=II+1
    TDEGK=TDEGK+TDELTR
    IF(II.EQ.2) GOTO 40
    HS1=H
C ** Calculating the entropy at an incrementally higher temperature
    GOTO 20
40  HS2=H
    RETURN
    END
```

Appendix D
SAMPLE PROCESS INPUT AND OUTPUT FILES

The amount of information generated from the numerous computer simulations is too large to include in its entirety. Instead a number of representative files have been included. These are:

(i) Input and output files for the basic novel refrigeration cycle with methyldiethylamine and water as working fluids.

(ii) Input and output files for the novel refrigeration cycle with absorbent phase distillation employing dimethylethylamine and water as working fluids.

(iii) Input and output files for the modified aqua-ammonia refrigeration cycle without precooling.

(iv) Input and output files for the conventional aqua-ammonia refrigeration cycle without precooling.

(v) Input and output files for the basic novel absorption cycle heatpump with cyclohexane and aniline as working fluids.

PROCESS™ Input and Output File Listings

BASIC NOVEL REFRIGERATION CYCLE WITH METHYLDIETHYLAMINE AND WATER

```
TITLE PROJECT=MDEAM REFRIG, DATE=8-7-90
    CALC NOTRIAL=10
    TOLERANCE PROP=0.0005,TEMP=-0.002,STREAM=0.0001,-0.002
    DIMENSION SI,TEMP=C,PRESSURE=MMHG
    PRINT INPUT=NONE

COMP DATA
    LIBID 2,H2O
    NONLIBRARY 1,MDEAMI
    MW 1,87.17
    SPGR 1,0.72
    NBP 1,66
    TC 1,235
    PC 1,25081
    ACENTRIC 1,0.3039
    FORMATION(KJ,KG) 1,-79,102.0
    VP(MMHG) CORR=21,LOG,TEMP=C,DATA=1,,,6.91578,-1184.8,227.67
    HIDEAL(KJ,KG,MOLE) CORR=1,TEMP=K,DATA=1,,,+16.447,-12.348E-3,*
     0.30138E-3,-1.2027E-7,2.1425E-11
    LATENT(KJ,KG) CORR=43,TEMP=K,DATA=1,,,336.2,0.38
    HLIQ(KJ,KG,MOLE) CORR=1,TEMP=C,DATA=1,,,0.0,0.2022

THERMO DATA
    TYPE KTYP=LACT,LACT,HTYP=LIBRARY,STYP=SRK
    HLSET KSET=1,SETNO=1
    KSET SETNO=1,NOTEMP=3
    SUBSET 1,10
    NRTL 1,2,,207.7790,,586.1201,0.50213
    SUBSET 2,30
    NRTL 1,2,,468.6817,,810.0509,0.50213
    SUBSET 3,50.00
    NRTL 1,2,,729.5844,,1033.9817,0.50213
    KSET SETNO=2
    NRTL 1,2,,674.6857,,1379.9828,0.4108

STREAM DATA
    PROPERTY STRM=3,TEMP=80,PRES=2500,RATE=1542,COMP=1,1.08/2,98.92
    PROPERTY STRM=12,TEMP=20,PRES=2500,RATE=1521,COMP=1,4.42/2,95.58
    PROPERTY STRM=4,TEMP=80,PRES=2500,RATE=328,COMP=1,65.0/2,35.0
    PROPERTY STRM=9,TEMP=10,PRES=2500,RATE=298,COMP=1,60.7/2,39.3
```

```
UNIT OPERATIONS
HX UID=HX22
    HOT FEED=4,L=5
    COLD FEED=9,L=19
    SPEC HICO=2
    DATA KSET=1
FLASH UID=F2
    FEED 5
    PROD V=7,L=8
    TPSPEC TEMP=10
    SPEC STRM=8,RATE=0.66,REFS=5
PUMP UID=P1
    FEED 8
    PROD L=9
    OPER PRES=2500,EFF=60
HX UID=HX2
    HOT FEED=3,L=6
    COLD FEED=12,L=22
    SPEC HOCI=2
    DATA KSET=1
FLASH UID=F1
    FEED 7,6
    PROD V=10V,L=10L
    ADIA
MIXER UID=M4
    FEED 10V,10L
    PROD M=10
HX UID=HX4
    HOT FEED=10,L=11
    SPEC HOT,LFRACT=1.0
    UTILITY WATER,TIN=15,TOUT=17
```

```
PUMP UID=P2
    FEED 11
    PROD L=12
    OPER PRES=2500,EFF=60
CONTROL UID=CON1
    SPEC STRM=11,TEMP=20
    PARAM STRM=3,MAXI=150000,MINI=100,EST2=1200,RETURNUNIT=HX2


MIXER UID=M3
    FEED 22,19
    PROD M=23
SEPARATOR UID=S1
    FEED 23
    OVHD STRM=4,PHASE=L,TEMP=80
    BTMS STRM=3,TEMP=80
    XOVHD 1,1,0.65
    XBTMS 2,2,0.989


RECYCLE
    LOOP NO=1,START=HX22,END=P1
    LOOP NO=2,START=HX2,END=P2
    LOOP NO=3,START=HX22,END=S1
```

```
 STRM: 3    T=  80.0 P= 2500.0 RATE= 5968.    DTEMP=   0.00 DCOMP=   0.0185
 STRM: 4    T=  80.0 P= 2500.0 RATE= 326.1    DTEMP=   0.00 DCOMP=   0.0057
 UNIT   1, HX22,    SOLVED
 UNIT   2, F2 ,    SOLVED
 UNIT   3, P1 ,    SOLVED
LOOP  1 NOT SOLVED AFTER   1 TRIALS
 STRM: 9    T=  10.1 P= 2500.0 RATE= 215.3    DTEMP=   0.00 DCOMP=   0.0057
 UNIT   1, HX22,    SOLVED
 UNIT   2, F2 ,    SOLVED
 UNIT   3, P1 ,    SOLVED
LOOP  1    SOLVED AFTER   2 TRIALS
 STRM: 9    T=  10.1 P= 2500.0 RATE= 215.3    DTEMP=   0.00 DCOMP=   0.0000
 UNIT   4, HX2 ,    SOLVED
 UNIT   5, F1 ,    SOLVED
 UNIT   6, M4 ,    SOLVED
 UNIT   7, HX4 ,    SOLVED
 UNIT   8, P2 ,    SOLVED
LOOP  2 NOT SOLVED AFTER   1 TRIALS
 STRM: 12   T=  20.1 P= 2500.0 RATE= 6079.    DTEMP=  -0.02 DCOMP=   0.0039
 UNIT   4, HX2 ,    SOLVED
 UNIT   5, F1 ,    SOLVED
 UNIT   6, M4 ,    SOLVED
 UNIT   7, HX4 ,    SOLVED
 UNIT   8, P2 ,    SOLVED
LOOP  2    SOLVED AFTER   2 TRIALS
 STRM: 12   T=  20.1 P= 2500.0 RATE= 6079.    DTEMP=   0.00 DCOMP=   0.0000
 UNIT   9, CON1, NOT SOLVED
 UNIT   4, HX2 ,    SOLVED
 UNIT   5, F1 ,    SOLVED
 UNIT   6, M4 ,    SOLVED
 UNIT   7, HX4 ,    SOLVED
 UNIT   8, P2 ,    SOLVED
LOOP  2 NOT SOLVED AFTER   1 TRIALS
```

```
 STRM: 12   T=  20.1 P= 2500.0 RATE= 6077.    DTEMP=   0.00 DCOMP=   0.0003
 UNIT   4, HX2 ,    SOLVED
 UNIT   5, F1  ,    SOLVED
 UNIT   6, M4  ,    SOLVED
 UNIT   7, HX4 ,    SOLVED
 UNIT   8, P2  ,    SOLVED
LOOP  2    SOLVED AFTER   2 TRIALS
 STRM: 12   T=  20.1 P= 2500.0 RATE= 6077.    DTEMP=   0.00 DCOMP=   0.0000
 UNIT   9, CON1, NOT SOLVED
 UNIT   4, HX2 ,    SOLVED
 UNIT   5, F1  ,    SOLVED
 UNIT   6, M4  ,    SOLVED
 UNIT   7, HX4 ,    SOLVED
 UNIT   8, P2  ,    SOLVED
LOOP  2 NOT SOLVED AFTER   1 TRIALS
 STRM: 12   T=  20.1 P= 2500.0 RATE= 6125.    DTEMP=   0.03 DCOMP=   0.0080
 UNIT   4, HX2 ,    SOLVED
 UNIT   5, F1  ,    SOLVED
 UNIT   6, M4  ,    SOLVED
 UNIT   7, HX4 ,    SOLVED
 UNIT   8, P2  ,    SOLVED
LOOP  2    SOLVED AFTER   2 TRIALS
 STRM: 12   T=  20.1 P= 2500.0 RATE= 6125.    DTEMP=   0.00 DCOMP=   0.0000
 UNIT   9, CON1,    SOLVED
 UNIT  10, M3  ,    SOLVED
 UNIT  11, S1  ,    SOLVED
LOOP  3    SOLVED AFTER   2 TRIALS
 STRM: 3    T=  80.0 P= 2500.0 RATE= 6014.    DTEMP=   0.00 DCOMP=   0.0000
 STRM: 4    T=  80.0 P= 2500.0 RATE= 326.1    DTEMP=   0.00 DCOMP=   0.0000
```

**** PROBLEM SOLUTION REACHED ****

SUMMARY OF FLASH DRUMS,MIXER/SPLITTERS AND VALVES

UNIT ID	F2	F1	M4	M3
SEQ NO	2	5	6	10
TYPE	FLASH	FLASH	MIXER	MIXER
FEEDS	5	7	10V	22
		6	10L	19
PRODUCTS	7 (V)	10V (V)	10 (M)	23 (L)
	8 (L)	10L (L)		
TEMP, DEG C	10.0000	23.5314	23.5314	73.0058
PRESSURE, MMHG	67.2398	67.2398	67.2398	2500.0000
FRACTION LIQUID	0.66020	0.98393	0.98393	1.00000
DUTY, MM KJ /HR	2.21901	0.00000	0.00000	0.00000

SUMMARY OF HEAT EXCHANGE UNITS

1 UNIT HX22, , IS A HEAT EXCHANGER

*** OPERATING CONDITIONS		
DUTY, MM KJ /HR	3.74538	
LMTD, DEG C	8.391	
F FACTOR	1.00000	
MTD , DEG C	8.391	
U * A, KJ /HR DEG C	446350.094	
*** HOT SIDE CONDITIONS	INLET	OUTLET
FEED(S)	4	
LIQUID PRODUCT		5
VAPOR, KG MOLS/HR	0.0000	0.0000
M KGS/HR	0.0000	0.0000
CP, KJ /KG - DEG C	0.0000	0.0000
LIQUID, KG MOLS/HR	326.1363	326.1363
M KGS/HR	20.5354	20.5354
CP, KJ /KG - DEG C	2.5074	2.5057
TOTAL, KG MOLS/HR	326.1363	326.1363
CONDENS(VAPORIZ)ATION, KG MOLS/HR		0.0000
TEMPERATURE, DEG C	80.000	32.319
PRESSURE, MMHG	2500.000	2500.000
*** COLD SIDE CONDITIONS	INLET	OUTLET
FEED(S)	9	
LIQUID PRODUCT		19
VAPOR, KG MOLS/HR	0.0000	0.0000
M KGS/HR	0.0000	0.0000
CP, KJ /KG - DEG C	0.0000	0.0000
LIQUID, KG MOLS/HR	215.3148	215.3148
M KGS/HR	11.7442	11.7442
CP, KJ /KG - DEG C	2.6106	2.6115
TOTAL, KG MOLS/HR	215.3148	215.3148
CONDENS(VAPORIZ)ATION, KG MOLS/HR		0.0000
TEMPERATURE, DEG C	10.124	78.000
PRESSURE, MMHG	2500.000	2500.000

4 UNIT HX2 , , IS A HEAT EXCHANGER

*** OPERATING CONDITIONS		
DUTY, MM KJ /HR	27.80338	
LMTD, DEG C	4.375	
F FACTOR	1.00000	
MTD , DEG C	4.375	
U * A, KJ /HR DEG C	6354704.500	
*** HOT SIDE CONDITIONS	INLET	OUTLET
FEED(S)	3	
LIQUID PRODUCT		6
VAPOR, KG MOLS/HR	0.0000	0.0000
M KGS/HR	0.0000	0.0000
CP, KJ /KG - DEG C	0.0000	0.0000
LIQUID, KG MOLS/HR	6013.9165	6013.9165
M KGS/HR	112.9155	112.9155
CP, KJ /KG - DEG C	4.0988	4.0859
TOTAL, KG MOLS/HR	6013.9165	6013.9165
CONDENS(VAPORIZ)ATION, KG MOLS/HR		0.0000
TEMPERATURE, DEG C	80.000	22.124
PRESSURE, MMHG	2500.000	2500.000
*** COLD SIDE CONDITIONS	INLET	OUTLET
FEED(S)	12	
LIQUID PRODUCT		22
VAPOR, KG MOLS/HR	0.0000	0.0000
M KGS/HR	0.0000	0.0000
CP, KJ /KG - DEG C	0.0000	0.0000
LIQUID, KG MOLS/HR	6124.7388	6124.7388
M KGS/HR	121.7068	121.7068
CP, KJ /KG - DEG C	3.9625	3.9681
TOTAL, KG MOLS/HR	6124.7388	6124.7388
CONDENS(VAPORIZ)ATION, KG MOLS/HR		0.0000
TEMPERATURE, DEG C	20.124	71.857
PRESSURE, MMHG	2500.000	2500.000

7 UNIT HX4 , , IS A HEAT EXCHANGER

*** OPERATING CONDITIONS	
DUTY, MM KJ /HR	6.89870
LMTD, DEG C	5.731
F FACTOR	1.00000
MTD , DEG C	5.731
U * A, KJ /HR DEG C	1203654.625

*** HOT SIDE CONDITIONS	INLET	OUTLET
FEED(S)	10	
LIQUID PRODUCT		11
VAPOR, KG MOLS/HR	98.4507	0.0000
M KGS/HR	6.4087	0.0000
CP, KJ /KG - DEG C	1.6889	0.0000
LIQUID, KG MOLS/HR	6026.2881	6124.7388
M KGS/HR	115.2981	121.7068
CP, KJ /KG - DEG C	4.0435	3.9626
TOTAL, KG MOLS/HR	6124.7388	6124.7388
CONDENS(VAPORIZ)ATION, KG MOLS/HR		98.4507
TEMPERATURE, DEG C	23.531	20.000
PRESSURE, MMHG	67.240	67.240

*** COLD SIDE CONDITIONS	INLET	OUTLET
COOLING WATER, KG /HR	823859.125	823859.125
TEMPERATURE, DEG C	15.000	17.000

SUMMARY OF COMPRESSOR/EXPANDER/PUMP/TURBINE UNITS

3 UNIT P1 , , IS A PUMP
*** FEED STREAMS ARE 8
*** LIQUID PRODUCT IS STREAM 9
*** OPERATING CONDITIONS

WORK, KW	2.33
EFFICIENCY, PERCENT	60.00

	INLET	OUTLET
MOLE FRACTION LIQUID	1.0000	1.0000
TEMPERATURE, DEG C	10.000	10.124
PRESSURE, MMHG	67.2398	2500.0000
HEAD, M		72.9743
HOT VOLUME, M3/HR	15.546	15.546

- -

8 UNIT P2 , , IS A PUMP
*** FEED STREAMS ARE 11
*** LIQUID PRODUCT IS STREAM 12
*** OPERATING CONDITIONS

WORK, KW	19.24
EFFICIENCY, PERCENT	60.00

	INLET	OUTLET
MOLE FRACTION LIQUID	1.0000	1.0000
TEMPERATURE, DEG C	20.000	20.124
PRESSURE, MMHG	67.2398	2500.0000
HEAD, M		58.0193
HOT VOLUME, M3/HR	128.086	128.092

SUMMARY OF COMPONENT SEPARATORS

UNIT ID	S1
SEQ NO	11
FEEDS	23

PRODUCTS	4 (L)	3 (L)
TEMP, DEG C	80.0000	80.0000
PRESSURE, MMHG	2500.0000	2500.0000
FRACTION LIQUID	1.00000	1.00000
DUTY, MM KJ /HR	-4.60207	

STREAM COMPONENT FLOW RATES - KG MOLS/HR

STREAM ID	3	4	5	6
PHASE	LIQUID	LIQUID	LIQUID	LIQUID
1 MDEAMI	66.1525	211.9901	211.9889	66.1531
2 H2O	5947.7617	114.1489	114.1475	5947.7632
TOTALS	6013.9141	326.1390	326.1363	6013.9165
TEMPERATURE, DEG C	80.0000	80.0000	32.3190	22.1237
PRESSURE, MMHG	2500.0000	2500.0000	2500.0000	2500.0000
H, MM KJ /HR	36.3002	4.6987	0.9532	8.4968
MOLE FRACT LIQUID	1.0000	1.0000	1.0000	1.0000
RECYCLE CONVERGENCE	0.0000	0.0000	0.0000	0.0000

STREAM ID	7	8	9	10
PHASE	VAPOR	LIQUID	LIQUID	MIXED
1 MDEAMI	98.2549	113.7340	113.7340	164.4080
2 H2O	12.5673	101.5802	101.5802	5960.3306

TOTALS	110.8222	215.3142	215.3142	6124.7388
TEMPERATURE, DEG C	10.0000	10.0000	10.1239	23.5314
PRESSURE, MMHG	67.2398	67.2398	2500.0000	67.2398
H, MM KJ /HR	3.9787	-0.8065	-0.7981	12.4755
MOLE FRACT LIQUID	0.0000	1.0000	1.0000	0.9839
RECYCLE CONVERGENCE	0.0000	0.0000	0.0000	0.0000

STREAM ID	11	12	19	22
PHASE	LIQUID	LIQUID	LIQUID	LIQUID
1 MDEAMI	164.4080	164.4080	113.7346	164.4080
2 H2O	5960.3306	5960.3306	101.5803	5960.3306
TOTALS	6124.7388	6124.7388	215.3148	6124.7388
TEMPERATURE, DEG C	19.9996	20.1237	78.0000	71.8572
PRESSURE, MMHG	67.2398	2500.0000	2500.0000	2500.0000
H, MM KJ /HR	5.5768	5.6461	2.9473	33.4494
MOLE FRACT LIQUID	1.0000	1.0000	1.0000	1.0000
RECYCLE CONVERGENCE	0.0000	0.0000	0.0000	0.0000

STREAM COMPONENT FLOW RATES - KG MOLS/HR

STREAM ID	23	10L	10V
PHASE	LIQUID	LIQUID	VAPOR
1 MDEAMI	278.1425	97.3828	67.0252
2 H2O	6061.9106	5928.9053	31.4253
TOTALS	6340.0532	6026.2881	98.4505
TEMPERATURE, DEG C	73.0058	23.5314	23.5314
PRESSURE, MMHG	2500.0000	67.2398	67.2398
H, MM KJ /HR	36.3968	8.5777	3.8978
MOLE FRACT LIQUID	1.0000	1.0000	0.0000
RECYCLE CONVERGENCE	0.0000	0.0000	0.0000

PROCESS™ Input and Output File Listings

NOVEL REFRIGERATION CYCLE WITH ABSORBENT PHASE DISTILLATION

```
TITLE PROJECT=MDEAM REFRIG, DATE=8-7-90
  CALC NOTRIAL=20
  TOLERANCE PROP=0.0005,TEMP=-0.002,STREAM=0.0001,-0.05
  DIMENSION SI,TEMP=C,PRESSURE=MMHG
  PRINT INPUT=NONE

COMP DATA
  LIBID 2,H2O
  NONLIBRARY 1,DMEAMI
  MW 1,73.14
  SPGR 1,0.69
  NBP 1,36.47
  TC 1,238
  PC 1,30007
  ACENTRIC 1,0.3039
  FORMATION(KJ,KG) 1,-58,39.70
  VP(MMHG) CORR=21,LOG,TEMP=C,DATA=1,,,7.06702,-1171.74,243.43
  HIDEAL(KJ,KG,MOLE) CORR=1,TEMP=K,DATA=1,,,+23.228,-11.439E-3,*
     0.2539E-3,-1.0213E-7,1.845E-11
  LATENT(KJ,KG) CORR=43,TEMP=K,DATA=1,,,317.6,0.38
  HLIQ(KJ,KG,MOLE) CORR=1,TEMP=C,DATA=1,,,0.0,0.1718

THERMO DATA
  TYPE KTYP=LACT,LACT,HTYP=LIBRARY,STYP=SRK
  HLSET KSET=1,SETNO=1
  KSET SETNO=1,NOTEMP=3
  SUBSET 1,10
  NRTL 1,2,,1104.7582,,388.6270,0.61462
  SUBSET 2,30
  NRTL 1,2,,856.4556,,586.5607,0.61462
  SUBSET 3,50.00
  NRTL 1,2,,608.1530,,784.4944,0.61462
  KSET SETNO=2
  NRTL 1,2,,674.6857,,1379.9828,0.4108

STREAM DATA
  PROPERTY STRM=31,TEMP=49.4,PRES=1100,COMP=1,582.5/2,30.27
  PROPERTY STRM=17,TEMP=83.0,PRES=1100,COMP=1,42.7/2,6311.6
  PROPERTY STRM=7,TEMP=30.1,PRES=1100,COMP=1,438.5/2,6318.9
  PROPERTY STRM=9A,TEMP=74.3,PRES=3500,COMP=1,116.4/2,198.2
  PROPERTY STRM=9,TEMP=102,PRES=3500,COMP=1,116.4/2,198.2
  PROPERTY STRM=10,TEMP=102,PRES=3500,COMP=1,322.1/2,6120.7

UNIT OPERATIONS
MIXER UID=M1
  FEED 9A,31
  PROD M=1
HX UID=HX5
  HOT FEED=1,L=2
  SPEC HOT,TEMP=30.0
  UTILITY WATER,TIN=20,TOUT=25
```

```
FLASH UID=F1
  FEED 2
  PROD V=5,L=6
  TPSPEC TEMP=10.
  SPEC STRM=6,COMP=1,FRACT=0.58
PUMP UID=P1
  FEED 6
  PROD L=26
  OPER PRES=3500,EFF=60
COLUMN UID=C1
  FEED 10,5/26,1
  PRODUCT OVHD=31,613,BTMS=17
  PARAMETER TRAY=6,SURE=20
  HEAT 1,6,5.94
  PSPEC TOP=1100
  SPEC TRAY=6,TEMP=83
  LIQUID 1,488.3/2,461.5/3,379.3/4,281.9/5,7847.6/6,6354.2
  VAPOUR 1,612.7/2,771.1/3,744.2/4,662.1/5,564.7/6,58.2
  TEMP 1,49.4/2,49.8/3,52.5/4,62.2/5,77.0/6,83.0
  PRINT TRAY=10
  VARIABLE HEAT=1

HX UID=HX7
  HOT FEED=17,L=11
  COLD FEED=7,M=15
  SPEC HOCI=5
  DATA KSET=1
FLASH UID=F2
  FEED 5,11
  PROD M=12
  ADIA
HX UID=HX4
  HOT FEED=12,L=13
  SPEC HOT,LFRACT=1.0
  UTILITY WATER,TIN=20,TOUT=25
PUMP UID=P2
  FEED 13
  PROD L=7
  OPER PRES=3500,EFF=60

CONTROL UID=CON2
  SPEC STRM=13,TEMP=30
  PARAM STRM=17,MAXI=20000,MINI=100,EST2=10300,IPRINT,RETURNUNIT=HX7

HX UID=HX1
  HOT FEED=9,L=9A
  COLD FEED=15,M=15A
  SPEC HOCI=5
HX UID=HX6
  COLD FEED=15A,L=15B
  SPEC COLD,TEMP=102
  UTILITY STEAM,TSAT=120
```

```
SEPARATOR UID=S1
  FEED 15B
  OVHD STRM=9,PHASE=L,TEMP=102
  BTMS STRM=10,PHASE=L,TEMP=102
  XOVHD 1,1,0.37
  XBTMS 2,2,0.95



CALCULATOR UID=CAL1
  RETRIEVE P(1),UNIT=C1,IDNO=1,DUTY
  RETRIEVE P(2),UNIT=F1,DUTY
  RETRIEVE P(3),UNIT=HX6,DUTY
  PROCEDURE
$ R(1) IS COEFFICIENT OF PERFORMANCE

  R(1)=P(1)+P(3)
  R(1)=P(2)/R(1)
  RETURN


OPTIMIZER UID=OPT1
  OBJECTIVE UNIT=CAL1,RESULT,IDNO=1,MAXIMISE
  PARAMETER UNIT=F1,SPEC,MINI=0.4,MAXI=0.60,EST2=0.585,STEPSIZE=0.005
  PARAMETER UNIT=C1,SPEC=1,MINI=50,MAXI=102,EST2=83.5,STEPSIZE=0.5
  OPTPARA METHOD=1,IPRINT=1

RECYCLE
  LOOP NO=1,START=M1,END=C1,TRIAL=15,TOLE=0.001,WEGS=4,,0.5,0.5
  LOOP NO=2,START=HX7,END=P2,TRIAL=10
  LOOP NO=3,START=HX1,END=S1,TRIAL=10
  LOOP NO=4,START=M1,END=S1,TRIAL=15,TOLE=0.0015
```

```
 UNIT  1, M1 ,    SOLVED
 UNIT  2, HX5 ,   SOLVED
 UNIT  3, F1 ,    SOLVED
 UNIT  4, P1 ,    SOLVED
 UNIT  5, C1 ,    SOLVED
LOOP 1   SOLVED AFTER  5 TRIALS
 STRM: 31  T=  58.9 P= 1100.0 RATE= 573.9    DTEMP=  0.00 DCOMP=  0.0003
 UNIT  6, HX7 ,   SOLVED
 UNIT  7, F2 ,    SOLVED
 UNIT  8, HX4 ,   SOLVED
 UNIT  9, P2 ,    SOLVED
LOOP 2   SOLVED AFTER  1 TRIALS
 STRM: 7   T=  30.2 P= 3500.0 RATE= 8697.    DTEMP=  0.00 DCOMP=  0.0000
 CONTROLLER UNIT 10, CON2, AT ITERATION  1
        SPECIFICATION VALUE =  0.30000E+02,  CALC =  0.29988E+02
        PARAMETER  CURRENT =  0.82880E+04,  NEXT =  0.82880E+04
 UNIT 10, CON2,   SOLVED
 UNIT 11, HX1 ,   SOLVED
 UNIT 12, HX6 ,   SOLVED
 UNIT 13, S1 ,    SOLVED
LOOP 3   SOLVED AFTER  1 TRIALS
 STRM: 9   T= 102.0 P= 3500.0 RATE= 53.86    DTEMP=  0.00 DCOMP=  0.0000
LOOP 4   SOLVED AFTER  6 TRIALS
 STRM: 9A  T=  75.2 P= 3500.0 RATE= 53.86    DTEMP=  0.00 DCOMP=  0.0000
 STRM: 10  T= 102.0 P= 3500.0 RATE= 8643.    DTEMP=  0.00 DCOMP=  0.0000
 UNIT 14, CAL1,   SOLVED
** AFTER  3 CYCLES
** CONVERGENCE METHOD  1 - SECOND ESTIMATE(S) LIMITING -
** BETTER SECOND ESTIMATE(S) MAY IMPROVE RESULTS.
   OPTIMIZATION HISTORY
   CYCLE        1        2        3
   PARA 1    5.8000E-01  5.8500E-01  5.8500E-01
   PARA 2    8.3000E+01  8.3000E+01  8.3500E+01
   OBJ.      2.5083E-01  2.5083E-01  2.5080E-01
    UNIT 15, OPT1,   SOLVED


   VERSION O484                    SM
   SIMULATION SCIENCES, INC.      PROCESS              PAGE  4
   PROJECT  MDEAM REFRIG
   PROBLEM                  SOLUTION          8-7-90



            **** PROBLEM SOLUTION REACHED ****
```

SUMMARY OF FLASH DRUMS,MIXER/SPLITTERS AND VALVES

UNIT ID	M1	F1	F2
SEQ NO	1	3	7
NAME			
TYPE	MIXER	FLASH	FLASH
FEEDS	9A	2	5
	31		11
PRODUCTS	1 (M)	5 (V)	12 (M)
		6 (L)	
TEMP, DEG C	58.9466	10.0000	37.9171
PRESSURE, MMHG	1100.0000	236.0427	236.0427
FRACTION LIQUID	0.07623	0.34896	0.96176
DUTY, MM KJ /HR	0.00000	7.10457	0.00000

SUMMARY OF HEAT EXCHANGE UNITS

2 UNIT HX5 , , IS A HEAT EXCHANGER

*** OPERATING CONDITIONS		
DUTY, MM KJ /HR	16.80980	
LMTD, DEG C	19.593	
F FACTOR	1.00000	
MTD , DEG C	19.593	
U * A, KJ /HR DEG C	57950.438	
*** HOT SIDE CONDITIONS	INLET	OUTLET
FEED(S)	1	
LIQUID PRODUCT		2
VAPOR, KG MOLS/HR	579.9301	0.0000
M KGS/HR	38.6136	0.0000
CP, KJ /KG - DEG C	1.7066	0.0000
LIQUID, KG MOLS/HR	47.8534	627.7835
M KGS/HR	1.6901	40.3037
CP, KJ /KG - DEG C	2.9901	2.4322
TOTAL, KG MOLS/HR	627.7835	627.7835
CONDENS(VAPORIZ)ATION, KG MOLS/HR		579.9301
TEMPERATURE, DEG C	58.947	30.000
PRESSURE, MMHG	1100.000	1100.000
*** COLD SIDE CONDITIONS	INLET	OUTLET
COOLING WATER, KG /HR	802987.188	802987.188
TEMPERATURE, DEG C	20.00	25.000

6 UNIT HX7 , , IS A HEAT EXCHANGER

*** OPERATING CONDITIONS		
DUTY, MM KJ /HR	30.58462	
LMTD, DEG C	8.476	
F FACTOR	1.00000	
MTD , DEG C	8.476	
U * A, KJ /HR DEG C	3608280.250	
*** HOT SIDE CONDITIONS	INLET	OUTLET
FEED(S)	17	
LIQUID PRODUCT		11
VAPOR, KG MOLS/HR	0.0000	0.0000
M KGS/HR	0.0000	0.0000
CP, KJ /KG - DEG C	0.0000	0.0000
LIQUID, KG MOLS/HR	8288.0313	8288.0313
M KGS/HR	152.2455	152.2455
CP, KJ /KG - DEG C	4.1505	4.1309
TOTAL, KG MOLS/HR	8288.0313	8288.0313
CONDENS(VAPORIZ)ATION, KG MOLS/HR		0.0000
TEMPERATURE, DEG C	83.500	35.174
PRESSURE, MMHG	1100.000	1100.000
*** COLD SIDE CONDITIONS	INLET	OUTLET
FEED(S)	7	
LIQUID PRODUCT		15
VAPOR, KG MOLS/HR	0.0000	0.0000
M KGS/HR	0.0000	0.0000
CP, KJ /KG - DEG C	0.0000	0.0000
LIQUID, KG MOLS/HR	8696.7061	8696.7061
M KGS/HR	181.5915	181.5915
CP, KJ /KG - DEG C	3.8453	3.8525
TOTAL, KG MOLS/HR	8696.7061	8696.7061
CONDENS(VAPORIZ)ATION, KG MOLS/HR		0.0000
TEMPERATURE, DEG C	30.174	70.221
PRESSURE, MMHG	3500.000	3500.000

8 UNIT HX4 , , IS A HEAT EXCHANGER

*** OPERATING CONDITIONS	
DUTY, MM KJ /HR	18.93911
LMTD, DEG C	11.390
F FACTOR	1.00000
MTD , DEG C	11.390
U * A, KJ /HR DEG C	1662783.125

*** HOT SIDE CONDITIONS	INLET	OUTLET
FEED(S)	12	
LIQUID PRODUCT		13
VAPOR, KG MOLS/HR	332.5957	0.0000
M KGS/HR	20.5528	0.0000
CP, KJ /KG - DEG C	1.7560	0.0000
LIQUID, KG MOLS/HR	8364.1455	8696.7412
M KGS/HR	161.0399	181.5928
CP, KJ /KG - DEG C	4.0215	3.8455
TOTAL, KG MOLS/HR	8696.7412	8696.7412
CONDENS(VAPORIZ)ATION, KG MOLS/HR		332.5957
TEMPERATURE, DEG C	37.917	29.988
PRESSURE, MMHG	236.043	236.043

*** COLD SIDE CONDITIONS	INLET	OUTLET
COOLING WATER, KG /HR	904702.000	904702.000
TEMPERATURE, DEG C	20.000	25.000

11 UNIT HX1 , , IS A HEAT EXCHANGER

*** OPERATING CONDITIONS	
DUTY, MM KJ /HR	0.21926
LMTD, DEG C	14.394
F FACTOR	1.00000
MTD , DEG C	14.394
U * A, KJ /HR DEG C	15232.754

*** HOT SIDE CONDITIONS	INLET	OUTLET
FEED(S)	9	
LIQUID PRODUCT		9A
VAPOR, KG MOLS/HR	0.0000	0.0000
M KGS/HR	0.0000	0.0000
CP, KJ /KG - DEG C	0.0000	0.0000
LIQUID, KG MOLS/HR	53.8621	53.8621
M KGS/HR	2.0689	2.0689
CP, KJ /KG - DEG C	2.9017	2.8931
TOTAL, KG MOLS/HR	53.8621	53.8621
CONDENS(VAPORIZ)ATION, KG MOLS/HR		0.0000
TEMPERATURE, DEG C	102.000	75.221
PRESSURE, MMHG	3500.000	3500.000

*** COLD SIDE CONDITIONS	INLET	OUTLET
FEED(S)	15	
LIQUID PRODUCT		15A
VAPOR, KG MOLS/HR	0.0000	0.0000
M KGS/HR	0.0000	0.0000
CP, KJ /KG - DEG C	0.0000	0.0000
LIQUID, KG MOLS/HR	8696.7061	8696.7061
M KGS/HR	181.5915	181.5915
CP, KJ /KG - DEG C	3.8525	3.8527
TOTAL, KG MOLS/HR	8696.7061	8696.7061
CONDENS(VAPORIZ)ATION, KG MOLS/HR		0.0000
TEMPERATURE, DEG C	70.221	70.513
PRESSURE, MMHG	3500.000	3500.000

12 UNIT HX6 , , IS A HEAT EXCHANGER

*** OPERATING CONDITIONS	
DUTY, MM KJ /HR	23.42941
LMTD, DEG C	31.134
F FACTOR	1.00000
MTD , DEG C	31.134
U * A, KJ /HR DEG C	752533.188

*** HOT SIDE CONDITIONS	INLET	OUTLET
STEAM, KG /HR	10642.438	10642.438
SATURATION PRESSURE, MMHG		1478.249
SATURATION TEMPERATURE, DEG C		120.000

*** COLD SIDE CONDITIONS	INLET	OUTLET
FEED(S)	15A	
LIQUID PRODUCT	15B	
VAPOR, KG MOLS/HR	0.0000	0.0000
M KGS/HR	0.0000	0.0000
CP, KJ /KG - DEG C	0.0000	0.0000
LIQUID, KG MOLS/HR	8696.7061	8696.7061
M KGS/HR	181.5915	181.5915
CP, KJ /KG - DEG C	3.8527	3.8792
TOTAL, KG MOLS/HR	8696.7061	8696.7061
CONDENS(VAPORIZ)ATION, KG MOLS/HR		0.0000
TEMPERATURE, DEG C	70.513	102.000
PRESSURE, MMHG	3500.000	3500.000

SUMMARY OF COMPRESSOR/EXPANDER/PUMP/TURBINE UNITS

4 UNIT P1 , , IS A PUMP

*** FEED STREAMS ARE 6
*** LIQUID PRODUCT IS STREAM 26
*** OPERATING CONDITIONS

WORK, KW	3.04
EFFICIENCY, PERCENT	60.00

	INLET	OUTLET
MOLE FRACTION LIQUID	1.0000	1.0000
TEMPERATURE, DEG C	10.000	10.183
PRESSURE, MMHG	236.0427	3500.0000
HEAD, M		101.8107
HOT VOLUME, M3/HR	15.081	15.081

- -

9 UNIT P2 , , IS A PUMP

*** FEED STREAMS ARE 13
*** LIQUID PRODUCT IS STREAM 7
*** OPERATING CONDITIONS

WORK, KW	40.19
EFFICIENCY, PERCENT	60.00

	INLET	OUTLET
MOLE FRACTION LIQUID	1.0000	1.0000
TEMPERATURE, DEG C	29.988	30.173
PRESSURE, MMHG	236.0427	3500.0000
HEAD, M		81.2327
HOT VOLUME, M3/HR	199.433	199.449

SUMMARY OF COMPONENT SEPARATORS

UNIT ID	S1	
SEQ NO	13	
NAME		
FEEDS	15B	
PRODUCTS	9 (L)	10 (L)
TEMP, DEG C	102.0000	102.0000
PRESSURE, MMHG	3500.0000	3500.0000
FRACTION LIQUID	1.00000	1.00000
DUTY, MM KJ /HR	-0.15790	

SUMMARY OF CALCULATOR UNITS
REPORT OF RESULTS VECTORS

UNIT ID	CAL1
SEQ NO	14
NAME	

R(1)	2.50798E-01
R(2)	UNDEFINED
R(3)	UNDEFINED
R(4)	UNDEFINED
R(5)	UNDEFINED
R(6)	UNDEFINED
R(7)	UNDEFINED
R(8)	UNDEFINED

I SUMMARY FOR COLUMN UNIT 5 - C1 ,

1 TOTAL NUMBER OF ITERATIONS

FAST METHOD	0
SURE METHOD	117

2 COLUMN SUMMARY

TRAY	TEMP DEG C	PRESS MMHG	NET FLOW RATES, KG MOLS/HR LIQUID PHASE(L)	VAPOR PHASE(V)	FEED	PRODUCT	HEAT(COOL)ER DUTIES MM KJ /HR
1	58.9	1100.00	225.7		219.1L	573.9V	
2	71.6	1100.00	190.1	580.5			
3	78.2	1100.00	191.7	544.9			
4	78.6	1100.00	191.8	546.5			
5	78.7	1100.00	8333.1	546.6	8642.8L		
6	83.5	1100.00		45.1		8288.0L	4.8985

3 FEED AND PRODUCT STREAMS	MASS RATES KG MOLS/HR	HEAT RATES MM KJ /HR
* FEED STREAMS:		
10 TO TRAY 5 IS LIQUID FROM UNIT 13, S1	0.86428E+04	0.66631E+02
26 TO TRAY 1 IS LIQUID FROM UNIT 4, P1	0.21907E+03	-0.47215E+00
* PRODUCT STREAMS:		
17 IS LIQUID STREAM FROM TRAY 6	0.82880E+04	0.51509E+02
31 IS VAPOR STREAM FROM TRAY 1	0.57389E+03	0.19549E+02
OVERALL MASS BALANCE, (FEEDS - PRODS)	0.00000E+00	
OVERALL HEAT BALANCE, (HIN - HOUT)		-0.61798E-03

4 SPECIFICATION VALUES

PARAMETER TYPE	TRAY NO	COMP. NO	SPECIFICATION TYPE	SPECIFIED VALUE	CALCULATED VALUE
TRAY	6		TEMP	0.8350E+02	0.8350E+02

IIA TRAY COMPOSITIONS

TRAY	-------- 1 --------		-------- 2 --------	
COMPONENT	X	Y	X	Y
1 DMEAMI	0.3167E+00	0.8822E+00	0.1936E-01	0.7762E+00
2 H2O	0.6833E+00	0.1184E+00	0.9806E+00	0.2244E+00
KG MOLS/HR	0.2257E+03	0.5739E+03	0.1901E+03	0.5805E+03
TRAY	-------- 3 --------		-------- 4 --------	
COMPONENT	X	Y	X	Y
1 DMEAMI	0.1020E-01	0.7024E+00	0.9826E-02	0.6970E+00
2 H2O	0.9898E+00	0.2979E+00	0.9902E+00	0.3032E+00
KG MOLS/HR	0.1917E+03	0.5449E+03	0.1918E+03	0.5465E+03

TRAY	-------- 5 --------		-------- 6 --------	
COMPONENT	X	Y	X	Y
1 DMEAMI	0.9804E-02	0.6965E+00	0.6428E-02	0.6304E+00
2 H2O	0.9902E+00	0.3035E+00	0.9936E+00	0.3696E+00
KG MOLS/HR	0.8333E+04	0.5466E+03	0.8288E+04	0.4509E+02

STREAM COMPONENT FLOW RATES - KG MOLS/HR

STREAM ID	1	2	5	6
NAME				
PHASE	MIXED	LIQUID	VAPOR	LIQUID
1 DMEAMI	525.9717	525.9717	398.8082	127.1635
2 H2O	101.8119	101.8119	9.9025	91.9094
TOTALS	627.7835	627.7835	408.7106	219.0729
TEMPERATURE, DEG C	58.9466	30.0000	10.0000	10.0000
PRESSURE, MMHG	1100.0000	1100.0000	236.0427	236.0427
H, MM KJ /HR	20.0650	3.2552	10.8429	-0.4831
MOLE FRACT LIQUID	0.0762	1.0000	0.0000	1.0000
RECYCLE CONVERGENCE	0.0000	0.0000	0.0000	0.0000

STREAM ID	7	9	10	11
NAME				
PHASE	LIQUID	LIQUID	LIQUID	LIQUID
1 DMEAMI	452.0813	19.9285	432.1414	53.2731
2 H2O	8244.6602	33.9336	8210.7021	8234.7578
TOTALS	8696.7412	53.8621	8642.8438	8288.0313
TEMPERATURE, DEG C	30.1733	102.0000	102.0000	35.1735
PRESSURE, MMHG	3500.0000	3500.0000	3500.0000	1100.0000
H, MM KJ /HR	12.9730	0.7330	66.6313	20.9243
MOLE FRACT LIQUID	1.0000	1.0000	1.0000	1.0000
RECYCLE CONVERGENCE	0.0000	0.0000	0.0000	0.0000

STREAM ID	12	13	15	17
NAME				
PHASE	MIXED	LIQUID	LIQUID	LIQUID
1 DMEAMI	452.0813	452.0813	452.0699	53.2731
2 H2O	8244.6602	8244.6602	8244.6357	8234.7578
TOTALS	8696.7412	8696.7412	8696.7061	8288.0313
TEMPERATURE, DEG C	37.9171	29.9883	70.2207	83.5000
PRESSURE, MMHG	236.0427	236.0427	3500.0000	1100.0000
H, MM KJ /HR	31.7674	12.8283	43.5578	51.5089
MOLE FRACT LIQUID	0.9618	1.0000	1.0000	1.0000
RECYCLE CONVERGENCE	0.0000	0.0000	0.0000	0.0000

STREAM COMPONENT FLOW RATES - KG MOLS/HR

STREAM ID NAME	26	31	9A	15A
PHASE	LIQUID	VAPOR	LIQUID	LIQUID
1 DMEAMI	127.1635	505.9881	19.9285	452.0699
2 H2O	91.9094	67.8982	33.9336	8244.6357
TOTALS	219.0729	573.8863	53.8621	8696.7061
TEMPERATURE, DEG C	10.1830	58.8779	75.2207	70.5128
PRESSURE, MMHG	3500.000	1100.0000	3500.0000	3500.0000
H, MM KJ /HR	-0.4721	19.5493	0.5137	43.7770
MOLE FRACT LIQUID	1.000	0.0000	1.0000	1.0000
RECYCLE CONVERGENCE	0.0000	0.0003	0.0000	0.0000

STREAM ID NAME	15B
PHASE	LIQUID
1 DMEAMI	452.0699
2 H2O	8244.6357
TOTALS	8696.7061
TEMPERATURE, DEG C	102.0000
PRESSURE, MMHG	3500.0000
H, MM KJ /HR	67.2064
MOLE FRACT LIQUID	1.0000
RECYCLE CONVERGENCE	0.0000

PROCESS™ Input and Output File Listings

THE MODIFIED AQUA-AMMONIA REFRIGERATION CYCLE WITHOUT PRECOOLING

```
TITLE PROJECT=MDEAM REFRIG, DATE=8-7-90
  TOLER PROP=0.0005,TEMP=-0.002,STREAM=0.0001,-0.002,0.0001
  CALC NOTRIAL=10
  EXERGY
  DIMENSION SI,TEMP=C,PRESS=ATM
  PRINT INPUT=NONE

COMP DATA
  LIBID 1,NH3/2,H2O
  THERMO DATA
  YPE KTYP=U2,HTYP=U3,STYP=U4

STREAM DATA
  PROPERTY STRM=3,TEMP=156.7,PRES=17.05,RATE=521,COMP=1,17.95/2,82.05
  PROPERTY STRM=2,TEMP=44.4,PRES=17.1,RATE=650.,COMP=1,36.78/2,63.22
  PROPERTY STRM=5,TEMP=44.,PRES=17.05,RATE=162,COMP=1,99.69/2,0.31



UNIT OPERATIONS

FLASH UID=F2
  FEED 5
  PROD V=7,L=8
  TPSPEC TEMP=-10.
  SPEC STRM=8,RATE=0.043,REFS=5
  DATA KSET=1

PUMP UID=P1
  FEED 8
  PROD L=8A
  OPER PRES=17.1,EFF=60

HX UID=HX2,PLOT,ZONES=5
  HOT FEED=3,L=6
  COLD FEED=2A,L=12
  SPEC HOCI=10
  DATA KSET=1
  CONF U=3600
```

```
MIXER UID=M2
  FEED 6,7
  PROD M=15
HX UID=HX4
  HOT FEED=15,L=11,DP=0.12
  SPEC HOT,LFRACT=1.0
  UTILITY WATER,TIN=27,TOUT=40
  DATA KSET=1
  CONF U=3600
PUMP UID=P2
  FEED 11
  PROD L=2
  OPER PRES=17.1,EFF=60
MIXER UID=M1
  FEED 2,8A
  PROD M=2A
CONTROL  UID=CON2
  SPEC STRM=11,TEMP=44.0
  PARAM STRM=3,MAXI=3000,MINI=100,EST2=2500
COLUMN UID=COL1
  PARA TRAY=7,FAST=5,SURE=30
  FEED 12,4
  PRODUCT OVHD=5,BTMS=3,1662
  PSPEC TOP=17.1
  CONDENSER TYPE=3
  HEAT  1,7,5.30/2,1,-3.56
  PRINT TRAY=10
  SPEC TRAY=7,TEMP=154.00
  SPEC TRAY=1,PHASE=L,RATE=70
  VARIABLE HEAT=1,2
  TEMP  1,44.0/2,65.6/3,99.8/4,105.7/5,107.6/6,117.8/7,149.7
  VAPOUR  1,147.6/2,180.8/3,161.3/4,158.9/5,155.7/6,153/7,145.1
  LIQUID  1,33./2,13.6/3,11.3/4,578.3/5,575.7/6,567.8/7,422.7
  DATA KSET=1
```

```
HX UID=REB1
  ATTACHED COLUMN=COL1,TYPE=2
  UTILITY STEAM,TSAT=170
  CONF U=3600

HX UID=COND1
  ATTACHED COLUMN=COL1,TYPE=1
  UTILITY WATER,TIN=27,TOUT=40
  CONF U=3600

CONTROL  UID=CON1
  SPEC STRM=5,TEMP=44.0
  PARAM UNIT=COL1,SPEC=2,MAXI=300,MINI=2,EST2=96,IPRINT,STEPSIZE=4,NOST

CALCULATOR UID=CAL1
  RETRIEVE P(1),UNIT=HX2,AREA
  RETRIEVE P(2),UNIT=HX4,AREA
  RETRIEVE P(3),UNIT=COND1,AREA
  RETRIEVE P(4),UNIT=REB1,AREA
  RETRIEVE P(5),UNIT=F2,DUTY
  RETRIEVE P(6),UNIT=COL1,IDNO=1,DUTY
  PROCEDURE

  $R(1) IS EVAPORATOR AREA
  $R(2) IS TOTAL EXCHANGER AREA
  $R(3) IS EXCHANGER AREA FOR 2.5 MMKJ/HR OF REFRIGERATION
  $R(4) IS COST OF HEAT EXCHANGERS
  $R(5) IS COEFFICIENT OF PERFORMANCE
  $R(6) IS COST OF COOLING WATER FOR 3 YRS
  $R(7) IS COST OF COOLING WATER FOR 3 YRS + EXCHANGER COST
```

```
  R(1)=P(5)/0.036
  R(2)=R(1)+P(1)
  R(2)=R(2)+P(2)
  R(2)=R(2)+P(3)
  R(2)=R(2)+P(4)
  R(3)=R(2)/P(5)
  R(3)=R(3)*45.36
  R(4)=R(3)*550
  R(4)=R(4)+78500
  R(5)=P(5)/P(6)
  R(6)=P(5)+P(6)
  R(6)=R(6)/P(5)
  R(6)=R(6)*45.36
  R(6)=R(6)*22500
  R(7)=R(4)+R(6)
  RETURN

OPTIMIZER UID=OPT
  OBJECTIVE UNIT=CAL1,RESULT,IDNO=7,MINIMISE
  PARAMETER UNIT=F2,SPEC,MINI=0.02,MAXI=0.13,EST2=0.041,STEPSIZE=0.002
  PARAMETER UNIT=HX2,SPEC,MINI=4,MAXI=50,EST2=9,STEPSIZE=1
  PARAMETER UNIT=COL1,SPEC=1,MINI=105,MAXI=160,EST2=155,STEPSIZE=1
  OPTPARA METHOD=1,IPRINT=1

RECYCLE
  LOOP NO=1,START=HX2,END=M1
  LOOP NO=2,START=F2,END=CON1,TRIAL=25
```

UNIT 1, F2 , SOLVED

UNIT 2, P1 , SOLVED

UNIT 3, HX2 , SOLVED

UNIT 4, M2 , SOLVED

UNIT 5, HX4 , SOLVED

UNIT 6, P2 , SOLVED

UNIT 7, M1 , SOLVED

LOOP 1 SOLVED AFTER 1 TRIALS

STRM: 2A T= 44.6 P= 17.1 RATE= 662.5 DTEMP= 0.00 DCOMP= 0.0000

UNIT 8, CON2, SOLVED

UNIT 9, COL1, SOLVED

CONTROLLER UNIT 12, CON1, AT ITERATION 1

SPECIFICATION VALUE = 0.44000E+02, CALC = 0.44002E+02

PARAMETER CURRENT = 0.62587E+02, NEXT = 0.62587E+02

UNIT 12, CON1, SOLVED

LOOP 2 SOLVED AFTER 5 TRIALS

STRM: 3 T= 157.0 P= 17.1 RATE= 500.6 DTEMP= 0.00 DCOMP= 0.0000

STRM: 5 T= 44.0 P= 17.1 RATE= 161.9 DTEMP= 0.00 DCOMP= 0.0000

UNIT 10, REB1, SOLVED

UNIT 11, COND, SOLVED

UNIT 13, CAL1, SOLVED

** AFTER 10 CYCLES

** CONVERGENCE METHOD 1 - OBJECTIVE FUNCTION NO LONGER IMPROVES.

OPTIMIZATION HISTORY

CYCLE	1	2	3	4	5
PARA 1	4.3000E-02	4.1000E-02	4.1000E-02	4.1000E-02	4.0426E-02
PARA 2	1.0000E+01	1.0000E+01	9.0000E+00	9.0000E+00	8.9144E+00
PARA 3	1.5400E+02	1.5400E+02	1.5400E+02	1.5500E+02	1.5595E+02
OBJ.	6.4509E+06	6.4390E+06	6.4354E+06	6.3958E+06	6.3618E+06

OPTIMIZATION HISTORY

CYCLE	6	7	8	9	10
PARA 1	3.9853E-02	3.9279E-02	3.7937E-02	3.9902E-02	4.1053E-02
PARA 2	8.8288E+00	8.7433E+00	8.8288E+00	7.8325E+00	9.6241E+00
PARA 3	1.5691E+02	1.5786E+02	1.5662E+02	1.5683E+02	1.5700E+02
OBJ.	6.3358E+06	6.3436E+06	6.3659E+06	6.3752E+06	6.3738E+06

** BEST OBJECTIVE FUNCTION = 6.33576E+06 AT CYCLE NUMBER 6

UNIT 2, P1 , SOLVED

UNIT 3, HX2 , SOLVED

UNIT 4, M2 , SOLVED

UNIT 5, HX4 , SOLVED

UNIT 6, P2 , SOLVED

UNIT 7, M1 , SOLVED

LOOP 1 SOLVED AFTER 1 TRIALS

STRM: 2A T= 44.6 P= 17.1 RATE= 664.2 DTEMP= 0.00 DCOMP= 0.0000

UNIT 8, CON2, SOLVED

UNIT 9, COL1, SOLVED

CONTROLLER UNIT 12, CON1, AT ITERATION 1

SPECIFICATION VALUE = 0.44000E+02, CALC = 0.44003E+02

PARAMETER CURRENT = 0.62587E+02, NEXT = 0.62587E+02

UNIT 12, CON1, SOLVED

LOOP 2 SOLVED AFTER 7 TRIALS

STRM: 3 T= 156.9 P= 17.1 RATE= 502.3 DTEMP= 0.00 DCOMP= 0.0000

STRM: 5 T= 44.0 P= 17.1 RATE= 161.8 DTEMP= 0.00 DCOMP= 0.0000

UNIT 10, REB1, SOLVED

UNIT 11, COND, SOLVED

UNIT 13, CAL1, SOLVED

UNIT 14, OPT , SOLVED

**** PROBLEM SOLUTION REACHED ****

SUMMARY OF FLASH DRUMS,MIXER/SPLITTERS AND VALVES

UNIT ID	F2	M2	M1
EQ NO	1	4	7
NAME			
TYPE	FLASH	MIXER	MIXER
FEEDS	5	6	2
		7	8A
PRODUCTS	7 (V)	15 (M)	2A (L)
	8 (L)		
TEMP, DEG C	-10.0000	68.2266	44.5615
PRESS, ATM	2.8055	2.8055	17.1000
FRACT LIQUID	0.03985	0.82309	1.00000
DUTY, MM KJ /HR	2.72702	0.00000	0.00000

SUMMARY OF HEAT EXCHANGE UNITS

3 UNIT HX2 , , IS A HEAT EXCHANGER

*** OPERATING CONDITIONS

DUTY, MM KJ /HR	4.09450
WEIGHTED LMTD, DEG C	19.654
F FACTOR	1.00000
MTD , DEG C	19.654
U * A, KJ /HR DEG C	208326.109
U, KJ /HR DEG C SQ M	3600.000
A, SQ M	57.868

*** HOT SIDE CONDITIONS	INLET	OUTLET
FEED(S)	3	
LIQUID PRODUCT		6
VAPOR, KG MOLS/HR	0.0000	0.0000
M KGS/HR	0.0005	0.0000
CP, KJ /KG - DEG C	2.6914	0.0000
LIQUID, KG MOLS/HR	502.3283	502.3283
M KGS/HR	8.9604	8.9609
CP, KJ /KG - DEG C	4.6546	4.3167
TOTAL, KG MOLS/HR	502.3283	502.3283
CONDENS(VAPORIZ)ATION, KG MOLS/HR		0.0000
TEMPERATURE, DEG C	156.908	53.391
PRESSURE, ATM	17.100	17.100

*** COLD SIDE CONDITIONS	INLET	OUTLET
FEED(S)	2A	
MIXED PRODUCT		12
VAPOR, KG MOLS/HR	0.0000	15.4922
M KGS/HR	0.0000	0.2648
CP, KJ /KG - DEG C	0.0000	2.7243
LIQUID, KG MOLS/HR	664.1602	648.6680
M KGS/HR	11.7172	11.4523
CP, KJ /KG - DEG C	4.4855	4.7239
TOTAL, KG MOLS/HR	664.1602	664.1602
CONDENS(VAPORIZ)ATION, KG MOLS/HR		15.4922
TEMPERATURE, DEG C	44.562	114.607
PRESSURE, ATM	17.100	17.100

5 UNIT HX4 , , IS A HEAT EXCHANGER

*** OPERATING CONDITIONS	
DUTY, MM KJ /HR	4.46875
LMTD, DEG C	22.131
F FACTOR	1.00000
MTD , DEG C	22.131
U * A, KJ /HR DEG C	201921.375
U, KJ /HR DEG C SQ M	3600.000
A, SQ M	56.089

*** HOT SIDE CONDITIONS	INLET	OUTLET
FEED(S)	15	
LIQUID PRODUCT		11
VAPOR, KG MOLS/HR	116.356	0.0000
M KGS/HR	1.9899	0.0000
CP, KJ /KG - DEG C	2.2962	0.0000
LIQUID, KG MOLS/HR	541.3550	657.7112
M KGS/HR	9.6173	11.6072
CP, KJ /KG - DEG C	4.3809	4.4904
TOTAL, KG MOLS/HR	657.7112	657.7112
CONDENS(VAPORIZ)ATION, KG MOLS/HR		116.3562
TEMPERATURE, DEG C	68.227	43.984
PRESSURE, ATM	2.805	2.685

*** COLD SIDE CONDITIONS	INLET	OUTLET
COOLING WATER, KG /HR	82102.953	82102.953
TEMPERATURE, DEG C	27.000	40.000

10 UNIT REB1, , IS A HEAT EXCHANGER

*** OPERATING CONDITIONS		
DUTY, MM KJ /HR	5.94961	
LMTD, DEG C	24.952	
F FACTOR	1.00000	
MTD , DEG C	24.952	
U * A, KJ /HR DEG C	238443.094	
U, KJ /HR DEG C SQ M	3600.000	
A, SQ M	66.234	
*** HOT SIDE CONDITIONS	INLET	OUTLET
STEAM, KG /HR	2830.137	2830.137
SATURATION PRESSURE, ATM		7.780
SATURATION TEMPERATURE, DEG C		170.000
*** COLD SIDE CONDITIONS	INLET	OUTLET
STREAM IS FROM COLUMN COL1, UNIT 9		
VAPOR, KG MOLS/HR	0.0000	158.0592
M KGS/HR	0.0000	2.7376
CP, KJ /KG - DEG C	0.0000	2.6913
LIQUID, KG MOLS/HR	660.4044	502.3452
M KGS/HR	11.6987	8.9612
CP, KJ /KG - DEG C	4.7049	4.6546
TOTAL, KG MOLS/HR	660.4044	660.4044
CONDENS(VAPORIZ)ATION, KG MOLS/HR		158.0592
TEMPERATURE, DEG C	127.592	156.896
PRESSURE, ATM	17.100	17.100

11 UNIT COND, , IS A HEAT EXCHANGER

*** OPERATING CONDITIONS		
DUTY, MM KJ /HR	4.24328	
LMTD, DEG C	14.471	
F FACTOR	1.00000	
MTD , DEG C	14.471	
U * A, KJ /HR DEG C	293219.938	
U, KJ /HR DEG C SQ M	3600.000	
A, SQ M	81.450	
*** HOT SIDE CONDITIONS	INLET	OUTLET
STREAM IS FROM COLUMN COL1, UNIT 9		
VAPOR, KG MOLS/HR	224.3906	0.0000
M KGS/HR	3.8218	0.0000
CP, KJ /KG - DEG C	3.1813	0.0000
LIQUID, KG MOLS/HR	0.0000	224.3906
M KGS/HR	0.0000	3.8218
CP, KJ /KG - DEG C	0.0000	5.0297
TOTAL, KG MOLS/HR	224.3906	224.3906
CONDENS(VAPORIZ)ATION, KG MOLS/HR		224.3906
TEMPERATURE, DEG C	52.236	43.964
PRESSURE, ATM	17.100	17.100
*** COLD SIDE CONDITIONS	INLET	OUTLET
COOLING WATER, KG /HR	77960.492	77960.492
TEMPERATURE, DEG C	27.000	40.000

SUMMARY OF COMPRESSOR/EXPANDER/PUMP/TURBINE UNITS

2 UNIT P1 , , IS A PUMP

*** FEED STREAMS ARE 8

*** LIQUID PRODUCT IS STREAM 8A

*** OPERATING CONDITIONS

WORK, KW		0.11
EFFICIENCY, PERCENT		60.00
	INLET	OUTLET
MOLE FRACTION LIQUID	1.0000	1.0000
TEMPERATURE, DEG C	-10.000	-9.415
PRESSURE, ATM	2.8055	17.1000
HEAD, M		374.9895
HOT VOLUME, M3/HR	0.167	0.168

- -

6 UNIT P2 , , IS A PUMP

*** FEED STREAMS ARE 11

*** LIQUID PRODUCT IS STREAM 2

*** OPERATING CONDITIONS

WORK, KW		9.92
EFFICIENCY, PERCENT		60.00
	INLET	OUTLET
MOLE FRACTION LIQUID	1.0000	1.0000
TEMPERATURE, DEG C	43.984	44.410
PRESSURE, ATM	2.6855	17.1000
HEAD, M		313.7579
HOT VOLUME, M3/HR	14.670	14.670

SUMMARY OF CALCULATOR UNITS

REPORT OF RESULTS VECTORS

UNIT ID	CAL1	
SEQ NO	13	
NAME		
R(1)		7.57507E+01
R(2)		3.32762E+02
R(3)		5.53500E+03
R(4)		3.12275E+06
R(5)		4.58353E-01
R(6)		3.24727E+06
R(7)		6.37002E+06
R(8)		UNDEFINED

I SUMMARY FOR COLUMN UNIT 9 - COL1,

1 TOTAL NUMBER OF ITERATIONS

FAST METHOD	0
SURE METHOD	170

2 COLUMN SUMMARY

TRAY	TEMP	PRESS	NET FLOW RATES, KG MOLS/HR				HEAT(COOL)ER DUTIES
			LIQUID	VAPOR			
	DEG C	ATM	PHASE(L)	PHASE(V)	FEED	PRODUCT	MM KJ /HR
1	44.0	17.10	62.6			161.8L	-4.2433
2	52.2	17.10	30.6	224.4			
3	98.8	17.10	21.0	192.4			
4	114.6	17.10	668.9	182.8	664.2M		
5	117.0	17.10	666.3	166.6			
6	127.6	17.10	660.4	164.0			
7	156.9	17.10	158.1			502.3L	5.9496

3 FEED AND PRODUCT STREAMS	MASS RATES	HEAT RATES
* FEED STREAMS:	KG MOLS/HR	MM KJ /HR
12 TO TRAY 4 IS MIXED FROM UNIT 3, HX2	0.66416E+03	0.35989E+01
* PRODUCT STREAMS:		
3 IS LIQUID STREAM FROM TRAY 7	0.50233E+03	0.47243E+01
5 IS LIQUID STREAM FROM TRAY 1	0.16183E+03	0.58013E+00

OVERALL MASS BALANCE, (FEEDS - PRODS)	0.00000E+00
OVERALL HEAT BALANCE, (HIN - HOUT)	0.76151E-03

4 SPECIFICATION VALUES

PARAMETER TYPE	TRAY NO	COMP. NO	SPECIFICATION TYPE	SPECIFIED VALUE	CALCULATED VALUE
TRAY	7		TEMP	0.1569E+03	0.1569E+03
TRAY LIQD	1		ML RATE	0.6259E+02	0.6259E+02

IIA TRAY COMPOSITIONS

TRAY	-------- 1 --------		-------- 2 --------	
COMPONENT	X	Y	X	Y
1 NH3	0.9991E+00	0.9991E+00	0.8110E+00	0.9990E+00
2 H2O	0.8502E-03	0.8502E-03	0.1890E+00	0.8501E-03
KG MOLS/HR	0.6259E+02	0.1618E+03	0.3058E+02	0.2244E+03

TRAY	-------- 3 --------		-------- 4 --------	
COMPONENT	X	Y	X	Y
1 NH3	0.4440E+00	0.9689E+00	0.3658E+00	0.9355E+00
2 H2O	0.5560E+00	0.3076E-01	0.6342E+00	0.6454E-01
KG MOLS/HR	0.2096E+02	0.1924E+03	0.6689E+03	0.1828E+03

TRAY	-------- 5 --------		-------- 6 --------	
COMPONENT	X	Y	X	Y
1 NH3	0.3543E+00	0.9284E+00	0.3053E+00	0.8905E+00
2 H2O	0.6457E+00	0.7158E-01	0.6947E+00	0.1095E+00
KG MOLS/HR	0.6663E+03	0.1666E+03	0.6604E+03	0.1640E+03

TRAY	-------- 7 --------	
COMPONENT	X	Y
1 NH3	0.1792E+00	0.7059E+00
2 H2O	0.8208E+00	0.2942E+00
KG MOLS/HR	0.5023E+03	0.1581E+03

STREAM COMPONENT FLOW RATES - KG MOLS/HR

STREAM ID	2	3	5	6
PHASE	LIQUID	LIQUID	LIQUID	LIQUID
1 NH3	245.3941	90.0117	161.6943	90.0119
2 H2O	412.3170	412.3166	0.1376	412.3164
TOTALS	657.7112	502.3284	161.8319	502.3283
TEMPERATURE, DEG C	44.4103	156.9083	44.0035	53.3908
PRESSURE, ATM	17.1000	17.1000	17.1000	17.1000
H, MM KJ /HR	-0.4892	4.7243	0.5801	0.6298
MOLE FRACT LIQUID	1.0000	1.0000	1.0000	1.0000
RECYCLE CONVERGENCE	0.0000	0.0000	0.0000	0.0000

STREAM ID	7	8	11	12
PHASE	VAPOR	LIQUID	LIQUID	MIXED
1 NH3	155.3822	6.3121	245.3941	251.7040
2 H2O	0.0007	0.1369	412.3170	412.4562
TOTALS	155.3829	6.4490	657.7112	664.1602
TEMPERATURE, DEG C	-10.0000	-10.0000	43.9835	114.6066
PRESSURE, ATM	2.8055	2.8055	2.6855	17.1000
H, MM KJ /HR	3.3140	-0.0069	-0.5249	3.5989
MOLE FRACT LIQUID	0.0000	1.0000	1.0000	0.9767
RECYCLE CONVERGENCE	0.0000	0.0000	0.0000	0.0000

STREAM ID	15	2A	8A
PHASE	MIXED	LIQUID	LIQUID
1 NH3	245.3941	251.7062	6.3121
2 H2O	412.3170	412.4539	0.1369
TOTALS	657.7112	664.1602	6.4490
TEMPERATURE, DEG C	68.2266	44.5615	-9.4154
PRESSURE, ATM	2.8055	17.1000	17.1000
H, MM KJ /HR	3.9439	-0.4956	-0.0065
MOLE FRACT LIQUID	0.8231	1.0000	1.0000
RECYCLE CONVERGENCE	0.0000	0.0000	0.0000

------ ------------ -----

STREAM AVAILABILITY TABLE
TZERO = 15.00 DEG C

ID	NAME	RATE	ENTHALPY	ENTROPY	B=(H-T0S)
		KG MOLS/HR	MM KJ /HR	MM KJ /HR K	MM KJ /HR
2		6.577E+02	-4.892E-01	2.108E-03	-1.097E+00
3		5.023E+02	4.724E+00	1.556E-02	2.416E-01
5		1.618E+02	5.801E-01	1.980E-03	9.736E-03
6		5.023E+02	6.298E-01	4.492E-03	-6.644E-01
7		1.554E+02	3.314E+00	1.284E-02	-3.850E-01
8		6.449E+00	-6.856E-03	-2.231E-05	-4.277E-04
11		6.577E+02	-5.249E-01	2.055E-03	-1.117E+00
12		6.642E+02	3.599E+00	1.396E-02	-4.231E-01
15		6.577E+02	3.944E+00	1.696E-02	-9.437E-01
2A		6.642E+02	-4.956E-01	2.111E-03	-1.104E+00
8A		6.449E+00	-6.451E-03	-2.168E-05	-2.029E-04

UNIT AVAILABILITY BALANCE

---- ---------- -------

UID	NAME	DELTA-B	W-EXT	DUTY
		---------- MM KJ /HR ----------		
F2		3.951E-01	0.000E+00	2.727E+00
P1		-2.248E-04	4.043E-04	0.000E+00
HX2		2.252E-01	0.000E+00	0.000E+00
M2		-1.057E-01	0.000E+00	0.000E+00
HX4		1.734E-01	0.000E+00	4.469E+00
P2		-2.058E-02	3.571E-02	0.000E+00
M1		7.203E-03	0.000E+00	0.000E+00
COL1		-6.744E-01	0.000E+00	5.950E+00
				-4.243E+00
REB1		0.000E+00	0.000E+00	5.950E+00
COND		0.000E+00	0.000E+00	4.243E+00

PROCESS™ Input and Output File Listings

CONVENTIONAL AQUA-AMMONIA REFRIGERATION CYCLE WITHOUT PRECOOLING

```
TITLE PROJECT=MDEAM REFRIG, DATE=8-7-90
   TOLER PROP=0.0005,TEMP=-0.002,STREAM=0.0001,-0.002
   CALC NOTRIAL=10
   DIMENSION SI,TEMP=C,PRESS=ATM
   PRINT INPUT=NONE

COMP DATA
   LIBID 1,NH3/2,H2O

THERMO DATA
   TYPE KTYP=U2,HTYP=U3,STYP=U4

STREAM DATA
   PROPERTY STRM=3,TEMP=145,PRES=17.05,RATE=678,COMP=1,22.54/2,77.46
   PROPERTY STRM=12,TEMP=44,PRES=17.05,RATE=894,COMP=1,44.46/2,55.54
   PROPERTY STRM=5,TEMP=44,PRES=17.05,RATE=253,COMP=1,99.41/2,0.59


UNIT OPERATIONS

FLASH UID=F2
   FEED 5
   PROD V=7,L=8
   TPSPEC TEMP=-10.0
   SPEC STRM=8,RATE=0.14,REFS=5

PUMP UID=PP1
   FEED 8
   PROD L=4
   OPER PRES=17.1,EFF=60


HX UID=HX2,ZONES=5,PLOT
   HOT FEED=3,L=6
   COLD FEED=12,L=22
   SPEC HOCI=13
   CONF U=3600

MIXER UID=M2
   FEED 7,6
   PROD M=15
```

```
HX UID=HX4
    HOT FEED=15,L=11,DP=0.12
    SPEC HOT,LFRACT=1.0
    UTILITY WATER,TIN=27,TOUT=40
    CONF U=3600

PUMP UID=P2
    FEED 11
    PROD L=12
    OPER PRES=17.1,EFF=60

CONTROL  UID=CON2
    SPEC STRM=11,TEMP=44.0
    PARAM STRM=3,MAXI=1200,MINI=200,EST2=2500,IPRINT,NOSTOP


COLUMN UID=COL1
    PARA TRAY=7,FAST=5,SURE=30
    FEED 22,4/4,1
    PRODUCT OVHD=40,BTMS=3,678
    PSPEC TOP=17.05
    HEAT 1,7,7.8
    PRINT TRAY=10
    SPEC TRAY=7,TEMP=153.00
    VARIABLE HEAT=1
    TEMP 1,63.4/2,104.4/3,113.1/4,114/5,116.5/6,125/7,153
    VAPOUR 1,287.9/2,261.3/3,255.8/4,255.4/5,242.5/6,239.1/7,231
    LIQUID 1,32.4/2,26/3,25/4,1040./5,1037./6,1028./7,797.8

HX UID=REB1
    ATTACHED COLUMN=COL1,TYPE=2
    UTILITY STEAM,TSAT=170
    CONF U=3600

HX UID=COND1
    HOT FEED=40,L=5
    SPEC HOT,LFRACT=1.0
    UTILITY WATER,TIN=27,TOUT=40
    CONF U=3600
```

```
CONTROL  UID=CON1
    SPEC STRM=5,TEMP=44.0
    PARAM UNIT=F2,SPEC,MAXI=0.25,MINI=0.06,EST2=0.11,RETURNUNIT=F2,*
        STEPSIZE=0.02


CALCULATOR UID=CAL1
    RETRIEVE P(1),UNIT=HX2,AREA
    RETRIEVE P(2),UNIT=HX4,AREA
    RETRIEVE P(3),UNIT=COND1,AREA
    RETRIEVE P(4),UNIT=REB1,AREA
    RETRIEVE P(5),UNIT=F2,DUTY
    RETRIEVE P(6),UNIT=COL1,IDNO=1,DUTY
    PROCEDURE
    $R(1) IS EVAPORATOR AREA
    $R(2) IS TOTAL EXCHANGER AREA
    $R(3) IS EXCHANGER AREA FOR 2.5 MMKJ/HR OF REFRIGERATION
    $R(4) IS COST OF HEAT EXCHANGERS
    $R(5) IS COEFFICIENT OF PERFORMANCE
    $R(6) IS COST OF COOLING WATER FOR 3 YRS
    $R(7) IS COST OF COOLING WATER + EXCHANGERS

    R(1)=P(5)/0.036
    R(2)=R(1)+P(1)
    R(2)=R(2)+P(2)
    R(2)=R(2)+P(3)
    R(2)=R(2)+P(4)
    R(3)=R(2)/P(5)
    R(3)=R(3)*45.36
    R(4)=R(3)*550
    R(4)=R(4)+78500
    R(5)=P(5)/P(6)
    R(6)=P(5)+P(6)
    R(6)=R(6)/P(5)
    R(6)=R(6)*45.36
    R(6)=R(6)*22500
    R(7)=R(4)+R(6)
    RETURN
```

```
OPTIMIZER UID=OPT
    OBJECTIVE UNIT=CAL1,RESULT,IDNO=7,MINIMISE
    PARAMETER UNIT=HX2,SPEC,MINI=10,MAXI=50,STEPSIZE=1,EST2=14
    PARAMETER UNIT=COL1,SPEC,MINI=105,MAXI=160,STEPSIZE=1,EST2=152
    OPTPARA METHOD=1,IPRINT=1


RECYCLE
    LOOP NO=1,START=HX2,END=P2
    LOOP NO=2,START=F2,END=CON1,TRIAL=15,WEGS=3
```

```
 UNIT  3, HX2 ,    SOLVED
 UNIT  4, M2  ,    SOLVED
 UNIT  5, HX4 ,    SOLVED
 UNIT  6, P2  ,    SOLVED
LOOP  1    SOLVED AFTER  2 TRIALS
 STRM: 12  T=  44.4 P=  17.1 RATE= 1032.    DTEMP=  0.00 DCOMP=  0.0000
  CONTROLLER UNIT  7, CON2, AT ITERATION  1
       SPECIFICATION VALUE =  0.44000E+02,  CALC =  0.44011E+02
       PARAMETER  CURRENT =  0.79835E+03,  NEXT =  0.79835E+03
 UNIT  7, CON2,    SOLVED
 UNIT  8, COL1,    SOLVED
 UNIT 10, COND,    SOLVED
   CONTROLLER UNIT 11, CON1, AT ITERATION  1
       SPECIFICATION VALUE =  0.44000E+02,  CALC =  0.44017E+02
       PARAMETER  CURRENT =  0.20307E+00,  NEXT =  0.20307E+00
 UNIT 11, CON1,    SOLVED
LOOP  2    SOLVED AFTER  3 TRIALS
 STRM: 3   T= 154.0 P=  17.0 RATE= 798.3    DTEMP=  0.00 DCOMP=  0.0000
 STRM: 5   T=  44.0 P=  17.0 RATE= 293.2    DTEMP=  0.00 DCOMP=  0.0000
 UNIT  9, REB1,    SOLVED
 UNIT 12, CAL1,    SOLVED
** AFTER  5 CYCLES
** ALL NEW PARAMETERS SAME AS CYCLE   1 **
   OPTIMIZATION HISTORY
   CYCLE          1             2             3             4             5
   PARA  1    1.3000E+01  1.4000E+01  1.3000E+01  1.2149E+01  1.1298E+01
   PARA  2    1.5300E+02  1.5300E+02  1.5200E+02  1.5352E+02  1.5405E+02
   OBJ.       6.1808E+06  6.1833E+06  6.1823E+06  6.1767E+06  6.1783E+06
    UNIT 13, OPT ,    SOLVED

   VERSION O484                    SM
   SIMULATION SCIENCES, INC.       PROCESS              PAGE  4
   PROJECT  MDEAM REFRIG
   PROBLEM                  SOLUTION          8-7-90

                **** PROBLEM SOLUTION REACHED ****
```

SUMMARY OF FLASH DRUMS,MIXER/SPLITTERS AND VALVES

UNIT ID	F2	M2
SEQ NO	1	4
TYPE	FLASH	MIXER
FEEDS	5	7
		6
PRODUCTS	7 (V)	15 (M)
	8 (L)	
TEMP, DEG C	-10.0000	67.7289
PRESSURE, ATM	2.8154	2.8154
FRACTION LIQUID	0.20307	0.82672
DUTY, MM KJ /HR	3.88149	0.00000

SUMMARY OF HEAT EXCHANGE UNITS

3 UNIT HX2 , , IS A HEAT EXCHANGER

*** OPERATING CONDITIONS		
DUTY, MM KJ /HR	6.19046	
WEIGHTED LMTD, DEG C	22.222	
F FACTOR	1.00000	
MTD , DEG C	22.222	
U * A, KJ /HR DEG C	278572.875	
U, KJ /HR DEG C SQ M	3600.000	
A, SQ M	77.381	

*** HOT SIDE CONDITIONS	INLET	OUTLET
FEED(S)	3	
LIQUID PRODUCT		6
VAPOR, KG MOLS/HR	0.0000	0.0000
M KGS/HR	0.0003	0.0000
CP, KJ /KG - DEG C	2.6923	0.0000
LIQUID, KG MOLS/HR	798.3464	798.3464
M KGS/HR	14.2325	14.2328
CP, KJ /KG - DEG C	4.6588	4.3224
TOTAL, KG MOLS/HR	798.3464	798.3464
CONDENS(VAPORIZ)ATION, KG MOLS/HR		0.0000
TEMPERATURE, DEG C	154.050	55.735
PRESSURE, ATM	17.050	17.050

*** COLD SIDE CONDITIONS	INLET	OUTLET
FEED(S)	12	
MIXED PRODUCT		22
VAPOR, KG MOLS/HR	0.0000	15.6759
M KGS/HR	0.0000	0.2680
CP, KJ /KG - DEG C	0.0000	2.7241
LIQUID, KG MOLS/HR	1031.9690	1016.2931
M KGS/HR	18.2116	17.9436
CP, KJ /KG - DEG C	4.4815	4.7236
TOTAL, KG MOLS/HR	1031.9690	1031.9690
CONDENS(VAPORIZ)ATION, KG MOLS/HR		15.6759
TEMPERATURE, DEG C	44.438	114.768
PRESSURE, ATM	17.100	17.100

5 UNIT HX4 , , IS A HEAT EXCHANGER

*** OPERATING CONDITIONS

DUTY, MM KJ /HR	6.85472
LMTD, DEG C	21.935
F FACTOR	1.00000
MTD , DEG C	21.935
U * A, KJ /HR DEG C	312499.125
U, KJ /HR DEG C SQ M	3600.000
A, SQ M	86.805

*** HOT SIDE CONDITIONS	INLET	OUTLET
FEED(S)	15	
LIQUID PRODUCT		11
VAPOR, KG MOLS/HR	178.8232	0.0000
M KGS/HR	3.0578	0.0000
CP, KJ /KG - DEG C	2.2967	0.0000
LIQUID, KG MOLS/HR	853.1458	1031.9690
M KGS/HR	15.1538	18.2116
CP, KJ /KG - DEG C	4.3835	4.4907
TOTAL, KG MOLS/HR	1031.9690	1031.9690
CONDENS(VAPORIZ)ATION, KG MOLS/HR		178.8232
TEMPERATURE, DEG C	67.729	44.011
PRESSURE, ATM	2.815	2.695

*** COLD SIDE CONDITIONS	INLET	OUTLET
COOLING WATER, KG /HR	125939.641	125939.641
TEMPERATURE, DEG C	27.000	40.000

9 UNIT REB1, , IS A HEAT EXCHANGER

*** OPERATING CONDITIONS

DUTY, MM KJ /HR	8.69016
LMTD, DEG C	27.637
F FACTOR	1.00000
MTD , DEG C	27.637
U * A, KJ /HR DEG C	314440.781
U, KJ /HR DEG C SQ M	3600.000
A, SQ M	87.345

*** HOT SIDE CONDITIONS	INLET	OUTLET
STEAM, KG /HR	4133.773	4133.773
SATURATION PRESSURE, ATM		7.780
SATURATION TEMPERATURE, DEG C		170.000

*** COLD SIDE CONDITIONS	INLET	OUTLET
STREAM IS FROM COLUMN COL1, UNIT 8		
VAPOR, KG MOLS/HR	0.0000	232.3383
M KGS/HR	0.0000	4.0188
CP, KJ /KG - DEG C	0.0000	2.6920
LIQUID, KG MOLS/HR	1030.6936	798.3553
M KGS/HR	18.2518	14.2329
CP, KJ /KG - DEG C	4.7062	4.6590
TOTAL, KG MOLS/HR	1030.6936	1030.6936
CONDENS(VAPORIZ)ATION, KG MOLS/HR		232.3383
TEMPERATURE, DEG C	126.026	154.045
PRESSURE, ATM	17.050	17.050

10 UNIT COND, , IS A HEAT EXCHANGER

*** OPERATING CONDITIONS

DUTY, MM KJ /HR	5.77634
LMTD, DEG C	21.062
F FACTOR	1.00000
MTD , DEG C	21.062
U * A, KJ /HR DEG C	274260.250
U, KJ /HR DEG C SQ M	3600.000
A, SQ M	76.183

*** HOT SIDE CONDITIONS	INLET	OUTLET
FEED(S)	40	
LIQUID PRODUCT	5	
VAPOR, KG MOLS/HR	293.1537	0.0000
M KGS/HR	4.9937	0.0000
CP, KJ /KG - DEG C	2.9862	0.0000
LIQUID, KG MOLS/HR	0.0000	293.1537
M KGS/HR	0.0000	4.9937
CP, KJ /KG - DEG C	0.0000	5.0273
TOTAL, KG MOLS/HR	293.1537	293.1537
CONDENS(VAPORIZ)ATION, KG MOLS/HR		293.1537
TEMPERATURE, DEG C	65.702	44.017
PRESSURE, ATM	17.050	17.050

*** COLD SIDE CONDITIONS	INLET	OUTLET
COOLING WATER, KG /HR	106126.930	106126.930
TEMPERATURE, DEG C	27.000	40.000

SUMMARY OF COMPRESSOR/EXPANDER/PUMP/TURBINE UNITS

2 UNIT PP1 , , IS A PUMP
*** FEED STREAMS ARE 8
*** LIQUID PRODUCT IS STREAM 4
*** OPERATING CONDITIONS

WORK, KW	1.04
EFFICIENCY, PERCENT	60.00

	INLET	OUTLET
MOLE FRACTION LIQUID	1.0000	1.0000
TEMPERATURE, DEG C	-10.000	-9.413
PRESSURE, ATM	2.8154	17.1000
HEAD, M		375.1443
HOT VOLUME, M3/HR	1.548	1.548

6 UNIT P2 , , IS A PUMP
*** FEED STREAMS ARE 11
*** LIQUID PRODUCT IS STREAM 12
*** OPERATING CONDITIONS

WORK, KW	15.56
EFFICIENCY, PERCENT	60.00

	INLET	OUTLET
MOLE FRACTION LIQUID	1.0000	1.0000
TEMPERATURE, DEG C	44.011	44.438
PRESSURE, ATM	2.6954	17.1000
HEAD, M		313.6260
HOT VOLUME, M3/HR	23.023	23.024

SUMMARY OF CALCULATOR UNITS

REPORT OF RESULTS VECTORS

UNIT ID CAL1

SEQ NO 12

R(1)	1.07819E+02
R(2)	4.34727E+02
R(3)	5.08031E+03
R(4)	2.87267E+06
R(5)	4.46654E-01
R(6)	3.30559E+06
R(7)	6.17826E+06
R(8)	UNDEFINED

I SUMMARY FOR COLUMN UNIT 8 - COL1,

1 TOTAL NUMBER OF ITERATIONS

FAST METHOD	0
SURE METHOD	150

2 COLUMN SUMMARY

TRAY	TEMP	PRESSURE	NET FLOW RATES, KG MOLS/HR				HEAT(COOL)ER
	DEG C	ATM	LIQUID	VAPOR	FEED	PRODUCT	DUTY MM kJ/hr
1	65.7	17.05	33.4		59.5L	293.2V	
2	105.7	17.05	27.8	267.0			
3	113.9	17.05	27.3	261.4			
4	115.0	17.05	1042.5	260.9	1032.0M		
5	116.9	17.05	1039.3	244.2			
6	126.0	17.05	1030.7	240.9			
7	154.0	17.05		232.3		798.3L	8.6902

3 FEED AND PRODUCT STREAMS	MASS RATES	HEAT RATES
* FEED STREAMS:	KG MOLS/HR	MM KJ /HR
22 TO TRAY 4 IS MIXED FROM UNIT 3, HX2	0.10320E+04	0.54233E+01
4 TO TRAY 1 IS LIQUID FROM UNIT 2, PP1	0.59531E+02	-0.56731E-01
* PRODUCT STREAMS:		
3 IS LIQUID STREAM FROM TRAY 7	0.79835E+03	0.72404E+01
40 IS VAPOR STREAM FROM TRAY 1	0.29315E+03	0.68167E+01
OVERALL MASS BALANCE, (FEEDS - PRODS)	0.00000E+00	
OVERALL HEAT BALANCE, (HIN - HOUT)		-0.32806E-03

4 SPECIFICATION VALUES

PARAMETER TYPE	TRAY NO	COMP. NO	SPECIFICATION TYPE	SPECIFIED VALUE	CALCULATED VALUE
TRAY	7		TEMP	0.1540E+03	0.1540E+03

IIA TRAY COMPOSITIONS

TRAY	-------- 1 --------		-------- 2 --------	
COMPONENT	X	Y	X	Y
1 NH3	0.6536E+00	0.9971E+00	0.4087E+00	0.9573E+00
2 H2O	0.3464E+00	0.3579E-02	0.5913E+00	0.4327E-01
KG MOLS/HR	0.3336E+02	0.2932E+03	0.2778E+02	0.2670E+03

TRAY	-------- 3 --------		-------- 4 --------	
COMPONENT	X	Y	X	Y
1 NH3	0.3686E+00	0.9376E+00	0.3631E+00	0.9340E+00
2 H2O	0.6314E+00	0.6281E-01	0.6369E+00	0.6597E-01
KG MOLS/HR	0.2728E+02	0.2614E+03	0.1043E+04	0.2609E+03

TRAY	-------- 5 --------		-------- 6 --------	
COMPONENT	X	Y	X	Y
1 NH3	0.3540E+00	0.9283E+00	0.3117E+00	0.8965E+00
2 H2O	0.6460E+00	0.7163E-01	0.6883E+00	0.1035E+00
KG MOLS/HR	0.1039E+04	0.2442E+03	0.1031E+04	0.2409E+03

TRAY	-------- 7 --------	
COMPONENT	X	Y
1 NH3	0.1902E+00	0.7292E+00
2 H2O	0.8098E+00	0.2708E+00
KG MOLS/HR	0.7983E+03	0.2323E+03

STREAM COMPONENT FLOW RATES - KG MOLS/HR

STREAM ID	3	4	5	6
PHASE	LIQUID	LIQUID	LIQUID	LIQUID
1 NH3	151.8803	58.4794	292.1052	151.8812
2 H2O	646.4661	1.0517	1.0485	646.4652
TOTALS	798.3464	59.5311	293.1537	798.3464
TEMPERATURE, DEG C	154.0498	-9.4127	44.0166	55.7352
PRESSURE, ATM	17.0500	17.1000	17.0500	17.0500
H, MM KJ /HR	7.2404	-0.0567	1.0404	1.0499
MOLE FRACT LIQUID	1.0000	1.0000	1.0000	1.0000
RECYCLE CONVERGENCE	0.0000	0.0000	0.0000	0.0000

STREAM ID	7	8	11	12
PHASE	VAPOR	LIQUID	LIQUID	LIQUID
1 NH3	233.6217	58.4794	385.5029	385.5029
2 H2O	0.0009	1.0517	646.4661	646.4661
TOTALS	233.6226	59.5311	1031.9690	1031.9690
TEMPERATURE, DEG C	-10.0000	-10.0000	44.0109	44.4375
PRESSURE, ATM	2.8154	2.8154	2.6954	17.1000
H, MM KJ /HR	4.9823	-0.0605	-0.8225	-0.7665
MOLE FRACT LIQUID	0.0000	1.0000	1.0000	1.0000
RECYCLE CONVERGENCE	0.0000	0.0000	0.0000	0.0000

STREAM ID	15	22	40
PHASE	MIXED	MIXED	VAPOR
1 NH3	385.5029	385.5029	292.1052
2 H2O	646.4661	646.4661	1.0485
TOTALS	1031.9690	1031.9690	293.1537
TEMPERATURE, DEG C	67.7289	114.7675	65.7017
PRESSURE, ATM	2.8154	17.1000	17.0500
H, MM KJ /HR	6.032	5.4233	6.8167
MOLE FRACT LIQUID	0.8267	0.9848	0.0000
RECYCLE CONVERGENCE	0.0000	0.0000	0.0000

PROCESS™ Input and Output File Listings

BASIC NOVEL ABSORPTION CYCLE HEATPUMP WITH CYCLOHEXANE AND ANILINE

```
TITLE PROJECT=POWER, DATE=8-7-90
  TOLER PROP=0.0005,TEMP=-0.002,STREAM=0.0005,-0.1
  DIMENSION SI,TEMP=C,PRESSURE=MMHG
  PRINT INPUT=NONE
  CALCULATION FLASH=0

COMP DATA
  LIBID 1,CH/2,ANLN

THERMO DATA
  TYPE KTYP=LACT,HTYP=LIBRARY,STYP=LK
  KSET SETNO=1,NOTEMP=3
  SUBSET 1,10.0
  NRTL  1,2,,683.9756,,547.9851,0.41076
  SUBSET 2,30.0
  NRTL  1,2,,692.3542,,499.4734,0.41076
  SUBSET 3,50.00
  NRTL  1,2,,700.7328,,450.9616,0.41076
  HLSET SETNO=1,KSET=1

STREAM DATA
  PROPERTY STRM=2,TEMP=25,PRES=1500,RATE=532,COMP=1,87.0/2,13.0
  PROPERTY STRM=1,TEMP=25,PRES=1500,RATE=2589,COMP=1,27.0/2,73.0
  PROPERTY STRM=5,TEMP=100,PRES=1500,RATE=373,COMP=1,82.5/2,17.5
  PROPERTY STRM=9A,TEMP=104,PRES=1500,RATE=2748,COMP=1,31.1/2,68.9


UNIT OPERATIONS

HX UID=HX1
  COLD FEED=2,L=3
  HOT FEED=5,L=6
  SPEC HOCI=2

FLASH UID=F1
  FEED 3
  PROD V=4,L=5
  TPSPEC TEMP=100
  SPEC STRM=5,RATE=0.90,REFS=3
```

```
HX UID=HX2
  COLD FEED=1,L=7
  HOT FEED=9A,L=10
  SPEC COLD,TEMP=102

HX UID=HX2A
  HOT FEED=7,L=7A
  SPEC HOT,TEMP=102
  UTILITY WATER,TIN=15,TOUT=60

MIXER UID=M1
  FEED 7A,4
  PROD M=8

HX UID=HX4
  HOT FEED=8,L=9
  SPEC HOT,LFRACT=1.00
  UTILITY WATER,TIN=15,TOUT=60

HX UID=HX4A
  HOT FEED=9,L=9A
  SPEC HOT,TEMP=104
  UTILITY WATER,TIN=15,TOUT=60

CONTROL UID=CON1
  SPEC STRM=9,TEMP=104
  PARAM STRM=7A,MAXI=30000,MINI=100,EST2=1550,RETURNUNIT=M1,NOSTOP

SET UID=SE1
  SPEC STRM=1,RATE=1,REFS=7A,RATIO

SEPARATOR UID=F2
  FEED 10,6
  OVHD STRM=2,PHASE=L,TEMP=25
  BTMS STRM=1,PHASE=L,TEMP=25
  XOVHD 1,1,0.87
  XBTMS 2,2,0.73
```

```
CALCULATOR UID=CAL1
  RETRIEVE P(1),UNIT=F1,DUTY
  RETRIEVE P(2),UNIT=HX4,DUTY
  PROCEDURE
$   R(1) IS COEFFICIENT OF PERFORMANCE
  R(1)=P(2)/P(1)
  RETURN


OPTIMIZER UID=OPT1
  OBJECTIVE UNIT=CAL1,RESULT,IDNO=1,MAXIMISE
  PARAMETER UNIT=F1,SPEC,MAXI=0.98,MINI=0.5,EST2=0.85,STEPSIZE=0.05
  OPTPARA METHOD=1,IPRINT=1


RECYCLE
  LOOP NO=1,START=HX1,END=F1,TRIAL=10
  LOOP NO=2,START=HX2,END=SE1,TRIAL=10
  LOOP NO=3,START=HX1,END=F2,TRIAL=10
```

```
      STRM: 1   T= 25.0 P= 1228.1 RATE=0.1279E+05 DTEMP= 0.00 DCOMP= 0.0000
      UNIT  11, CAL1,    SOLVED
** AFTER   6 CYCLES
** ALL NEW PARAMETERS SAME AS CYCLE   4 **
     OPTIMIZATION HISTORY
     CYCLE        1            2            3            4            5
     PARA  1   9.0000E-01  8.5000E-01  8.0000E-01  7.5000E-01  7.0000E-01
     OBJ.      5.1449E-01  5.2680E-01  5.3007E-01  5.3174E-01  5.3252E-01
     OPTIMIZATION HISTORY
     CYCLE          6
     PARA  1   6.5000E-01
     OBJ.      5.3091E-01
** BEST OBJECTIVE FUNCTION =  5.32517E-01  AT CYCLE NUMBER   5
      UNIT  12, OPT1, NOT SOLVED
      UNIT   2, F1 ,    SOLVED
     LOOP  1 NOT SOLVED AFTER   1 TRIALS
      STRM: 5   T= 100.0 P= 1230.2 RATE= 3178.    DTEMP=   0.00 DCOMP=   0.0845
      UNIT   1, HX1 ,    SOLVED
      UNIT   2, F1 ,    SOLVED
     LOOP  1    SOLVED AFTER   2 TRIALS
      UNIT   3, HX2 ,    SOLVED
      UNIT   4, HX2A,    SOLVED
      UNIT   5, M1 ,    SOLVED
      UNIT   6, HX4 ,    SOLVED
      UNIT   7, HX4A,    SOLVED
        CONTROLLER UNIT  8, CON1, AT ITERATION  1
             SPECIFICATION VALUE =  0.10400E+03,  CALC =  0.10402E+03
             PARAMETER   CURRENT =  0.11029E+05,  NEXT =  0.11029E+05
      UNIT   8, CON1,    SOLVED
      UNIT   9, SE1 ,    SOLVED
     LOOP  2    SOLVED AFTER   5 TRIALS
      STRM: 9A  T= 104.0 P= 1228.1 RATE=0.1239E+05 DTEMP=0.00 DCOMP=0.0000
      UNIT  10, F2 ,    SOLVED
     LOOP  3    SOLVED AFTER   1 TRIALS
      STRM: 2   T=  25.0 P= 1228.1 RATE= 4540.    DTEMP=   0.00 DCOMP=   0.0002
      STRM: 1   T=  25.0 P= 1228.1 RATE=0.1103E+05 DTEMP=0.00 DCOMP=0.0000
      UNIT  11, CAL1,    SOLVED
      UNIT  12, OPT1,    SOLVED
```

**** PROBLEM SOLUTION REACHED ****

SUMMARY OF FLASH DRUMS,MIXER/SPLITTERS AND VALVES

UNIT ID	F1	M1
SEQ NO	2	5
TYPE	FLASH	MIXER
FEEDS	3	7A
		4
PRODUCTS	4 (V)	8 (M)
	5 (L)	
TEMP, DEG C	100.0000	106.1630
PRESSURE, MMHG	1230.1661	1228.0967
FRACTION LIQUID	0.70000	0.92246
DUTY, MM KJ /HR	57.47249	0.00000

SUMMARY OF HEAT EXCHANGE UNITS

1 UNIT HX1 , , IS A HEAT EXCHANGER

*** OPERATING CONDITIONS

DUTY, MM KJ /HR	39.56242
LMTD, DEG C	8.398
F FACTOR	1.00000
MTD , DEG C	8.398
U * A, KJ /HR DEG C	4710785.000

*** HOT SIDE CONDITIONS	INLET	OUTLET
FEED(S)	5	
LIQUID PRODUCT		6
VAPOR, KG MOLS/HR	0.0000	0.0000
M KGS/HR	0.0000	0.0000
CP, KJ /KG - DEG C	0.0000	0.0000
LIQUID, KG MOLS/HR	3177.8674	3177.8674
M KGS/HR	272.4743	272.4743
CP, KJ /KG - DEG C	2.1444	1.7719
TOTAL, KG MOLS/HR	3177.8674	3177.8674
CONDENS(VAPORIZ)ATION, KG MOLS/HR		0.0000
TEMPERATURE, DEG C	100.000	27.000
PRESSURE, MMHG	1230.174	1230.174

*** COLD SIDE CONDITIONS	INLET	OUTLET
FEED(S)	2	
LIQUID PRODUCT		3
VAPOR, KG MOLS/HR	0.0000	0.0000
M KGS/HR	0.0000	0.0000
CP, KJ /KG - DEG C	0.0000	0.0000
LIQUID, KG MOLS/HR	4539.0259	4539.0259
M KGS/HR	387.3458	387.3458
CP, KJ /KG - DEG C	1.8009	2.0374
TOTAL, KG MOLS/HR	4539.0259	4539.0259
CONDENS(VAPORIZ)ATION, KG MOLS/HR		0.0000
TEMPERATURE, DEG C	25.000	77.777
PRESSURE, MMHG	1228.097	1228.097

3 UNIT HX2 , , IS A HEAT EXCHANGER

*** OPERATING CONDITIONS

DUTY, MM KJ /HR	137.94331
LMTD, DEG C	5.915
F FACTOR	1.00000
MTD , DEG C	5.915
U * A, KJ /HR DEG C	23319504.000

*** HOT SIDE CONDITIONS	INLET	OUTLET
FEED(S)	9A	
LIQUID PRODUCT		10
VAPOR, KG MOLS/HR	0.0000	0.0000
M KGS/HR	0.0000	0.0000
CP, KJ /KG - DEG C	0.0000	0.0000
LIQUID, KG MOLS/HR	12390.7490	12390.7490
M KGS/HR	1115.8488	1115.8488
CP, KJ /KG - DEG C	2.1479	1.5882
TOTAL, KG MOLS/HR	12390.7490	12390.7490
CONDENS(VAPORIZ)ATION, KG MOLS/HR		0.0000
TEMPERATURE, DEG C	104.000	38.132
PRESSURE, MMHG	1228.097	1228.097

*** COLD SIDE CONDITIONS	INLET	OUTLET
FEED(S)	1	
LIQUID PRODUCT		7
VAPOR, KG MOLS/HR	0.0000	0.0000
M KGS/HR	0.0000	0.0000
CP, KJ /KG - DEG C	0.0000	0.0000
LIQUID, KG MOLS/HR	11029.0400	11029.0400
M KGS/HR	1000.9313	1000.9313
CP, KJ /KG - DEG C	1.5932	2.1185
TOTAL, KG MOLS/HR	11029.0400	11029.0400
CONDENS(VAPORIZ)ATION, KG MOLS/HR		0.0000
TEMPERATURE, DEG C	25.000	102.000
PRESSURE, MMHG	1228.097	1228.097

4 UNIT HX2A, , IS A HEAT EXCHANGER

*** OPERATING CONDITIONS		
DUTY, MM KJ /HR	0.00000	
LMTD, DEG C	61.793	
F FACTOR	1.00000	
MTD , DEG C	61.793	
U * A, KJ /HR DEG C	0.000	
*** HOT SIDE CONDITIONS	INLET	OUTLET
FEED(S)	7	
LIQUID PRODUCT		7A
VAPOR, KG MOLS/HR	0.0000	0.0000
M KGS/HR	0.0000	0.0000
CP, KJ /KG - DEG C	0.0000	0.0000
LIQUID, KG MOLS/HR	11029.0400	11029.0400
M KGS/HR	1000.9313	1000.9313
CP, KJ /KG - DEG C	2.1185	2.1185
TOTAL, KG MOLS/HR	11029.0400	11029.0400
CONDENS(VAPORIZ)ATION, KG MOLS/HR		0.0000
TEMPERATURE, DEG C	102.000	102.000
PRESSURE, MMHG	1228.097	1228.097
*** COLD SIDE CONDITIONS	INLET	OUTLET
COOLING WATER, KG /HR	0.000	0.000
TEMPERATURE, DEG C	15.000	60.000

6 UNIT HX4 , , IS A HEAT EXCHANGER

*** OPERATING CONDITIONS		
DUTY, MM KJ /HR	30.34591	
LMTD, DEG C	65.262	
F FACTOR	1.00000	
MTD , DEG C	65.262	
U * A, KJ /HR DEG C	464985.719	
*** HOT SIDE CONDITIONS	INLET	OUTLET
FEED(S)	8	
LIQUID PRODUCT		9
VAPOR, KG MOLS/HR	960.7344	0.0000
M KGS/HR	81.1752	0.0000
CP, KJ /KG - DEG C	1.4986	0.0000
LIQUID, KG MOLS/HR	11430.0127	12390.7471
M KGS/HR	1034.6734	1115.8486
CP, KJ /KG - DEG C	2.1121	2.1155
TOTAL, KG MOLS/HR	12390.7471	12390.7471
CONDENS(VAPORIZ)ATION, KG MOLS/HR		960.7344
TEMPERATURE, DEG C	106.163	104.018
PRESSURE, MMHG	1228.097	1228.097
*** COLD SIDE CONDITIONS	INLET	OUTLET
COOLING WATER, KG /HR	161065.906	161065.906
TEMPERATURE, DEG C	15.000	60.000

7 UNIT HX4A, , IS A HEAT EXCHANGER

*** OPERATING CONDITIONS		
DUTY, MM KJ /HR	0.12034	
LMTD, DEG C	63.891	
F FACTOR	1.00000	
MTD , DEG C	63.891	
U * A, KJ /HR DEG C	1883.569	
*** HOT SIDE CONDITIONS	INLET	OUTLET
FEED(S)	9	
LIQUID PRODUCT		9A
VAPOR, KG MOLS/HR	0.0000	0.0000
M KGS/HR	0.0000	0.0000
CP, KJ /KG - DEG C	0.0000	0.0000
LIQUID, KG MOLS/HR	12390.7471	12390.7471
M KGS/HR	1115.8486	1115.8486
CP, KJ /KG - DEG C	2.1155	2.1479
TOTAL, KG MOLS/HR	12390.747	12390.7471
CONDENS(VAPORIZ)ATION, KG MOLS/HR		0.0000
TEMPERATURE, DEG C	104.018	104.000
PRESSURE, MMHG	1228.097	1228.097
*** COLD SIDE CONDITIONS	INLET	OUTLET
COOLING WATER, KG /HR	638.744	638.744
TEMPERATURE, DEG C	15.000	60.000

SUMMARY OF COMPONENT SEPARATORS

UNIT ID	F2
SEQ NO	10
NAME	
FEEDS	10
	6

PRODUCTS	2 (L)	1 (L)
TEMP, DEG C	25.0000	25.0000
PRESSURE, MMHG	1228.0967	1228.0967
FRACTION LIQUID	1.00000	1.00000
DUTY, MM KJ /HR	27.00710	

SUMMARY OF CALCULATOR UNITS
REPORT OF RESULTS VECTORS

UNIT ID	CAL1
SEQ NO	11
NAME	

R(1)	5.28008E-01
R(2)	UNDEFINED
R(3)	UNDEFINED
R(4)	UNDEFINED
R(5)	UNDEFINED
R(6)	UNDEFINED
R(7)	UNDEFINED
R(8)	UNDEFINED

STREAM COMPONENT FLOW RATES - KG MOLS/HR

STREAM ID	1	2	3	4
PHASE	LIQUID	LIQUID	LIQUID	VAPOR
1 CH	2977.7939	3949.5825	3948.9534	1327.1575
2 ANLN	8051.0728	590.1665	590.0723	34.5492
TOTALS	11028.8672	4539.7490	4539.0259	1361.7067
TEMPERATURE, DEG C	25.0000	25.0000	77.7772	100.0000
PRESSURE, MMHG	1228.0967	1228.0967	1228.0967	1230.1661
H, MM KJ /HR	60.6893	20.0612	59.6211	62.0289
MOLE FRACT LIQUID	1.0000	1.0000	1.0000	0.0000
RECYCLE CONVERGENCE	0.0000	0.0002	0.0000	0.0000

STREAM ID	5	6	7	8
PHASE	LIQUID	LIQUID	LIQUID	MIXED
1 CH	2621.7957	2622.3787	2977.8398	4304.9976
2 ANLN	555.5230	555.4886	8051.2002	8085.7495
TOTALS	3177.3186	3177.8674	11029.0400	12390.7471
TEMPERATURE, DEG C	100.0000	27.0000	102.0000	106.1630
PRESSURE, MMHG	1230.1661	1230.1742	1228.0967	1228.0967
H, MM KJ /HR	55.0647	15.5113	198.6335	260.6624
MOLE FRACT LIQUID	1.0000	1.0000	1.0000	0.9225
RECYCLE CONVERGENCE	0.0002	0.0000	0.0000	0.0000

STREAM ID	9	10	7A	9A
PHASE	LIQUID	LIQUID	LIQUID	LIQUID
1 CH	4304.9976	4304.9976	2977.8398	4304.9976
2 ANLN	8085.7495	8085.7510	8051.2002	8085.7495
TOTALS	12390.7471	12390.7490	11029.0400	12390.7471
TEMPERATURE, DEG C	104.0178	38.1323	102.0000	104.0000
PRESSURE, MMHG	1228.0967	1228.0967	1228.0967	1228.0967
H, MM KJ /HR	230.3165	92.2463	198.6335	230.1962
MOLE FRACT LIQUID	1.0000	1.0000	1.0000	1.0000
RECYCLE CONVERGENCE	0.0000	0.0000	0.0000	0.0000

BIBLIOGRAPHY

Abello, L., Servais, B., Kern, M. and Pannetier, G., *"Studies of Hydrogen Bonding N-H..N. XII. Thermodynamic Study of the Self Association of Aniline and N-Methylaniline in Cyclohexane"*, Bull. Soc. Chim. Fr., 11, 4360 (1968)

Altenkirch, E., *Absorptionskaltemaschinen*, VEB - Verlag Technik, Berlin (1954)

Ando, E. and Takeshita, I., *"Residential Gas-Fired Absorption Heat Pump Based on R22-DEGDME Pair. Part 1 Thermodynamic Properties of the R22-DEGDME Pair"*, Int. J. Refrig., 7, 181 (1984)

Asselineau, L. and Renon, H., *"Extension de l'Equation NRTL pour la Representation de l'Ensemble des Donnees d'Equilibre Binaire, Liquide-Vapeur et Liquide-lLquide"*, Chem. Eng. Sci., 25, 1211 (1970)

Auh, P.C., *"A Survey of Absorption Cooling Technology in Cooling Applications"*, B.N.L. Report No. 50704 (1977)

Backstrom, M., *Kaltetechnik*, Verlag G Braun, Karlsruhe (1953)

Bett, K.E., Rowlinson, J.S. and Saville, G., *Thermodynamics for Chemical Engineers*, MIT Press (1975)

Blass, E., "*Capacity Increase of NH_3 H_2O Absorption Refrigeration Plants for Industrial Refrigeration"*, DKV - Tagungsbericht, Nurnberg, 145 (1974)

Bogart, M., *Ammonia Absorption Refrigeration in Industrial Processes*, Gulf Pub. Co., (1981)

Briggs, S.W., *"Second-Law Analysis of Absorption Refrigeration"*, Proc. AGA & IGT Conf. on Natural Gas Res. & Tech., Chicago (1971)

Buchner, E.H. and Kleyn, D., Recl. Trav. Chim. Pays-Bas., 43, 153 (1924)

Buffington, R.M., *"Qualitative Requirements for Absorbent-Refrigerant Combinations"*, Refrig. Eng., 57, 343 (1949)

Cockshoot, J.E., Proc. 4th Aust. Chem. Eng. Conf., Adelaide, 330 (1976)

Copp, J.L., *"Thermodynamics of Binary Systems Containing Amines; Part 2"*, Trans. Faraday Soc., 51, 1056 (1955)

Copp, J.L. and Everett, D.H., *"Thermodynamics of Binary Systems Containing Amines; Part 3"*, Trans. Faraday Soc., 53, 9 (1957)

Copp, J.L. and Everett, D.H., *"Thermodynamics of Binary Systems Containing Amines"*, Faraday Soc. Discussions, 15, 174 (1953)

Chueh, C.F. and Swanson, A.C., *"Estimating Liquid Heat Capacity"*, Chem. Eng. Progr., 69, 83 (1973)

Chun, K.W., Clikscales, T.C. and Davison, R.R., *"Vapour-Liquid Equilibrium of Triethylamine-Water and Methyldiethylamine-Water"*, J. Chem. Eng. Data, 16, 443 (1971)

Dalichaouch, M., *"Energy Analysis of Absorption-Refrigeration Cycles"*, J. Inst. Energy, 63, 167 (1990)

Davison, R.R., *"Vapour-Liquid Equilibria of Water-Diisopropylamine and Water-Di-n-Propylamine"*, J. Chem. Eng. Data, 13, 348 (1968)

Davison, R.R., Smith W.H. and Chun K.W., *"A Static Vapour Pressure Apparatus for Mixtures"*, AIChE Journal, 13, 590 (1967)

Davison, R.R., Smith W.H. and Hood D.W., *"Phase Equilibria of Desalination Solvents: Water-NaCl-Amines"*, J. Chem. Eng. Data, 1, 304 (1966)

Davison, R.R., Smith W.H. and Hood D.W., *"Structure and Amine-Water Solubility in Desalination by Solvent Extraction"*, J. Chem. Eng. Data, 5, 420 (1960)

Felsing, W.A. and Phillips, B.A., *"Partial Vapour Pressures of Aqueous Methylamine Solution"*, J. Am. Chem. Soc., 58, 1973 (1936)

Gmehling, J., Onken, U. and Arlt, W., *Vapour - Liquid Data Collection*, Dechema Chemistry Data Series, Frankfurt (1977 -)

Grover, G.S., Devotta, S. and Holland, F.A., *"Performance of an Experimental Absorption Cooler Using Aqueous LiCl and LiCl/LiBr Solutions"*, Ind. Eng. Chem. Res., 28, 250 (1989)

Holldorff, G., *"Revisions Up Absorption Refrigeration Efficiency"*, Hydrocarbon Processing, 58, 149 (1979)

Hood, D.W. and Davison, R.R., *"The Place of Solvent Extraction in Saline Water Conversion"*, Advan. Chem. Series No 27, 40 (1960)

Hosseini, S.M. and Schneider, G., *"Evaporation Equilibria in Hydrocarbon - Aniline Systems (III)"*, Z. Phys. Chem. (Frankfurt), 36, 137 (1963)

Hunter, T.G.and Brown, T., *"Distribution in Hydrocarbon-Solvent Systems"*, Ind. Eng. Chem., 39, 1343 (1947)

Iedema, P.D., *"Mixtures for the Absorption Heat Pump"*, Int. J. Refrig., 5, 262 (1982)

Jacob, X., Albright, C.F. and Tucker, W.H., *"Factors Affecting the Coefficient of Performance for Absorption Air-Conditioning Systems"*, ASHRAE Trans., 75, 103 (1969)

Joback, K.G., Thesis, Massachusetts Institute of Technology, Cambridge, Mass. (1984),

Kandlikar, S.G., *"A New Absorber Heat Recovery Cycle to Improve COP of Aqua-Ammonia Absorption Refrigeration System"*, ASHRAE Trans., 88, 141 (1982)

Karakas, A., Egrican, N. and Uygur, S., *"Second-Law Analysis of Solar Absorption-Cooling Cycles using Lithium Bromide/ Water and Ammonia/ Water as Working Fluids"*, Applied Energy, 37, 169 (1990)

Kaushik, S.C. and Kaudinya, J.V., *"Open-Cycle Solar Absorption Cooling. A Review"*, Energy Convers. Mgmt., 29, 84 (1989)

Korteum, G. and Frier, H.J., *"Isothermal Vapour-Pressure Diagrams of Binary and Ternary Liuquid Mixtures by a Simplified Static Method"*, Chem. Ing. Tech., 26, 670 (1954)

Kriebel, M. and Loffler, H.J., *"Thermodynamische Eigenschaften des Binaren Systems R22 - Tetraathylenglykol dimethylather"*, Kaltetechnik, 17, 266 (1965)

Kumar, R. and Kaushik, S.C., *"Thermoynamic Evaluation of a modified Aqua-Ammonia Absorption Refrigeration System"*, Energy Convers. Mgmt., 32, 191 (1991)

Lange, N.A., *Handbook of Chemistry 10th ed.*, McGraw - Hill, New York, .(1961)

Lenz, T., Loef, G., Kaushik, V. and Sandell, G., *"Open-Cycle Solar Absorption Cooling"*, Proc. 9th Cong. Int. Solar Energy Soc., Montreal (1985)

Linnhoff, B. and Ahmad, S., *"Cost Optimum Heat Exchanger Networks -1. Minimum Energy and Capital Using Simple Models for Capital Cost"*, Computers Chem. Engng., 14, 729 (1990)

Linnhoff, B. and Carpenter, K.J., *"Energy Conservation by Exergy Analysis - The Quick and Simple Way"*, Proc. 2nd. World Cong. Chem. Eng., Montreal (1981)

Ludwig, E.E., Applied Process Design for Chemical and Petrochemical Plants, Gulf Pub. Co. (1965)

Macriss, R.A., *"Selecting Refrigerant Absorbent Fluid Systems for Solar Energy Utilization"*, ASHRAE Trans., 82, 975 (1976)

Maiuri, G., Z. f. ges Kalte Ind., 46, 169 (1939)

Manscori, G.A. and Patil, V., *"Thermodynamic Basis for the Choice of Working Fluids for Solar Absorption Cooling Systems"*, Solar Energy, 22, 483 (1979)

Mehta, G.D., *"Liquid Phase Separation in Absorption Refrigeration"*, U.S. Patent No. 4,283,918 (1981)

Morrissey, A.J. and O'Donnell, J.P., *"Endothermic Solutions and their Application in Absorption Heat Pumps"*, Chem. Eng. Res. Des., 64, 404 (1986)

O'Neill, B.K. and Roach, J.R., *"Organic-Fluid Absorption-Cooling Systems: An Assessment of the Theoretical Performance Limits"*, Proc. 18th Aust. Chem. Eng. Conf., Auckland, 330 (1990)

Peters, M.S. and Timmerhaus, K.D., *Plant Design and Economics for Chemical Engineers*, McGraw-Hill (1991)

Press, W.H., Flannery, B.P., Teukolsky, S.A. and Vetterling, W.T., *Numerical Recipes: The Art of Scientific Computing*, Cambridge University Press (1989)

Reid, R.C., Prausnitz, J.M. and Poling, B.E., *The Properties of Gases & Liquids 4ed*, McGraw Hill (1987)

Renon, H. and Prausnitz, J.M., *"Local Compositions in Thermodynamic Excess Functions for Liquid Mixtures"*, AIChE Journal, 14, 135 (1968)

Riedel, L., *"Extension of the Theorem of Corresponding States. III Critical Coefficient, Density of Saturated Vapour, and Latent Heat of Vaporization"*, Chem. Ing. Tech., 26, 679 (1954)

Roeck, H. and Sieg, L., *"Measurement of Evaporation Equilibria in a Modernized By-pass Apparatus"*, Z. Phys. Chem. (Frankfurt), 3, 355 (1955)

Skjold-Jorgensen, S., Rasmussen, P. and Fredenslund, AA, *"On the Temperature Dependence of the Uniquac/Unifac Models"*, Chem. Eng. Sci., 35, 2389 (1980)

Stephan, K., *"History of Absorption Heat Pumps and Working Pair Developments in Europe"*, Int. J. Refrig., 6, 160 (1983)

Tan, T.C. and Ti, H.C., *"Predicting Effect of Dissolved Solute on the Vapour-Liquid Equilibria of Organic Solvent Mixtures and Aqueous Organic Acid Solutions"*, Chem. Eng. Res. Des., 67, 79 (1989)

Ting, A.M., Lynn, S. and Prausnitz, J.M., *"Liquid-Liquid Equilibria for Aqueous Systems Containing N,N-Diethylmethylamine and Sodium Chloride or Sodium Sulfate"*, J. Chem. Eng. Data, 37, 252 (1992)

Trepp, Ch., *"History and Perspectives of Heat Transformation"*, Int. J. Refrig., 6, 309 (1983)

Uemura, T. and Hasaba, S., *"Studies on the R22-Absorbent Absorption Refrigerating Machine"*, Reito, 43, 1241 (1968)

Zellhoefer, G.F., *"Solubility of Halogenated Hydrocarbon Refrigerants in Organic Solvents"*, Ind. Eng. Chem., 29, 548 (1937)

Ziegler, B. and Trepp, Ch., *"Equation of State for Ammonia-Water Mixtures"*, Int. J. Refrig., 7, 101 (1984)

PUBLICATIONS RESULTING FROM THIS STUDY

White, S.D. and O'Neill, B.K., *"Phase Equilibria for Dimethylethylamine-Water and Trimethylamine-Water Mixtures"* , J. Chem. Eng. Data, in press

White, S.D. and O'Neill, B.K., *"Performance of a Novel Absorption Refrigeration Cycle"*, Proc. 18th Aust. Chem. Eng. Conf., Canberra, Part 2, 360 (1992)

White, S.D. and O'Neill, B.K., *"A Novel Absorption Cycle Heat Pump; Part I - Refrigeration"*, submitted to Int. J. Refrig

White, S.D. and O'Neill, B.K., *"A Novel Absorption Cycle Heat Pump; Part II - Heating"*, submitted to Int. J. Refrig

White, S.D. and O'Neill, B.K., *"An Improved Absorption Refrigeration Cycle"*, Provisional Patent

ADDENDA

Section 2.1, page 4, insert following paragraph before paragraph 1

Plattens and Munter modified the conventional absorption refrigeration cycle to eliminate the necessity for mechanical pumping. The Electrolux domestic absorption refrigerators, which employ this cycle, have been extremely popular in situations where electricity is not available or is unreliable.

Section 2.3, page 8, insert following paragraph before paragraph 1

The conventional absorption refrigeration cycle is illustrated in figure 2.1. High pressure liquid refrigerant exiting the top of the distillation column is depressured across an expansion valve and fed to the evaporator. The reduction in pressure causes the refrigerant to boil at low temperature. Consequently, useful refrigeration is obtained by boiling the refrigerant in the evaporator. The resulting low pressure refrigerant vapour is dissolved/condensed in lean absorbent at low pressure. Refrigerant rich absorbent, exiting the absorber, is then pumped back to high pressure and the refrigerant is recovered from the absorbent in the distillation column. Improved efficiency can be obtained by (i) preheating the distillation column feed with hot lean absorbent exiting the bottom of the distillation column and (ii) precooling liquid refrigerant with cold refrigerant vapour exiting the evaporator (figure 8.1).

Section 3.1.2, page 28, insert following paragraph before paragraph 2

Within the accuracy of the experimental technique, there was no change in the measured concentrations when the mixture was allowed a longer equilibration time.

Section 6.3, page 94, Insert new section 6.3.4 as follows

6.3.4 Exergy Analysis of the Variations to the Novel Absorption Cycle.

The performance of a number of variations of the novel absorption refrigeration cycle have been examined using dimethylethylamine and water as the refrigerant and absorbent respectively. Unfortunately, the performance of each novel cycle variation was shown to be inferior to the conventional absorption refrigeration cycle. In an attempt to explain the decline in performance obtained with the novel cycle variations, an exergy analysis has been performed on each of the cycles examined.

To enable exergy losses in each cycle to be compared, the evaporator temperature and duty were set at 15°C and 0.7 MW. Process data, for each variation analysed, are presented in figures 6.5, 6.6, 6.8 and 6.10. Steam at 110°C was used as the heat source and heat was rejected to an ambient temperature of 20°C. The simplified equations presented by Linnhoff and Carpenter (1981) were used for calculating exergy losses in each unit. Exergy losses for each cycle variation are presented in table 6.1.

Comparison of the total exergy losses incurred in each cycle can be used to rank the thermodynamic performance of the cycles. Examination of table 6.1 confirms that exergy losses from the conventional cycle are less than those obtained in the novel cycle variations. The novel cycle with refrigerant rectification appears to be the best of the novel cycle variations. These results agree with the COP comparisons presented in section 6.3.3.

Examination of the source of exergy losses, in each of the cycle variations, confirms that the addition of the liquid phase separation step has successfully led to a reduction in exergy losses in the distillation column. Unfortunately, the resulting increase in the required absorption fluid circulation rate has led to a significant increase in losses in the absorbent heat recovery exchanger. Heating the absorption fluid to effect liquid phase separation also results in significant losses.

Unit	Conventional Cycle Exergy Loss (kW)	Novel Cycle with Absorbent Phase Distillation Exergy Loss (kW)	Novel Cycle with Refrigerant Phase Rectification Exergy Loss (kW)	Novel Cycle with Evaporator Blowdown Recovery Exergy Loss (kW)
Distillation column	170.3	86.0	139.7	176.3
Absorber	239.1	290.2	204.5	341.7
Absorbent heat recovery exchanger	38.9	60.2	77.1	88.1
Evaporator	14.4	15.1	14.5	23.5
Liquid-liquid separation	–	102.8	48.1	neg
Liquid-liquid separation preheater	–	3.5	–	neg
TOTAL	462.7	557.8	483.9	629.6

TABLE 6.1. COMPARISON OF EXERGY LOSSES FOR NOVEL CYCLE VARIATIONS

The exergy losses from the absorber is also of interest. The exergy losses in the absorber of the refrigerant phase rectification cycle are significantly lower than those obtained in the conventional cycle. This can be explained by the higher pressure observed in the absorber and highlights the importance of absorber pressure on the overall performance of absorption refrigeration cycles. This will be discussed in more detail in chapter 8.

Section 7.5, page 122, the following paragraphs are to be inserted after paragraph 4

Numerous alternative mixtures, exhibiting upper critical solution temperature phase behaviour, could have been chosen to demonstrate the feasibility of the novel heat pump cycles. The furfural/water absorbent/refrigerant pair is one candidate pair that may have proved more attractive. Phase equilibrium data for this pair is presented in Appendix E.

There is a large difference between the boiling point of furfural and water and the liquid-liquid phase envelope straddles the vapour-liquid azeotrope. This enables relatively impure volatile working fluid to be completely boiled off in the evaporator without lowering the boiling point difference between the evaporator and the absorber.

The boiling point difference between coexisting liquid phases must be zero. With increasing temperature the boiling point difference will increase to enable a boiling point difference to be obtained between the evaporator and the absorber in the novel heat pump cycle. Unfortunately, for all conceivable mixtures, the boiling point difference does not increase rapidly with increasing temperature. Consequently, the liquid phase separation step will never contribute significantly to the boiling point elevation which can be achieved between the evaporator and the absorber in these cycles.

For mixtures exhibiting upper critical solution temperature behaviour, the forces of interaction are physical in nature. Consequently, the impact of changing temperature on mixture properties will be small compared with the changes observed in tertiary amine-water mixtures, which are strongly influenced by hydrogen bonding.

Add a new Appendix E as follows

Appendix E

THERMODYNAMIC EQUILIBRIUM DATA FOR CYCLOHEXANE - ANILINE AND FURFURAL - WATER MIXTURES

Cyclohexane - aniline and furfural - water mixtures were selected for further investigation as candidate working fluid pairs in the novel heat pump cycle and its variations. While no experimental phase equilibrium data was obtained for these mixtures, a summary of available experimental data from the literature is presented below .

(i) Cyclohexane - Aniline

P (mmHg)	x (mole fraction)	y (mole fraction)
273.0	0	0
262.2	0.061	0.007
255.5	0.126	0.0095
251.2	0.206	0.011
248.8	0.287	0.011
246.2	0.392	0.011
245.7	0.418	0.011
245.0	0.438	0.011
243.5	0.514	0.0115
241.3	0.606	0.012
237.4	0.640	0.012
229.6	0.716	0.012
219.1	0.774	0.013
200.0	0.832	0.016
163.3	0.891	0.021
119.2	0.936	0.028
3.47	1.0	1.0

TABLE E. 1 : VAPOUR-LIQUID EQUILIBRIUM FOR MIXTURES OF ANILINE AND CYCLOHEXANE AT 50.2°C, ABELLO ET. AL. (1968)

P (mmHg)	x (mole fraction)	y (mole fraction)
151.6	0	0
145.2	0.063	0.005
142.9	0.111	0.007
141.4	0.166	0.008
140.4	0.267	0.008
140.4	0.304	0.008
139.8	0.354	0.008
139.7	0.454	0.008
139.4	0.530	0.008
139.0	0.606	0.008
138.3	0.638	0.008
136.2	0.708	0.0085
131.3	0.773	0.009
116.1	0.853	0.010
105.8	0.883	0.012
1.3	1.0	1.0

TABLE E. 2 : VAPOUR-LIQUID EQUILIBRIUM FOR MIXTURES OF ANILINE AND CYCLOHEXANE AT 35.2°C, ABELLO ET. AL. (1968)

P (mmHg)	x (mole fraction)	y (mole fraction)
511.06	0.0910	0.0116
504.92	0.1130	0.0127
489.41	0.2110	0.0154
478.79	0.3235	0.0169
469.04	0.4278	0.0180
461.33	0.5100	0.0186
452.18	0.5720	0.0192
439.86	0.6314	0.0200
413.30	0.7353	0.0216
385.35	0.7879	0.0236
343.62	0.8385	0.0270
315.79	0.8630	0.0299

TABLE E. 3 : VAPOUR-LIQUID EQUILIBRIUM FOR MIXTURES OF ANILINE AND CYCLOHEXANE AT 70.0°C, HOSSEINI AND SCHNEIDER (1963)

P (mmHg)	x (mole fraction)	y (mole fraction)
184.3	0.00104	0.000168
184.0	0.00203	0.000332
184.0	0.00402	0.000636
183.4	0.00718	0.00111
183.2	0.00825	0.00124
182.9	0.01036	0.00157
183.0	0.01108	0.00165
182.3	0.01499	0.00216
182.2	0.0156	0.00225
182.0	0.0143	0.0021
181.5	0.0213	0.0029
181.1	0.0232	0.0031
181.2	0.0238	0.0031
180.5	0.0305	0.0038
180.2	0.0318	0.0039
180.4	0.0322	0.0039
180.1	0.0324	0.004
179.2	0.0419	0.0046
178.9	0.043	0.0049
178.0	0.0536	0.0055
177.0	0.0657	0.0061
176.8	0.0675	0.0062
175.7	0.0826	0.0068
174.8	0.0981	0.0074
173.6	0.1134	0.0078
172.4	0.1412	0.0082
172.0	0.1597	0.0084
171.1	0.1958	0.0087
170.3	0.2365	0.0088
170.0	0.2715	0.0089

TABLE E. 4 : VAPOUR-LIQUID EQUILIBRIUM FOR MIXTURES OF ANILINE AND CYCLOHEXANE AT 40.0°C, ROECK AND SIEG (1955)

(ii) Furfural - Water

T (°C)	x (mole fraction)	y (mole fraction)
161.7	0	0
158.8	0.02	0.1
154.8	0.04	0.19
146.0	0.06	0.36
122.5	0.08	0.68
109.5	0.1	0.81
100.6	0.2	0.89
98.7	0.3	0.905
97.9	0.96	0.908
98.07	0.98	0.92
98.56	0.99	0.945
100	1.0	1.0

TABLE E. 5 : VAPOUR-LIQUID EQUILIBRIUM FOR MIXTURES OF FURFURAL AND WATER AT 760MMHG, MAINS (1922)

T (°C)	x (mole fraction)	y (mole fraction)
85.4	0	0
42.2	0.0981	0.9154
40.6	0.2192	0.9202
40.2	0.9796	0.9275
40.4	0.9911	0.9426
40.7	0.9962	0.9674
40.9	0.9981	0.9805
41.2	1.0	1.0

TABLE E. 6 : VAPOUR-LIQUID EQUILIBRIUM FOR MIXTURES OF FURFURAL AND WATER AT 55MMHG, TSIRLIN (1962)

T (°C)	x (mole fraction)	y (mole fraction)
153.2	0	0
123.0	0.0981	0.5557
100.0	0.2192	0.8311
92.7	0.3721	0.9008
91.8	0.4848	0.9079
91.5	0.9679	0.9115
91.7	0.9796	0.9206
92.2	0.9911	0.9443
92.8	0.9962	0.9732
93.2	0.9981	0.9875
93.3	1.0	1.0

TABLE E. 7 : VAPOUR-LIQUID EQUILIBRIUM FOR MIXTURES OF FURFURAL AND WATER AT 600MMHG, TSIRLIN (1962)

ERRATA

Section 2.3, page 8, paragraph 2 to read as follows

An investigation into the losses encountered in conventional absorption refrigeration cycles provides a starting point in the search for new cycles. Recent papers by Briggs (1971) and Karakas et. al. (1990) have detailed an exergy balance on the conventional absorption refrigeration cycle with refrigerant precooling illustrated in figure 8.1. The exergy losses calculated by Briggs (1971) are summarised in table 2.1. These studies demonstrate that the majority of losses occur in the absorber and the generator.

Section 2.3.1, page 10, replace old figure 2.1 with new figure 2.1 as follows

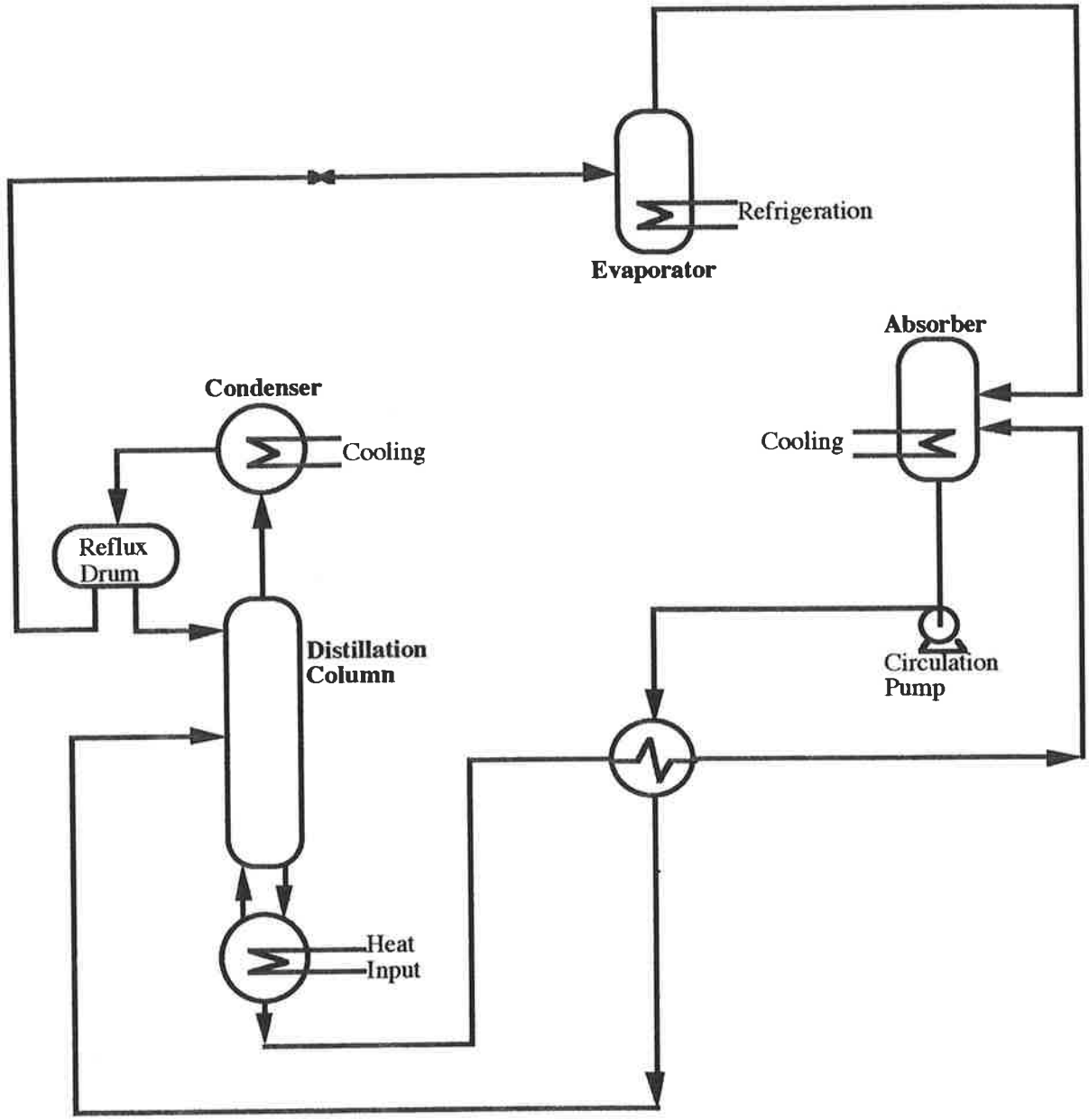

Section 2.3.1, page 11, replace old figure 2.2 with new figure 2.2 as follows

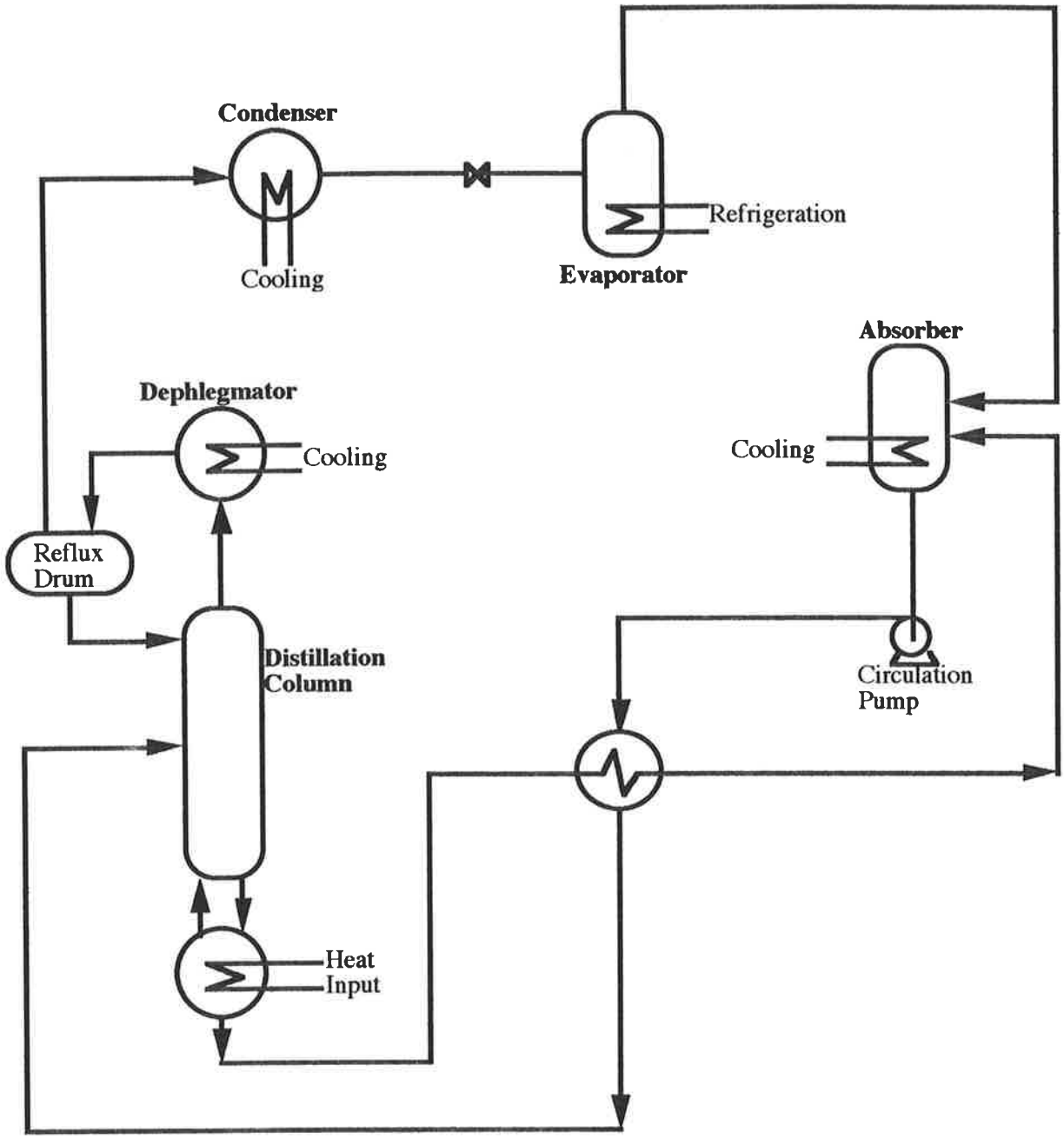

Section 2.3.1, page 13, replace old figure 2.3 with new figure 2.3 as follows

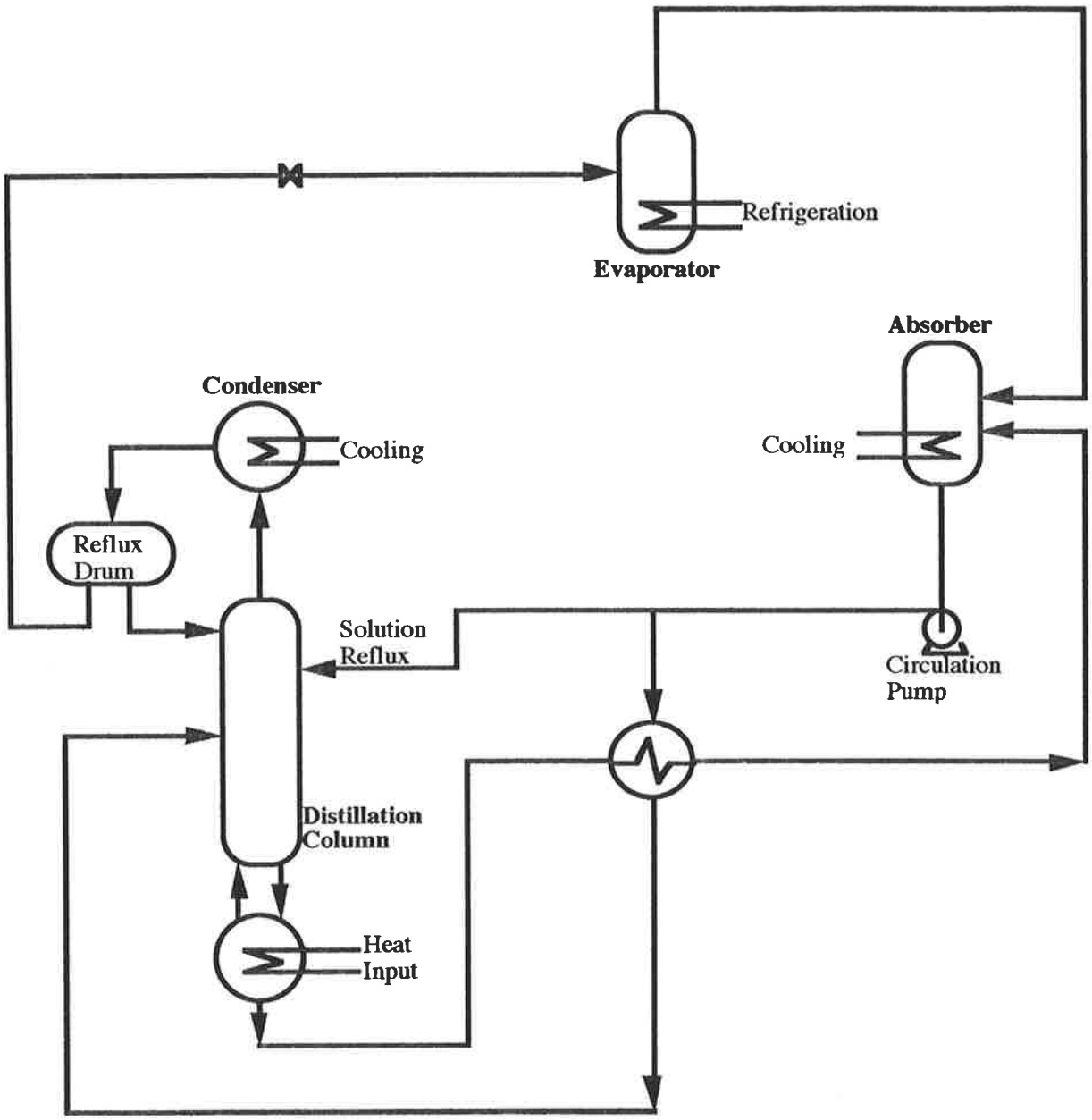

Section 2.3.1, page 14, line 16: delete "Holldorf, 1979" and insert "Holldorff, 1979".

Section 2.4, page 16, line 16: delete "Lenz et. al., 1986" and insert "Lenz et. al., 1985".

Section 2.5, page 18, line 13: delete "comopounds" and insert "compounds".

Section 3.1, page 22, last line: delete "occured" and insert "occurred".

Section 4.1, 4.2.1 and 4.3, pages 28, 44, 45, 46 and 48,

Units on the x-axis of figures 4.1, 4.2, 4.3, 4.4, 4.5, 4.6, 4.7, 4.8 and 4.9 are mole fractions.

Section 4., page 34, line 3: delete "are" and insert "is".

Section 4.2.1, page 42, last line: delete "table 1" and insert "table 4.1".

Section 5.5.3, page 74, line 4: delete "Linhoff" and insert "Linnhoff".

Section 6.3.1, page 87, replace old figure 6.6 with new figure 6.6 as follows

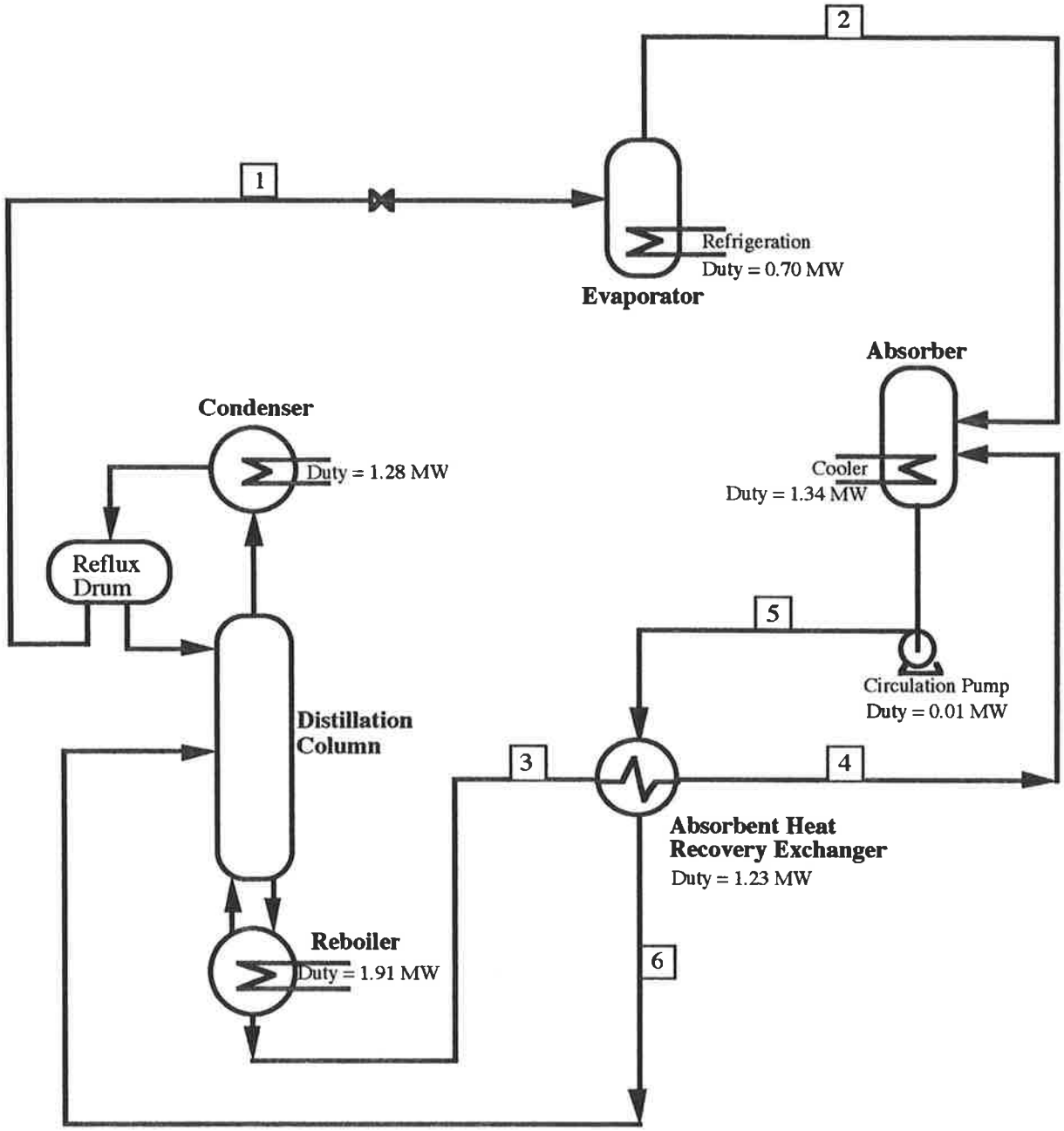

STREAM NO	1	2	3	4	5	6
Flowrate (kmol h^{-1})	127	127	1350	1350	1477	1477
Composition (mol %)	95.1	95.1	1.1	1.1	9.2	9.2
Temperature (°C)	30.0	15.0	77.7	35.2	30.2	59.7
Pressure (kPa)	146.6	39.6	146.6	146.6	146.6	146.6
Liquid Fraction	1.0	0.056	1.0	1.0	1.0	1.0

Section 7.2, page 110, Paragraph 3 is to read

Conveniently, a large body of experimental data is available for the development of an accurate thermodynamic model for mixtures of cyclo-hexane and aniline (Abello et. al., 1968, Hosseini and Schneider, 1963, Korteum and Freier, 1954, Roeck and Sieg, 1955, Buchner and Kleyn, 1924 and Hunter and Brown, 1947). Selected experimental thermodynamic data, obtained from these references, is presented in Appendix E. The five-parameter NRTL model described in chapter 4 was used to predict the phase behaviour of these mixtures. By comparison of model predictions and experimental data, the thermodynamic model was shown to predict mixture vapour pressure with an average accuracy of ±1.8%.

Section 8.2, page 131, line 21: delete "Holldorf, 1979" and insert "Holldorff, 1979".

Section 8.2, page 131, line 22: delete "Linhoff" and insert "Linnhoff".

Section 8.3, page 133, line 4: delete "Holldorf, 1979" and insert "Holldorff, 1979".

Section 8.3, page 133, line 8: delete "cost" and insert "costs".

Section 8.3, page 136, line 7: delete "Peters and Timmerhaus, 1990" and insert "Peters and Timmerhaus, 1991".

Section 8.3, page 136, line 8: delete "Peters and Timmerhaus (1990)" and insert "Peters and Timmerhaus (1991)".

Bibliography, page 1, number 4 to read

Asselineau, L. and Renon, H., "Extension de l'Equation NRTL pour la Representation de l'Ensemble des Donnees d'Equilibre Binaire, Liquide-Vapeur et Liquide-Liquide", Chem. Eng. Sci., 25, 1211 (1970)

Bibliography, page 2, number 1 to read

Cockshott, J.E., Proc. 4th Aust. Chem. Eng. Conf., Adelaide, 330 (1976)

Bibliography, page 3, number 11 to read

Korteum, G. and Freier, H.J., "Isothermal Vapour-Pressure Diagrams of Binary and Ternary Liquid Mixtures by a Simplified Static Method", Chem. Ing. Tech., 26, 670 (1954)